Pages 107N–116N, 1101–1234 ISSN 0003-2654

The Analyst

An international research journal dealing with all branches of analytical science and technology

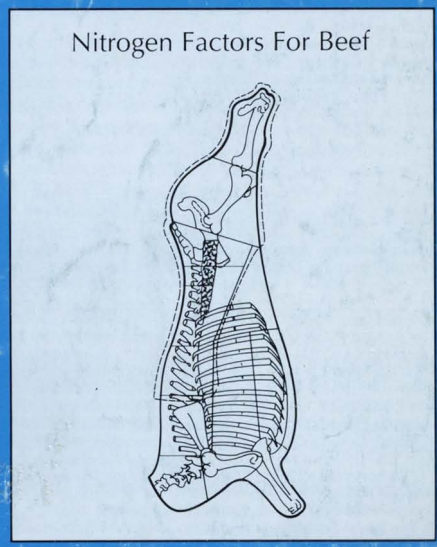

Vol.118 No.9 September 1993

The Analyst

The Analytical Journal of The Royal Society of Chemistry

Editorial Manager, Analytical Journals: Janice M. Gordon

Editor, *The Analyst*
Harpal S. Minhas
The Royal Society of Chemistry,
Thomas Graham House, Science Park,
Milton Road, Cambridge, UK CB4 4WF
Telephone +44(0)223 420066.
Fax +44(0)223 420247. Telex No. 818293 ROYAL.

US Associate Editor, *The Analyst*
Dr Julian F. Tyson
Department of Chemistry,
University of Massachusetts,
Amherst MA 01003, USA
Telephone +1 413 545 0195
Fax +1 413 545 4490

Senior Assistant Editor
Paul Delaney

Assistant Editor
Sheryl Youens

Editorial Secretary: Claire Harris

Advertisements: Advertisement Department, The Royal Society of Chemistry, Burlington House, Piccadilly, London, UK W1V 0BN. Telephone +44(0)71-287 3091. Telex No. 268001. Fax +44(0)71-494 1134.

Information for Authors

Full details of how to submit material for publication in *The Analyst* are given in the Instructions to Authors in the January issue. Separate copies are available on request.

The Analyst publishes papers on all aspects of the theory and practice of analytical chemistry, fundamental and applied, inorganic and organic, including chemical, physical, biochemical, clinical, pharmaceutical, biological, environmental, automatic and computer-based methods. Papers on new approaches to existing methods, new techniques and instrumentation, detectors and sensors, and new areas of application with due attention to overcoming limitations and to underlying principles are all equally welcome. There is no page charge.

The following types of papers will be considered:

Full research papers.

Communications, which must be on an urgent matter and be of obvious scientific importance. Rapidity of publication is enhanced if diagrams are omitted, but tables and formulae can be included. Communications receive priority and are usually published within 5–8 weeks of receipt. They are intended for brief descriptions of work that has progressed to a stage at which it is likely to be valuable to workers faced with similar problems. A fuller paper may be offered subsequently, if justified by later work. Although publication is at the discretion of the Editor, communications will be examined by at least one referee.

Full critical reviews, which must be a critical evaluation of the existing state of knowledge on a particular facet of analytical chemistry.

Every paper (except Communications) will be submitted to at least two referees, by whose advice the Editorial Board of *The Analyst* will be guided as to its acceptance or rejection. Papers that are accepted must not be published elsewhere except by permission. Submission of a manuscript will be regarded as an undertaking that the same material is not being considered for publication by another journal.

Regional Advisory Editors. For the benefit of potential contributors outside the United Kingdom and North America, a Group of Regional Advisory Editors exists. Requests for help or advice on any matter related to the preparation of papers and their submission for publication in *The Analyst* can be sent to the nearest member of the Group. Currently serving Regional Advisory Editors are listed in each issue of *The Analyst.*

Manuscripts (four copies typed in double spacing) should be addressed to:

H. S. Minhas, Editor, *or*
J. F. Tyson, US Associate Editor

Particular attention should be paid to the use of standard methods of literature citation, including the journal abbreviations defined in Chemical Abstracts Service Source Index. Wherever possible, the nomenclature employed should follow IUPAC recommendations, and units and symbols should be those associated with SI.

All queries relating to the presentation and submission of papers, and any correspondence regarding accepted papers and proofs, should be directed either to the Editor, or Associate Editor, *The Analyst* (addresses as above). Members of the Analytical Editorial Board (who may be contacted directly or via the Editorial Office) would welcome comments, suggestions and advice on general policy matters concerning *The Analyst.*

Fifty reprints are supplied free of charge.

The Analyst (ISSN 0003–2654) is published monthly by The Royal Society of Chemistry, Thomas Graham House, Science Park, Milton Road, Cambridge, UK CB4 4WF. All orders, accompanied with payment by cheque in sterling, payable on a UK clearing bank or in US dollars payable on a US clearing bank, should be sent directly to The Royal Society of Chemistry, Turpin Distribution Services Ltd., Blackhorse Road, Letchworth, Herts, UK SG6 1HN. Turpin Distribution Services Ltd., is wholly owned by the Royal Society of Chemistry. 1993 Annual subscription rate EC £301.00, USA $662.00, Canada £348.00 (excl. GST), Rest of World £331.00. Purchased with *Analytical Abstracts* EC £656.00, USA $1444.00, Canada £758.00 (excl. GST), Rest of World £722.00. Purchased with *Analytical Abstracts* plus *Analytical Proceedings* EC £774.40, USA $1703.68, Canada £894.00 (excl. GST), Rest of World £851.84. Purchased with *Analytical Proceedings* EC £383.00, USA $842.00, Canada £442.00 (excl. GST), Rest of World £421.00. Air freight and mailing in the USA by Publications Expediting Inc., 200 Meacham Avenue, Elmont, NY 11003.

USA Postmaster: Send address changes to: *The Analyst,* Publications Expediting Inc., 200 Meacham Avenue, Elmont, NY 11003. Second class postage paid at Jamaica, NY 11431. All other despatches outside the UK by Bulk Airmail within Europe, Accelerated Surface Post outside Europe. PRINTED IN THE UK.

Under-determination of Strontium-90 in Soils Containing Particles of Irradiated Uranium Oxide Fuel

Deborah H. Oughton and B. Salbu
Isotope and Electron Microscopy Laboratories, Agricultural University of Norway, 1432 Ås, Norway
Tom L. Brand and J. Philip Day
Department of Chemistry, University of Manchester, Manchester, UK M13 9PL
Asker Aarkrog
Environmental Science and Technology Department, Risø National Laboratory, DK-4000, Denmark

A much used method for the determination of ^{90}Sr in soil depends on extraction of the soil with 6 mol l^{-1} HCl, followed by β-counting. For soils containing particles of irradiated uranium oxide, we postulate that this extraction could result in a variable underestimate owing to incomplete chemical recovery of strontium from the uranium oxide matrix. In experiments on two soils, collected from near Windscale (now Sellafield) in 1956 and near Chernobyl in 1990, about 25% of the total ^{90}Sr present in the soil was recovered in 24 h by HCl extraction at room temperature, and the presence of high-radioactivity particles both before and after extraction was demonstrated by autoradiography. For a further 11 particle-containing Chernobyl soils, ^{90}Sr determination, based on classical HCl extraction, yielded, on average, 54% (range 33–85%) of the total ^{90}Sr, as determined by oxidative alkaline fusion. While we accept that HCl extraction is well established as a reliable method for the determination of soil ^{90}Sr derived from weapons fallout, we conclude that more rigorous analytical pre-treatment is essential in instances where the ^{90}Sr may be associated with fuel particles.

Keywords: *Strontium-90 determination; soil extraction; uranium oxide fuel particle; Windscale; Chernobyl*

Historically, on at least two occasions, particles of uranium oxide from irradiated reactor fuel have been released in significant amounts into the environment.[1] In the early 1950s, the operation of the two Windscale piles (at Sellafield, UK) resulted in the continuous release over several years of an estimated 20 kg of uranium, in the form of relatively large particles (up to 700 μm in length) of oxidized uranium fuel.[2] More recently, the Chernobyl Reactor accident, in 1986, released a large amount of radioactive particles.[3–7] These varied in size, shape and composition, but were mainly of two types. Firstly, fragmentation of the reactor core during the initial explosion released about 3.5% of the irradiated uranium dioxide fuel: the larger fuel particles (20–400 μm) were deposited within about 60 km of the reactor, while smaller particles were carried at least 1500 km. Secondly, during combustion of the reactor core, following the explosion, small particles of irradiated fuel and 'condensation' particles (*i.e.*, inactive or active materials on which the volatile fission products had condensed) were released. These particles were carried considerable distances from Chernobyl, and constituted the major component of long-lived fission products deposited at distances over 30 km (that is, outside the so-called '30 km exclusion zone').

The radiochemical analysis of soils containing discrete radioactive particles can present special problems, apart from the difficulty of obtaining representative samples. In direct γ-ray spectrometry (*e.g.*, for ^{137}Cs), inhomogeneity could clearly give rise to errors in calibration, whereas for determinations requiring chemical isolation of the nuclides, for example, in the determination of ^{90}Sr or actinides, problems arise if the analyte nuclide is not completely extracted (or, more precisely, in instances in which a yield monitor is used if complete exchange between the analyte and yield monitor nuclides is not achieved). Such problems have been recognized for some time, and the subject has been reviewed recently.[8] In particular, Sill and co-workers[9,10] showed that, for soils containing particles of refractory uranium or plutonium oxides, extraction methods involving HCl and/or HNO_3, which would be appropriate for soils containing only weapons fallout, achieve very low recoveries (typically <30%) of plutonium and other actinides. In such instances, fusion techniques, resulting in complete dissolution of the sample, were recommended.[10]

In relation to ^{90}Sr determination in soils containing fuel particles, a crucial part of the analytical procedure is the initial chemical extraction of the ^{90}Sr from within the fuel particle matrix. Traditionally, the determination of ^{90}Sr in soil has depended upon an extraction procedure using HCl, typically 6 mol l^{-1} HCl at room temperature.[11,12] This extraction step, which was developed in the 1950s and remains a recommended procedure,[8,13] achieves good recovery of ^{90}Sr originating from weapons fallout, where ^{90}Sr is deposited in condensed, sub-micrometre particles. However, general problems of incomplete recovery have been recognized, and some laboratories now routinely use much more vigorous conditions to ensure complete extraction of strontium.[8] As uranium oxide is relatively inert to cold HCl (although more reactive in oxidizing conditions),[14] it would be expected that complete recovery of ^{90}Sr from fuel particles might not be attained by HCl extraction alone. Hence, in instances where the fuel particle component was significant, the method could give rise to an underestimate of deposited ^{90}Sr in soils.

To test this hypothesis, ^{90}Sr determinations have been carried out by HCl extraction of particle-containing soils from two sources: from near Sellafield (then Windscale), collected in 1956; and from within 15 km of Chernobyl, collected in 1990 and 1991. The efficiency of the HCl extraction was then assessed by determination of the remaining ^{90}Sr, following total dissolution of the residues.

Experimental

Two types of experiment have been carried out. In the first, intended to examine the behaviour of identifiable radioactive particles during extraction, samples of Chernobyl and Windscale soil were sequentially extracted with HCl (6 mol l^{-1}; two portions), ammonium acetate and finally (for total analysis) a mixture of HF and HNO_3. The presence of radioactive particles in the samples was demonstrated by autoradiography both before and after the HCl extractions.

In the second experiment, intended to investigate the extent to which ^{90}Sr in particle-containing soils might be under-

estimated in normal laboratory practice, ^{90}Sr in 11 samples of Chernobyl soil was determined by using HCl extraction, and the results were compared with the total obtained following oxidative alkaline fusion of the residues.

Sample Origins and Preparation

The Chernobyl soils were taken to a depth of 5 cm, from Bourykovka (May, 1990 and 1991) and from Novo Shepilichi (May, 1991), 15 and 5 km, respectively, from the Chernobyl reactor. Stones and roots were removed, and the soils were dried, crushed and homogenized by gentle grinding. Soils from these locations have previously been characterized both at the Isotope Laboratory, Norway, and the Risø National Laboratory, Denmark, and were found to contain relatively high activities of the refractory fission products (*e.g.*, ^{144}Ce), consistent with the presence of fuel particles.[7,15]

The Windscale soil was one of a number of grass and topsoil samples collected between 1955 and 1957 from a garden in the village of Seascale, approximately 3 km from the Windscale piles, as part of a contemporary investigation of the emissions of oxidized fuel particles. The piles operated from 1951 to 1957, when both were shut down because of a major fire in one of them.[16] Particle releases were first discovered in mid-1955, and were caused by oxidation of incorrectly discharged (metallic uranium) fuel elements in the ducts leading from the air-cooled reactor core to the discharge stack, which housed an ineffective filter system.[2,17] One such particle (approximately 300 μm in length) was isolated, at the time, from the Seascale garden[18] and some of its characteristics have already been reported.[7] The Seascale soil samples were stored dry and intact, together with their surface vegetation, until 1991, when they were delivered to the University of Manchester, and thereafter to the Isotope Laboratory in Norway. A number of additional experiments to characterize these materials have now been carried out, and will be reported separately.

The Windscale soil sample described in the present paper had been collected in February, 1956, to a depth of approximately 1 cm. In 1991, the vegetation and obvious stones were removed, and the soil (15.2 g) was further dried, crushed, and mixed gently, yielding seven 2 g portions for further investigation. These were first screened by γ-ray spectrometry. The only fission product readily detectable was ^{137}Cs, averaging 0.12 ± 0.05 Bq g^{-1} in six of the sub-samples. The seventh portion contained (in total) 22.8 Bq of ^{137}Cs, and was assumed to contain one or more fuel particles. This high-activity portion, and a low-activity sample for control purposes, was further examined by autoradiography and then subjected to chemical extraction with HCl.

Sequential Extraction Experiments

Two 2 g samples of one particular Chernobyl soil (Bourykovka, 1990) were compared with two 2 g samples of the Windscale soil (*i.e.*, the active sample and the control, as described earlier). Sample preparation, autoradiography and chemical extractions were carried out in Norway, at the Isotope Laboratory. Extracts and residues were then divided, and radiochemical measurements were carried out in duplicate, both at the Isotope Laboratory and at the University of Manchester (actinides were also determined at Manchester, and will be reported separately). Measurement differences between the two laboratories for parallel samples did not exceed 10%. As the soils were known to contain small radioactive particles, the loss of even a very small fraction of the sample could potentially affect the results disproportionately. Therefore, at all stages in the experiment the ^{137}Cs content of the samples, sub-samples, residues and empty containers was monitored. No losses were detected.

For autoradiography, the soils (the initial 2 g portions and the corresponding dried residues after the solution extractions) were examined for the presence of β/γ-emitting hot particles using standard X-ray film (Kodak X-OMAT AR-5). The samples were thinly spread on paper, covered with a thin polyethylene membrane, and the X-ray film was placed in close contact on top for 2 weeks exposure. The results are shown in Fig. 1.

After the first autoradiographic exposures, the soil samples were treated sequentially with two portions of 6 mol l^{-1} HCl (20 ml each for 12 h with gentle shaking at 20 °C) and one of 1 mol l^{-1} ammonium acetate (20 ml for 2 h, intended as a precautionary measure to ensure that none of the extracted ^{137}Cs would be re-adsorbed by soil components). Strontium chloride (20 mg of Sr) was added as a yield monitor/carrier with each treatment, and on each occasion the residue was washed with water (10 ml), and the washings were added to the appropriate extractant solution. The ^{137}Cs was determined in the initial starting materials, the extracting solutions at each stage, and in the residues. To determine total ^{90}Sr, the extracted residues were totally dissolved in a 1 + 1 mixture of 60% HF and 16 mol l^{-1} HNO_3, the solutions were evaporated to dryness, and the residual solids were dissolved in 4 mol l^{-1} HNO_3.

Comparative Analysis of Chernobyl Soils

Strontium-90 was determined in 11 samples of Chernobyl soils (five from Bourkovka and six from Novo Shepilichi, collected in May, 1991) using a standard HCl extraction technique, and the residual ^{90}Sr was then recovered by oxidative alkaline fusion.[19,20] Duplicate 1 g portions of each soil were treated with cold 6 mol l^{-1} HCl for 24 h, with occasional stirring. The residual solids from the HCl extractions were fused with a mixture of NaOH (41 g), $NaKCO_3$ (14 g) and KNO_3 (0.7 g). The fused mixture was extracted with HNO_3, and ^{90}Sr was determined in both sets of extracts.

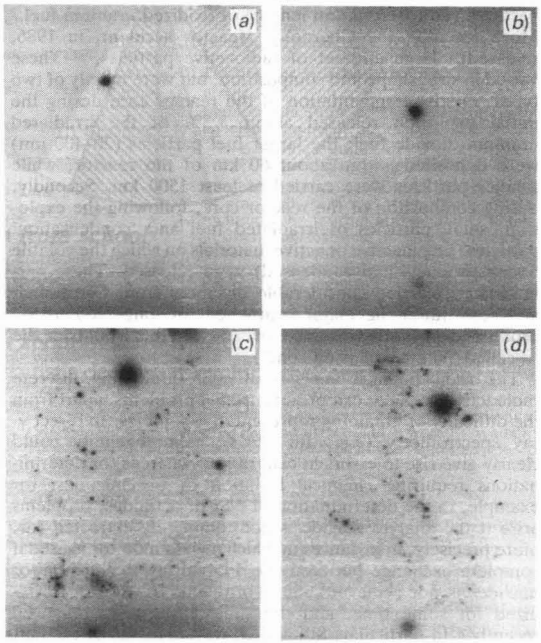

Fig. 1 Autoradiographs of Windscale and Chernobyl soils: (*a*) Windscale soil before chemical extraction; (*b*) Windscale soil after extraction; (*c*) Chernobyl soil before chemical extraction; and (*d*) Chernobyl soil after extraction. The light patch on the top edge of (*a*), (*c*) and (*d*) is due to exposure from exterior light

Radiochemical Measurements

At the Isotope Laboratory, ^{90}Sr was determined by an established laboratory procedure involving extraction of equilibrated ^{90}Y.[21] Solutions were evaporated to dryness, the residues were ashed at 400 °C, and the ashes were dissolved in 1 mol l^{-1} HCl, with addition of natural yttrium and strontium carriers. Yttrium was isolated by extraction into toluene containing 5% of bis(2-ethylhexyl) hydrogen phosphate (HDEHP), back-extracted into 3 mol l^{-1} HNO_3 and finally determined by Cerenkov counting (Quantilus 1220 low-level liquid scintillation spectrometer; LKB-Wallac, Turku, Finland). Chemical yields were determined by complexometric titration. The ^{137}Cs in solids was determined by means of an HPGe (high-purity germanium) detector, and in the extractant solutions using a sodium iodide well (MiniAxi) detector (Canberra Packard Benelux, Tilburg, The Netherlands), cross-calibrated against the HPGe system.

At the University of Manchester, strontium (*i.e.*, carrier plus ^{90}Sr) was isolated from 4 mol l^{-1} HNO_3 by chromatography on a strontium-specific solid phase (Sr-SPEC; EI-Chrom Industries, Chicago, IL, USA) and subsequently eluted with water.[22] The chemical yield was determined by analysis for total strontium (inductively coupled plasma atomic emission spectrometry; Perkin- Elmer Model 6500, Norwalk, CT, USA), and ^{90}Sr (with equilibrated ^{90}Y) was determined after 3 weeks by liquid scintillation spectrometry [Canberra (Pangbourne, Dorset, UK) Model 2250CA], using an equilibrated (^{90}Sr–^{90}Y) low-level standard for calibration (National Physical Laboratory, Ref. R715). Caesium-137 was determined by γ-ray spectrometry.

At the Risø National Laboratory, ^{90}Sr was determined in all extracts using the classical technique of precipitation with fuming HNO_3, and β-counting (after 3 weeks).[19,20] Yields were monitored with ^{85}Sr.

Results and Discussion

Autoradiography

The autoradiographs for the high-activity Windscale soil, before and after HCl extraction, are shown in Fig. 1(*a*) and (*b*), respectively. The low activity (control) Windscale soil produced no visible effect on the X-ray film. The analogous autoradiographs for one of the Chernobyl soil samples are shown in Fig. 1(*c*) and (*d*) (both Chernobyl samples yielded similar results). At the pre-extraction stage, the presence of a considerable number of particles is clearly seen in the Chernobyl soil, while one particle is visible in the active Windscale soil.

The resistance of these particles to HCl extraction is demonstrated by the post-extraction autoradiographs [Fig. 1(*b*) and (*d*), Windscale and Chernobyl, respectively], although the Windscale particle appears to have broken into two pieces during extraction. Using the particle positions identified by the autoradiograph [Fig. 1(*b*)], the bulk of the residue was physically separated from the two particles. It was found that most of the ^{137}Cs activity was still associated with the particles, not with the bulk soil. Hence, the possibility that ^{137}Cs had been extracted from the particle and resorbed by the soil fraction can be excluded.

Sequential HCl Extraction

Results for the Windscale soil are summarized in Table 1. The total ^{137}Cs activity of the soil plus particle was 22.8 ± 0.5 Bq, whereas that of the control soil was 0.24 ± 0.02 Bq (both 2 g). It seems reasonable to infer that, in the more active sample, at least 99% of the ^{137}Cs (and presumably ^{90}Sr) activity was associated with the one particle observed by autoradiography. For this particle, totals of 23 and 25% of the ^{137}Cs and ^{90}Sr, respectively (*i.e.*, within experimental error, the same relative amounts), were extracted. Additionally, the ^{90}Sr : ^{137}Cs ratio (mean 1.7; range 1.5–2.0) does not vary markedly as between the various extracts or between extract and residue. These results suggest strongly that the extraction process results essentially from dissolution of the particle matrix itself.

It might also be noted that the ^{90}Sr : ^{137}Cs ratio observed is higher than that assumed (0.9 : 1.0) for the irradiated fuel that was released.[2] The reason for the discrepancy is not clear, but could reflect preferential removal of Cs nuclides (*e.g.*, by volatilization) at some stage in the life of the uranium fuel, perhaps during its oxidation and the formation of particles, which occurred in a hot-air stream over a long period. Possible, but in our view less likely, would be preferential extraction of caesium relative to strontium from the fuel particle after deposition, by weathering processes in the soil.

For the analogous sequential extraction of the Chernobyl soil (Table 2), the relative amounts of ^{137}Cs and ^{90}Sr extracted by HCl were 66 and 26%, respectively. The result for ^{90}Sr, taken together with the demonstration by autoradiography of the presence of extraction-resistant particles, clearly demonstrates the ineffectiveness of HCl extraction for the determination of total ^{90}Sr in this soil. However, the greater extractability of ^{137}Cs relative to ^{90}Sr, which is also reflected by the

Table 1 ^{90}Sr and ^{137}Cs activities in sequential extracts and residue from a soil sample collected from near Windscale in February, 1956

Component	^{137}Cs/Bq*	Amount (%)	^{90}Sr/Bq*	Amount (%)	^{90}Sr : ^{137}Cs ratio
1. 6 mol l^{-1} HCl (12 h)	3.3 ± 0.1	14.5	5.1 ± 0.1	14.5	1.5
2. 6 mol l^{-1} HCl (12 h)	1.6 ± 0.1	7.0	3.2 ± 0.1	9.1	2.0
3. 1 mol l^{-1} NH_4OAc (1 h)	0.3 ± 0.1	1.3	0.5 ± 0.1	1.4	1.7
Total extracted	5.2 ± 0.3	22.8	8.8 ± 0.3	25.0	1.7
Residue (measured)	17.6 ± 0.2	77.2	26.4 ± 2	75.0	1.5
Total in 2 g sample	22.8	100.0	35.2	100.0	1.54

* Activity ± standard deviation (counting statistics).

Table 2 ^{90}Sr and ^{137}Cs activities in sequential extracts and residue from a soil sample collected from near Chernobyl in May, 1990

Component	^{137}Cs/Bq*	Amount (%)	^{90}Sr/Bq*	Amount (%)	^{90}Sr : ^{137}Cs ratio
1. 6 mol l^{-1} HCl (12 h)	84.7 ± 0.1	57.8	6.6 ± 0.2	22.7	0.078
2. 6 mol l^{-1} HCl (12 h)	10.9 ± 0.1	7.4	0.7 ± 0.1	2.4	0.064
3. 1 mol l^{-1} NH_4OAc (1 h)	1.0 ± 0.3	0.7	0.3 ± 0.1	1.0	0.30
Total extracted	96.6 ± 0.5	65.9	7.6 ± 0.4	26.2	0.079
Residue (measured)	50.0 ± 1	34.1	21.4 ± 1.5	73.8	0.43
Total in 2 g sample	146.6	100.0	29.0	100.0	0.198

* Activity ± standard deviation; mean of two 2 g samples.

differing ^{90}Sr : ^{137}Cs ratios in the residue and the HCl-extractable component (0.43 and 0.079, respectively), also suggests that a significant amount of the total ^{137}Cs activity is bound to a matrix other than fuel particles.

In relation to the analytical determination of ^{90}Sr in particle-containing soils, the hypothesis outlined in the introduction to this paper has been substantiated by these experiments. In both instances, the HCl extraction method recovered about 20–26% of the total ^{90}Sr present in the soil samples. For the Windscale soil, the incomplete extraction was shown to be due to the presence of a single fuel particle, resistant to extraction by the technique used, and a similar explanation is likely for the low ^{90}Sr recoveries from the Chernobyl soil.

Comparative Analysis of Chernobyl Soils

In general, it might be expected that the fraction of the total ^{90}Sr extracted from a soil sample would be affected by the fraction of the isotope associated with radioactive particles, the properties of the particles themselves (composition, size/surface area, degree of post-depositional weathering, *etc.*) and by factors related to sample preparation (*e.g.*, drying temperature or amount of sample grinding) and chemical extraction (*e.g.*, temperature, agitation or length of extraction processes). In the sequential extraction experiments reported above, we deliberately reduced the mechanical factors thought likely to affect particle dissolution (*e.g.*, we avoided fine grinding of the soil before extraction). Hence, while demonstrating that large, intact particles are resistant to chemical attack by HCl, our sequential extraction experiments may not be fully representative of routine laboratory soil analysis.

In order to evaluate whether HCl extraction underestimates ^{90}Sr in normal practice, we have also carried out determinations on 11 particle-containing soil samples from the Chernobyl area by the procedure (based on HCl extraction) routinely used at the Risø National Laboratory, and which follows a long established and widely used protocol[19,20] (although we recognize that soil pre-treatment methods for ^{90}Sr determination vary considerably between laboratories, as indeed do the extraction methods themselves).

The results for these soil analyses are presented in Table 3. The fractional ^{90}Sr recovery by HCl extraction (relative to that obtained by alkaline fusion and complete dissolution) ranged from 33 to 85%, with a mean of 54%. It is clear that, for soils containing uranium oxide fuel particles, extraction by cold 6 mol l^{-1} HCl is not a satisfactory technique for the determination of total ^{90}Sr.

A significant deposit of condensation-type particles, in addition to fuel particles, in this soil is suggested by the relatively low values for the ^{90}Sr : ^{137}Cs ratios (range 0.27–0.62), which are below the average ratio (0.71) for the irradiated fuel at the time of the accident.

Extraction by HCl and the Alternatives

Under conditions in which ^{90}Sr has been deposited in submicrometre particles, and probably in an acid-soluble matrix, as is the case with weapons fallout, HCl extraction has been demonstrably and understandably effective.[8,12] However, extraction of trace nuclides from larger particles of a refractory oxide presents a very different problem, as was identified some years ago by Sill and co-workers,[9,10] in relation to actinide determination. At that time, plutonium in soil from weapons fallout was determined accurately and reliably by an extraction procedure involving HCl or a mixture of HCl and HNO_3. Sill[9] demonstrated that, for soils contaminated by 'an accidental release of plutonium' (site not stated), the standard extraction failed to recover all the plutonium, and additionally, if the soil had been strongly heated before extraction, recoveries as low as 5–30% were obtained. He concluded that treatment with these acids alone 'is grossly inadequate for dissolution of refractory compounds of plutonium'. Sill *et al.*[10] concluded that only complete dissolution of the sample initially could ensure reliable analysis, and they evolved a method of sample pre-treatment based on a combination of KF and pyrosulfate fusions to meet this problem.

Oxides of the lower oxidation states of uranium are only easily soluble in acids under oxidizing conditions.[14] In our view, the HCl extraction method is ineffective for soils containing fuel particles, in part because of the lack of oxidizing capability (hence, extraction is enhanced by the use of H_2O_2 and/or HNO_3[15]). However, in instances in which fuel particles could be involved, even more rigorous oxidizing conditions might be needed. Additionally, thorough grinding of a sample to reduce the particle size (and increase the relative surface area) of the chemically resistant components would clearly assist recovery in instances where an acid-extraction method is to be used (in this context, we are aware of recent work[23] in which a Windscale soil, similar to our own, afforded good recovery of ^{90}Sr when extracted with 6 mol l^{-1} HCl; however, it is probable that the soil sample was ground to a much finer powder than in our extraction experiments, which could explain the difference in the results obtained).

It has been suggested to us[24] that the HCl extraction technique for ^{90}Sr determined in soil is no longer in common usage, and that soil extraction with hot *aqua regia* (HCl–HNO_3, 3 + 1), which is more likely to achieve complete recovery, is now more commonplace. Traditionally, recommended alternatives to acid extraction, for intractable matrices, have been alkaline and/or fluoride fusion under oxidizing conditions (as outlined earlier in this paper).[6,7]

Table 3 ^{90}Sr determination (Bq g^{-1}) by HCl extraction (and subsequent oxidative alkaline fusion of the residue) for samples of 11 soils containing radioactive particles, collected from near Chernobyl in May, 1991

Sample	Location*	^{90}Sr/Bq g^{-1} in soil		Amount in HCl extract (%)	Isotope ratio (^{90}Sr : ^{137}Cs)
		HCl extract	Residue		
B2-11	BK	11.3 ± 0.2	9.9 ± 0.1	53	0.62
B2-11	BK	6.2 ± 0.1	5.3 ± 0.1	54	0.39
C2-7	BK	27 ± 0.4	12.3 ± 0.2	69	0.30
C2-8	BK	23 ± 0.3	18.7 ± 0.2	55	0.29
C2-9	BK	42 ± 0.6	7.4 ± 0.1	85	0.37
E2-9	NS	58 ± 0.8	42 ± 0.6	58	0.43
E2-10	NS	49 ± 0.7	66 ± 0.8	43	0.42
E2-11	NS	59 ± 0.7	59 ± 0.8	50	0.39
F2-9	NS	134 ± 2.0	122 ± 2.0	52	0.27
F2-10	NS	132 ± 2.0	270 ± 4.0	33	0.43
F2-11	NS	155 ± 2.0	230 ± 3.0	40	0.41

* BK = Bourykovka; NS = Novo Shepilichi (15 and 5 km, respectively, from the Chernobyl reactor site).

These methods are all discussed in the recent RADREM (Radioactivity Research and Environment Monitoring Committee) report,[8] and it does indeed seem likely that many UK laboratories would now not use HCl extraction routinely for soil analysis.

However, we also note that the use of HCl extraction for the determination of ^{90}Sr in soils, including those which could contain fuel particles, is specifically recommended in the recent IAEA (International Atomic Energy Agency) 'Guidebook' for environmental radionuclide determination,[13] intended particularly to establish 'reliable analytical methods to obtain data capable of inter-comparison in the case of radioactive releases'. In the recommended procedure, soil is first dried, weighed, and crushed to pass through a 4 mm mesh sieve. The dry soil (500 g recommended) is then treated with 6 mol l^{-1} HCl and allowed to stand, with occasional stirring, for at least 8 h. After filtration, the procedure is repeated and the extracts are combined. This procedure is almost identical with that originally described in 1957 by Bryant *et al.*[11] and used (scaled down) by ourselves in the present work.

It now seems clear, both from the earlier work and from our own experiments, that HCl extraction is an unreliable method for the extraction of nuclides from soils, at least in instances where fuel particles are likely to be involved. Therefore, we suggest that the IAEA recommendation[13] should be viewed with considerable caution. In our view, in instances where oxide fuel particles are likely to be present, only methods based on complete dissolution of the sample should initially be assumed to be reliable, and although methods based on mixed-acid extraction (HCl–HNO_3–HF) could be effective, they should be evaluated for the particular circumstances of the analysis.

Re-evaluation of Previous Results

In view of our conclusions above, it may be necessary to examine the reported experimental methods carefully when evaluating determinations of soil ^{90}Sr reported in connection with the Chernobyl accident, certainly for locations close to the site. Similarly, the determinations of ^{90}Sr in soil near Sellafield in the period following the Windscale pile fire (October, 1957) are likely to have been affected by the presence of uranium oxide particles, as it was established at the time that most of the soil ^{90}Sr identified within 10 km of Sellafield originated from particle emissions that had taken place before the fire.[25] It seems to us possible that in both instances the total release of ^{90}Sr will have been underestimated as a result of the analytical problems we have discussed.

We thank Dr. F. Leslie, formerly resident in Seascale, for supplying materials used in this investigation, H. N. Lien of the Isotope Laboratory, Agricultural University of Norway, for carrying out analyses for ^{90}Sr, and Drs. F. R. Livens (University of Manchester) and B. T. Wilkins (UK National Radiological Protection Board), and also the two (anonymous) referees of this paper, for helpful comments and suggestions.

References

1 Eisenbud, M., *Environmental Radioactivity* Academic Press, New York, 3rd edn., 1987, pp. 244–391.
2 Chamberlain, A. C., *Sci. Total. Environ.*, 1987, **63**, 139.
3 Loshchilov, N. A., Kashparov, V. A., Yudin, Ye. B., Protsak, V. P., Zhurba, M. A., and Parshakov, A. E., in *The Radiobiological Impact of Hot Beta-Particles from the Chernobyl Fallout: Risk Assessment*, IAEA, Vienna, 1992, Part I, pp. 34–39.
4 Bogatov, S. A., and Borovoy, A. A., in *The Radiobiological Impact of Hot Beta-Particles from the Chernobyl Fallout: Risk Assessment*, IAEA, Vienna, 1992, Part II, pp. 1–16.
5 Salbu, B., in *Proceedings of an International Workshop (Thueren, FRG)*, eds. von Philipsborn, H., and Steinhausler, F., Bergbau- und Industriemuseums, Thueren, 1988, vol. 16, pp. 83–84.
6 Sandells, F. J., Segal, M. G., and Victorova, N., *J. Environ. Radioact.*, 1993, **18**, 5.
7 Salbu, B., Krekling, T., Oughton, D. H., Ostby, G., Kashparov, V. A., and Day, J. P., *Proceedings of the International Symposium on Radioecology. Chemical Speciation–Hot Particles*, CEC/IUR Joint Workshop on Hot Particles, Prague, TUR-European Branch, Znojmo, Czechoslovakia, 1992, pp. 108–110.
8 *Sampling and Measurements of Radionuclides in the Environment*, UK Department of the Environment, RADREM Report, HM Stationery Office, London, 1989.
9 Sill, C. W., *Health Phys.*, 1975, **29**, 619.
10 Sill, C. W., Hindman, F. D., and Anderson, J. I., *Anal. Chem.*, 1979, **51**, 1307.
11 Bryant, F. J., Chamberlain, A. C., Morgan, A., and Spicer, G. S., Radiostrontium Fallout in Environmental Materials in Britain, Report AERE HP/R.2056 (unclassified), AERE, Harwell, UK, 1957.
12 Wilken, R. D., and Diehl, R., *Radiochim. Acta*, 1987, **41**, 157.
13 *Measurement of Radionuclides in Food and the Environment: a Guidebook*, Technical Report series, No. 295, IAEA, Vienna, 1989.
14 Katz, J. J., and Rabinovitch, E., *The Chemistry of Uranium*, Dover Publications, New York, 1951, p. 322.
15 Oughton, D. H., Salbu, B., Riise, G., Lien, H., Østby, G., and Nøren, A., *Analyst*, 1992, **117**, 481.
16 Arnold, L., *The Windscale Fire, 1957, Anatomy of a Nuclear Accident*, Macmillan Press, London, 1992.
17 Howells, H., Ross, A. E., and Gausden, R., The Release of Oxide from Irradiated Uranium in the Windscale Area Since October 1955, UKAEA Report No. IGO/TM/W036, 1957 (available from the Public Records Office, UK).
18 Leslie, F. R., personal communication, 1990.
19 Harley, J. H., *Health and Safety Laboratory Procedures Manual*, HASL-300, US Energy Research and Development Administration, New York, 1972.
20 Aarkrog, A., Environmental Studies on Radioecological Sensitivity and Variability With Special Emphasis on the Fallout Nuclides ^{90}Sr and ^{137}Cs, Risø-R-437, Risø National Laboratory, Roskilde, Denmark, 1979.
21 Bjørnstad, H. E., Lien, H. N., Yu-Fu, Y., and Salbu, B., *J. Radioanal. Nucl. Chem.*, 1992, **156**, 165.
22 Horwitz, E. P., Diety, M. L., and Fisher, D. E., *Anal. Chem.*, 1991, **63**, 522.
23 McMahon, A. W., Toole, J., Jones, S. R., and Gray, J., unpublished work.
24 Wilkins, B. T., personal communication, 1992.
25 Bryant, F. J., Spicer, G. S., Chamberlain, A. C., Morgan, A., and Templeton, W. L., Radiostrontium in Soil, Grass, Vegetables and Milk from Seven Farms in the Windscale Area. Report No. HP/R-2636, AERE, Harwell, UK, 1958.

Paper 2/05139G
Received September 25, 1992
Accepted February 11, 1993

Estimating and Using Sampling Precision in Surveys of Trace Constituents of Soils

Michael Thompson and Michael Maguire
Department of Chemistry, Birkbeck College, Gordon House, 29 Gordon Square, London, UK WC1H 0PP

Sampling variance and analytical variance have been estimated in a survey of concentrations of trace metals in soils from public gardens in an inner London borough. Robust analysis of variance was used for this purpose and found to be appropriate. The resulting statistics were used to define criteria that identified unusual measurements for the purpose of checking or further investigation. The statistics were further used to assess the analytical and sampling protocols in respect of their fitness for the task of producing data of appropriate quality, in the light of the variation in the concentrations among the various gardens. Criteria for this latter purpose were also suggested.

Keywords: *Sampling precision; analytical precision; analysis of variance; robust statistics; soil survey*

It has become almost a *cliché* to say that sampling errors are more of a problem than analytical errors, and yet it is seldom that any attempt is made to quantify sampling errors. It is perhaps more seldom that the combined errors resulting from sampling and analysis are formally demonstrated to be of a magnitude appropriate to the task of interpreting the resulting data. This omission is surprising because the requisite information can be obtained by means of a simple experiment.[1–3] Moreover, the information on sampling and analytical errors is essential if reliable and economic decisions are to be made from the data. If the errors are too large they can obscure the information and lead to incorrect decisions. If the errors are very small, it may be that excessive effort (and therefore cost) is being put into the sampling and analytical methodology.

This paper describes a hierarchical randomized replicated experiment applied to the study of toxic metals in the soils of urban public gardens. The purpose of the experiment, apart from obtaining preliminary values for the concentrations of the metals, was the estimation of sampling and analytical errors, and their assessment in relation to the actual variation between gardens. This procedure can be seen as a preliminary method of validating sampling and analytical protocols before undertaking a wider survey, an undertaking known as an 'orientation survey' in applied geochemistry.[4] Although the immediate application of the present paper lies in the environmental field, the experimental design is suitable for a wide range of applications.

Nested analysis of variance (ANOVA) is the standard method of treating the data from such experiments. In this paper the use of a relatively new approach is advocated, namely, robust ANOVA.[3,5]

Theoretical

Classical ANOVA

Consider a single measurement (x), obtained by applying the sampling protocol once to a particular site and analysing the sample once, then

x = true value for site + sampling error + analytical error

Assuming for the moment that the sources of variation are independent, the variance of x is given by

$$\mathrm{var}(x) = \sigma^2_{\mathrm{site}} + \sigma^2_{\mathrm{sam}} + \sigma^2_{\mathrm{an}}$$

where σ^2_{site} is the variance of the true values of the sites, σ^2_{sam} is the variance of true values of random samples taken from a site (the sampling variance), and σ^2_{an} is the variance of analytical measurements performed on random test portions from a sample (the analytical variance). These three variances can be estimated from the results of an experiment with the design shown in Fig. 1, with duplicated sampling and analysis. The computations for the classical ANOVA are shown in Table 1, using the following conventions, where x_{ijk} is the kth analysis on the jth sample taken from the ith of l sites:

$$\bar{x}_{ij} = (x_{ij1} + x_{ij2})/2$$
$$\bar{x}_i = (\bar{x}_{i1} + \bar{x}_{i2})/2$$
$$\bar{x} = \Sigma_i \bar{x}_i/l$$

Estimates ($\hat{\sigma}$) of the variances are obtained by equating the expected mean square to the calculated value, *i.e.*,

$$\hat{\sigma}^2_{\mathrm{an}} = MS_{\mathrm{an}}$$
$$\hat{\sigma}^2_{\mathrm{sam}} = (MS_{\mathrm{sam}} - MS_{\mathrm{an}})/2$$
$$\hat{\sigma}^2_{\mathrm{site}} = (MS_{\mathrm{site}} - MS_{\mathrm{sam}})/4$$

Robust ANOVA

A classical estimate of a variance σ^2 is based on a sum of squares of the form $\Sigma_i(y_i - \bar{y})^2$. Such a sum can be dominated by a small proportion of discrepant values of y_i because of the squared terms. This has the unfortunate effect of unduly emphasizing the effects of unusual observations and discounting the majority of 'normal' observations. This is the antithesis of what is required in orientation surveys where the objective is to define criteria, based on normal observations, that enable the investigator to identify unusual observations in subsequent studies. An alternative approach that achieves the desired end is to use robust methods,[6] where the square function is replaced, yielding $\Sigma_i\Psi(y_i - \bar{y})$. The function Ψ is the square near zero, and the absolute value is outside the limits of $\pm k\sigma$.

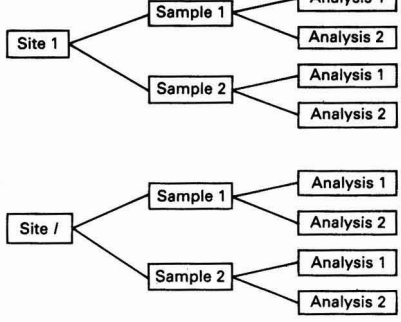

Fig. 1 Design of the hierarchical duplicated experiment executed at l sites

Table 1 ANOVA table for an experiment with duplicated sampling and analysis at l sites

Source of variation	Sum of squares	Degrees of freedom	Mean square	Expected mean square
Between sites	$4\Sigma_i(\bar{x}_i - \bar{x})^2$	$l-1$	MS_{site}	$\sigma^2_{an} + 2\sigma^2_{sam} + 4\sigma^2_{site}$
Between samples	$\Sigma_i(\bar{x}_{i1} - \bar{x}_{i2})^2$	l	MS_{sam}	$\sigma^2_{an} + 2\sigma^2_{sam}$
Within samples/between analyses	$\frac{1}{2}\Sigma_i\Sigma_j(x_{ij1} - x_{ij2})^2$	$2l$	MS_{an}	σ^2_{an}

A common choice is $k = 1.5$. The application of this method to ANOVA has been discussed in the context of interlaboratory trials,[5] and is adapted here for studies of sampling error. The method downweights the influence of outliers in the estimation of statistics, and simultaneously corrects for the downweighting.

According to a general principle stated by Rousseeuw,[7] 'outliers can easily be identified by comparing data with a robust fit'. This principle can be applied to the data obtained in orientation surveys and, with caution, to data collected in subsequent surveys. As the purpose is to enable the investigator to identify unusual observations for further study, and not to conduct tests of significance, approximate criteria suffice. Moreover, it must be remembered that no simple exact frequency distributions can be attributed to robust estimates.

Potentially anomalous sites are, therefore, a possibility when

$$|\bar{x}_i - \bar{\bar{x}}|/\sqrt{(l-1)\boldsymbol{MS}_{site}/4l} > 2$$

where $\bar{\bar{x}}$ or $\boldsymbol{MS}$ in bold typeface indicates that the statistic is obtained by the robust method.

Unusually discrepant duplicate samples are indicated when

$$|\bar{x}_{i1} - \bar{x}_{i2}|/\sqrt{\boldsymbol{MS}_{sam}} > 2$$

Possibly spurious duplicate determinations are indicated when

$$|x_{ij1} - x_{ij2}|/\sqrt{2\boldsymbol{MS}_{an}} > 2$$

Appropriate Magnitudes of Sampling Variance and Analytical Variance

Consider the variance of a mean result ($\bar{x}$) for a site, based on the collection of m samples each analysed n times. The value is

$$\text{var}(\bar{x}) = \sigma^2_{site} + (\sigma^2_{sam} + \sigma^2_{an}/n)/m$$

If we define technical variance as the total variance introduced by the methodology, *i.e.*,

$$\sigma^2_{tech} = (\sigma^2_{sam} + \sigma^2_{an}/n)/m$$

then we have

$$\text{var}(\bar{x}) = \sigma^2_{site} + \sigma^2_{tech}$$

where the magnitude of σ^2_{tech} can be adjusted by altering the values of m and n.

Normally in environmental studies, one of two possibilities is required: to discriminate among background (normal) sites or to distinguish between background and anomalous sites. Both of these requirements are jeopardized if σ^2_{tech} is relatively large. For example, if $\sigma^2_{tech} = \sigma^2_{site}$, the information in $\bar{x}$ about variation among sites would be compromised by experimental 'noise'. Accordingly, we should seek to obtain lower values of σ^2_{tech}. However, reducing its value to below about 0.1 σ^2_{site} is probably unproductive, as it has little effect on var($\bar{x}$), but almost certainly costs more to achieve than a higher value. Hence, an 'ideal' value of $\sigma^2_{tech}/\sigma^2_{site} \approx 0.3$ can be formulated.

Consider now the relative sizes of σ^2_{sam} and σ^2_{an}. Unless the survey material is almost homogeneous (rare in soil sampling), it is normally observed that $\sigma^2_{sam} > \sigma^2_{an}$. However, there is little benefit to the investigator if $\sigma^2_{sam} \gg \sigma^2_{an}$, because σ^2_{an}/n then makes little contribution to σ^2_{tech}. Again, we suggest an 'ideal' value of $\sigma^2_{an}/n\sigma^2_{sam} \approx 0.3$.

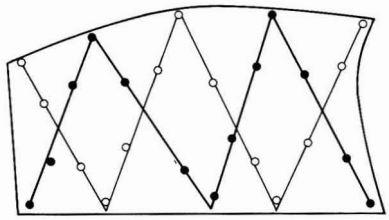

Fig. 2 Illustration of the sampling protocol applied to a roughly rectangular site, showing the first sampling walk (bold line), the duplicate sampling walk (light line) and the points where increments were collected

Experimental

Sampling Sites

Sixteen sites, consisting of grassed recreational spaces, within the London Borough of Lambeth were selected for investigation, so as to provide a reasonably even coverage of the borough. Most were small gardens typically 2000–10 000 m^2. Some were discrete plots of comparable size at the edge of large parks. While some sites had remained virtually unmodified since urbanization in the middle of the 19th century, others were sites where houses had previously been destroyed by war damage or demolition. The latter sites consisted of rubble covered with a layer of soil, possibly from a distant source. One site had been subject to remediation after an earlier industrial pollution event. All sites were, at the time of sampling, subject to varying degrees of pollution from road traffic exhaust fumes and, in the past, from coal smoke. Sites previously built upon were possibly also contaminated with paint residues.

Sampling Protocol

Duplicate samples were collected at each site. The first such sample was obtained by aggregating 13 increments, three collected on each leg of an 'M' that was walked across the site. Fig. 2 shows how this was done for a roughly rectangular site. The duplicate sample was obtained by reversing the walk, *i.e.*, with a 'W'. Each increment was collected to a depth of 5 cm with a 25 mm auger.

Mechanical Preparation

The aggregate samples were dried, broken down by light compression, passed through a 2 mm sieve to remove stones, roots, *etc.*, and reduced to a manageable bulk by dividing with a riffle. The resulting laboratory sample was ground to a fine powder (−80 mesh) and dried at 105 °C for 16 h.

Analysis

Duplicate test portions (0.250 g) of each sample were weighed into test-tubes and treated with nitric acid (70% m/m, 1.0 ml) at 100–105 °C for 1 h. The resulting mixture was diluted to 25 ml with water. Determination of cadmium, copper, lead and zinc was accomplished by flame atomic absorption spectrometry under standard conditions. Analysis was conducted

Table 2 Analytical data (μg g^{-1})

Site	Sample	Analysis	Cadmium	Copper	Lead	Zinc	Site	Sample	Analysis	Cadmium	Copper	Lead	Zinc
1	1	1	1.90	68	539	295	9	1	1	1.29	64	406	269
		2	1.30	68	511	297			2	1.94	65	406	220
	2	1	1.28	71	522	314		2	1	1.94	77	405	249
		2	1.07	64	467	307			2	1.89	76	386	250
2	1	1	3.23	159	863	1221	10	1	1	1.26	51	377	306
		2	2.34	149	825	1070			2	0.88	50	383	287
	2	1	1.54	137	809	508		2	1	1.71	48	341	685
		2	2.55	144	900	557			2	0.84	47	348	735
3	1	1	1.75	49	539	260	11	1	1	1.26	54	511	252
		2	1.04	47	482	241			2	0.63	57	537	248
	2	1	2.41	87	728	407		2	1	1.51	82	692	246
		2	1.27	85	722	419			2	1.50	79	715	408
4	1	1	2.19	67	345	242	12	1	1	1.05	51	365	242
		2	2.45	66	326	246			2	0.82	71	382	229
	2	1	3.25	72	544	420		2	1	1.27	54	356	238
		2	2.64	71	620	379			2	1.68	54	333	148
5	1	1	1.07	32	181	154	13	1	1	1.10	47	486	164
		2	1.51	36	195	149			2	1.08	49	486	168
	2	1	2.35	51	176	294		2	1	1.30	47	336	204
		2	1.55	47	177	297			2	1.05	45	329	144
6	1	1	4.51	64	271	229	14	1	1	2.87	65	281	256
		2	7.24	69	300	239			2	2.56	65	289	558
	2	1	5.24	77	327	286		2	1	2.59	49	331	206
		2	5.65	65	323	268			2	2.16	52	339	210
7	1	1	2.21	116	838	643	15	1	1	4.41	50	474	287
		2	2.86	134	815	671			2	3.84	77	488	382
	2	1	1.77	116	828	455		2	1	3.64	79	741	391
		2	1.95	122	788	462			2	4.41	81	739	401
8	1	1	1.09	97	524	178	16	1	1	1.04	80	503	284
		2	1.51	82	511	177			2	0.83	82	526	290
	2	1	0.61	58	577	183		2	1	1.06	93	630	354
		2	1.02	56	634	185			2	1.10	93	645	292

directly on the resulting solutions after the suspended matter had settled, or with dilution, as appropriate. The determinations for each element were carried out in a random order as a single analytical run.

Computing

Robust and classical estimates of the three variances were calculated by ANOVA on the unedited data in Table 2, by using a program supplied by Professor B. D. Ripley, Department of Statistics, University of Oxford.

Results and Discussion

Results

The raw results of the study are presented in Table 2, and the statistics in Table 3. It is of interest to note that the mean concentrations (in μg g^{-1}) fall well below the levels recommended by the Department of the Environment as maxima for land to be used for parks and playing fields,[8] namely, Cd 15, Cu 1000, Pb 2000, and Zn 1000. The same comment applies to nearly all individual samples also.

Applicability of Robust Statistics

The results of robust and classical ANOVA can be compared in Table 3. No substantial difference between the respective pairs of estimates is evident in the instance of lead. Zinc, however, displays a different behaviour, with the robust estimates considerably smaller than the classical. It is interesting to analyse the differences.

Table 3 Statistics obtained by robust and classical ANOVA (μg g^{-1})

Analyte	Method	$\bar{x}$	$\hat{\sigma}_{an}$	$\hat{\sigma}_{sam}$	$\hat{\sigma}_{site}$
Cd	Robust	1.81	0.45	0.21	0.74
	Classical	2.05	0.52	0.00	1.24
Cu	Robust	67.5	3.3	10.5	14.3
	Classical	72.8	5.8	11.0	25.7
Pb	Robust	489	18.7	86.0	169.5
	Classical	496	22.8	88.7	172.0
Zn	Robust	310	22.2	107.3	78.9
	Classical	341	48.5	147.5	130.4

For $\hat{\sigma}_{an}$ the classical and robust estimates are 48.5 and 22.2, respectively. The difference is almost entirely accounted for by a few discrepant analytical duplicates (absolute differences of 90, 95, 162, 194 and 302 μg g^{-1}). These discrepancies greatly exceed those for any of the remaining 27 duplicate pairs (Fig. 3) and are readily identified as exceeding the criterion of 63 μg g^{-1} derived from MS_{an}. No immediate explanation for the discrepancies is apparent, but once they are identified, the results can be checked by re-analysis. Use of a criterion based on classical statistics (137 μg g^{-1}) would fail to identify the lower discrepant duplicates, so the robust value is preferred.

For $\hat{\sigma}_{sam}$ the difference between the estimates can be attributed largely to two occurrences of discrepant duplicate samples, yielding mean absolute differences of 413 and 591 μg g^{-1}. These values are easily visible in Fig. 4 and are identified by exceeding the criterion of 307 μg g^{-1} derived from MS_{sam}. In these instances, there is no doubt that the duplicate samples are genuinely different. Large sampling

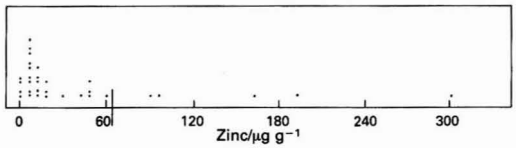

Fig. 3 Absolute differences between analytical duplicates $|x_{ij1} - x_{ij2}|$ for zinc. The robust criterion for unusually high values $2\sqrt{2MS_{an}}$ is also shown as a vertical bar

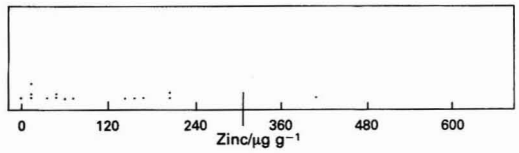

Fig. 4 Absolute differences between duplicate sample means $|\bar{x}_{i1} - \bar{x}_{i2}|$ for zinc. The robust criterion for unusually high values $2\sqrt{MS_{sam}}$ is also shown as a vertical bar

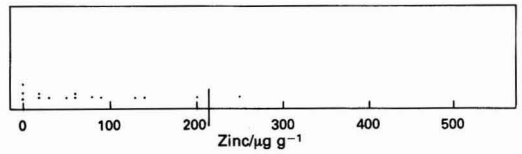

Fig. 5 Absolute deviations of the site means from the robust grand mean $|\bar{x}_i - \bar{\bar{x}}|$ for zinc. The robust criterion for unusually high values $\sqrt{(15MS_{site})}/4$ is also shown as a vertical bar

variations are often observed at polluted sites, because, in general, contamination is unlikely to be uniform. This is particularly true for zinc where contamination of soil from corroded galvanized objects would be very localized. In fact, both of the sites that gave rise to discrepant samples have anomalously high average zinc contents. Moreover, one of these samples gave rise to a suspect analytical duplicate, which is thereby, explained (higher analytical variability is expected at higher concentrations).

Again, for the orientation survey, the variation within the background sites is of primary concern, so the robust estimate is preferred, as the sites with higher sampling discrepancies are from anomalous sites. Moreover, a criterion based on the classical mean square (428 μg g^{-1}) fails to identify one of the suspect samples.

The use of the robust estimate also helps to maintain independence between the sources of variation. At an anomalously high (polluted) site, the sampling and analytical variances are almost certain to be considerably higher than at background sites. The use of the robust estimate removes this type of dependence.

For $\hat{\sigma}^2_{site}$ the difference between the robust and the classical estimates is explained by the influence of two sites identified as anomalous by the criterion based on MS_{site}, with mean concentrations of 829 and 558 μg g^{-1} (Fig. 5). As the purpose of an extended survey would be to characterize the variation among the background sites and thereby identify sites that do not conform to the general picture, the use of the robust statistic is justified. The criterion based on classical estimation is higher and less likely to identify anomalous sites.

Observations similar to the above apply to the results for cadmium and copper.

Suitability of Sampling and Analytical Protocols

The robust variance estimates are presented in Table 4, together with the ratios $\hat{\sigma}^2_{an}/\hat{\sigma}^2_{sam}$ and $\hat{\sigma}^2_{tech}/\hat{\sigma}^2_{site}$, calculated for single samples at each site and single determinations on each sample ($n = m = 1$). Only the statistics for lead fulfil the previously derived criteria, *i.e.*, the two ratios below the 'ideal' value of 0.3.

Table 4 Variances and variance ratios obtained by robust ANOVA (basic unit: μg g^{-1})

Analyte	$\hat{\sigma}^2_{an}$	$\hat{\sigma}^2_{sam}$	$\hat{\sigma}^2_{site}$	$\hat{\sigma}^2_{an}/\hat{\sigma}^2_{sam}$	$\hat{\sigma}^2_{tech}/\hat{\sigma}^2_{site}$
Cd	0.202	0.044	0.548	4.6	0.45
Cu	10.9	110	204	0.1	0.59
Pb	350	7396	28651	0.05	0.27
Zn	493	11513	6225	0.04	1.93

The results for cadmium show that the analysis is unduly variable compared with sampling. This is because the analytical method was being used at a concentration of cadmium not greatly above its detection limit. The only means by which the data quality could be significantly improved would be by using a different analytical method. Analytical replication ($n > 1$) would not help here unless an unacceptable number of replicates were performed.

For copper and zinc, the analytical precision is satisfactory, but the sampling precision falls short of requirements. For copper, the situation could be alleviated by duplicate sampling ($m = 2$, $n = 1$) or by the equivalent method of preparing the aggregate sample by combining twice the number of increments given in the original protocol. This strategy would make $\hat{\sigma}^2_{an}/n\hat{\sigma}^2_{sam} = 0.2$ and $\hat{\sigma}^2_{tech}/\hat{\sigma}^2_{site} = 0.3$. For zinc, the situation could be remedied only by greatly increasing the number of increments that are aggregated, or perhaps by redefining the nature or size of the sampling targets.

Conclusions

The results of this study show that an orientation survey consisting of a hierarchical replicated experiment followed by robust ANOVA provided valuable information on the magnitude of sampling and analytical errors and also on the concentrations of the analytes. Knowledge of the robust mean squares allowed unusual measurements to be identified for checking or further investigation more certainly than did their classical counterparts. Moreover, the results provided a direct means of establishing whether the sampling and analytical protocols were satisfactory for the application. In instances where sampling precision was found to be unsatisfactory, a remedial strategy was immediately apparent.

It is also noteworthy that the sampling precision (in terms of relative standard deviation) was greater for zinc than for the other analytes. This serves to emphasize that the sampling protocol could need to be validated separately for each analyte.

References

1 Meisch, A. T., in *Computers in the Mineral Industry. Part 1*, ed. Parks, G. A., Stanford University Publications in Geological Science, 1964, vol. 9, pp. 156–170.
2 Garrett, R. G., in *Statistics and Data Analysis in Geochemical Prospecting*, ed. Howarth, R. J., Elsevier, Amsterdam, 1983, pp. 83–107.
3 Ramsey, M. H., Thompson, M., and Hale, M., *J. Geochem. Explor.*, 1992, **44**, 23.
4 Rose, A. W., Hawkes, H. E., and Webb, J. S., *Geochemistry in Mineral Exploration*, Elsevier, Amsterdam, 1979, pp. 34–35, 320–329.
5 Analytical Methods Committee, *Analyst*, 1989, **114**, 1699.
6 Huber, P., *Robust Statistics*, Wiley, New York, 1981.
7 Rousseeuw, P. J., *J. Chemometr.*, 1991, **5**, 1.
8 *Problems Arising from the Redevelopment of Gas Works and Similar Sites*, Department of the Environment, London, 2nd edn., 1986.

Paper 3/01533E
Received March 17, 1993
Accepted April 21, 1993

Spectroscopic Probes for Hydrogen Bonding, Extraction Impregnation and Reaction in Supercritical Fluids*

Andrew I. Cooper, Steven M. Howdle,† Catherine Hughes, Margaret Jobling, Sergei G. Kazarian,‡ Martyn Poliakoff† and Lindsey A. Shepherd
Department of Chemistry, University of Nottingham, Nottingham, UK NG7 2RD
Keith P. Johnston
Department of Chemical Engineering, University of Texas, Austin, TX 78712, USA

Spectroscopy is used for monitoring a number of processes relevant to solution, extraction and impregnation in supercritical CO_2 ($scCO_2$). Examples include: a combined infrared (IR) and ultraviolet study of the interaction between *para*-hydroquinone (HQ) and tributyl phosphate in $scCO_2$, which reveals hydrogen bonding, detected by the characteristic ν(O–H) IR bands; IR measurement of the solubility of $CpMn(CO)_3$ (Cp = η^5–C_5H_5) in $scCO_2$ as a function of temperature and pressure; an investigation of the uniformity of supercritical impregnation of $CpMn(CO)_3$ into 4 mm diameter pellets of polyethylene (PE) using Fourier-transform infrared (FTIR) microscopy and FTIR depth profiling by photoacoustic detection; and an IR study of the photochemical reaction of $CpMn(CO)_3$ with N_2 with PE film.

Keywords: *Supercritical fluid; hydrogen bonding; impregnation; polyethylene; photochemical reaction*

The role of supercritical fluids in analytical chemistry is the focus of increasing interest not only because of the inherent potential of supercritical fluids[1–3] themselves but also because they represent an environmentally more acceptable alternative to many of the solvents currently in use in the analytical laboratory. Most of the work in this area has concentrated, quite rightly, on applications of supercritical fluids, particularly in the areas of extraction and use of modifiers to enhance the solubility of individual solutes.[2] By contrast, there has been relatively little development of spectroscopic techniques to probe and monitor these processes *in situ*.

It is the purpose of this paper to describe new applications of infrared (IR) spectroscopy to a range of problems associated with the use of supercritical fluids in an analytical context. These applications have largely evolved from the study of chemical reactions in supercritical fluids at Nottingham,[4–8] which required, *inter alia*, the development of versatile IR and ultraviolet (UV) cells for monitoring the progress of the reactions.[9–11] Our results are divided into three sections: (*i*) a combined IR and UV study to establish the role of hydrogen bonding in the action of tributyl phosphate (TBP) as a modifier for the solubilization of hydroquinone in supercritical CO_2 ($scCO_2$); (*ii*) the use of IR techniques for monitoring the impregnation and extraction of organometallic compounds from polyethylene (PE); and (*iii*) a study of photochemical reactions of organometallics within polymers to explore the potential of these compounds for *in situ* derivatization and spectroscopic labelling of polymer additives.

Experimental

Spectroscopy

The UV spectra were obtained on a Perkin-Elmer Lambda 5 spectrometer with Epson data station. Transmission IR spectra were recorded on a Nicolet Model 730 interferometer and 680D data system (16K data collection, 32K transform points, 2 cm^{-1} resolution). Fourier-transform infrared (FTIR) microscopy was carried out at 8 cm^{-1} resolution with a NicPlan IR microscope with SpectraTech automatic translation stage, using a Nicolet Model 730 interferometer. Photoacoustic measurements were made at 8 cm^{-1} on a Bio-Rad Model 896 step-scan FTIR interferometer equipped with a demodulator accessory for phase modulation experiments and fitted with an MTEC photoacoustic detector.

Materials

The following reagents were all used without further purification: $CpMn(CO)_3$ (Cp = η^5-C_5H_5) (Strem), TBP (BDH), *para*-hydroquinone (HQ; BDH), CO_2 (Air Products SFC grade), N_2 (Air Products) and low density PE pellets (BP Research) were used without further purification. The PE film was formed from powdered, low-density PE (Aldrich) using a constant thickness melt press Specac (Model 15620).[12] Supercritical impregnation was carried out as described in detail elsewhere,[11,12] by immersing PE pellets overnight in a near-saturated solution of $CpMn(CO)_3$ in $scCO_2$ at about 40 °C and 2000 psi pressure (145 psi ≈ 1 MPa) with a modified Nupro TF Series in-line filter, 5 μm pore size, as the pressure vessel.[12] Pellets were sectioned with a Leitz sledge microtome.

Results and Discussion

Hydrogen Bonding

Hydrogen bonding has been intensively studied for many years and the process is well understood in both gas and condensed phases.[13] Supercritical fluids offer the unique opportunity to observe the effect on hydrogen bonding of varying the density of the medium without altering the concentrations of either proton donor or acceptor.[14,15] More importantly, hydrogen bonding appears to be a major factor in the action of many, if not the majority, of the modifiers currently used to enhance the solubility of particular components in supercritical extraction. A better understanding of hydrogen bonding in supercritical fluids should, therefore, lead eventually to a more rational approach to the design and choice of modifiers for individual applications.

There have been a number of studies of supercritical hydrogen bonding,[14,15] particularly by Yee *et al.*[14] The usual approach has been to use IR spectroscopy to detect the characteristic shift in the ν(O–H) vibration of the proton

* Based on a lecture presented at the Current and Future Applications of Supercritical Fluid Extraction meeting of the Western Region of the Analytical Division of The Royal Society of Chemistry, Cardiff, UK, October 2, 1992.

† To whom correspondence should be addressed.

‡ Permanent address: Institute of Spectroscopy, Russian Academy of Sciences, 142092 Troitzk, Moscow Region, Russia.

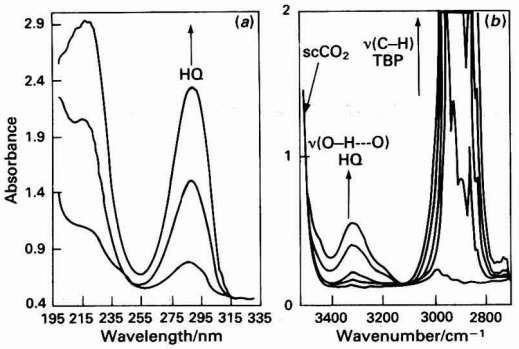

Fig. 1 (*a*) UV and (*b*) IR absorption spectra showing the effect of increasing amounts of TBP on the solubility of HQ in $scCO_2$. The IR spectra cover the ν(C–H) region of TBP itself and the ν(O–H) bands of the hydrogen-bonded HQ–TPB complex. Each trace (UV or IR) was recorded with a separate solution with a different concentration of TBP but the IR and UV spectra for the same concentration of TBP were recorded from the same solution in the same cell (2 ml volume and optical pathlength 5 mm). In each case, a measured amount of TBP was syringed into the cell, containing excess solid HQ. The cell was then pressurized with $scCO_2$ to 3700 psi (≙ 25 MPa). The traces in the UV spectra (*a*) correspond to additions of 4, 14 and 24 μl of TBP and those in the IR spectra (*b*) to 0, 4, 14, 24 and 34 μl of TBP

donor, which occurs on formation of a hydrogen bond. One problem is that, in $scCO_2$, the absorptions of the $scCO_2$ itself obscure the ν(O–H) bands of the free proton donor or, with deuteriated donors, the ν(O–D) of the D-bonded complex.[14] Clearly, this limitation can be overcome by switching to fluids that do not absorb in this region of the spectrum (*e.g.*, C_2H_6[14] or SF_6[15,16]) but this option is not open if the aim is to study bonding in $scCO_2$ under realistic analytical conditions. Here, we illustrate a different approach, the combined use of UV and IR spectroscopy.

Tributyl phosphate is well known for its use in a wide range of extraction processes in conventional solvents and for its ability to form hydrogen bonds.[17] Recently, Lemert and Johnston[18] reported how TBP could be used as a far more effective modifier than CH_3OH in $scCO_2$ to increase the solubility of HQ by over two orders of magnitude. *para*-Hydroquinone has a higher melting point and lower vapour pressure than the *ortho*-isomer; the consequence of intermolecular hydrogen bonding. It was, therefore, postulated[18] that the effect of TBP as a modifier is to hydrogen bond to the OH groups of HQ. This proposition has now been tested spectroscopically. The strategy has been to use UV absorption to detect the total amount of HQ in solution and IR spectroscopy not only to establish the amount of TBP in solution but also to detect the presence of hydrogen bonding *via* the shifted ν(O–H) bands.

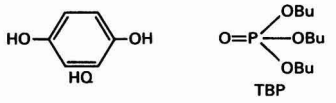

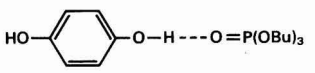

1

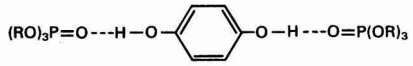

2

Fig. 1 shows the IR and UV spectra of a series of solutions in $scCO_2$ containing increasing amounts of TBP and in each case saturated with HQ. The UV spectra, [Fig. 1(*a*)], clearly confirm that the concentration of HQ in $scCO_2$ increases with an increasing concentration of TBP. At the same time the IR spectra, [Fig. 1(*b*)] indicate increasing concentrations of hydrogen-bonded species in solution, thus supporting the postulation that, in this case, the role of TBP involves hydrogen bonding. Unfortunately, IR is not a precise enough technique to distinguish easily between the bands caused by hydrogen bonding to one or to both of the OH groups in HQ, *i.e.*, structures **1** and **2**, or indeed to identify species containing more than one molecule of HQ. However, mathematical modelling[18] of the effects of TBP on the solubility of HQ favoured the formation of an $HQ{\cdot}(TBP)_2$ adduct (**2**). Currently, we are applying similar techniques to simpler systems to quantify the role of the supercritical solvent in hydrogen bonding,[16] using $(CF_3)_3COH$ as the proton donor; $(CF_3)_3COH$ has the advantage that it does not self-associate to any significant extent, thus simplifying the systems even further.

Impregnation of Polymers

In a supercritical extraction experiment, it is usually much easier to measure the amount of material, extracted into the fluid, which is initially 'clean', than it is to measure the amount of guest material remaining in the host matrix. Impregnation is the inverse of extraction and the converse is true of the ease of measurement. In impregnation experiments, it is much easier to measure spectroscopically how much material has penetrated the host matrix because, at the start of the experiment, the host matrix does not normally contain any of the guest material to be impregnated.

Transition metal carbonyl compounds are particularly suited to impregnation experiments. They are relatively volatile, strongly hydrophobic compounds with very intense IR absorptions, due to ν(C–O) vibrations, the wavenumbers of which are highly sensitive to the environment.[11] Thus it is possible to distinguish spectroscopically between a compound dissolved in $scCO_2$ and the same compound impregnated into PE. The way in which this property can be exploited for monitoring the impregnation and extraction of $CpMn(CO)_3$ in thin <500 μm PE film has recently been described.[11] In this paper, the work is concentrated on investigating more bulky samples, specifically, near spherical pellets about 4 mm in diameter. Such pellets are of considerable relevance to current models of supercritical extraction, including the Leeds 'Hot-Ball' model.[19,20]

Briefly, the impregnation experiment[11,12] involves immersing the polymer pellet in a solution of $CpMn(CO)_3$ in $scCO_2$. Impregnation is allowed to occur, the pressure is vented and the pellet removed. This study has had two aims: (*i*) to establish the uniformity of the impregnation of the pellets; and (*ii*) to investigate the solid residue left on the surface of the polymer, when the supercritical solution is depressurized. There have been relatively few studies[21] on the solubility of carbonyl compounds in $scCO_2$ and no data were available for $CpMn(CO)_3$. Therefore, a brief study of solubility as a function of temperature and pressure using the circulating system illustrated in Fig. 2 was carried out, by monitoring the concentration of dissolved $CpMn(CO)_3$ by FTIR.

The results are summarized in Fig. 3. Like other solutes,[1] the solubility of $CpMn(CO)_3$ in $scCO_2$ increases sharply with pressure and decreases with temperature at a constant pressure under the conditions used. Thus, although impregnation would be expected to proceed more effectively at higher temperatures, the concentration of $CpMn(CO)_3$ in supercritical solution will be lower if the pressure is not increased. In the present experiments, therefore, a temperature close to the critical point of CO_2 was used.

Once the pellet is impregnated, the strategy has been to microtome thin sections from the pellet and then to scan the section using an IR microscope with a 100 μm spot-size to measure the distribution of the impregnated carbonyl compound. Fig. 4 shows the result of one such scan across the diameter of a section, which indicates that the impregnation is remarkably uniform. Although, the concentration of $CpMn(CO)_3$ is higher close to the outside of the pellet, overall it varies by less than 30%. Two dimensional scans, such as that illustrated in Fig. 5, provide very similar results and the high symmetry of the contours in Fig. 6 suggest that sectioning of the pellet with the microtome causes minimal distortion of the pellet and has little effect on the distribution of $CpMn(CO)_3$.

As the overall procedure (impregnation, sectioning, spectroscopy) was relatively drawn out, these results do not show the distribution of $CpMn(CO)_3$ within the pellet at the moment immediately following the end of impregnation. Recent experiments in our laboratory[22] have suggested that molecules the size of $CpMn(CO)_3$ are relatively mobile, at least over short distances, in PE at room temperature over a period of minutes. Nevertheless, the fact that the present experiments revealed a slightly higher concentration of $CpMn(CO)_3$ close to the outside of the pellet suggests that bulk diffusion of $CpMn(CO)_3$ within the PE must be slow on the timescale of the experiment (*i.e.*, over a period of days).

Experiments with finely powdered KBr have shown[11] that $CpMn(CO)_3$ deposited from $scCO_2$ solution onto the surface has an IR spectrum with relatively sharp ν(C–O) bands, a spectrum quite distinct from the very broad bands normally observed with bulk solid $CpMn(CO)_3$, possibly due to the amorphous nature of the deposited material. Although the IR spectrum of this deposited $CpMn(CO)_3$ is also significantly different from that of the compound impregnated into PE, it is a challenging task to use IR spectroscopy for the characterization of the deposits of $CpMn(CO)_3$ on the surface of the 4 mm PE pellets. Direct transmission spectroscopy is not practic-

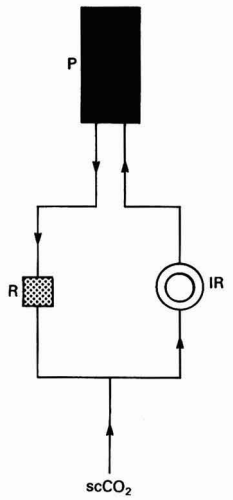

Fig. 2 Schematic diagram of the system used for monitoring the solubility of $CpMn(CO)_3$ in $scCO_2$. The components are marked as follows; P, Micropump Model 180SC ultrahigh pressure circulating pump; IR, cell of 1 mm pathlength for IR detection of $CpMn(CO)_3$; and R, Nupro in-line filter to act as a reservoir for solid $CpMn(CO)_3$. All components, except the cell, were placed in a heated box; the cell itself and connecting pipework were heated with heating tape. Additional $scCO_2$ was added as appropriate from a Lee Scientific Model 501 syringe pump. The whole system was allowed to equilibrate for 30–40 min before each measurement

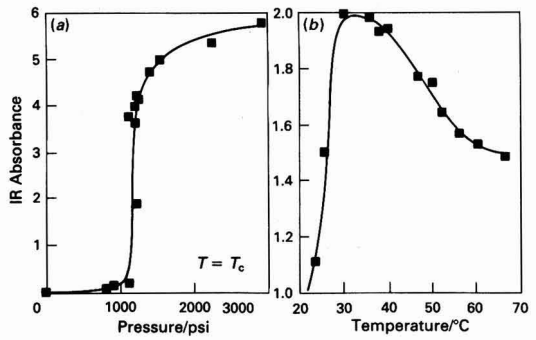

Fig. 3 IR spectra obtained with the apparatus illustrated in Fig. 2, showing the qualitative effects of (*a*) pressure and (*b*) temperature on the solubility of $CpMn(CO)_3$ in $scCO_2$. (*a*) Effect of pressure at 32 °C. The ordinate scale refers to the absorbance of the a_1 ν(C–O) band of $CpMn(CO)_3$ and the maximum absorbance value, about 6, corresponds to an approximate concentration of 2×10^{-2} mol l^{-1}. (*b*) Effect of temperature at a constant pressure of 2000 psi (≏ 13.8 MPa). Note that in (*a*), the data are presented as if IR absorbance can be measured accurately to a value of >6. In reality, these high absorbance values were obtained by a two stage process: (*i*) while the ν(C–O) bands were in the absorbance range 2–3, the absorbance values were measured for the first overtone and combination bands about 4000 cm^{-1}, which are inherently much weaker than the fundamental vibrations, and their intensities relative to the fundamental bands were established; (*ii*) when the intensity of the ν(C–O) bands exceeded an absorbance of 3, the absorbance values of the overtones could be used to calculate the 'absorbance' of the fundamental bands

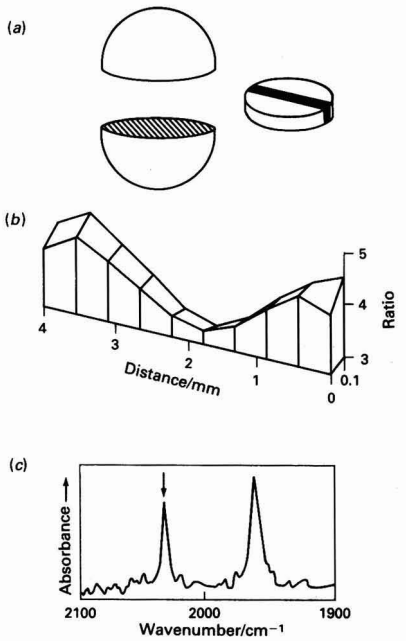

Fig. 4 Results of the FTIR microscopic investigation (100 μm spot size) to establish the distribution of $CpMn(CO)_3$, impregnated into a PE pellet. (*a*) Schematic view of the pellet showing a section (about 50 μm thick) and the path scanned across it by the FTIR microscope. (*b*) Computer-generated display of the distribution of $CpMn(CO)_3$ across the pellet. The ordinate axis shows the ratio of the absorbance the a_1 band of $CpMn(CO)_3$ to the absorbance of a weak band of PE itself (2017 cm^{-1}). By using the ratio of bands rather than the absorbance, any effects that might be caused by non-uniformity in the thickness of the section can be eliminated. (*c*) A spectrum showing the ν(C–O) bands of impregnated $CpMn(CO)_3$ with the a_1 mode arrowed and absorptions of PE removed

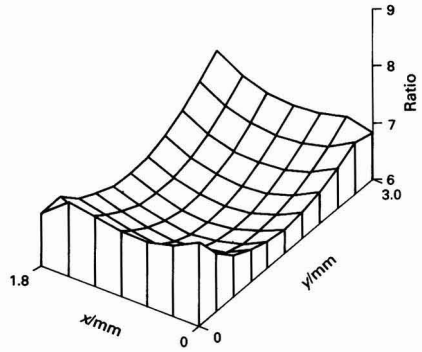

Fig. 5 Two-dimensional FTIR microscope scan of a microtomed section obtained by exactly the same method as that described for Fig. 4

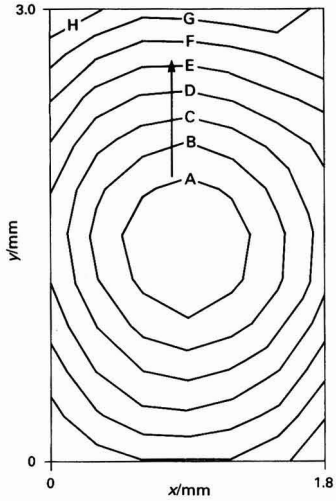

Fig. 6 FTIR contour plot corresponding to the data illustrated in a perspective view in Fig. 5. The contours give the values of the absorbance ratio (as defined in Fig. 4), which increase in the direction of the arrow and are plotted from (A) 6.3 to (G) 8.1, at intervals of 0.3. Note in particular, that the contours are essentially circular. If the microtome were distorting the pellet severely during sectioning, one would expect a corresponding distortion of the contours

able, because the thickness of the surface layer is undoubtedly small compared with the dimensions of the pellet. Equally, the layer is thin compared with the diameter of the spot viewed through the IR microscope. Although diffuse reflectance infrared Fourier-transform spectroscopy (DRIFTS) has been highly successful in making such measurements on impregnated PE powder,[11] we have found DRIFTS difficult to use with these pellets because the surface gives rise to sufficient specular reflection to degrade the spectrum.

The solution to these problems has been to use FTIR with photoacoustic detection, because this technique has a relatively shallow penetration depth and, furthermore, offers the possibility of depth profiling.[23–28] Photoacoustic detectors rely on absorption of IR radiation by the sample to heat a carrier gas, causing a pressure rise which is detected with a sensitive microphone. Depth profiling of a sample can be achieved in two ways, by varying the scan velocity or by so-called 'step' scanning.

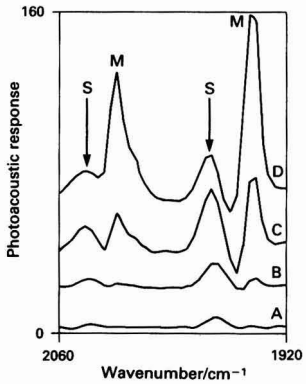

Fig. 7 FTIR photoacoustic depth profiling of an intact impregnated PE pellet by means of interferometer mirror velocity. In this case, mirror velocity is defined by the frequency at which the data points are recorded. Spectrum A was obtained with the highest frequency, 20 kHz, corresponding to the shallowest depth of sampling. The other spectra were recorded at: B, 800 Hz; C, 200 Hz; and D, 50 Hz, corresponding to increasing depths of penetration. The bands are labelled as follows: S, surface deposited solid $CpMn(CO)_3$; M, molecular $CpMn(CO)_3$, impregnated into the bulk of the solid PE. Note that this particular sample was washed with heptane prior to recording the spectrum in an attempt to reduce the thickness of the surface layer. Given the restricted wavenumber region of the spectra, the 'photoacoustic response' of the ordinate scale of the spectra can be reasonably equated to absorbance.

Altering the mirror velocity of the FTIR interferometer alters the modulation frequency of the IR radiation incident on the sample. In general, the more rapid the modulation, the shallower the depth of sample from which the photoacoustic signal can originate; fast mirror velocities yield information only from the surface region, whereas lower velocities provide the sum of the spectra from the surface and from the layers beneath it.[23–25] Fig. 7 shows a set of photoacoustic spectra of an impregnated pellet, recorded with different mirror velocities. These spectra confirm the existence of the surface layer but not its thickness. There is a clear transition from the bands of solid $CpMn(CO)_3$, arrowed, to the superimposed spectra of solid and impregnated $CpMn(CO)_3$ as the mirror velocity is reduced.

Step-scanning is a relatively new feature in commercial FTIR instrumentation.[26–28] Although the detailed mechanics of the process are intricate,[26–28] the principle of operation is straightforward.

In a conventional interferometer, the IR signal is not measured continuously but at regularly spaced points along the path of the moving mirror, points determined by the calibrating He/Ne laser. In a step-scan instrument, the moving mirror appears to spend a relatively long time stationary at one measurement position and then jumps almost instantaneously to the next position.[26–28] This behaviour permits additional modulation of the IR beam at a frequency that is fast compared with the time spent by the mirror at each measurement point. When this double modulation is applied to photoacoustic experiments, the detector can be linked to a phase-sensitive amplifier and, as described elsewhere,[26–28] varying the phase of detection relative to the phase of modulation allows spectra to be obtained from different depths within the sample, the larger the phase angle the greater the depth. Fig. 8 illustrates the effect of varying the phase angle in phase modulated photoacoustic spectra of a PE pellet impregnated with $CpMn(CO)_3$. The spectra show a good transition from the spectrum of pure solid $CpMn(CO)_3$ to that of pure impregnated $CpMn(CO)_3$, in a manner that the spectra in Fig. 7 do not. However, the technique does not have

an inherent scale of depth so, again, the precise thickness of the surface layer (probably only a few μm) cannot be established from these spectra. It is therefore, clear that step-scan photoacoustic measurements of this type have considerable promise for probing such samples but without extensive calibration the results are only semi-quantitative.

Photochemical Reactions Within the Polymer

Currently, there is considerable interest in the use of supercritical fluid extraction (SFE) for identification and quantification of polymer additives.[2,29] Unfortunately, some classes of additives, *e.g.*, those with amine functions, are often almost insoluble in $scCO_2$ because of reaction with the CO_2 itself.[1] However, transition metal carbonyl complexes, *e.g.*, $CpMn(CO)_3$, undergo facile photochemical reactions with many such compounds.[30] Work is currently underway to explore the feasibility of using carbonyl complexes for reactive extraction of additives, exploiting the carbonyl not only to sequester the reactive functional group of the additive but also to provide an excellent spectroscopic label. Carbonyl compounds have intense absorptions in both IR and UV and, therefore, should greatly increase the sensitivity of spectroscopic detection of the complexed additives. For example, $(C_6H_3Me_3)Cr(CO)_3$ has an injected minimum detectable quantity of only 20 pg for capillary supercritical fluid chromatography–FTIR.[31]

As the first step in this investigation, the photochemical reactions of carbonyl compounds in pure PE film were examined. Fig. 9 shows spectra obtained during and after the UV irradiation of $CpMn(CO)_3$, previously impregnated into low-density PE film, under a high pressure of N_2 gas, as the added reactant. It can be seen that there are in fact two products, not only the expected dinitrogen complex[32] $CpMn(CO)_2N_2$ but also a complex formed by coordination of the $CpMn(CO)_2$ moiety to the pendant olefinic C=C bonds, which occur at random intervals down the polymer chain.[2,33] This olefinic product can also be formed in the absence of N_2 and appears not to be easily extractable from the polymer by subsequent SFE with $scCO_2$. There are two reasons why this experiment is of relevance to reactive extraction. Firstly, it demonstrates that there is sufficient mobility within the polymer matrix for photochemical reactions of $CpMn(CO)_3$ to occur. Secondly, it shows that, although reaction between carbonyl and polymer would clearly consume some of the carbonyl compound, such products will be unextractable so may well not interfere with the overall SFE process.

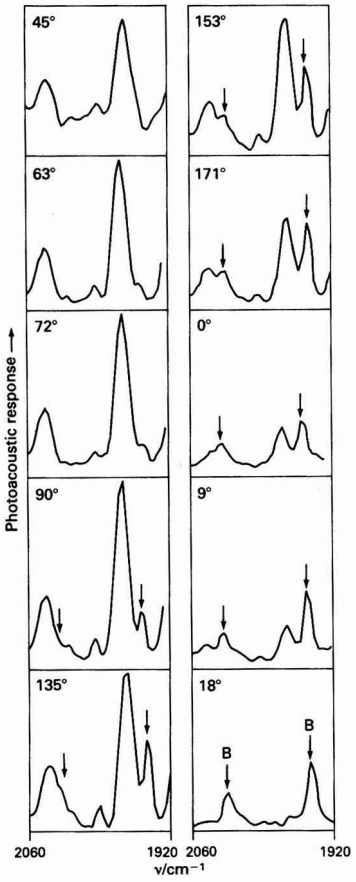

Fig. 8 FTIR photoacoustic depth profiling of an intact impregnated PE pellet using step-scan phase modulation. Spectra were recorded as the phase angle was varied from 0° to 180° in steps of 9° and a representative set of spectra are shown. From 45° to about 90° the bands in the spectra are those of solid $CpMn(CO)_3$ and from 90° the arrowed bands of $CpMn(CO)_3$ impregnated into the bulk of the PE gradually increase so that by 18° all trace of the surface bands have disappeared. In principle, the surface species might be expected to appear at a phase angle of 0 ° but the nature of the equipment appears to generate a phase shift of about 45 °. As in Fig. 7, 'photoacoustic response' can be reasonably equated to absorbance

Conclusions

The experiments described in this paper have shown the IR and, to a lesser extent, UV spectroscopy can provide valuable *in situ* monitoring of processes of importance to the exploitation of supercritical fluids in analytical chemistry. Transition metal carbonyl complexes, a range of compounds not normally associated with this area of chemistry, have the

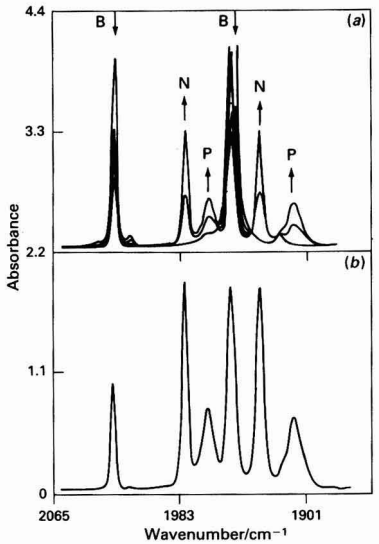

Fig. 9 IR spectra illustrating the photochemical reaction of $CpMn(CO)_3$ with N_2 in low density PE film, 500 μm thickness. The film was first impregnated with $CpMn(CO)_3$ at 3000 psi (≙ 20.7 MPa). The CO_2 was vented, excess solid $CpMn(CO)_3$ removed and the cell refilled with N_2 at 3000 psi. (*a*) Spectra recorded over a 60 min period of UV irradiation, showing the decay of the bands, B, of impregnated $CpMn(CO)_3$ and the growth of bands N, of $CpMn(CO)_2(N_2)$ and P, of $CpMn(CO)_2(\eta^2$-polymer)

spectroscopic properties needed for probing the impregnation and extraction of polymers. Supercritical fluid extraction is still a largely empirical technique. We believe that, in the near future, spectroscopic investigations will provide a new approach for studying supercritical extraction, an approach which will complement the methods in use today and will help to reach a better understanding of SFE.

We thank SERC (Grant No. GR/G0823), the Royal Society, the Nuffield Foundation, Nicolet Instruments Ltd. and BP International Ltd. for support. We are particularly grateful to Dr. S. F. Parker and Dr. C. Baker for their help with the FTIR microscopy and Dr. A. Grady for his assistance with the photoacoustic measurements. We thank Dr. I. G. Anderson, J. A. Banister, Dr. G. Davidson, J. G. Gamble, Dr. T. J. Jenkins, Dr. M. A. Healy, T. Lynch, K. Stanley and Professor J. J. Turner for their help and advice.

References

1 McHugh, M. A., and Krukonis, V. J., *Supercritical Fluid Extraction*, Butterworth, Boston, 1986.
2 *Analytical Supercritical Chromatography and Extraction*, eds. Lee, M. L., and Markides, K. E., Chromatography Conferences, Provo, UT, 1990.
3 Vigdergauz, M. S., Lobachev, A. L., Lobacheva, I. V., and Platonov, I. A., *Russian Chem. Rev.*, 1992, **61**, 267.
4 Howdle, S. M., and Poliakoff, M., *J. Chem. Soc. Chem. Commun.*, 1989, 1099.
5 Howdle, S. M., Grebenik, P., Perutz, R. N., and Poliakoff, M., *J. Chem. Soc. Chem. Commun.*, 1989, 1517.
6 Howdle, S. M., Poliakoff, M., and Healy, M. A., *J. Am. Chem. Soc.*, 1990, **112**, 4804.
7 Jobling, M., Howdle, S. M., Healy, M. A., and Poliakoff, M., *J. Chem. Soc., Chem. Commun.*, 1990, 1278.
8 Howdle, S. M., Jobling, M., George, M. W., and Poliakoff, M., *Proceedings of the Second International Symposium on Supercritical Fluids (Boston)*, ed. McHugh, M. A., Johns Hopkins University, MD, 1991, p. 189.
9 Poliakoff, M., Howdle, S. M., Healy, M. A., and Whalley, J. M., *Proceedings of the International Symposium on Supercritical Fluids*, ed. Perrut, M., Societé Franc. de Chimie, 1988, p. 967.
10 Howdle, S. M., Jobling, M., and Poliakoff, M., *Supercritical Fluid Technology; Theoretical and Applied Approaches in Analytical Chemistry*, eds. Bright, F. V., and McNally, M. E., *ACS Symposium Series*, 1992, **488**, 121.
11 Cooper, A. I., Howdle, S. M., and Ramsay, J. M., *J. Polymer Sci. Polymer Phys.*, in the press.
12 Jobling, M., Ph.D. Thesis, University of Nottingham, UK, 1992.
13 *The Hydrogen Bond—Recent Developments in Theory and Experiment*, eds. Schuster, P., Zundel, G., and Sandorfy, C., North Holland, Amsterdam, 1976.
14 Yee, G. G., Fulton, J. L., and Smith, R. D., *J. Phys. Chem.*, 1992, **96**, 6172, and references therein.
15 Gupta, R. B., Combes, J. E., and Johnston, K. P., *J. Phys. Chem.*, 1993, **97**, 707.
16 Kazarian, S. G., Gupta, R. B., Johnston, K. P., and Poliakoff, M., unpublished work.
17 Ferraro, J. R., and Peppard, D. F., *J. Phys. Chem.*, 1961, **65**, 539.
18 Lemert, R. M., and Johnston, K. P., *Ind. Eng. Chem. Res.*, 1991, **30**, 1222.
19 Bartle, K. D., Boddington, T., Clifford, A. A., Cotton, N. J., and Dowle, C. J., *Anal. Chem.*, 1991, **63**, 2371.
20 Bartle, K. D., Clifford, A. A., and Cotton, N. J., *Analyst*, submitted for publication.
21 Warzinski, R. P., and Holder, G. D., *Proceedings of the Second International Symposium on Supercritical Fluids (Boston)*, ed. McHugh, M. A., Johns Hopkins University, MD, 1991, p. 161.
22 Cooper, A. I., Kazarian, S. G., and Poliakoff, M., *Chem. Phys. Lett.*, 1993, **206**, 175.
23 Graham, J. A., Grim, W. M., III, and Fateley, W. G., in *Fourier Transform Infrared Spectroscopy: Industrial and Laboratory Chemical Analysis*, eds. Ferraro, R., and Krishnan, K., Academic Press, New York, vol. 4, 1990.
24 Urban, M. W., *Polym. Mater. Sci. Eng.*, 1991, **64**, 31.
25 Yang, C. Q., *Appl. Spectrosc.*, 1991, **45**, 102.
26 Crocombe, R. A., Curbelo, R., Leonardi, J., and Johnson, D. B., in *Eighth International Conference on Fourier Transform Spectroscopy*, eds. Heise, H. M., Korte, E. H., and Seisler, H. W., *Proc. SPIE Int. Soc. Opt. Eng.*, 1992, **1575**, 189.
27 Crocombe, R. A., Compton, S. V., and Leonardi, J., in *Eighth International Conference on Fourier Transform Spectroscopy*, eds. Heise, H. M., Korte, E. H., and Seisler, H. W., *Proc. SPIE Int. Soc. Opt. Eng.*, 1992, **1575**, 193.
28 Lerner, B., *Nicolet FTIR Technical Note, TN-9253*, Nicolet Instruments, Madison, WI, 1992.
29 Ashraf-Khorassani, M., Boyer, D. S., Cross, K., Levy, J. M., and Houck, R. K., *Proceedings of the Second International Symposium on Supercritical Fluids (Boston)*, ed. McHugh, M. A., Johns Hopkins University, 1991, MD, p. 219.
30 Geoffroy, G. L., and Wrighton, M. S., *Organometallic Photochemistry*, Academic Press, New York, 1979.
31 Jenkins, T. J., Kaplan, M., Davidson, G., Healy, M. A., and Poliakoff, M., *J. Chromatogr.*, 1992, **626**, 53.
32 Sellmann, D., *Angew. Chem. Int. Ed. Engl.*, 1971, **10**, 919.
33 Cooper, A. I., Clark, M., Jobling, M., Howdle, S. M., and Poliakoff, M., unpublished work.

Paper 3/012711
Received March 4, 1993
Accepted May 5, 1993

Determination of Derivatized Urea Herbicides in Water by Solid-phase Extraction, Methylation and Gas Chromatography With a Nitrogen–Phosphorus Detector

Steven Scott
Essex Water Co., Trace Organics Laboratory, South Hanningfield, Chelmsford, Essex, UK

Four urea herbicides, isoproturon, chlorotoluron, linuron and diuron, were determined by gas chromatography (GC) with a nitrogen–phosphorus detector (NPD) after derivatization, with detection limits of 0.035, 0.039, 0.041 and 0.036 μg l^{-1}, respectively. The concentrations of all analytes were linear over the range 0.1–8.0 μg l^{-1}, with recoveries in excess of 75% from spiked potable waters. In their standard, underivatized form the herbicides were found to be thermally unstable on passage through a GC column. After derivatization, by methylation using iodomethane and a strong base, the resulting compounds were found to be stable at elevated temperatures, and so could be determined by GC. The derivatized herbicides were also analysed by GC–mass spectrometry, in order to elucidate the structures of the derivatized compounds. Each compound yielded a different product with a different retention time. The reaction was of the type typical of nucleophilic displacement, with the methyl group attacking the nitrogen of the amide group, forming a stable tertiary amide and hydrogen iodide gas. This method was found to be more selective than the Standing Committee of Analysts' method owing to the nature of the analysis. Firstly, GC, compared with high-performance liquid chromatography, offers better resolution. There are many ultraviolet absorbers in water which can be detected by the standard method, but use of a specific detector, such as an NPD, offers better selectivity. The method was also applied to other urea herbicides, including monuron, methabenzthiazuron and tebuthiuron, which were also successfully determined, although no quantitative data have been obtained.

Keywords: *Urea herbicide; gas chromatography with a nitrogen–phosphorus detector; methylation; water; solid-phase extraction*

As stated in *Guidance on Safeguarding the Quality of Public Water Supplies*,[1] urea herbicides[2] are persistent in water and most damaging to the aquatic environment[3] and are likely to reach water supplies. The maximum values for isoproturon and diuron within the Essex Water Company boundary of supply[4] were 0.39 and 0.14 μg l^{-1}, found in potable waters in weeks 4 and 35 of 1992, respectively. Raw water samples reached 1.6 μg l^{-1} for isoproturon, 0.36 μg l^{-1} for chlorotoluron and 0.5 μg l^{-1} for diuron during 1992. The Water Supply (Water Quality) Regulations 1989 state that individual pesticides and related products must not exceed 0.1 μg l^{-1}, or 0.5 μg l^{-1} for total substances. As these limits are not uncommonly exceeded, it is necessary to have a consistent method with good resolution and that is free from interference.

The standard Standing Committee of Analysts' (SCA) method of analysis[5] [double solvent extraction, one in alkaline conditions and the other in acidic conditions, followed by detection by high-performance liquid chromatography (HPLC) with ultraviolet (UV) absorbance at two wavelengths] suffers interference from other UV absorbers, and from a poor resolution of analytes (Figs. 1 and 2).

The proposed method is intended to provide a better alternative method of analysis. It involves derivatization of the urea herbicides by methylation of the amide group followed by separation by capillary gas chromatography (GC) and detection by a nitrogen–phosphorus detector (NPD). The method was assessed for consistency of results, limits of detection, rates of recovery and linearity over the specified range, together with limits of determination of the derivatized products by GC–mass spectrometry (MS).

Experimental

Reagents and Glassware

All solvents were of HPLC grade (FSA Laboratory Supplies, Loughborough, Leicestershire, UK), with the water and methanol filtered through 0.45 μm membranes. The sodium hydride was in 80% dispersion with mineral oil (Aldrich Chemicals, Gillingham, Dorset, UK), the iodomethane (99%) was stabilized with copper (Aldrich) and the dimethyl sulfoxide was also of HPLC grade (Aldrich).

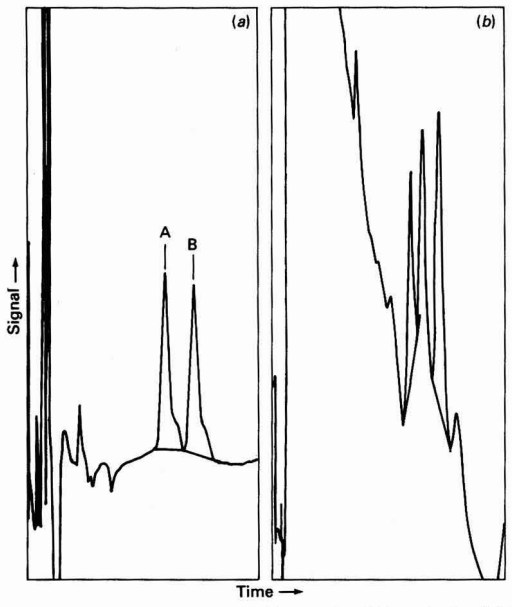

Fig. 1 Spiked recovery from potable water by SCA method. (*a*) 0.1 μg ml^{-1} standard and (*b*) 0.1 μg l^{-1} spiked sample. Peak A = isoproturon and peak B = chlorotoluron

The extraction cartridges were Octadecyl C_{18} (1 g) reversed-phase columns (J. T. BV Baker, Deventer, The Netherlands) fitted to a vacuum chamber (Supelchem UK, Saffron Walden, Essex, UK), with a vacuum pump (Charles Austin Pumps, Weybridge, Surrey, UK).

Glassware for sample collection was rinsed with acetone, then with tap-water followed by ultra-high purity (UHP) water (Elgastat double ion-exchange resin and activated carbon columns, Elga, High Wycombe, Buckinghamshire, UK) and then with the sample. Glassware for analysis was washed with detergent and heated to 100 °C, cooled and rinsed with approximately 10% HCl, washed in acetone and finally in UHP water before baking for 1 h at 100 °C.

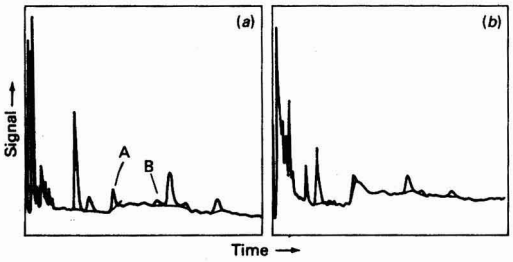

Fig. 2 Spiked recovery from potable water by SCA method. (*a*) 0.1 μg ml^{-1} standard and (*b*) 0.1 μg l^{-1} spiked sample. Peak A = linuron and peak B = diuron

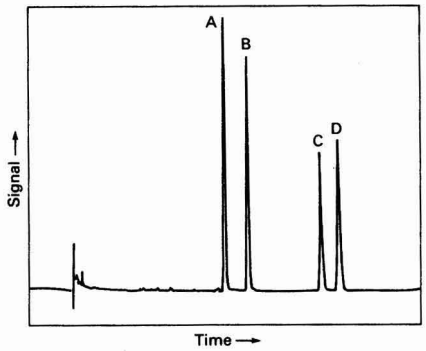

Fig. 3 Mixed urea herbicide standard. 1.0 μg ml^{-1} standard. A, Isoproturon; B, chlorotoluron; C, linuron; and D, diuron

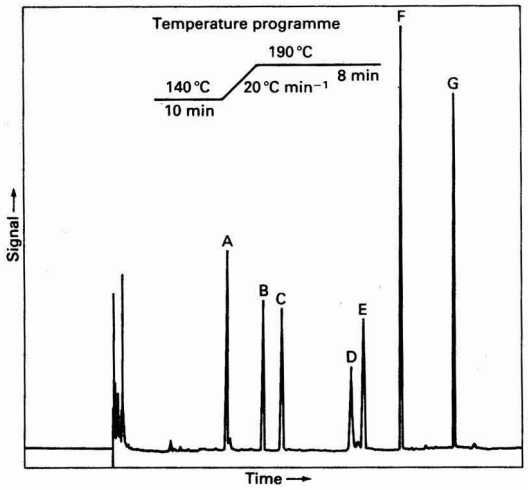

Fig. 4 Urea herbicides by proposed method (2.0 μg ml^{-1} standard). A, Monuron; B, isoproturon; C, chlorotoluron; D, linuron; E, diuron; F, methabenzthiazuron; and G, tebuthiuron

Extraction

Fix the solid-phase cartridges to a suitable vacuum chamber capable of reaching a maximum of 20 in (50.8 cm) of Hg vacuum. Condition the cartridges with 6 ± 0.2 ml of filtered methanol followed by 6 ± 0.2 ml of filtered water, making sure that the cartridges do not become dry.

With vacuum off, apply 3 ml of UHP filtered water to the column. Add 1.0 l ± 10 ml of sample *via* poly(tetrafluoroethylene) (PTFE) tubing and suitable PTFE connectors. Aspirate at a flow rate of 15 ± 2 ml min^{-1}. Wash the column with 3 ± 0.5 ml of UHP filtered water. Dry under vacuum for 5 min.

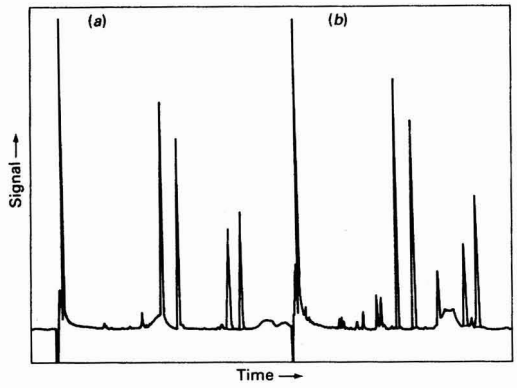

Fig. 5 Spiked potable water (1 l). (*a*) 0.1 μg ml^{-1} standard and (*b*) spiked sample

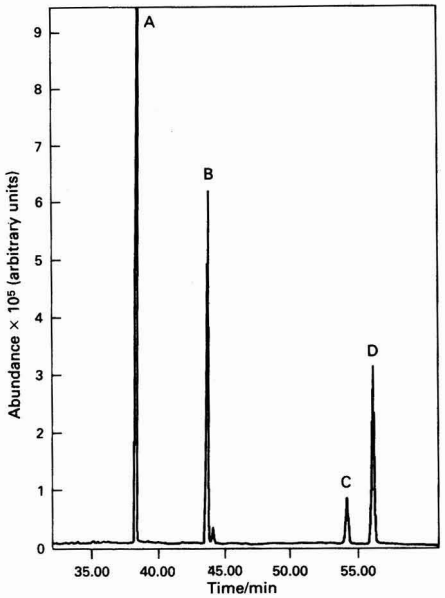

Fig. 6 Derivatized standard by GC–MS in SIM mode. Mixed standard, 5.0 μg ml^{-1}. A, Isoproturon; B, chlorotoluron; C, linuron; and D, diuron

Table 1 Analysis of variance: proposed method

	Mean	s_w*	s_b†	s_t‡	Recovery (%)	Degrees of freedom§
Linford water/0.1 μg l^{-1} *spike*—						
Isoproturon	0.089	0.0122	0.0001	0.0122	89.2	18.9
Chlorotoluron	0.083	0.0106	0.0106	0.0159	83.1	13.9
Linuron	0.087	0.0129	0.0129	0.0135	87.4	18.6
Diuron	0.082	0.0099	0.0099	0.0183	82.3	12.1
Linford water/1.0 μg l^{-1} *spike*—						
Isoproturon	0.913	0.1625	0.0001	0.1625	91.3	18.9
Chlorotoluron	0.845	0.1148	0.1141	0.1618	84.5	14.6
Linuron	0.757	0.1815	0.0796	0.1982	75.7	18.2
Diuron	0.856	0.1249	0.1057	0.1637	85.6	15.6
UHP water/0.1 μg l^{-1} *spike*—						
Isoproturon	0.091	0.0105	0.0081	0.0132	90.9	16.1
Chlorotoluron	0.088	0.0118	0.0102	0.0156	87.5	15.4
Linuron	0.081	0.0125	0.0125	0.0177	79.8	14.5
Diuron	0.083	0.0108	0.0123	0.0164	82.9	13.8
UHP water/1.0 μg l^{-1} *spike*—						
Isoproturon	0.936	0.0726	0.1453	0.1624	93.6	10.9
Chlorotoluron	0.886	0.1046	0.1141	0.1547	88.6	13.9
Linuron	0.792	0.1211	0.1311	0.1784	79.2	14.1
Diuron	0.889	0.1157	0.0907	0.1471	88.9	15.9

Limits of detection/μg l^{-1}—

	Linford water	UHP water
Isoproturon	0.041	0.035
Chlorotoluron	0.035	0.039
Linuron	0.043	0.041
Diuron	0.033	0.036

* s_w = Within-batch standard deviation.
† s_b = Between-batch standard deviation.
‡ s_t = Total-batch standard deviation.
§ Ref. 6.

Table 2 Analysis of variance: SCA method

	Mean	s_w*	s_b†	s_t‡	Recovery (%)	Degrees of freedom§
Linford water/0.1 μg l^{-1} *spike*—						
Isoproturon	0.076	0.009	0.014	0.017	76.1	12.1
Chlorotoluron	0.076	0.011	0.006	0.012	76.1	16.8
Linuron	0.073	0.018	0.019	0.026	72.5	4.7
Diuron	0.078	0.023	0.019	0.029	77.7	5.4
Linford water/1.0 μg l^{-1} *spike*—						
Isoproturon	0.768	0.103	0.103	0.103	76.8	19.1
Chlorotoluron	0.815	0.073	0.073	0.094	81.5	15.9
Linuron	ND¶	ND	ND	ND	ND	ND
Diuron	ND	ND	ND	ND	ND	ND
UHP water/0.1 μg l^{-1} *spike*—						
Isoproturon	0.067	0.007	0.007	0.009	67.1	14.5
Chlorotoluron	0.071	0.014	0.005	0.015	71.1	18.4
Linuron	0.059	0.014	0.001	0.015	59.4	6.8
Diuron	0.076	0.013	0.014	0.019	76.1	4.9
UHP water/1.0 μg l^{-1} *spike*—						
Isoproturon	0.781	0.064	0.067	0.093	78.1	14.3
Chlorotoluron	0.825	0.081	0.086	0.117	82.5	14.1
Linuron	0.657	0.244	0.224	0.331	65.7	5.1
Diuron	0.661	0.086	0.001	0.086	66.1	6.8

Limits of detection/μg l^{-1}—

	Linford water	UHP water
Isoproturon	0.031	0.023
Chlorotoluron	0.036	0.046
Linuron	0.059	0.046
Diuron	0.076	0.043

* s_w = Within-batch standard deviation.
† s_b = Between-batch standard deviation.
‡ s_t = Total-batch standard deviation.
§ Ref. 6.
¶ ND = Not determined.

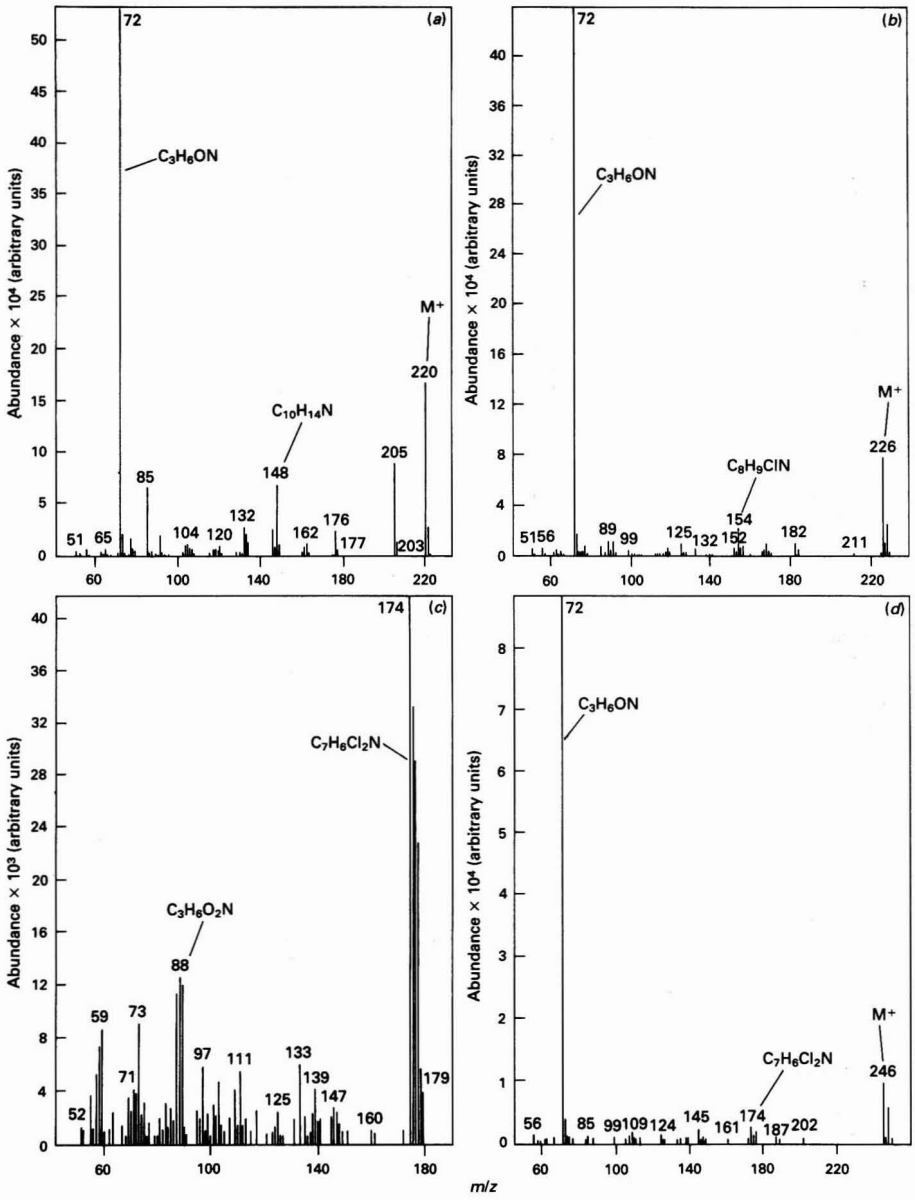

Fig. 7 Mass spectra after derivatization. (*a*) Isoproturon, (*b*) chlorotoluron, (*c*) linuron and (*d*) diuron

Elute the urea herbicides with 6 ± 0.2 ml of filtered methanol, at a flow rate of 6 ml min^{-1}, into a 10 ml centrifuge tube.

Derivatization

Evaporate the solvent residue to incipient dryness under a stream of nitrogen, while warming to approximately 40 °C. The nitrogen supply should be adjusted such that the surface of the solvent is just indented and no splashing occurs.

Remove the tube from the nitrogen supply. Place approximately 0.2 g of sodium hydride in a separate round-bottomed centrifuge tube, followed by 1 ± 0.2 ml of diethyl ether. Evaporate to dryness under a stream of nitrogen. Add 1.5 ± 0.2 ml of dimethyl sulfoxide to the tube and mix to form a suspension. One tube is required for three samples.

Place approximately 300 ± 50 μl of the sodium hydride suspension in the sample tube using a disposable pipette, and immediately add 50 ± 5 μl of iodomethane. Leave standing in a fume cupboard for 10 min.

In a fume cupboard add 1 ± 0.2 ml of UHP water to the samples, taking care not to add too much too quickly as the sample can effervesce vigorously.

Add 8 ± 0.2 ml of diethyl ether to the sample, stopper the tube and shake vigorously for 2 min. Once the two phases have

separated, remove the supernatant organic phase with a clean disposable pipette and place in a clean, pointed centrifuge tube.

Evaporate the extract to incipient dryness, accurately dilute to 1 ml with diethyl ether, and stopper the tube tightly.

An analysis of variance (ANOVA)[6] was carried out over 10 d to ensure at least ten degrees of freedom to assess the performance of the method (Table 1).

Instrumentation

The GC analyses were carried out using an AMS 92 gas chromatograph (Analytical Instrumentation, Cambridge, UK), fitted with an NPD, with the injector operated in split mode at a ratio of 30:1.

The column was a fused-silica BP1 (25 m × 0.22 mm i.d., 0.25 μm film thickness) capillary column [SGE (UK), Milton Keynes, Buckinghamshire, UK]. The operating parameters were: injector temperature 250 °C, detector temperature 250 °C, and column temperature 150 °C (isothermal). The total run time was approximately 8 min.

The NPD was operated with the following gas flow rates: carrier (helium) 25 ml min^{-1}, hydrogen 3 ml min^{-1}, and air 150 ml min^{-1}. The output was linked to an SP4400 Chromjet integrator (Spectra-Physics Analytical, Fremont, CA, USA).

The GC–MS analysis was performed using an HP 5980 Series II gas chromatograph (Hewlett-Packard, Avondale, PA, USA) with an HP 5971A mass-selective detector; splitless injection was carried out for 1.5 min using an HP 7673 auto-injector. The fused-silica capillary column was a DB1701 (60 m × 0.32 mm i.d., 0.15 μm film thickness) column (J & W Scientific, Folsom, CA, USA). Data acquisition and processing were performed by Microsoft MS-DOS 3.3 (Microsoft, Redmond, WA, USA], with mass calibration based on perfluorotributylamine (PFTBA). All mass spectra were obtained under electron-impact conditions (70 eV). The mass spectra were continuously scanned over the mass range 50–450 u at 0.5 s $decade^{-1}$.

Results

Under the conditions described, separation of the four derivatized products was achieved (Fig. 3). With slight temperature programming, seven derived herbicides could be resolved (Fig. 4). Spiked recoveries were carried out on UHP water and a well water supply (Linford Well, Essex, UK) (see Table 1).

A spiked recovery was also performed on a river-derived potable water (Hanningfield Final Water, Essex, UK), which shows few interference peaks (Fig. 5).

Calibration was over the range 0.1–8.0 μg l^{-1} within which all analytes provided a linear response passing through the origin.

Derivatized standards of 5.0 μg l^{-1} were run on the mass spectrometer as described (Fig. 6). From the data obtained it was possible to elucidate the structures of the derivatized products (Figs. 1 and 2).

Discussion

It can be seen that interference peaks and relatively poor recoveries make the previous methods for the determination of herbicides unsuitable for low-level analysis of river and potable waters (Figs. 7 and 8).

The proposed method is based on methylation of the amide NH group to form a stable tertiary amide (Fig. 8). The reaction is a typical nucleophilic substitution reaction of the type shown below, where X is a readily displaced, stable leaving group

$$\text{Sample—NH} \xrightarrow[\text{Base}]{\text{R—X}} \text{Sample—N—R} + \text{HX}$$

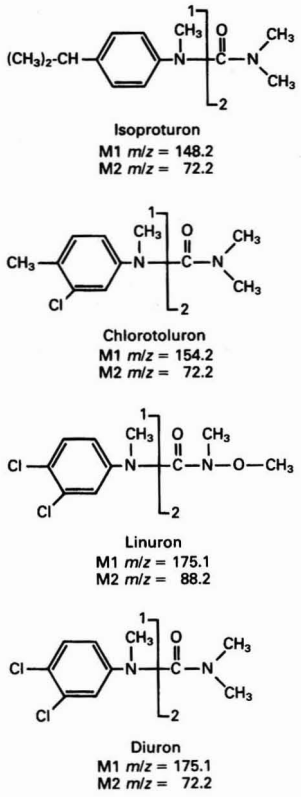

Fig. 8 Structures of derivatized herbicides showing major fragmentation

For urea herbicides, the leaving group is iodine, with the sodium hydride acting as a strong basic catalyst, and the reaction being achieved at ambient temperature. Effervescence of the acrid hydrogen iodide can be seen during the reaction.

Separation of the four urea herbicides is achieved easily without the need for temperature programming, and although other peaks can be detected, they do not generally have the same retention time as the analytes and are of lower frequency than those for analysis by HPLC with UV detection.

The limits of detection, calculated by multiplying the standard deviation of the mean of the low spikes by 3.3 (WRC, NS30, Revised June 1989)[6] (Table 1), are, in reality, much lower than the values stated, with peaks of concentration 0.02 μg l^{-1} being seen for all analytes. The blank samples yielded no response and so could not be used for determining the limits of detection.

For further confirmation of the derivatized product, the samples can be analysed by GC–MS in the selective-ion mode (SIM), searching for the base peak and molecular ion (Fig. 6).

Comparison With Standard SCA Methods

The standard SCA method[5] for the determination of urea herbicides involves sample concentration by extraction, evaporation of the extract to incipient dryness, dissolution of the residue in the mobile phase, and analysis, using polar solvents, by HPLC with UV detection.

In order to determine the four urea herbicides mentioned here, it is necessary to perform two separate extractions, one in alkaline conditions for isoproturon and chlorotoluron, and the other in acidic conditions for linuron and diuron. To gain the best response, they should be analysed at two separate wavelengths, *viz.*, 240 and 220 nm, respectively.

Although reasonable separation and response can be achieved by using this standard method (Figs. 1 and 2), at low levels of analyte in water ($<0.1\ \mu g\ l^{-1}$), background peaks are significant and, without additional quantitative data, should be regarded as maxima (Figs. 1 and 2).

Phenoxy acidic herbicides are a known contaminant, and, when present, the ureas have to be re-analysed at 270–280 nm. Because of the nature of UV detection and the fact that river and potable waters contain many UV absorbers, it is clear that analysis by GC–NPD will be much more selective.

Recoveries performed on the same waters, and at the same concentrations, are generally about 10% lower for the SCA method, with comparable limits of detection (Tables 1 and 2).

References

1 Department of the Environment Welsh Office, *Guidance on Safeguarding the Quality of Public Water Supplies*, HM Stationery Office, London, 1990, pp. 99–102.
2 Worthing, C. R., and Hance, R. J., *The Pesticide Manual*, British Crop Protection Council, Farnham, Surrey, 9th edn., 1991, pp. 161, 322, 507 and 520.
3 Ivens, G. W., *The UK Pesticide Guide*, British Crop Protection Council, Cambridge, UK, 1992, p. 18.
4 Essex Water Co., *Water Quality Register*, Chelmsford, Essex, 1992.
5 Standing Committee of Analysts, *The Determination of Carbamates, Thiocarbamates, Related Compounds and Ureas in Water*, HM Stationery Office, London, 1987, pp. 15–21.
6 Water Research Centre, NS30—*A Manual on Analytical Quality Control for the Water Industry*, Marlow, Buckinghamshire, 1989, pp. 57 and 131.

Paper 2/06602E
Received December 14, 1992
Accepted February 25, 1993

Comparison of Liquid Chromatographic Methods for Analysis of Homologous Alkyl Esters of Biphenyl-4,4′-dicarboxylic Acid*

Joel K. Swadesh
Alpha-Beta Technology, Innovation Drive, Worcester, MA 01060, USA
Charles W. Stewart Jr.† and Peter C. Uden‡
Department of Chemistry, University of Massachusetts, Amherst, MA 01003, USA

Homologous series of compounds are generated in systematic studies of liquid crystals, petroleum fractions and pharmaceutical compounds. The paper describes the separation of a series of homologous liquid crystalline alkyl esters of biphenyl-4,4′-dicarboxylic acid by high-performance liquid chromatography. High-performance gel-permeation chromatography (HPGPC) was capable of separating compounds differing by a single carbon, and is, therefore, similar in resolving power to either normal- or reversed-phase liquid chromatography. High-performance gel-permeation chromatography has the advantage of permitting the analysis of compounds of widely differing polarity. If the resolution of GPC can be increased slightly by reducing the particle size and decreasing the pore size to maximize resolution in the range of 250–500 u, it could become a primary analytical technique in the organic synthetic laboratory.

Keywords: *Comparative high-performance liquid chromatography; high-performance gel-permeation chromatography; biphenyldicarboxylic acid ester; mono- and diester homologous series*

Separation of members of a series of homologous compounds is often required in the course of studying liquid crystals,[1] pharmaceutical structure–activity relationships,[2] alkanes[3] and chromatographic phases,[4,5] and in the conductance of other activities of industrial and theoretical importance. Resolution of a compound of interest from synthetic precursors and contaminants can require the development of separate methods for different members of the series. Demands on the analytical procedure are particularly high in the characterization of a homologous series of alkyl-substituted liquid crystals. Firstly, the physical properties of homologues are extremely similar, differing by the effects of a single methylene unit. Secondly, rigorous measurement of purity is desired, as the thermal properties are highly dependent on purity. Finally, predicted contaminants of a given homologue often include related homologues or structural isomers of the desired compound.

The separation of homologues differing by a single methylene is not an unknown problem in chromatographic science. Homologous parabens in cosmetics have been separated by reversed-phase chromatography.[6] Homologous phthalate plasticizers have been separated by size-exclusion chromatography,[3,7–9] as have alkanes.[3,8,10] Reversed-phase liquid chromatography (RPLC) has been used to separate alkanes, alkyl benzenes and fatty acid methyl esters.[4] Homologous alcohols have been separated by size-exclusion chromatography in micelles.[11]

The syntheses and thermotropic transitions of 14 liquid crystalline alkyl monoesters of 4,4′-biphenyldicarboxylic acid (R_nBDCA–H) were first described in 1981.[1] The corresponding diesters (R_nBDCA–R_n), which are synthetic precursors, were found to exhibit no liquid crystalline mesophases. The monoesters, however, display a rich range of mesomorphism, including three distinct smectic phases and at least one nematic phase. At the time at which this class of liquid crystals was first synthesized, qualitative thin-layer chromatography was used for characterization. Since then, high-performance liquid chromatography (HPLC) has become more generally available. In the present work, a number of the members of the homologous series of R_nBDCA–R_n and R_nBDCA–H were separated by HPLC.

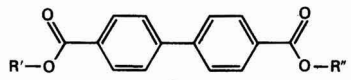

R_nBDCA–R_n: R′ = R″ = *n*-alkyl
R_nBDCA–H: R′ = *n*-alkyl, R″ = H

Experimental

Materials

The synthesis of R–BDCA–R and R–BDCA has been described. Briefly, BDCA was esterified to the diester, then hemihydrolysed to the corresponding monoester. The purity of the monoester was monitored by thin-layer chromatography on silica, using a 75 + 25 mixture of chloroform–methanol. Some preparations were sublimed to remove BDCA and other non-volatile impurities.

Chromatographic solvents were of HPLC grade. Unstabilized tetrahydrofuran (THF) (J. T. Baker, Phillipsburg, NJ, USA) was used for gel-permeation chromatography (GPC). Methanol, acetic acid, hexane and chloroform were from Fisher Scientific (Fairlawn, NJ, USA). For GPC, four 30 × 7.5 mm poly(styrene–divinylbenzene) columns packed with 5 μm diameter, 50 Å porosity particles (Polymer Laboratories Ltd., Church-Stretton, Shropshire, UK) were connected in series. For normal-phase liquid chromatography (NPLC), a 150 × 4.6 mm silica column (MacMod Analytical, Chadds Ford, PA, USA) in 90 + 10 hexane–chloroform was used for the separation of the diesters. It was not possible to elute the monoesters from this column. The monoesters were instead chromatographed by reversed-phase in ion suppression mode on a 150 × 4.6 mm octadecylsilylated silica column (MacMod Analytical), using 92 + 8 methanol–water, with the apparent pH of the mixture adjusted to 2.8 with acetic acid.

* Presented at the 21st Northeast Regional Meeting of the American Chemical Society, June, 1991 as *HPLC Analysis of the n-Alkyl Esters of Biphenyl-4,4′-Dicarboxylic Acid.*

† Present Address: Department of Chemistry, Hartwick College, Oneonta, NY 13820-4020, USA.

‡ To whom correspondence should be addressed.

Equipment

The liquid chromatographic system used for GPC was a Hewlett-Packard (Avondale, PA, USA) Model 1090 chromatograph equipped with a diode-array detector. Elution was performed at ambient temperature and 1 ml min^{-1}. Ultraviolet detection at 260 nm was used. The injection volume was 5 μl, with the analyte at a concentration of about 1 mg ml^{-1} in eluent. A small portion of toluene was added as a flow rate marker. The monoesters and diesters of BDCA were chromatographed on this system.

The instrumentation used for NPLC and RPLC consisted of a Series 10 pump and Model LC 75 UV detector (Perkin-Elmer, Norwalk, CT, USA), equipped with a Model 7010 injector (Rheodyne, Cotati, CA, USA). The injection volume was 10 μl, with the analyte at a concentration of about 40 μg ml^{-1}. Detection was at 254 nm.

Results

The principal results are summarized in two of the figures, demonstrating the separation of selected monoesters R_n–BDCA by GPC [Fig. 1(*a*)] and RPLC [Fig. 1(*b*)] and selected diesters R_n–BDCA–R_n by GPC [Fig. 2(*a*)] and NPLC [Fig. 2(*b*)]. Fig. 1(*a*) shows the GPC separation of the C_3, C_4, C_8, C_{11} and C_{15} monoesters of R_n–BDCA from 24 and 28 min, with the toluene flow rate marker eluting at 35 min, whereas Fig. 1(*b*) shows the C_4, C_6, C_8, C_{11} and C_{12} monoesters separated by RPLC from 2 to 13 min. Fig. 2(*a*) shows the C_1, C_2, C_3, C_4, C_9, C_{11} and C_{16} diesters separated by GPC from 23–30 min, with toluene eluting at 35 min. Fig. 2(*b*) shows the C_1, C_2, C_3, C_{10}, C_{12}, C_{14} and C_{16} diesters separated by NPLC from 5 to 25 min; biphenyl elutes at about 2 min. The void (exclusion) volume in GPC is difficult to determine precisely due to hydrodynamic chromatographic effects; apparatus to determine it was not accessible, however, a reasonable estimate is about 20 ml, based on the manufacturer's literature. The retention data is summarized in Table 1.

Gel-permeation chromatography was found to be capable of detecting impurities at levels of less than 0.1% peak area at 260 nm, as long as these were well-resolved from the principal peak. Of the diesters examined, the following purities were noted: methyl, 98.8; ethyl, 95.0; propyl, 99.6; butyl, 100; nonyl, 100; decyl, 100; undecyl, 99.9; dodecyl, 100; and hexadecyl, 100. Of the monoesters examined by GPC, the following purities were observed: propyl, 97.4; butyl, 99.6; pentyl, 100; hexyl, 99.8; heptyl, 99.7; octyl, 99.8; octyl, 99.8; tridecyl, 99.7; and pentadecyl, 98.0. On RPLC and NPLC, detection limits were of the order of 2%, and no impurities were detected.

Detectability is, of course, dependent on resolution. The resolution between adjacent homologues was estimated as $R_s = (t_2 - t_1)/4_{st}$, where t_2 and t_1 are the retention times of adjacent homologues, and s_t is the standard deviation, estimated as the peak width at half-height.[12] The GPC elution times of the membranes of each homologous series were flow corrected and fitted to a third-order polynomial to estimate

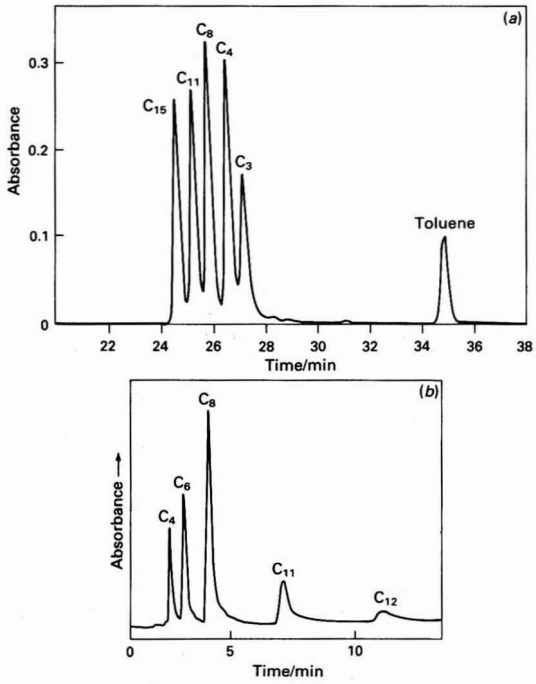

Fig. 1 Separation of monoesters of biphenyl-4,4′-dicarboxylic acids by gel-permeation chromatography (*a*) and reversed-phase chromatography (*b*). GPC with four 50 Å 30 × 0.8 cm columns in THF at 1 ml min^{-1}. RPLC using a 150 × 4.6 mm ODS column, mobile phase 92 + 8 v/v methanol–water (adjusted to pH 2.8 with acetic acid) 1 ml min^{-1}

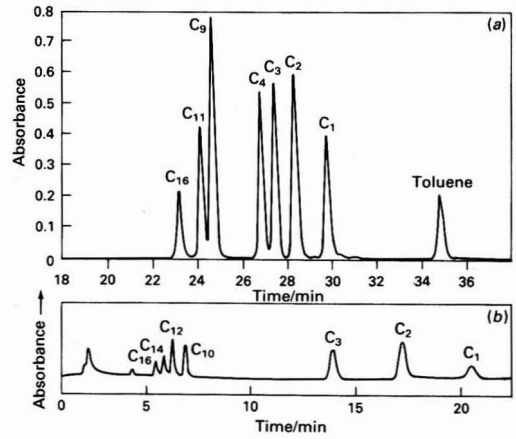

Fig. 2 Separation of diesters of biphenyl-4,4′-dicarboxylic acids by gel-permeation chromatography (*a*) and normal-phase chromatography (*b*). GPC column and conditions as in Fig. 1(*a*). NPLC 150 × 4.6 mm silica column, mobile phase 90 + 10 v/v hexane–chloroform 1 ml min^{-1}

Table 1 Retention data for mono and diesters of biphenyl-4,4′-dicarboxylic acids, chromatographic conditions as in the text

Compound alkyl chain	Monoester retention and peak width/min		Diester retention and peak width/min	
	GPC	RPLC	GPC	NPLC
Methyl			29.82, 0.29	24.44, 1.13
Ethyl			28.40, 0.26	20.31, 1.00
Propyl	27.22, 0.31		27.51, 0.26	16.13, 0.88
Butyl	26.62, 0.28	2.13, 0.38	26.88, 0.25	
Pentyl	26.35, 0.27			
Hexyl	26.11, 0.25	2.18, 0.50		
Heptyl	26.10, 0.27			
Octyl	25.88, 0.27	4.06, 0.88		
Nonyl			24.75, 0.25	
Decyl			24.58, 0.24	7.44, 0.38
Undecyl	25.30, 0.27	7.63, 1.00	24.20, 0.25	
Dodecyl		12.63, 1.38	24.09, 0.25	6.63, 0.38
Tridecyl	24.73, 0.27			
Tetradecyl				6.13, 0.25
Pentadecyl	24.66, 0.31		23.58, 0.22	
Hexadecyl			23.18, 0.26	5.63, 0.25

the resolution as a function of carbon number. Taking the peak width at half-height to be about 0.25 min, the resolution of a monoester of carbon number n from homologue $n + 1$ is

$$R_s\,(\text{mono, GPC}) = 0.4272 - 4.961 \times 10^{-2}n + 2.3629 \times 10^{-3}n^2$$

whereas the diester resolution is

$$R_s\,(\text{di, GPC}) = 1.278\text{–}0.1940n + 8.61 \times 10^{-3}n^2$$

The corresponding values were estimated for NPLC separations and diester separations by calculating interpolated values for retention times and peak least squares. The estimated values of resolution were

$$R_s\,(\text{mono, RPLC}) = -0.3248 + 0.4096n - 8.896 \times 10^{-2}n^2 + 5.710 \times 10^{-3}n^3$$

and

$$R_s\,(\text{di, NPLC}) = 1.25 - 0.1521n + 5.569 \times 10^{-3}n^2$$

The shape of the resolution curves is shown in Fig. 3. The carbon number is plotted on the x axis, and the resolution of adjacent homologues is plotted on the y axis. Values for resolution were estimated as $R_s = (t_2 - t_1)/4s_t$, where t_2 and t_1 are the interpolated retention times of adjacent homologues, and s_t is the standard deviation, estimated as the interpolated peak width at half-height.

Discussion and Conclusions

Gel-permeation chromatography is comparable in analysis time to both RPLC or NPLC reversed or normal phase chromatography, but is inferior in resolution. All homologues elute in less than 30 min from GPC and in less than 25 min from both RPLC and NPLC. The RPLC and NPLC separations could, of course, be accelerated without significant loss of resolution by the use of a gradient. The RPLC and NPLC chromatograms exhibit tailing, complicating the use of these techniques for analysis of purity. In contrast, peak symmetry in GPC is close to unity, with no tailing observed. Therefore, although resolution between adjacent homologues is greater in RPLC or NPLC than in GPC, the detectability of contaminants may be better in GPC. Also, the resolution in GPC is not greatly inferior to that observed in RPLC and NPLC. By reducing the pore size and particle size, it might be possible to obtain high-performance GPC, with resolution and separation time equivalent to that of isocratic NPLC or RPLC. No difference in peak widths was observed between larger and smaller homologues. This suggests that frictional drag in the mass transfer of solutes between mobile and static phases would not be a problem with reduced pore sizes. In GPC, gels of different porosities are often mixed, leading to a very wide distribution of pore size, without a concomitant loss of resolution being observed beyond that ascribed to diffusional broadening. Reproducibility of isocratic liquid chromatographic exclusion and partition methods might be considered to be generally similar. Comparisons or reproducibility among methods was not a part of the present study, particularly as data were obtained with different instrumental systems. It is also clear that although gradient elution reproducibilities approach those of isocratic modes if equipment quality and operation are of a sufficiently high standard, there always exists the possibility of greater irreproducibility in gradient elution by virtue of the additional operational parameters inherent in this method.

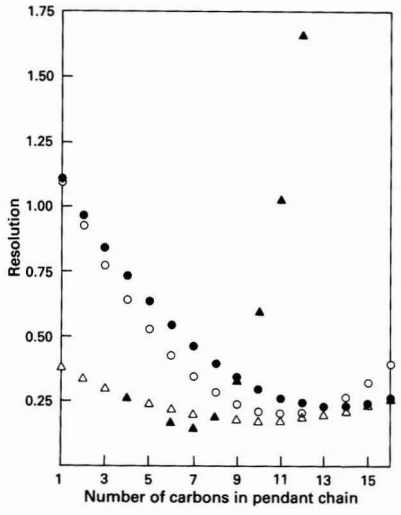

Fig. 3 Resolution of adjacent homologues by gel-permeation chromatography, reversed-phase chromatography and normal-phase chromatography. ●, Diesters on NPLC; ○, diesters on GPC; ▲, monoesters on NPLC; and △, monoesters on RPLC

Gel-permeation chromatography is extremely attractive as an analytical method for the separation of small molecules, as the only strict chromatographic requirement is that the analytes be soluble in a common solvent. Even analytes of widely different polarity can be chromatographed on a single system. It should be noted that secondary equilibria of the monoesters appears to be unimportant as little difference is observed in peak widths and/or symmetries between the monoesters and diesters. Analytes of greatly different polarity are often encountered in synthetic organic chemistry. This was the case in the present work. The principal contaminants in the R_n–BDCA monoesters are predicted to be the R_n–BDCA–R_n diester precursors and homologues of similar carbon chain length. Each diester and its corresponding product monoester is well-separated on GPC except for those homologues near C_5. The possibility of co-elution of dissimilar molecules (such as monoesters with long R chains and diesters with short R chains) cannot, however, be ignored. As some measure of the practical utility of GPC, it should be noted that the GPC data described was obtained in about 36 h of laboratory time wheres the RPLC and NPLC methods took considerably more time to develop.

The generosity of Professor J. C. Poirier in making available the samples used in this work is greatly appreciated. Support from Merck, Sharp and Dohme Research Laboratories is gratefully acknowledged.

References

1 Cohen, S. D., Risinger-Diuguid, C. A., Poirier, J. C., and Swadesh, J. K., *Mol. Cryst. Liq. Cryst.*, 1981, **78**, 135.
2 Kaliszan, R., *J. Chromatogr. Sci.*, 1984, **22**, 362.
3 Krishen, A., *J. Chromatogr. Sci.*, 1984, **16**, 254.
4 Colin, H., and Guiochon, G., *J. Chromatogr. Sci.*, 1980, **18**, 54.
5 Colin, H., Guiochon, G., and Diez-Masa, J. C., *Anal. Chem.*, 1981, **53**, 146.
6 Dong, M. W., and DiCesare, J. L., *J. Chromatogr. Sci.*, 1982, **20**, 49.
7 Benson, J. R., and Woo, D. J., *J. Chromatogr. Sci.*, 1984, **22**, 386.
8 Russell, D. J., *J. Liq. Chromatogr.*, 1988, **11**, 383.
9 Dong, M. W., and DiCesare, J. L., *J. Chromatogr. Sci.*, 1982, **20**, 517.
10 Kirkland, J. J., and Antle, P. E., *J. Chromatogr. Sci.*, 1977, **15**, 137.
11 Terabe, S., Tanaka, H., Otsuka, K., and Ando, T., *J. Chromatogr. Sci.*, 1989, **27**, 653.
12 *An Introduction to Separation Science*, Karger, B. L., Snyder, L. R., and Horváth, Cs, John Wiley, New York, 1973, pp. 148–150.

Paper 2/05028E
Received September 21, 1992
Accepted May 11, 1993

Assessment of Three Azophenol Calix[4]arenes as Chromogenic Ligands for Optical Detection of Alkali Metal Ions

Mary McCarrick, Stephen J. Harris and Dermot Diamond*
School of Chemical Sciences, Dublin City University, Dublin 9, Ireland

Three novel chromogenic cone conformational calix[4]arene tetraesters bearing nitrophenylazophenol residues (mono-, di- and tetra-substituted) in the ester portion of the molecules have been synthesized and shown to display a dramatic change in absorbance spectrum upon complexation with lithium, and to a lesser extent sodium, in the presence of a base. An instantaneous colour change from yellow to red corresponding to a λ_{max} shift from 380 to 520 nm, is noted upon the addition of lithium perchlorate to a solution containing any of the three ligands with the intensity of the colour being concentration dependent. The best selectivity for lithium against sodium and potassium was exhibited by the mono-substituted derivative, ligand **4**, (approximately 70-fold selectivity in both cases). Although this is somewhat less than that required for clinical applications, it is anticipated that it can be further improved using a variety of approaches, which are the subject of further investigations. The interference from potassium is too small to be measured.

Keywords: *Chromoionophore; lithium; calixarene; optrode; alkali metal ion*

The development of methods of detection for clinically important species such as lithium, sodium and potassium has received much recent attention. One of the main subjects of investigation is the development of chromoionophores, *i.e.*, ionophoric macromolecules that incorporate a chromophoric group into their structure. The aim is to produce a ligand that exhibits a dramatic, concentration-dependent change in absorbance spectrum upon complexation with the target species.

The nitrophenylazophenol group has been used as the chromogenic moiety in many different cation binding systems. A crowned azophenol was shown to exhibit lithium specific colour changes in the presence of an amine.[1] A slightly larger crown ether, also containing a nitrophenylazophenol moiety as the chromogenic substituent, was found to change colour from yellow to purple upon complexation with potassium. However, the selectivity against sodium was too low to allow the determination of potassium levels in blood.[2] A number of amine selective azophenol crown ethers have also been described, with the nature of the amine (*i.e.*, primary, secondary or tertiary) determining the wavelength of the absorbance maximum of the complexed molecule with some of the compounds.[3]

A four-membered spherand containing the *p*-nitrophenylazophenol chromogenic group has been shown to display lithium selectivity under hydrophobic conditions with no interaction with any other metals being observed.[4] The six-membered analogue of this spherand was found to respond to sodium and lithium ions with very little response to any other metal ions.[5]

Calixarene derivatives, another major class of macrocyclic receptor molecules, have recently evoked interest as a source of novel chromogenic ligands. Two calix[4]arenes bearing azophenol moieties as the chromogenic component have been recently described in the literature,[6,7] and one has been found to display lithium selectivity in a solid–liquid two-phase extraction.[6] A dinitrophenylazophenol with a similar calixarene backbone was synthesized and found to respond to the lithium ion in the presence of a number of amines.[7] Another calixarene, bearing the nitrophenylazophenol chromophore (which showed excellent selectivity for potassium against sodium), has also been described.[8] In all three of these compounds, the phenol group (which is deprotonated in order to give the colour change upon complexation) is housed within the cavity into which the metal ion fits and complexation actually involves the phenolic oxygen atoms.

Recently, work was presented on cone conformational chromogenic calix[4]arenes with hydroxynitrobenzyl groups as the chromogenic moieties.[9] These compounds exhibited lithium selectivity against sodium and potassium and changed from colourless to yellow upon complexation with the metal ions in the presence of a suitable base. In an attempt to create compounds whose complexed form would have a longer wavelength absorbance maximum than the compounds containing the nitrophenol group, several tetrameric calixarenes have been synthesized, incorporating a nitrophenylazophenol group as the chromogenic moiety in the ester portion of the molecule. Compounds with longer absorbance maxima such as these are more useful from an optical sensor point of view owing to the cheap availability of blue light emitting diodes, which emit light in the range of the absorbance maxima of the azophenol group. Hence instrumentation development for these sensors is much simpler than for shorter wavelength analogues in which more complex excitation sources are required.

Experimental

Materials and Equipment

Tetrahydrofuran (THF), and lithium, sodium and potassium perchlorate, along with deuteriated chloroform and methanol were all obtained from Aldrich. Tridodecylamine (TDDA) was purchased from BDH Chemicals and triethylamine (TEA) and butan-1-ol were obtained from Riedel-De-Haen. The nuclear magnetic resonance (NMR) and ultraviolet–visible (UV/VIS) spectra were obtained with a Bruker AC-400 spectrometer and a Hewlett-Packard 8452A diode-array spectrophotometer, respectively.

Synthesis of Ligands

Ligand **1** was prepared from the known *p-tert*-butyl calix[4]arene tetraacetic acid.[10] Treatment with thionyl chloride furnished the tetraacid chloride, which upon treatment with 2-hydroxy-5-(4′-nitrophenylazo)benzyl alcohol (**2**) in THF containing pyridine furnished ligand **1** (80% yield; m.p. 111–115 °C) (Found: C, 65.6%; H, 5.6%. Calc. for $C_{104}H_{96}O_{24}N_{12}$: C, 65.8; H, 5.1%). In a similar fashion triester monoacid **3**[11] was transformed *via* its acid chloride into ligand **4** (70% yield; m.p. 60–64 °C) (Found: C, 66.33; H, 6.51; N,

* To whom correspondence should be addressed.

3.00%. Calc. for $C_{71}H_{84}O_{15}N_3$: C, 66.29; H, 6.65; N, 3.22%). The final ligand, ligand **5** was prepared from the diacetic acid derivative. Treatment with thionyl chloride gave the diacid chloride, which upon similar treatment to the above gave the required ligand **5** (72% yield; m.p. 65–68 °C) (Found: C, 67.74; H, 4.54; N, 7.10%. Calc. for $C_{64}H_{52}O_{14}N_6$: C, 68.08; H, 4.64; N, 7.44%). The diacetic acid derivative **6** was itself prepared from its diethyl acetate derivative by hydrolysis with KOH in ethanol and subsequent acidification (94% yield).[12] The diethyl acetate derivative in turn was prepared from 1,3-diallyloxycalix[4]arene (**7**) by treatment with ethyl bromoacetate and K_2CO_3 in acetone[13] (75% yield). The diallyl ether was prepared from the parent calix[4]arene (**8**),[14] by treatment with two equivalents of allyl bromide in the presence of K_2CO_3 in acetonitrile[15] (72% yield). At each stage, the product was purified by column chromatography using a neutral alumina column and dichloromethane as the eluent. The presence of the azo and carbonyl groups in the final product was confirmed from infrared absorbance spectra (not shown).

UV/VIS Absorbance Spectra of Ligand Complexation

Solutions (5×10^{-5} mol l^{-1}), of ligands **1**, and **4** and a 6×10^{-5} mol l^{-1} solution of ligand **5**, were made up in THF. A 2.5 ml aliquot of each ligand solution was taken and to this 100 μl of TDDA were added. Incremental concentrations of aqueous lithium perchlorate were added to give final metal perchlorate concentrations of 1×10^{-6} mol l^{-1}, to 0.1 mol l^{-1}. After gentle shaking, the clear yellow ligand solution changed colour to red immediately, with the intensity of the resultant colour being dependent on the metal perchlorate concentration. This colour change was examined using UV/VIS spectroscopy in the range 300–800 nm.

Selectivity Coefficient Determination

In order to determine the selectivity coefficients for lithium against sodium, a series of experiments was set up as described above, with the final lithium perchlorate concentration being varied in the range from 1×10^{-6} to 0.1 mol l^{-1}, in a fixed background concentration of interferent (0.05 mol l^{-1} and 0.1 mol l^{-1} sodium perchlorate). Spectra were obtained from 300–800 nm and graphs of absorbance at 520 nm *versus* the log of the concentration of lithium perchlorate concentration drawn. At high concentrations, the sodium ion has the effect of reducing the response of the ligand to low concentrations of lithium as it dominates the complexation process with the ligand and swamps any lithium ion effects. However, at higher lithium ion concentrations, a response will be observed because of greater affinity of the ligand for lithium ions. From these graphs, selectivity coefficients can be estimated from the ratio of the sodium and lithium ion concentrations at the intersection of the sodium and lithium dominant response regions of the curves.

Two-phase Examination of Ligands

In order to examine whether these compounds, in their complexed form could be retained in the organic phase of an organic–aqueous phase two-phase system, a number of solvents were examined (dichloromethane, butan-1-ol, butanone, 1,1,1-trichloroethane and butan-2-ol) by making up 5×10^{-5} mol l^{-1} solutions of ligand **1** in each solvent. Then 20 μl of TEA was added, followed by 10 μl of 1 mol l^{-1} aqueous lithium perchlorate and 2.5 ml of water. Any colour changes upon each addition were noted, as was the ability of any colour generated to remain in the organic layer. For comparative purposes, blank experiments were carried out for each solvent containing everything except the lithium perchlorate.

Results and Discussion

A slight colour change from yellow to bronze was noted upon the addition of the TDDA to the solution. This effect coincided with an increase in absorption at the uncomplexed wavelength absorbance maximum at 380 nm. No increase in intensity at 520 nm was noted. Fig. 1(*a*) (*b*) and (*c*) illustrates the effect of varying lithium perchlorate concentration on the absorbance spectrum of ligands **1**, **4** and **5**, respectively. As anticipated, complexation led to a shift in λ_{max} from 380 to 520 nm with an isosbestic point at 425 nm, and the increase in the absorbance at 520 nm being dependent on the concentration of lithium perchlorate. No colour change was observed in the absence of base. This is indicative of the deprotonation of the azophenol group upon metal ion complexation being the cause of the colour change, as the presence of the base facilitates the removal of the phenolic proton. Confirmation of metal complexation was carried out using proton NMR spectroscopy for ligand **1**. Upon addition of 1 molar equivalent of sodium thiocyanate in deuteriated methanol to a solution of ligand **1** in deuteriated chloroform, a complex sequence of peaks between 0.9 and 1.3 ppm due to the non-equivalence of the tertiary butyl protons in the free ligand [Fig. 2(*a*)], are resolved into a singlet at 1.2 ppm, indicating that a more ordered symmetry is forced on the molecule on complexation [Fig. 2(*b*)]. The characteristic AB quartet[16,17] of the bridging methylene protons of the calix[4]arene at 3.2 and 4.6 ppm were found to shift to 3.4 and 4.4 ppm, respectively, which is again indicative of metal complexation conferring a more ordered structure on the molecule[16,17] [Fig. 2(*b*)].

Fig. 3(*a*), (*b*) and (*c*) shows the absorbance at 520 nm *versus* the log of the lithium perchlorate concentration for ligands **1**, **4** and **5**, respectively, at each level of sodium perchlorate interferent. The monochromogenic ligand, **4**, displayed the best lithium against sodium selectivity. Selectivity coefficients of 73.5, 50.0 and 31.6 against 0.05 mol l^{-1} sodium and 73.3, 36.8 and 31.5 against 0.1 mol l^{-1} sodium for ligands **4**, **5** and **1**,

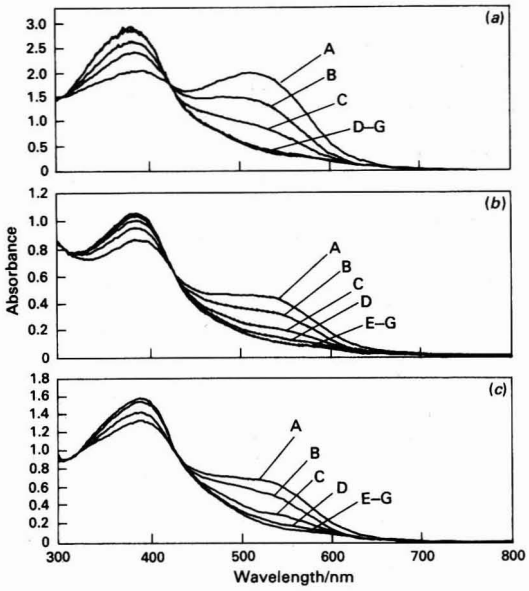

Fig. 1 One-phase investigation of changes in the absorbance spectrum of 2.5 ml of solutions of (*a*) 5.0×10^{-5} mol l^{-1} ligand **1**, and (*b*) 5.0×10^{-5} mol l^{-1} ligand **4** and (*c*) 6.0×10^{-5} mol l^{-1} ligand **5**, in THF with 100 μl of TDDA, upon addition of aqueous lithium perchlorate, with final lithium concentrations of: A, 0.1; B, 1×10^{-2}; C, 1×10^{-3}; D, 1×10^{-4}; E, 1×10^{-5}; F, 1×10^{-6} mol l^{-1}; and G, 0 mol l^{-1}

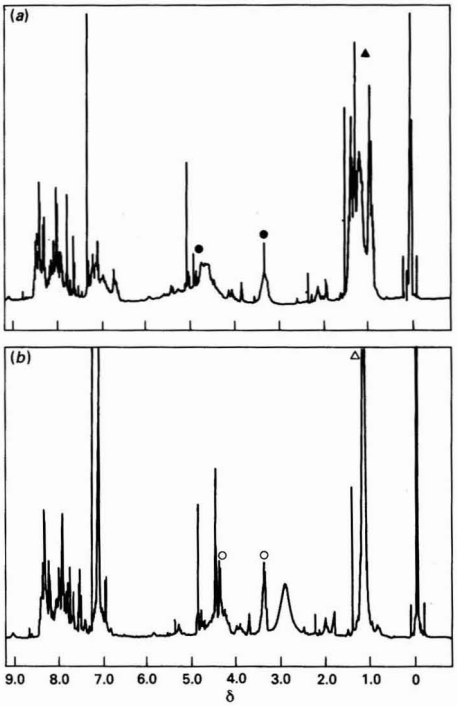

Fig. 2 Partial proton NMR spectra for ligand **1**. (*a*) Before addition of NaSCN. (*b*) After addition of 1 molar equivalent of sodium thiocyanate in deuteriated methanol to a solution of ligand **1** in deuteriated chloroform. Symbols: Δ and ▲, *tert*-butyl; ○ and ●, $ArCH_2Ar$ (filled symbol = before complexation with lithium ions, open symbol = after complexation with lithium ions)

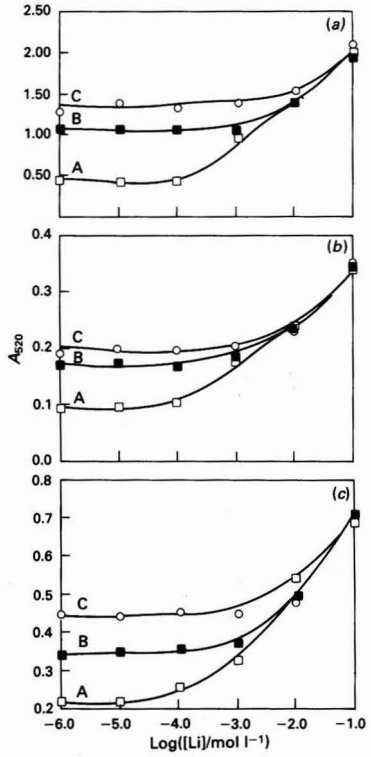

Fig. 3 One-phase studies of the optical response of 5.0×10^{-5} mol l^{-1} solutions of: (*a*) 5.0×10^{-5} mol l^{-1} ligand **1**, and (*b*) 5.0×10^{-5} mol l^{-1} ligand **4** and (*c*) 6.0×10^{-5} mol l^{-1} ligand **5**, in THF with 100 μl of TDDA, with varying concentrations of lithium perchlorate in the presence of fixed concentrations of sodium perchlorate. Response measured at 520 nm

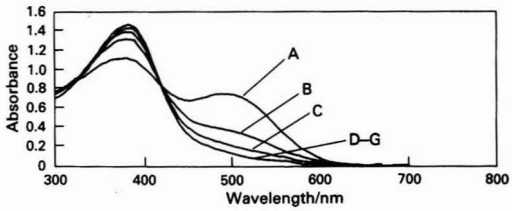

Fig. 4 One-phase investigation of changes in the absorbance spectrum of 2.5 ml of 5.0×10^{-5} mol l^{-1} solution of ligand **1** in butan-1-ol with 100 μl of TDDA, upon addition of lithium perchlorate, with final lithium concentrations of: A, 0.1; B, 1×10^{-2}; C, 1×10^{-3}; D, 1×10^{-4}; E, 1×10^{-5}; F, 1×10^{-6} mol l^{-1}; and G, 0 mol l^{-1}

respectively, were estimated. These values are an improvement on those obtained previously with the nitrophenol ligand.[9] When potassium perchlorate was used as the complexing metal, no colour or spectral change was observed until a final concentration of potassium perchlorate of 0.1 mol l^{-1} had been added, suggesting that all three ligands are very selective against this metal ion.

In the two-phase studies, the best results were obtained with butan-1-ol, which showed little or no leaching of the coloured complex into the aqueous phase. Hence, it was decided to examine further ligands **1**, **4** and **5**, in this solvent. It was found that by using TEA, a large increase in colour intensity, which was independent of metal perchlorate concentration was noticed upon addition of water to the system. It was therefore decided to use a weaker and more hydrophobic base, namely TDDA. Upon addition of TDDA to a solution of ligand **1** in butan-1-ol the colour changed from yellow to slightly orange. This colour was more intense than that observed when TDDA was added to solutions of the ligand in THF. This increased colour is indicative of a solvent dependency on coloration with, in this instance, butan-1-ol being a more basic solvent than THF. Fig. 4 shows the change in the UV/VIS absorbance spectra of ligand **1** dissolved in butan-1-ol, in the presence of TDDA, produced by varying concentrations of lithium perchlorate. Absorbance maxima at 500 nm and isosbestic points at 425 nm are obtained with all three ligands. Upon addition of water to the system, no colour transfer to the aqueous phase was noted even after a number of days. Of the three ligands, ligand **1** was the only one with which a discernible concentration dependent colour or spectral change was evident after the addition of the lithium perchlorate to the aqueous layer of the two-phase system.

Conclusion

Three new chromoionophores that exhibit a dramatic colour change upon complexation with lithium ions, and to a lesser extent sodium ions, have been synthesized. The colour change occurs only in the presence of a base. The base chosen affects the level of absorbance of the complexed compound, as does the solvent in which it is dissolved. Further work on two phase systems and on the incorporation of these compounds into optical sensors is in progress.

We gratefully acknowledge financial support for this research, which was jointly funded by the Irish Science and Technology Agency (Eolas) (grant no. SC/92/319) and Eolas/Amagruss Electrodes (Ireland) Ltd. (grant no. HEIC/91/327).

Appendix

Structures of Compounds Discussed in the Text

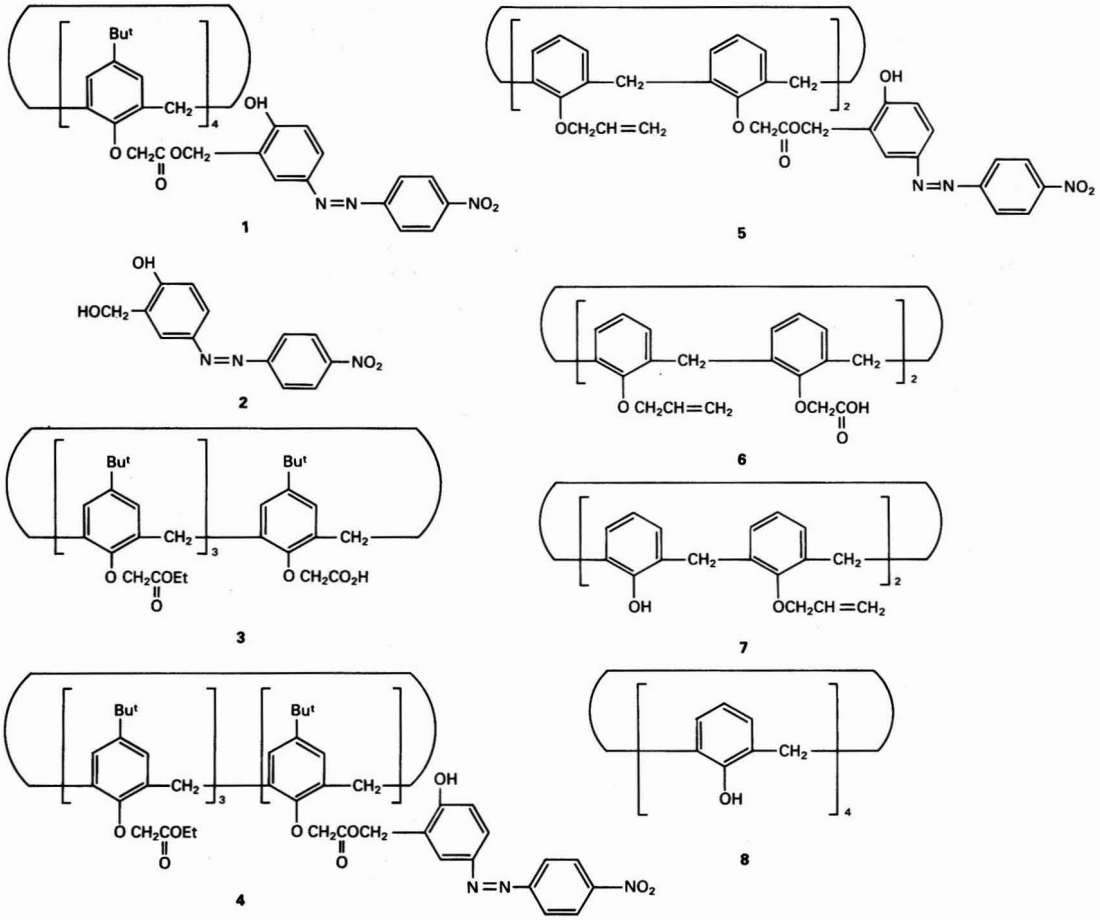

References

1 Kaneda, T., Sugihara, K., Kamiya, H., and Misumi, S., *Tetrahedron Lett.*, 1981, **22**, 4407.
2 Moss, R. E., and Sutherland, I. O., *Anal. Proc.*, 1988, **25**, 272.
3 Misumi, S., and Kaneda, T., *J. Inclusion Phenom. Mol. Recognit. Chem.*, 1989, **7**, 83.
4 Cram, D. J., *Angew. Chem., Int. Ed. Engl.*, 1986, **25**, 1039.
5 Cram, D. J., Carmack, R. A., and Helgeson, R. C., *J. Am. Chem. Soc.*, 1988, **110**, 571.
6 Shimizu, H., Iwamato, K., Fujimoto, K., and Shinkai, S., *Chem. Lett.*, 1991, 2147.
7 Nakamoto, Y., Nakayama, T., Yamagishi, T., and Ishida, S., Presented at the Workshop on Calixarenes and Related Compounds, Johannes Gutenberg-Universität, Mainz, Germany, August 28–30, 1991, Poster 1.
8 King, A. M., Moore, C. P., Sandanayake, K. R. A. S., and Sutherland, I. O., *J. Chem. Soc., Chem. Commun.*, 1992, 582.
9 McCarrick, M., Wu, B., Harris, S. J., Diamond, D, Barrett, G., and McKervey, M. A., *J. Chem. Soc., Chem. Commun.*, 1992, 1287.
10 Ungaro, R., Pochini, A., and Andretti, C. D., *J. Incl. Phenom.*, 1984, **2**, 199.
11 Böhmer, V., Vogt, W., Harris, S. J., Leonard, R. G., Collins, E. M., Deasy, M., McKervey, M. A., and Owens, M. J., *J. Chem. Soc., Perkin Trans. 1*, 1990, 431.
12 Harris, S. J., MacManus, M., and Guthrie, J., European Pat., EP 0309291A1, assigned to Loctite (Ireland) Ltd., March 29, 1889.
13 Harris, S. J., Woods, J. G., and Rooney, J. M., US Pat. 4642362, assigned to Loctite (Ireland) Ltd., February 10, 1987.
14 Arnaud-Neu, F., Collins, E. M., Laitner, B., Deasy, M., Ferguson, G., Harris, S. J., Lough, A. J., McKervey, M. A., Marques, E., Ruhl, B. L., Schwing-Weill, M. J., and Seward, E. M., *J. Am. Chem. Soc.*, 1989, **111**, 8681.
15 Van Loon, J. D., Arduini, A., Verboom, W., Ungaro, R., Van Hummel, G. J., Harkema, S., and Reinhoudt, D. N., *Tetrahedron Lett.*, 1989, **30**, 2681.
16 Jin, T., Ichikawa, I., and Koyama, T., *J. Chem. Soc., Chem. Commun.*, 1992, 499.
17 Arnaud-Neu, F., Barrett, G., Cremin, S., Deasy, M., Ferguson, G., Harris, S. J., Lough, A. J., Guerra, L., McKervey, M. A., Schwing-Weill, M. J., and Schwinte, P., *J. Chem. Soc., Perkin Trans. 2*, 1992, 1119.

Paper 3/01589K
Received March 19, 1993
Accepted May 4, 1993

Inverted Poly(vinyl chloride)–Liquid Membrane Ion-selective Electrodes for High-speed Batch Injection Potentiometric Analysis

Jianmin Lu and Qiang Chen
Department of Chemistry and Biochemistry, New Mexico State University, Las Cruces, NM 88003, USA

Dermot Diamond*
School of Chemical Sciences, Dublin City University, Dublin 9, Ireland

Joseph Wang*
Department of Chemistry and Biochemistry, New Mexico State University, Las Cruces, NM 88003, USA

Sodium and potassium ion-selective electrodes based on the ionophores valinomycin and tetramethyl-*p*-*tert*-butylcalix[4]arene tetraacetate immobilized in a poly(vinyl chloride) membrane were fabricated for use in an inverted configuration for batch injection (BI). The results suggest that BI can be used for routine assays involving these and similar electrodes. Peak shapes obtained under fast and zero stirring conditions are contrasted with those obtained using flow injection (FI). It is concluded that, unlike FI, BI peaks are primarily obtained under kinetically limiting conditions with negligible dispersion. This enables changes in over-all potential arising from surface and bulk effects to be clearly distinguished and will therefore provide an important tool for studying fundamental membrane exchange processes. The analytical performance is characterized by a fast, sensitive and reproducible response. Applicability to assays of mineral water is illustrated.

Keywords: *Batch injection; ion-selective electrode; membrane exchange; potassium and sodium; kinetics*

Ion-selective electrodes (ISEs) are widely used for the routine monitoring of various analytes.[1] Their success is based on the selective and fast response for the target species, low cost and simple, portable instrumentation. Cation-selective electrodes, particularly for Group I and II metal ions, are usually based on ionophores dissolved in a plasticizer that is dispersed as a liquid membrane in a poly(vinyl chloride) (PVC) supporting matrix.[2] These sensors have been successfully used for many years in batch assays[3] and more recently as detectors in flow injection (FI) systems.[4,5] The advantages offered by FI[6,7] such as reproducible sample handling, automation of sampling and sample processing and relative measurements (peak height) have enabled ISE determinations to be made with excellent precision and accuracy while achieving high sample throughputs.

The fact that batch injection (BI) can offer similar advantages to FI without the problems associated with valves, tubing, detector flow cells and pumps required by FI[8] prompted us to investigate the possibility of using liquid-membrane electrodes for BI. The technique involves injecting small sample volumes (10–100 μl) onto a flat sensor surface in a dilution cell and monitoring the transient response produced by the arrival, passage and dispersion of the sample zone over the sensor surface. Very reproducible and fast responses had been demonstrated previously with amperometric[8,9] and potentiometric[10] (crystalline membrane chloride and fluoride and glass pH) sensors using an Eppendorf pipette to inject the sample. The adaptation of liquid membrane ISEs to BI reported below greatly extends the scope of BI towards numerous ionic analytes for which these sensors are available. The resulting analytical performance compares favourably with that of analogous FI–ISE experiments. The challenge of employing inverted liquid-membrane ISEs (as required by the BI apparatus) and the analytical and fundamental opportunities accruing from such coupling are described below.

* Authors to whom correspondence should be addressed.

Experimental

Electrode Design

Preliminary experiments demonstrated that it was necessary to use the ISE in an inverted position in order to achieve reproducibly the 'wall-jet' effect needed in BI through precise control over the pipette tip to membrane distance and angle. This required modification of the usual PVC electrode design in order to prevent the internal electrolyte from reaching the solder joint between the cable and the internal Ag–AgCl reference electrode. In addition, the internal compartment had to be filled completely with the electrolyte to prevent air bubbles from rising to the internal PVC membrane boundary and affecting the electrode stability.

The design used in this study is shown in Fig. 1. The polycarbonate body was fabricated in two parts, which could be screwed together. An Ag–AgCl reference electrode was soldered to a BNC socket and the latter glued into place with epoxy resin. Silicone polymer was then used to fill the upper portion of the body completely and allowed to project out slightly from the screw-threaded area in order to prevent any cavity from forming on setting, which might allow air to be

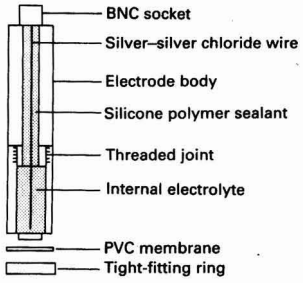

Fig. 1 Schematic diagram of electrode design developed for use in BI studies

trapped. Discs (diameter 10 mm) were cut from PVC membranes (see below) with a cork borer and securely clipped into place on the electrode tip using a tight-fitting polycarbonate ring to give a final exposed membrane disc of diameter 5 mm. A slight bevel on the inside edge of the ring prevents cutting of the PVC membrane as the ring is pressed onto the electrode body. The PVC serves as its own gasket and effectively seals the internal electrolyte from the external solution.

The lower electrode compartment was then back-filled with the internal electrolyte (0.1 mol l^{-1} chloride solution of the primary ion) and, when completely filled, screwed to the upper part of the body so that air was completely excluded. This electrode can then be used in an inverted position for extended time periods without adversely affecting the signal stability. Following attachment of a new membrane, electrodes were left to condition in a 0.1 mol l^{-1} solution of the primary ion chloride for at least 1 h prior to use. New electrodes were then checked in a series of primary ion solutions by means of conventional beaker-to-beaker steady-state measurements to ensure a satisfactory slope function ($S > 50$ mV per decade change in primary ion activity) prior to insertion in the BI cell. Electrode bodies were graduated for length to a resolution of 0.5 mm to facilitate pipette tip to ISE membrane separation studies. With this design, PVC membranes can be changed in a few seconds if problems arise with the ISE response.

PVC Membranes

Sodium- and potassium-selective PVC membranes were prepared in the following manner. A 10 mg amount of the ionophores (tetramethyl-*p*-*tert*-butylcalix[4]arene tetraacetate for sodium and valinomycin for potassium) and 2 mg of ion exchanger [potassium tetra-*p*-chlorophenylborate (KTpClPB)] were dissolved in 1 g of plasticizer [*o*-nitrophenyl octyl ether (*o*-NPOE)] and 0.5 g of high relative molecular mass PVC was added to give a slurry. Tetrahydrofuran (THF) was added dropwise until a clear solution was obtained and the resulting, slightly viscous solution was poured into a glass Petri dish and left covered with a loosely fitting lid for 24 h. Evaporation of the THF left clear PVC membranes of approximately 0.2 mm diameter, from which the sensor discs were cut. All the above materials were of Selectophore grade and obtained from Fluka, except for the sodium ionophore,[11] which was synthesized and purified as described previously.[12]

BI Cell and Procedure

The 600 ml volume cylindrical BI cell (see Fig. 2) was constructed from Plexiglas and is similar in design to those reported earlier,[13] with the exception of the use of an electronic stirrer consisting of a glass rod driven by a small d.c. motor (Model 273-223; Radio Shack) instead of a magnetic stirrer in order to minimize noise. In addition, a tapered injection port was incorporated to give very reproducible pipette positioning and hence reproducible angles and distances between the electrode surface and the pipette tip, a precondition if the constraints of the wall-jet hydrodynamics are to be met.[14] Injections are easy to perform and, given the short timescale involved in generating a result (about 30 s), large numbers of replicate measurements can be performed on relatively small sample volumes, giving high confidence in the final assay. These assays were carried out manually as described in earlier BI studies.[8–10] Injections (usually 100 μl) were made using an Eppendorf micropipette placed 2 mm from the ISE membrane. Owing to the very high selectivity of these ligands against lithium ions,[15] LiCl was used in most experiments as an ionic strength adjustment buffer in samples, standards and the cell filling solution, usually at a concentration of 0.1 mol l^{-1}. Measurements of physiological levels of sodium also employed 9.8 mmol l^{-1} NaCl in the cell solution. As in FI, ionic strength buffering is an important consideration if real responses are to be distinguished from electronic artifacts.

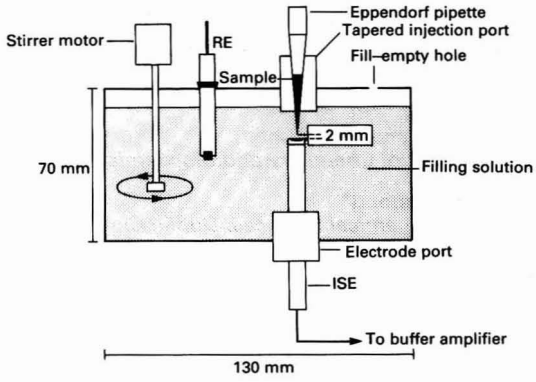

Fig. 2 Schematic diagram of cylindrical BI cell

Reagents and Instrumentation

Potassium (Fisher Scientific), sodium, ammonium, magnesium and lithium chloride, calcium nitrate and potassium hexacyanoferrate(II) (Baker Chemical) were of analytical-reagent grade. Mineral water samples (Naya Canadian Natural Spring Water, Gerolsteiner Sparking Mineral Water and Deming Waters 'Low-Sodium' Deep Well Mineral Water) were obtained in a local supermarket and were used as received.

Cell potentials were measured using a Bioanalytical Systems (BAS) *X–Y–t* recorder after impedance conversion with a laboratory-made voltage follower (input impedance $>10^{12}$ Ω). Two Ag–AgCl reference electrodes, BAS Model RE-1 and Cole-Parmer No. G-05992-20, were used for the potentiometric measurements. Amperometric measurements were made using a BAS glassy carbon electrode (MF 2012) with a platinum wire auxiliary electrode and a BAS Model RE-1 Ag–AgCl reference electrode, linked to a BAS CV27 potentiostat. All the amperometric measurements were obtained using a working electrode potential of +0.8 V *versus* the Ag–AgCl reference electrode. Prior to use, the glassy carbon electrode surface was prepared by polishing with 0.05 μm alumina slurry, rinsing with de-ionized water, sonicating for 5 min and then drying in air.

Results and Discussion

Stability of Sodium ISEs

An example of the high sample throughput coupled with excellent reproducibility obtained with the sodium electrode is illustrated in Fig. 3. Fig. 3(*a*) shows the peaks produced by alternately injecting 100 μl solutions of 16 and 12 mmol l^{-1} sodium chloride (pipette tip to ISE separation 2 mm) into a cell solution of 9.8 mmol l^{-1} sodium chloride (0.1 mol l^{-1} LiCl was used as an ionic strength adjustment buffer for cell and injection solutions). Fast stirring was employed during these measurements, producing peaks which are reminiscent of those obtained using FI, *i.e.*, a sharp profile with some tailing occurring over a time scale of around 30 s. This represents the detector output as sodium ions are transported towards and into the membrane (sharp rise) followed by efficient washout and dilution (dilution factor 6000) of the sample zone into the bulk filling solution (rapid fall). These characteristics are discussed in more detail under Dynamic Response Charac-

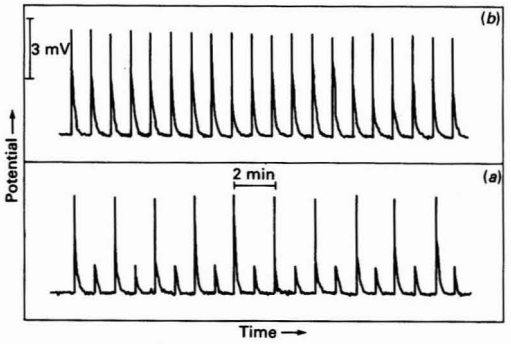

Fig. 3 (*a*) Carryover and (*b*) precision studies with the Na^+ ISE. Cell filling solution 600 ml of 9.8 mmol l^{-1} NaCl–0.1 mol l^{-1} LiCl in both instances. Transient signals produced with a 2 mm separation distance from the pipette tip to the ISE membrane under fast stirring with 100 μl injections of (*a*) 16 mmol l^{-1} NaCl (high) and 12 mmol l^{-1} NaCl (low) and (*b*) 16 mmol l^{-1} NaCl (part of a sequence of 40 injections, s_r = 1.7%)

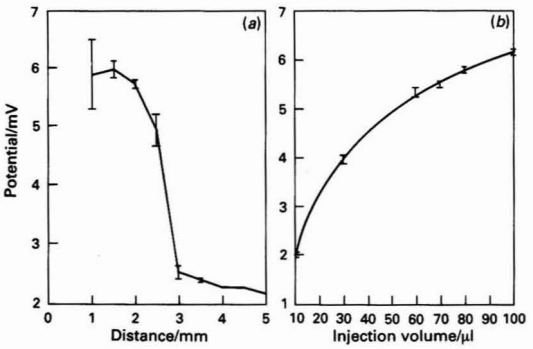

Fig. 4 (*a*) Optimization of the distance from the pipette tip to the ISE. Injections were of 100 μl 16 mmol l^{-1} NaCl into a cell filling solution of 9.8 mmol l^{-1} NaCl with 0.1 mol l^{-1} LiCl used as ionic strength adjustment buffer for both injection and cell filling solutions. (*b*) Optimization of injection volume, solutions used as for (*a*)

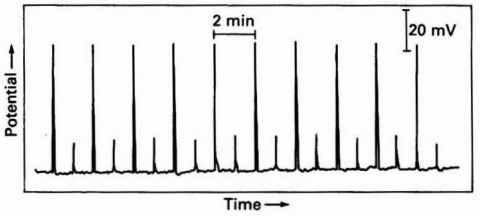

Fig. 5 Precision and carryover studies with the valinomycin K^+ ISE. Background electrolyte 10^{-3} mol l^{-1} LiCl in all solutions; injection volume 100 μl, pipette tip to ISE separation 2.0 mm, fast stirring, high response 10^{-4} mol l^{-1} KCl, s_r = 1.27%, n = 10, average response 66.15 mV; low response 10^{-5} mol l^{-1} KCl, s_r = 5.9%, n = 10, average response 16.85 mV

teristics. Most important is the lack of sample carryover between the two solutions. These results demonstrate that it is possible to perform many sample injections without adversely affecting the peak profile. As a result, replacement of the filling solution is required only after several hundred injections.

Fig. 3(*b*) demonstrates the good reproducibility obtained over a sequence of twenty 100 μl injections of 16 mmol l^{-1} NaCl (pipette tip to ISE separation 2 mm). The relative standard deviation (s_r) obtained over the entire sequence was 1.7% (n = 40), which is excellent considering the likely kinetic-limited nature of the response (the theoretical responses for injections of 16.0 and 12.0 mmol l^{-1} NaCl into 9.8 mmol l^{-1} NaCl are 12.6 and 5.2 mV, respectively, compared with averages of 5.18 and 1.56 mV obtained). Note also the stable baseline obtained during this prolonged experiment. These responses cover the sodium range normally found in blood samples after 10-fold dilution. We are therefore confident that this method could be used to determine blood sodium with good precision and accuracy. This would require proper attention to the disposal of the blood samples accumulated in the cell solution (on its replacement).

Optimization of Cell Parameters

Pipette tip to ISE separation

For these experiments, the cell was filled with 600 ml of a solution of 0.1 mol l^{-1} LiCl and 9.8 mmol l^{-1} NaCl. Using the graduated scale on the ISE body, the electrode was placed at positions from 5.0 to 1.0 mm (in 0.5 mm steps) from the pipette tip. Four injections of 16.0 mmol l^{-1} NaCl (in 0.1 mol l^{-1} LiCl) were made at each position. The results are shown in Fig. 4(*a*). It is clear that the separation should be no more than 2.0 mm if one is to obtain adequate sensitivity. However, as the separation distance decreases from 2.0 mm, there is a decrease in precision, possibly owing to minor variations in the pipette tip position during each injection, which become significant at shorter distances. Hence a separation of 2.0 mm was adopted for most measurements.

Injection volume

Fig. 4(*b*) shows the effect of varying the injection volume of 16.0 mmol l^{-1} NaCl samples into 9.8 mmol l^{-1} NaCl–0.1 mol l^{-1} LiCl from 10 to 100 μl under conditions of constant pipette tip to ISE separation (2.0 mm) and fast stirring. There is an exponential increase in the response, levelling off towards 100 μl although still increasing, suggesting that the theoretical response (12.6 mV) will eventually be reached. This volume represents a good compromise between sensitivity and amount of material and was used for most of the experimental work.

Performance of Valinomycin-based K^+ ISE

Experiments were also carried out using a valinomycin-based K^+ ISE to investigate whether the electrode design would perform satisfactorily with other ionophores. Fig. 5 shows the results obtained for alternating 100 μl injections of 10^{-4} mol l^{-1} (high) and 10^{-5} mol l^{-1} KCl (low) into a 10^{-3} mol l^{-1} LiCl cell filling solution (pipette tip to ISE separation 2 mm, fast stirring). These results strikingly demonstrate that even at the low concentrations used, the response is sensitive and reproducible (s_r = 1.27% for 10^{-4} mol l^{-1} and 5.9% for 10^{-5} mol l^{-1} injections, n = 10), with no observable carryover effects from high to low injections. An almost theoretical Nernstian difference (49.3 mV) is observed between the 10^{-5} and 10^{-4} mol l^{-1} injections.

Dynamic Response Characteristics

The effect of stirring on the response obtained from injecting 100 μl of 10^{-2} mol l^{-1} NaCl into 0.1 mol l^{-1} LiCl is illustrated in Fig. 6(*a*). Clearly, there is a dramatic decrease in the tailing of the peak as one moves from zero stirring (A) to gentle stirring (B) through to fast stirring (C). Interestingly, there is little effect on the peak height, suggesting that the peak

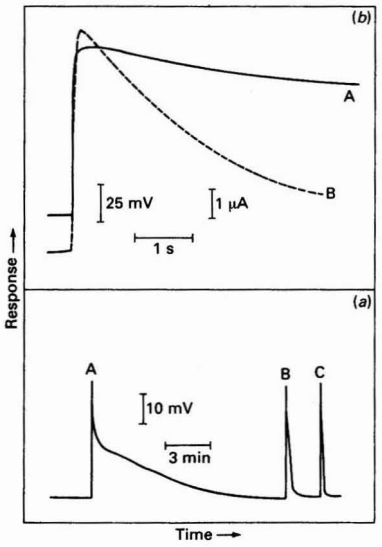

Fig. 6 (*a*) Response of Na^+ ISE to injections of 100 μl of 10^{-2} mol l^{-1} NaCl in 0.1 mol l^{-1} LiCl into 0.1 mol l^{-1} LiCl. A, No stirring; B, slow stirring; and C, fast stirring. (*b*) Response shown on expanded time scale under static (unstirred) conditions of A, K^+ ISE (solid line; 100 μl of 10^{-3} mol l^{-1} KCl in 10^{-3} mol l^{-1} LiCl injected into 10^{-3} mol l^{-1} LiCl); and B, bare glassy carbon electrode [broken line; 100 μl 10^{-3} mol l^{-1} $Fe(CN)_6^{4-}$ injected into 10^{-3} mol l^{-1} LiCl at +0.8 V *versus* Ag–AgCl]

response is primarily controlled by the active transport towards and away from the membrane provided by the wall-jet effect, whereas baseline recovery is controlled by the dynamics of diffusion into the bulk filling solution. This is consistent with the improvement in the washout conditions existing in stirred solutions which reduces the thickness of the Nernst diffusion layer at the electrode membrane and provides efficient mixing of the sample zone with the bulk filling solution. Similarly, the stirrer position had little effect on the peak height or shape (provided that it was at least 2 cm away from the ISE).

The opportunity offered by BI for fundamental studies is clearly evident from the transient profiles presented in Fig. 6(*b*), which compares the dynamic characteristics of the potentiometric response obtained with a valinomycin K^+ liquid membrane electrode (100 μl of 10^{-3} mol l^{-1} KCl injected into 10^{-3} mol l^{-1} LiCl) to the amperometric response of a glassy carbon electrode [100 μl of 10^{-3} mol l^{-1} $Fe(CN)_6^{4-}$ injected into 10^{-3} mol l^{-1} LiCl at +0.8 V *versus* Ag–AgCl] with no stirring. Unlike FI, the sample zone is not in contact with the walls of the tubing, and there is almost instantaneous transfer of the sample to the detector surface and hence nearly zero dispersion. Consequently, the detector output is a true record of its response to an undistorted 'square-wave' concentration impulse. These results demonstrate the almost instantaneous response of the valinomycin ISE to the arrival of the sample, which is even faster than that of the amperometric response of the well polished glassy carbon electrode. This is surprising, considering that the generation of the potentiometric response involves movement of primary ions into the diffusion (Nernst) layer at the ISE membrane boundary, complexation of the metal ions by the ionophore and transfer of the metal complexes into the ISE membrane. The immediate conclusion one can draw from this experiment is that the kinetics of metal ion uptake and complexation by the valinomycin membrane are extremely fast, even in comparison with the electron transfer processes occurring at

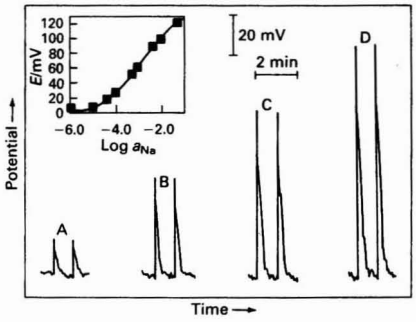

Fig. 7 Calibration graph obtained with Na^+ ISE, 10^{-3} mol l^{-1} LiCl background in all solutions and fast stirring. The electrode slope found by regression over the range from $10^{-4.5}$ to 0.1 mol l^{-1} NaCl is 35.7 mV per decade compared with 54.3 mV per decade obtained in steady-state batch measurements. The limit of detection is around 10^{-5} mol l^{-1} Na^+

the glassy carbon electrode surface. The wall-jet effect of the sample impinging normally onto the sensor surface also aids the dynamic response, as the ions are actively transported into the diffusion layer rather than passively diffusing from the bulk solution.[16]

In contrast, the decreasing signal indicating the diffusion of the sample into the bulk solution, and the consequent removal of primary ions from the diffusion layer and the ISE membrane, is much slower than the glassy carbon response to the $Fe(CN)_6^{4-}$ injection. This can be interpreted as follows. With the glassy carbon electrode, oxidation occurs only at the electrode surface. Hence, as the oxidation of $Fe(CN)_6^{4-}$ proceeds, its concentration in the diffusion layer decreases. With no replenishment available owing to the rapid dilution of the sample plug into the bulk solution, the signal decays relatively quickly. In contrast, K^+ ions can diffuse into the diffusion layer from the PVC liquid membrane phase in response to diffusion of K^+ into the bulk solution from the diffusion layer. Hence the PVC liquid membrane can supply primary ions to the diffusion layer as the concentration profile reverses on passage of the sample zone. In addition, these ions are exchanging reversibly across the membrane boundary and are still active in signal generation, unlike the $Fe(CN)_6^{3-}$ produced at the glassy carbon surface. Overall, these data demonstrate the suitability of BI for exploring the dynamic response behaviour of ISEs. Microcomputer-controlled, high-speed data capture using I/O cards will be used in further studies to examine these features more precisely.

Linear Range

Fig. 7 shows the response obtained to 100 μl injections of Na^+ covering the normal dynamic range of PVC membrane electrodes. Unlike the experiments described above, the cell was filled with 10^{-3} mol l^{-1} LiCl. This represents a compromise between the need for a low-resistance solution to minimize noise and accurate determinations of the sensor limit of detection and linear range. The calibration graph (inset) shows the response to be linear from about $10^{-4.5}$ mol l^{-1} upwards, with some decrease in slope possibly occurring at the upper end of the range. Interestingly, the slope is sub-Nernstian at 35.7 mV per decade compared with 54.3 mV per decade obtained in steady-state batch measurements. This strongly suggests that the electrode is functioning in a kinetic-limited regime under which the characteristics may be different compared with the normal Nernstian behaviour.[17] From the calibration graph, the limit of detection can be estimated to be around 10^{-5} mol l^{-1} Na^+.

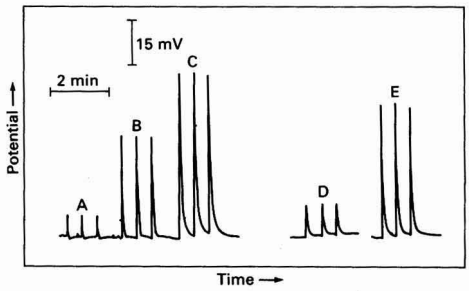

Fig. 8 Analysis of mineral water samples for sodium content. Injection volume 100 μl, pipette tip to ISE separation 2.0 mm, 0.1 mol l^{-1} LiCl filling solution, samples diluted 50 + 50 with 0.2 mol l^{-1} LiCl. A, Naya (labelled 2.6×10^{-4} mol l^{-1} Na^+); B, Deming (labelled 1.2×10^{-3} mol l^{-1} Na^+); C, Gerolsteiner (labelled 4.8×10^{-3} mol l^{-1} Na^+); D, Na^+ standard (10^{-4} mol l^{-1}); and E, Na^+ standard (10^{-3} mol l^{-1})

Table 1 Results of analysis of mineral water samples

	Sodium/mol l^{-1}	
Sample	Labelled	Found
Naya	2.6×10^{-4}	1.8×10^{-4}
Deming	2.7×10^{-3}	1.2×10^{-3}
Gerolsteiner	5.8×10^{-3}	4.8×10^{-3}

Fig. 8 illustrates some preliminary analytical data obtained with mineral water samples. Note again the rapid, sensitive and reproducible response obtained using the BI technique. There is relatively good agreement between the amounts specified on the bottle labels and our results (Table 1). These data suggest that BI coupled with liquid membrane ISEs can provide an inexpensive, reliable and rapid method for screening samples, even at the relatively low concentrations involved in this study.

Conclusions

From the results, we are confident that BI can be effectively used with any PVC liquid membrane electrode suitably modified for use in an inverted configuration. The unique almost zero dispersion conditions offered by the BI technique and the simplicity of the equipment involved will make it a valuable additional tool for both fundamental studies on liquid membrane and other selective sensors and for developing analytical methodologies for many applications in which traditional batch steady-state measurements are currently applied. The robust form of the cell coupled with the ease with which sensors and filling solutions can be changed and simple, inexpensive equipment will appeal to many industries. The performance can be expected to be particularly good when scavenging agents can be added to the cell filling solution in order to prevent the slow build-up of primary ion concentration during a long sequence of injections. Even when these are not readily available (as in the ion studies in this research), larger cells can be fabricated with the required dilution factor relatively inexpensively or, alternatively, the cell design can be modified to allow continuous addition of filling solution.[18] We are continuing our BI investigations into the dynamic response behaviour and applications of these and other PVC liquid membrane electrodes. Arrays of ISEs are also being explored in connection with multi-channel pipettes and a BI operation.

We acknowledge financial support from Dublin City University for D. D. to work at NMSU.

References

1 Arnold, M. A., and Solsky, R. L., *Anal. Chem.*, 1986, **58**, 84.
2 Moody, G. J., and Thomas, J. D. R., in *Chemical Sensors*, ed. Edmonds, T. E., Chapman and Hall, New York, 1988, ch. 3, p. 76.
3 Koryta, J., *Anal. Chim. Acta*, 1984, **159**, 1.
4 Meyerhoff, M., and Kovach, P., *J. Chem. Educ.*, 1983, **60**, 766.
5 Telting Diaz, M., Diamond, D., and Smyth, M. R., *Anal. Chim. Acta*, 1991, **251**, 149.
6 Růžička, J., and Hansen, E., *Flow-Injection Analysis*, Wiley, New York, 2nd edn., 1988.
7 Valcárcel, M., and Luque de Castro, M. D., *Flow-Injection Analysis*, Ellis Horwood, Chichester, 1987.
8 Wang, J., and Taha, Z., *Anal. Chem.*, 1991, **63**, 1053.
9 Chen, L., Wang, J., and Angnes, L., *Electroanalysis*, 1991, **3**, 773.
10 Wang, J., and Taha, Z., *Anal. Chim. Acta*, 1991, **252**, 215.
11 Diamond, D., Svehla, G., Seward, E., and McKervey, M. A., *Anal. Chim. Acta*, 1988, **204**, 223.
12 McKervey, M. A., Seward, E. R., Ferguson, G., Ruhl, B., and Harris, S. J., *J. Chem. Soc., Chem. Commun.*, 1985, 388.
13 Wang, J., *Microchem. J.*, 1992, **45**, 219.
14 Glauert, M. B., *J. Fluid Mech.*, 1956, **1**, 625.
15 Forster, R., Regan, F., and Diamond, D., *Anal. Chem.*, 1991, **63**, 876.
16 Gunasingham, H., and Fleet, B., in *Electroanalytical Chemistry*, ed. Bard, A. J., Marcel Dekker, New York, 1989, vol. 16, p. 99.
17 Diamond, D., and Forster, R. J., *Anal. Chim. Acta*, 1993, **276**, 75.
18 Amine, A., Kaufmann, J.-M., and Palleschi, G., *Anal Chim. Acta*, 1993, **273**, 213.

Paper 3/01324C
Received March 8, 1993
Accepted April 21, 1993

Titrations of Non-ionic Surfactants With Sodium Tetraphenylborate Using the Orion Surfactant Electrode

Robyn Dahl Gallegos
Technology Support Services, Ecolab Inc., St. Paul, MN 55102, USA

A method for the determination of non-ionic surfactants is described. The poly(oxyethylene) portion of non-ionic surfactants forms psuedo-crown compounds in the presence of barium ions. The Orion surfactant electrode is used as the end-point indicator in titrations of these compounds with sodium tetraphenylborate. Stoichiometric constants for the reaction of barium non-ionic complexes with sodium tetraphenylborate have been established. The results of titrations of several non-ionic surfactants indicate that an average of 5.16 oxyethylene units will form a complex with one tetraphenylborate ion. Empirical titration factors have also been established for several classes of non-ionic surfactants and used in the analysis for the non-ionic content of commercial detergent products. An average recovery of 96.4% was obtained in the analysis of three standard detergent products. The described method has been used successfully in the routine determination of non-ionic surfactants.

Keywords: *Non-ionic surfactant; sodium tetraphenylborate; ion-pair titration; Orion surfactant electrode*

Much research has been carried out in the area of potentiometric sensors for the determination of non-ionic surfactants. Vytřas *et al.*[1] prepared a poly(vinyl chloride) (PVC) coated-wire electrode (CWE) plasticized with 2,4-dinitrophenyl octyl ether for the titration of non-ionic surfactants with sodium tetraphenylborate ($NaBPh_4$). With CWEs, the consequence of the ill-defined solid-state internal-reference system is often an unstable reference potential from which a high drift can result. This affects the usefulness of these electrodes. Jones *et al.*[2] prepared a plasticized PVC membrane electrode doped with a barium–non-ionic–tetraphenylborate complex that responded to non-ionic surfactants. The electrode had a useful lifetime of less than 3 weeks. These workers suggested that new membranes are easily prepared, but when considering a sensor that will be used for routine analysis, the lack of convenience and the possibility of adversely affecting reproducibility make this undesirable. Given the problems cited for these electrodes, there remains a need for a stable, reproducible, long-lived electrode and accompanying methodology for the routine determination of non-ionic surfactants.

The Orion surfactant electrode has been commercially available for many years and has proved to be very useful for the determination of anionic and cationic surfactants. We have observed that this electrode also responds to the tetraphenylborate ion. Although the response is sub-Nernstian (36 mV decade^{-1}), it is stable and can be used to monitor the titrations of barium non-ionic complexes with $NaBPh_4$. The potential break at the equivalence-point (>100 mV) is more than adequate for an accurate end-point determination.

Several classes of non-ionic surfactants have been analysed. The experimentally determined constant for the number of oxyethylene units (OEUs) forming a complex with one mole of titrant is 5.16 ± 0.62, which is in agreement (within experimental error) with that reported by Vytřas *et al.*[1] (5.2 ± 0.6) and Sugawara *et al.*[3] (5.64–5.98). Empirical titration factors have been established and used in the determination of non-ionic surfactants in commercial detergent products. A comparison of the titration factors derived using two different electrodes indicates that the method is reproducible and can be used for routine analysis.

Experimental

Apparatus

Potentiometric titrations were carried out using a Brinkmann 670 Titroprocessor (Metrohm, Herisau, Switzerland). Automated titrations were performed by attaching a Brinkmann 665 Dosimat and 673 sample handler. The titrations were monitored using the Orion Model 93-42 surfactant electrode (Orion Research, Cambridge, MA, USA). The Orion Model 90-02 Ag–AgCl double-junction reference electrode, filled with saturated AgCl solution and 10% KNO_3 solution in the inner and outer chambers, respectively, was used as the reference half-cell.

Solutions

Solutions of $NaBPh_4$ (approximately 0.008 mol dm^{-3}) were prepared by dissolving analytical-reagent grade powder, puriss >99.5% (Fluka, Ronkonkoma, NY, USA) in de-ionized water, adjusting the solution to pH 9–10 with NaOH and diluting to 1 dm^{-3}. Thallium(I) nitrate (Fluka) solutions (0.01 mol dm^{-3}) were used for the standardization of $NaBPh_4$ solutions. A 0.2 mol dm^{-3} solution of $BaCl_2$ was prepared by dissolving analytical-reagent grade $BaCl_2 \cdot H_2O$ in distilled water. The source and type of non-ionic surfactants that were studied are summarized in Table 1. Surfactant solutions were prepared by dissolving these raw materials in distilled water.

Titration Procedure

An aliquot of surfactant solution was pipetted into a titration beaker and 2 cm^3 of 0.1 mol dm^{-3} HCl were added. Approximately 150 cm^3 of distilled water were added from a graduated cylinder. The titrator was programmed to dose 5

Table 1 Non-ionic surfactants studied

Surfactant	Manufacturer	Type	OEU
Igepal CO	Rhone-Poulenc	NPE*	9–20
Igepal CA	Rhone-Poulenc	OPE†	7–12
Surfonic N	Texaco	NPE	6–9.3
Tergitol NP	Union Carbide	NPE	6–9.5
Tergitol	Union Carbide	sec. alc-EO‡	9.0
Triton X	Union Carbide	OPE	9.5
Neodol	Shell	alc-EO§	6.5
Plurofac	BASF	alc-EO-PO	8.9

* NPE is a nonylphenoxypoly(ethyleneoxy)ethanol.
† OPE is an octylphenoxypoly(ethyleneoxy)ethanol.
‡ Tergitol 15-s-9 is an oxyethylenated alcohol with average alkyl and OEUs of C_{13} and 9, respectively.
§ Neodol 23–6.5 is an oxyethylenated linear primary alcohol with average alkyl and OEUs of C_{12} and 6.5, respectively.

cm^3 of 0.2 mol dm^{-3} $BaCl_2$ into the titration beaker at a rate of 5.0 cm^3 min^{-1}. The solution was then stirred for 240 s before the start of the titration. The titrations were performed according to a dynamic method in which the dose rate is governed by the change in potential so that the rate is decreased in the vicinity of the end-point. The maximum dose rate was set at 4 cm^3 min^{-1} with a drift requirement of 8 mV min^{-1}. The titrations were stopped with the identification of one equivalence-point, and the sample handler was then advanced to a conditioning solution. The conditioning solution was prepared by adding 2 cm^3 of 0.1 mol dm^{-3} HCl to approximately 150 cm^3 of distilled water. The electrodes were conditioned in this beaker, with stirring for 10 min, before the next titration.

The ternary complex, barium–non-ionic–tetraphenylborate, which is precipitated during the titration, is very insoluble in water and adsorbs onto the surfactant electrode materials. After several titrations have been performed, the electrode body and membrane can become coated with this complex. When the coating is dried on the membrane and not removed, both the accuracy and precision of the method are adversely affected. In order to improve the reproducibility and to ensure proper electrode care, the following analysis protocol was established. The titrations were performed in groups (all in 1 d rather than sporadically over the course of several days). All of the titrations were performed using an automatic titrator equipped with a sample handler. After a group of samples had been analysed, the electrode was allowed to air-dry. The membrane was then cleaned with gentle wiping and forced air before subsequent use. The reconditioning steps recommended by the manufacturer were also followed. We have observed an electrode lifetime of greater than 7 months and this can be extended with proper electrode care.

Results and Discussion

Electrode Response

The response of the Orion surfactant electrode to the ionic species involved in the determination of non-ionic surfactants is illustrated in Fig. 1. The slopes determined for the species that the electrode was designed to monitor, *i.e.*, sodium lauryl sulfate (SLS) and (diisobutylphenoxyethoxyethyl)dimethylbenzylammonium chloride (Hyamine 1622), are 46.0 and 51.1 mV $decade^{-1}$, respectively. The sub-Nernstian response to the tetraphenylborate ion is acceptable when considering the near-Nernstian reponse of the electrode to SLS and Hyamine 1622. The response to the tetraphenylborate ion is stable with less than 1 mV $decade^{-1}$ difference between the slopes determined using two different electrodes. Given that and the fact that a Nernstian response is not required when the electrode is used as an end-point indicator, we have found the Orion surfactant electrode suitable for this application.

It is known that after regular use with a strongly interfering ion the selectivity of an ion-selective electrode can change.[4] Because the Orion surfactant electrode is designed for the determination of anionic surfactants and it was found to respond to the tetraphenylborate ion, this ion can be considered as a strongly interfering species. An experiment was conducted in which the response of a new electrode, electrode A, was compared with the response of an electrode that had been used to monitor titrations of non-ionic surfactants for a period of 7 months, electrode B. The data summarized in Fig. 2 indicate that the response to SLS is decreased from 46.0 to 7.7 mV $decade^{-1}$ with repeated exposure to the tetraphenylborate ion. This is an indication that the membrane has been chemically altered.

The change in electrode response is most likely due to two key factors related to the membrane: the alteration of the bulk composition and the loss of free volume. Sugawara *et al.*[3] suggested that the partitioning of the hydrophobic ions between the membrane and sample solution phase dominates

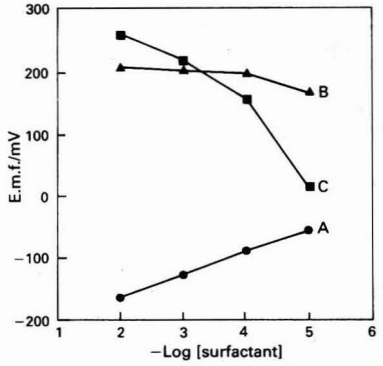

Fig. 1 Plot of potential *versus* −log [surfactant] obtained with the Orion surfactant electrode. A, $NaBPh_4$; B, Ba–Surfonic N95; and C, thallium nitrate

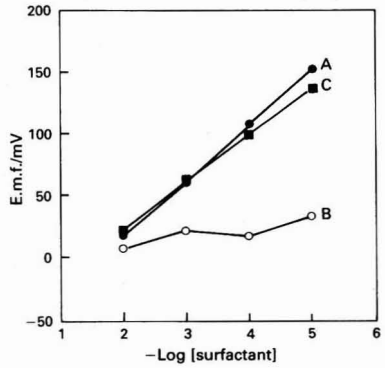

Fig. 2 Plot of potential *versus* −log [surfactant] obtained with the Orion surfactant electrode. A, Electrode A with SLS; B, electrode B with SLS; and C, electrode B after reconditioning with SLS

the electrode kinetics and establishes the interfacial potential. The hydrophobic tetraphenylborate ion favours the membrane phase and will most likely be absorbed by the membrane and dominate the measurement of the electrode potential. The long-term change in electrode response after exposure to the tetraphenylborate ion suggests that the ion is not only altering the membrane composition at the surface, but also diffusing into the bulk of the membrane. A qualitative analysis of the internal filling solution of an electrode used to monitor the titrations of non-ionic surfactants for a period greater than 5 months, using Fourier transform infrared spectroscopy, indicated the presence of $NaBPh_4$. As it is unlikely that this compound was a formulated species in the internal solution, this is a clear indication of the diffusion of this species into the bulk of the membrane. Cutler and Meares[5] suggested that the mobilities of ions in the membrane phase can be affected by the loss of free membrane volume that occurs with repeated use. The diffusion of the tetraphenylborate ion into the membrane has affected the response to SLS by both decreasing the free membrane volume and altering the interfacial potential.

If the analysis protocol that has been described is followed, the surfactant electrode will not be exposed to excess tetraphenylborate and the rate of change of the response to SLS will be greatly decreased. Moreover, as is illustrated in Fig. 2, the exposure of electrode B to SLS for 48 h increased the response to this species from 7.7 to 38.7 mV $decade^{-1}$. This clearly indicates that the change in electrode response is reversible.

Stoichiometry

Non-ionic surfactants will form complexes with a variety of monovalent and divalent cations. The stability of the metal non-ionic surfactant complex is dependent on the ionic radius of the metal ion in relation to the radius of the helical conformation of the psuedeo-crown complex that is formed by the oxyethylene portion of the non-ionic surfactant molecules. The structure of a pseudo-crown complex compared with that of a true crown ether complex is illustrated in Fig. 3. The metal ion is held in a 'cage' of the oxygen atoms of the poly(oxyethylene) portion of the non-ionic surfactant by an ion–dipole interaction.[6] Vytřas *et al.*[1] have confirmed that the stoichiometry of the complex formation of non-ionic surfactants with divalent cations requires that approximately 11 OEUs form a complex with one metal ion.

The use of barium to form complexes with non-ionic surfactants for subsequent titration with $NaBPh_4$ has been widely reported in the literature.[1,2,7,8] Sanchez and Vytřas[7] have shown that complex formation with Ba is preferred to that with Ca and Cd. They indicated that the potential break in titrations of metal ions with $NaBPh_4$ in the presence of poly(ethylene glycol) (PEG) decreased with decreasing ionic radius of the metal ion. In fact, because of the decrease in the stability of the metal–non-ionic surfactant complex with Ca and Cd, the shallowness of the titration curve, and the deviation from the theoretical equivalence-point, it was decided that these titrations are not suitable for practical use. It was also found that Ba is preferable to Ca in the titrations with the Orion electrode. A decrease in the potential break was observed in the titrations of calcium non-ionic complexes. Also, the nature of the precipitate and its adsorption onto the electrode materials were even more unfavourable than with the barium salt.

The stoichiometry of the complex-forming reaction is dependent on the ionic radius of the cation and on the chain length of the oxyethylene portion of the non-ionic surfactant, and this defines the stoichiometry of the reaction of these complexes with $NaBPh_4$. The results for the analysis of homologous series of nonylphenoxy and octylphenoxy poly(oxyethylene) surfactants are summarized in Table 2. The average value of 5.56 ± 0.40 OEUs per mole of titrant agrees well with that reported by Sugawara *et al.*[3] With the exception of Igepal CA620, the variation in stoichiometric constants within a homologous series is small. Samples from several classes of non-ionic surfactants were also titrated. The results are summarized in Table 3. An average stoichiometric constant, calculated from the results of determinations of all of the non-ionic surfactants studied, of 5.16 was obtained.

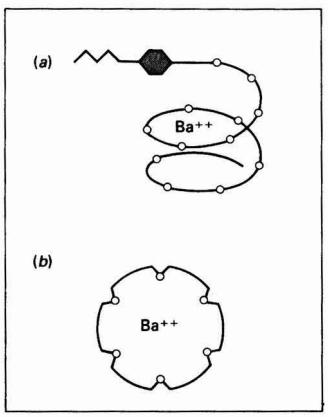

Fig. 3 Comparison of structures. (*a*) A pseudo-crown complex, (*b*) a crown ether complex

The factors affecting the complex formation of the OEUs include the polydispersity or distribution of oxyethylene chain length molecules within the non-ionic surfactant and the structure of the hydrophobic portion of the molecule. The average stoichiometric constant of 5.16 reported in this work most closely resembles the average value reported by Vytřas *et al.*[1] They obtained the average value of 5.2 from the analysis of several different classes of non-ionic surfactants forming complexes with several different cations. However, if the average constant is calculated from the data summarized in Table 2, the value obtained (5.56) most closely resembles those reported by Sugawara *et al.*[3] (5.64–5.98). They reported on the stoichiometric constants of the barium salts of poly(oxyethylene) mono(alkylphenyl)ether surfactants, which are similar to those summarized in Table 2. Vytřas *et al.*[1] also pointed out that only those non-ionic species with at least five OEUs are titratable. Igepal CA620 is the only surfactant in the series summarized in Table 2 with a stoichiometric constant of <5. It has an average OEU chain length of 7.2. In fact, all of the surfactants studied with calculated stoichiometric constants of <5 have an average OEU chain length of <8.5. With a lower average number of OEUs, it is more probable that a higher percentage of the molecules have chain lengths of <5. It is possible that the use of an average number of OEUs does not provide adequate information for interpreting these results and that information regarding the polydispersity of these surfactants could be used to understand fully the stoichiometric constants that have been reported here. Levins and Ikeda[8] suggested that the spatial arrangement of the atoms in the crystal lattice of the

Table 2 Results of titrations of homologous series of non-ionic surfactants

Non-ionic surfactant	Mean number of OEUs (Rhone-Poulenc)	Stoichiometric constant* (nOEU/$n$$BPh_4^-$)
Igepal CO630	9	5.56 ± 0.24
Igepal CO710	10.4	5.83 ± 0.22
Igepal CO720	12	5.94 ± 0.18
Igepal CO730	15	5.90 ± 0.17
Igepal CO850	20	5.54 ± 0.14
Igepal CA620	7.2	4.66 ± 0.48
Igepal CA630	9.5	5.62 ± 0.29
Igepal CA720	12.5	5.46 ± 0.02

* Stoichiometric constants are stated as the mean of three determinations plus or minus the range ($x_{max} - x_{min}$).

Table 3 Results of titrations of several classes of non-ionic surfactants

Non-ionic surfactant	Mean number of OEUs (^{13}C NMR)	M_r*/ g mol^{-1} (^{13}C NMR)	Titration factor† ($n$$BPh_4^-$/$n$ surfactant)	Stoichiometric constant (nOEU/n BPh_4^-)
Surfonic N95	8.3	585	1.87 ± 0.17‡	4.43 ± 0.40‡
Surfonic N60	5.3	453	1.28 ± 0.09	4.12 ± 0.29
Tergitol NP-9	8.6	598	1.69 ± 0.05	5.09 ± 0.15
Tergitol NP-9.5	8.8	607	1.74 ± 0.09	5.05 ± 0.26
Triton X-100	10.0	646	1.83 ± 0.06	5.47 ± 0.18
Tergitol 15-s-9	8.4	569	1.87 ± 0.09	4.48 ± 0.22
Neodol 23–6.5	7.6	527	1.85 ± 0.22	4.09 ± 0.49
Plurofac B255	8.9 PO§ 3.1	755	2.26 ± 0.10	5.32 ± 0.24

* Calculated from the average number of OEUs determined by ^{13}C nuclear magnetic resonance (NMR) spectroscopy.

† Empirical titration factors used in the calculation of % non-ionic surfactant in product mixtures.

‡ The values stated represent the mean of two determinations plus or minus the range (x_{max}–x_{min}).

§ PO = propylene oxide. Plurofac B255 includes approximately 3 PO units in addition to the OEUs.

ternary complex demands a minimum stoichiometric constant of 5.2.

The structure of the hydrophobic portion of these molecules could also affect the arrangement of the atoms in the crystal lattice and the stoichiometry of the complex formation. Izatt *et al.*[9] studied the ability of cations to form stable complexes with two isomers of cyclic polyethers. They suggested that the differences in the experimentally determined thermodynamic properties between the two isomers can be explained by the steric orientation of the hydrophobic cyclohexyl groups. It is possible that the increased variation in the stoichiometric constants reported in Table 3 could be explained by the various hydrophobic end-groups of the non-ionic surfactants affecting the complex formation and stoichiometry of these reactions. For instance, Tergitol NP-9 and 15-s-9 have similar average OEU chain lengths. The difference, 5.09 ± 0.15 and 4.48 ± 0.22, respectively, in the determined constant could be due to the difference in the hydrophobic portions of these molecules, nonylphenol and secondary tridecanol, respectively. As the manufacturer of these two surfactants is the same, a large change in polydispersity would not be expected. However, a summary of this work and the reported literature suggest that the length of the oxyethylene chain dominates the stoichiometry of these reactions.

Titrations

Vytřas[10] suggested that, if either the substance determined or titrant is changed, a membrane-conditioning step is needed. He chose to precede his analysis with one or two titrations. Levins and Ikeda[8] also conditioned the solid-state silver electrode that they used by making a rough titration with a PEG standard. We chose to perform three titrations of a non-ionic surfactant, which preceded all analyses each day for membrane conditioning. Standard titrations of thallium nitrate and of Surfonic N95 with $NaBPh_4$ are illustrated in Fig. 4. It is shown that the potential break at the equivalence-point (>100 mV) is more than adequate for precise and accurate end-point identification.

In order to establish an empirical titration factor (an experimentally determined factor indicating the volume of titrant required for a specific concentration of a surfactant), three titrations of the raw material were performed and the results were averaged. These values are reported in Table 3 for various surfactants. As the reproducibility of this determination affects the precision of the method, a titration factor was established for Surfonic N95 by titrating a solution five times using each of the two electrodes that have been previously described. It can be seen from the data summarized in Table 4 that the titration factors are very similar. A pooled variance *t*-test indicates that the difference is not statistically significant at the 95% confidence level. After a titration factor has been obtained for a specific surfactant, and a sample containing that surfactant has been titrated according to this method, the factor is then used in the determination of the non-ionic surfactant content of that product.

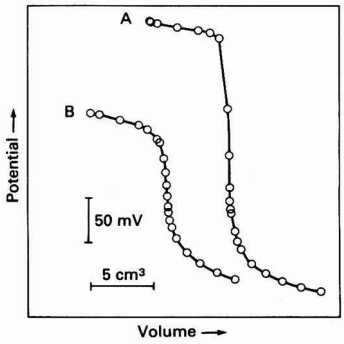

Fig. 4 Automated potentiometric titrations of samples with $NaBPh_4$ (about 0.008 mol dm^{-3}) as titrant using the Orion surfactant electrode as end-point indicator. A, Thallium nitrate (13.32 mg). B, Surfonic N95 (20 mg) in the presence of barium(II) chloride

Three laboratory-prepared samples of a laundry detergent in which the non-ionic content ranged from 13 to 39% were analysed according to this method. The empirical titration factor was determined by titrating the non-ionic surfactant that was used to make the products. The results are summarized in Table 5. An average recovery of 96.4 ± 4.3% was obtained. Although the data in Table 5 indicate an average recovery <100%, the accuracy of the method is acceptable for the determination of non-ionic surfactants in product systems. For the analysis of various detergent products, quaternary surfactants will be titrated by $NaBPh_4$ and these will interfere in the determination of non-ionic surfactants. The concentration of quaternary surfactant can be determined by another method[11] and then subtracted from the result of the titration with $NaBPh_4$ in order to determine the non-ionic surfactant content. Anionic surfactants could also interfere and should be removed before analysis.

Conclusion

Currently, most of the literature reports the use of laboratory-prepared CWEs or PVC membrane electrodes for the determination of non-ionic surfactants. The preparation of these electrodes is not convenient when considering their use in routine analysis. The Orion surfactant electrode has been used successfully as an end-point indicator in the automated titration of non-ionic surfactants with $NaBPh_4$. With proper electrode care, the electrode lifetime is greater than 7 months, and the apparent change in the selectivity of the electrode that occurs as a consequence of monitoring these titrations is reversible. Empirical titration factors can be established and

Table 4 Comparison of empirical titration factors determined by using electrodes of different ages

Titration of Surfonic N95	Orion surfactant electrode A (titration factor*)	Orion surfactant electrode B (titration factor*)
1	1.833	1.727
2	1.715	1.532
3	1.632	1.515
4	1.590	1.495
5	1.620	1.487
Mean	1.678	1.551
Relative standard deviation (%)	5.8	6.4

* Titration factors are expressed as moles of $NaBPh_4$ per mole of non-ionic surfactant. Electrode A: new electrode. Electrode B: electrode has been used to determine non-ionic surfactants for more than 7 months.

Table 5 Determination of the recovery of non-ionic surfactants in formulated products according to the titration with $NaBPh_4$

Detergent product formula (% non-ionic surfactant)	Titrated (% non-ionic surfactant)	Recovery (%)
13	11.9	91.5 ± 1.0
26	25.9	99.5 ± 1.0
39	38.4	98.4 ± 1.9

* Calculated as the mean of three determinations using the titration factor for the raw material and the formulated amount as the true value plus or minus the range (x_{max}–x_{min}).

used in the determination of non-ionic surfactants in commerical detergent products. An average recovery of greater than 96% has been achieved.

The author is indebted to Barbara L. Bohn for her dedication and assistance with the experimental work summarized in this paper. The author also thanks Dr. Martin P. Rigney for his thoughtful supervision and technical assistance with this work.

References

1 Vytřas, K., Dvořáková, V., and Zeman, I., *Analyst*, 1989, **114**, 1435.
2 Jones, D. L., Moody, G. J., Thomas, J. D. R., and Birch, B. J., *Analyst*, 1981, **106**, 974.
3 Sugawara, M., Nagasawa, S., and Ohashi, N., *J. Electroanal. Chem. Interfacial Electrochem.*, 1984, **176**, 183.
4 Evans, A., in *Potentiometry and Ion Selective Electrodes*, ed. James, A. M., Wiley, Chichester, 1987, ch. 3.
5 Cutler, S. G., and Meares, P., *J. Electroanal. Chem. Interfacial Electrochem.*, 1977, **85**, 145.
6 Thomas, J. D. R., *Analyst*, 1991, **116**, 1211.
7 Sanchez, M. L. R., and Vytřas, K., *Analyst*, 1988, **113**, 959.
8 Levins, R. J., and Ikeda, R. M., *Anal. Chem.*, 1965, **37**, 671.
9 Izatt, R. M., Nelson, D. P., Rytting, J. H., Haymore, B. L., and Christensen, J. J., *J. Am. Chem. Soc.*, 1971, **93**, 1619.
10 Vytřas, K., *Mikrochim. Acta*, 1984, **III**, 139.
11 Tsubouchi, M., Mitsushio, H., Yamasaki, N., *Anal. Chem.*, 1981, **53**, 1957.

Paper 2/05605D
Received October 20, 1992
Accepted January 29, 1993

Frequency Characteristics of an Electrode-separated Piezoelectric Crystal Sensor in Contact With a Liquid

Shen Dazhong, Lin Song, Kang Qi, Nie Lihua and Yao Shouzhuo*
New Material Research Institute, Hunan University, Changsha 410082, People's Republic of China

The equations characterizing the frequency response of an electrode-separated piezoelectric crystal (ESPC) sensor, with one side in contact with a liquid, to the properties of the liquid were derived from an electric equivalent circuit model and supported by experiments. The frequency shift of the ESPC can provide information on the permittivity, conductivity, density and viscosity of the liquid.

Keywords: *Frequency equation; electrode-separated piezoelectric sensor; solution properties*

There is increasing interest in the use of piezoelectric devices as liquid microsensors. Several papers have reviewed the applications of piezoelectric quartz crystals (PQCs) in the chemistry of solutions.[1–4] In most instances, the PQC is used to measure the mass change at the crystal surface, which is the basis of the work of Sauerbrey.[5] Besides the mass effect, the frequency of the PQC is also affected by the properties of liquids such as density, viscosity, specific conductivity and permittivity.[6–8] The non-mass effect is also useful in chemistry. For example, the PQC has been used as a viscosity sensor and applied to fermentation monitoring[9] and gelation monitoring in order to determine endotoxin or blood coagulation factors.[10,11] Some applications, based on the high-resolution frequency response of a PQC, to the specific conductivity of solutions were reported from this laboratory.[12–17]

Usually, a PQC is configured with electrodes on both sides of a thin disc of AT-cut quartz. Recently, a type of electrode-separated piezoelectric quartz crystal (ESPC) sensor was reported.[18] The electrodes on the surface of the crystal in the ESPC were separated by a liquid layer of a few tenths of a millimetre, and the high-frequency electric field was applied to the quartz disc through the liquid layers. As a result, it had a frequency response to the liquid properties more sensitive than that of a normal PQC, especially to the permittivity and specific conductivity. The behaviour of the ESPC in solution and its applications in analysis were also reported.[19–21] However, quantitative knowledge of ESPC behaviour in solution is still required if it is to be applied successfully in chemical analysis. Mo *et al.*[22] measured the electric equivalent circuit parameters of this kind of piezoelectric sensor in solution. It is worth pointing out that the resonant frequency of a piezoelectric sensor, as determined by an impedance analyser, differs from the oscillating frequency of the oscillator, because the oscillating frequency depends not only on the parameters of the crystal and the solution, but also on the properties of the oscillator.

In this paper, we have derived equations to describe the influence of the properties of a liquid on the oscillating frequency of an ESPC.

Theory

The configuration of the ESPC is illustrated in Fig. 1. From the point of view of an electric equivalent circuit, an ESPC can be represented by the series combination of equivalent circuits of a PQC and a liquid. The electric equivalent circuit of the ESPC, in the frequency range near the resonance of the PQC, is shown in Fig. 2. Its total impedance Z is given by

$$Z = R + \frac{NX_0}{M^2 + N^2} + j\left(\frac{MX_0}{M^2 + N^2} - X_0 - X_s\right) \qquad (1)$$

* To whom correspondence should be addressed.

where $R = G/(G^2 + \omega^2 C_s^2)$, $X_s = \omega C_s/(G^2 + \omega^2 C_s^2)$, $X_0 = 1/\omega C_0$, $N = R_q \omega C_0$, $M = 1 + C_0/C_q - \omega^2 L_q C_0$, $G = k\chi$, $C_s = k\varepsilon + C_p$; G is the solution conductivity ($G = 1/R_s$), and C_s is the solution capacitance; χ is the specific conductivity, and ε is the permittivity of the solution; k is the cell constant of the detection cell; C_p is the parasitic capacitance of the leading wires, with a typical value of 1.2 pF; ω is the angular frequency; C_0, L_q, C_q and R_q are the static capacitance, motional inductance, motional capacitance and motional resistance of the crystal, respectively; and $j = \sqrt{-1}$.

It is well known that there are two conditions that must be satisfied for oscillation to occur. One is that the phase shift around the loop should be zero; the other is that the loop gain should be unity. The loop is a closed path from the input of the amplifier through the amplifier to its output, and back to the input through the feedback circuit element. Usually, the loop gain condition can be easily satisfied because the gain of the amplifier is much greater than unity and will automatically adjust to unity. Hence, the oscillating frequency is mainly determined by the phase-shift condition.

If the amplifier used in an oscillator has a phase shift of θ, the feedback circuit element must have a phase shift of $-\theta$ in order to satisfy the phase-shift condition. When the ESPC is connected between the input and output of the amplifier, the ratio of imaginary to real parts of its impedance should be

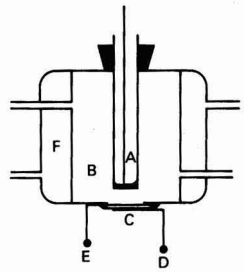

Fig. 1 Configuration of electrode separated piezoelectric crystal (ESPC) sensor: A, separated-electrode; B, detection cell; C, piezoelectric quartz crystal (PQC); D and E, silver electrode of PQC and leading wire; and F, water jacket

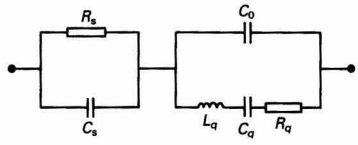

Fig. 2 Electric equivalent circuit of ESPC: R_s, solution resistance; C_s solution capacitance; C_0, static capacitance; L_q, motional inductance; C_q motional capacitance; and R_q motional resistance

equal to $\tan(-\theta)$ according to the phase-shift condition. Therefore, the following equation is obtained:

$$\frac{MX_0}{M^2+N^2} - X_0 - X_s = -Y\left(R + \frac{NX_0}{M^2+N^2}\right) \quad (2)$$

where $Y = \tan(\theta)$ is a parameter of the oscillator, which depends on the type of oscillator and its operating conditions. The typical Y value for the oscillator used in this paper is 1.83.

Because all the parameters in eqn. (2) are related to frequency, it is difficult to obtain an exact algebraic expression of the oscillating frequency of the ESPC from this equation. Fortunately, the relative change in oscillating frequency is small, only the value of M is sensitive to the slight frequency change. Therefore, the oscillating frequency can be approximately obtained from the value of M. Further, the values of X_0, X_s and R are calculated by using the resonance frequency of the crystal, as the relative difference between the oscillating frequency of the ESPC and the resonant frequency of the crystal is very small. Under this assumption, eqn. (2) is rewritten as

$$PM^2 - M + PN^2 - YN = 0 \quad (3)$$

where $P = 1 + (X_s - YR)\,\omega C_0$.

From eqn. (3), there are two roots for M. It is found that only the larger root is consistent with the experimental results, as the series oscillating frequency is monitored in our oscillator. This root is expressed as

$$M = [1 + (1 + 4PYN - 4P^2N^2)^{\frac{1}{2}}]/2P \quad (4)$$

According to the definition of $M = 1 + C_0/C_q - \omega L_q C_0$, the oscillating frequency of the ESPC is given by

$$F = F_s + \frac{F_s C_q}{2C_0}\left[1 - \frac{1 + (1 + 4YPN - 4P^2N^2)^{\frac{1}{2}}}{2P}\right] \quad (5)$$

where $F_s = 1/2\pi\sqrt{L_q C_q}$ is the resonant frequency of the crystal in hertz and F is the oscillating frequency of the ESPC in hertz.

Equation (5) is the fundamental equation characterizing the oscillation frequency of the ESPC. If an iterative method is used, the exact solution of eqn. (2) can be obtained even if only three iterations are used. In fact, the frequency calculated by eqn. (5) is very close to the results obtained from the iterative method.

If a non-electrolyte solution is used to fill the space between the separated electrode and the crystal, then $P = 1 + C_0/C_s$ for an ESPC under conditions of very low conductivity of the solution. Therefore, we have

$$F = F_s + \frac{F_s C_q}{2C_0}\left[1 - \frac{1 + (1 + 4HYN - 4H^2N^2)^{\frac{1}{2}}}{2H}\right] \quad (6)$$

where $H = 1 + C_0/C_s$.

Equation (7) indicates that increases in C_s or the permittivity of the solution correspond to a decrease in frequency. Because F_s decreases with the increment of the density and viscosity of solution,[16,23] the oscillating frequency of the ESPC also decreases with increasing density and viscosity of the solution.

In electrolyte solution, the permittivity of the solution hardly changes with the specific conductivity; hence, the value of P is mainly determined by the specific conductivity of the solution and the cell constant. According to the definition:

$$P = 1 + \frac{(\omega_0 C_s - Yk\chi)\omega_0 C_0}{k^2\chi^2 + \omega_0^2 C_s^2} \quad (7)$$

where $\omega_0 = 2\pi F_s$.

It can be seen that the P values decrease with the increment of specific conductivity until a minimum is reached, then increase as the specific conductivity continues to increase. According to eqn. (5), the variation trend in the oscillating frequency of an ESPC with the specific conductivity is similar to that of P, because the value of $1 + (1 + 4YPN - 4P^2N^2)^{\frac{1}{2}}$ is less sensitive to the change in P.

For the convenience of discussion, the square root in eqn. (5) is developed by Taylor' series, and eqn. (5) is approximately expressed as

$$F = F_s + \frac{F_s C_q}{2C_0}\left(1 - \frac{a}{2P} - \frac{YN}{b} + \frac{N^2P}{b}\right) \quad (8)$$

where $a = 1 + (1 + 2HNY)/b$, and $b = (1 + 4HNY)^{\frac{1}{2}}$.

The sensitivity to specific conductivity, *i.e.*, $\partial F/\partial\chi$, can be derived from eqn. (8) as follows:

$$\frac{\partial F}{\partial\chi} = -\pi F_s^2 k C_q (Y\omega_0^2 C_s^2 + 2G\omega_0 C_s - YG^2) \times \left\{\frac{N^2}{b(G^2+\omega_0^2C_s^2)^2} + \frac{a}{2[G^2 - YG\omega_0 C + \omega_0^2 C_s(C_s + C_0)]^2}\right\} \quad (9)$$

It transpires that the slope of frequency *versus* specific conductivity depends not only on the parameters of the crystal and circuit, but also on the solution conductivity and cell constant. In solutions of low conductivity, $G \ll \omega_0 C_s$, eqn. (9) can be simplified as

$$\frac{\partial F}{\partial\chi} = -\frac{kYC_q}{4\pi}\left[\frac{a}{2(C_0 + C_s)^2} + \frac{N^2}{bC_s^2}\right] \quad (10)$$

It can be seen that the slope is constant for solutions of low conductivity. That is to say, the frequency of the ESPC decreases linearly with the increment of the specific conductivity of the solution or the concentration of electrolyte. Besides, the influence of the cell constant on the sensitivity is slight, because C is proportional to the cell constant.

In highly conductive solutions, $G \gg \omega_0 C_s$, eqn. (9) can be simplified as

$$\frac{\partial F}{\partial\chi} = \frac{\pi Y F_s^2 C_q}{2k\chi^2}(a + 2N^2/b) \quad (11)$$

It was obvious that the values of $\partial F/\partial\chi$ become positive and decrease with the increase in specific conductivity. Hence, the frequency of the ESPC increases with increasing specific conductivity of the solution or the concentration of the electrolyte in highly conductive solutions. Additionally, the sensitivity is low and becomes less with larger cell constants in this range. If the conductivity of the solution is so great that the solution impedance can be neglected, the sensitivity to specific conductivity approaches zero.

In fact, a PQC with one side in contact with a liquid phase (PQC in the following discussion) can be treated as the special case of an ESPC. According to the equivalent circuit shown in Fig. 2, if $R_s = 0$, the ESPC is transformed into a PQC. Under such conditions, $P = 1$ and the oscillating frequency of the PQC is expressed as

$$F = F_s\{1 + [1 - (1 + 4YN - 4N^2)^{\frac{1}{2}}]C_q/4C_0\} \quad (12)$$

It seems that the oscillating frequency of the PQC is insensitive to the change in the specific conductivity and permittivity of the liquid, and depends mainly on the resonant frequency and motional resistance of the crystal.

For the situation between the two extreme examples, the change in sensitivity with specific conductivity is interesting. As the specific conductivity increases, the sensitivity increases until a maximum is reached, then it decreases through zero

and increases again towards positive values. When the positive maximum is obtained, the sensitivity decreases to zero again.

Generally, frequency shift is used in piezoelectric measurements. The frequency shift (ΔF) used in this paper is the frequency difference between test and reference solutions, *i.e.*, $\Delta F = F_1 - F_0$, where F_1 and F_0 are the frequencies in test and reference solutions, respectively. With the frequency in pure solvent serving as the reference, the frequency shift in electrolyte solution can be calculated as follows:

$$\Delta F = -\frac{F_s C_q}{4C_0}\left[\frac{a(G^2+\omega_0^2C_s^2)}{G^2+\omega_0^2C_s(C_s+C_0)-YG\omega_0C_0}-\frac{aC_s}{C_0+C_s}+\frac{2N^2}{b}\left(\frac{C_0}{C_s}-\frac{\omega_0^2C_sC_0-YG\omega_0C_0}{G^2+\omega_0^2C_s^2}\right)\right] \quad (13)$$

If a solution with specific conductivity of χ_0 is used as the reference solution, and the change in specific conductivity ($\Delta\chi$) is much less than χ_0, the frequency shift that reflects the change in specific conductivity is given by

$$\Delta F = -\frac{F_s C_q k \Delta\chi_0}{2C_0}\left[\frac{aG}{G_0^2-YG_0\omega_0C_0+\omega_0^2C_s(C_0+C_s)}-\frac{YN^2}{b(G_0^2+\omega_0^2C_s^2)}\right] \quad (14)$$

where $G_0 = k\chi_0$.

This equation reveals that the minute change in specific conductivity can be determined by an ESPC even in the presence of a highly conductive background. Moreover, the frequency shift is linearly related to the change in specific conductivity. The sensitivity can be improved if the value of the background specific conductivity is in the range where the frequency is sensitive to the change in specific conductivity.

Experimental

In the ESPC (Fig. 1), a platinum disc, with a diameter of 6 mm and a thickness of 1 mm, is attached to one end of a ground-glass tube with silicone resin; this is used as the separated electrode. An AT-cut 9 MHz piezoelectric crystal (12.5 mm diameter, with silver electrodes) is attached to the base of the detection cell with silicone resin. The distance between the separated electrode and the crystal is adjustable. For the purpose of measuring the parameters of the crystal and comparing the frequency characteristics of the ESPC and PQC, the silver electrodes are not dissolved. It is found that the response characteristics of the ESPC, with or without silver electrodes, remain almost the same. When the separated electrode and silver electrode (D) are used, the sensor is an ESPC. If both of the silver electrodes are connected, the sensor is converted into a normal PQC.

The oscillating frequency of the TTL-IC oscillator (made in this laboratory) is monitored by a frequency counter (Iwatsu; Model SC-7201). An impedance analyser (Hewlett-Packard, Avondale, PA, USA; Model 4192A) is used to measure the parameters of the crystal, oscillator and liquid. The solution capacitance and conductivity are measured between the separated electrode and silver electrode (E) at a frequency of 8 MHz.

Analytical-reagent grade chemicals and doubly distilled water were used. Test solutions were prepared with the reference solution (see under Results and Discussion).

The reference solution was introduced into the detection cell, the stable frequency (F_0) was recorded, then the reference solution was replaced by the test solution, and the stable frequency (F_1) was again recorded. The frequency shift, $\Delta F = F_1 - F_0$, was measured three times and the mean value was used. The equivalent circuit parameters of the crystal were measured by the admittance diagram method.[23]

Results and Discussion

Frequency Response of ESPC to Specific Conductivity

With pure water as the reference solution, the frequency shifts of the ESPC with different cell constants, in potassium chloride solutions of known specific conductivity, are illustrated in Fig. 3. The sensitivity, *i.e.*, $\partial F/\partial\chi$, is also shown in this figure. The solid lines are derived from eqns. (13) and (9), which are in good accord with the experimental points. As predicted above, the sensitivity is relevant to the cell constant with specific conductivities ranging from 0.003 to 0.3 S m^{-1}. A better sensitivity can be expected when an ESPC with a smaller cell constant is used in this range. Beyond this range, the influence of cell constants on the sensitivity is slight.

Frequency Response of ESPC to Permittivity

For a normal PQC operated in liquid, the frequency shift arising from permittivity change is slight[8] or negligible.[7] These results can be explained by eqn. (12), because the electric equivalent circuit shown in Fig. 2 is also suitable for a PQC with one or two sides in contact with a non-electrolyte solution. The frequency response of a PQC, with one side in contact with the liquid, is insensitive to the permittivity, because the permittivity of the liquid has a slight influence on the equivalent circuit parameters of the crystal. Although the C_0 value of a PQC immersed in non-electrolyte solution changes with the permittivity of the liquid, the frequency is insensitive to the change in C_0, according to eqn. (12). As seen in eqn. (6), the frequency of the ESPC is more sensitive to the change in the permittivity owing to the term $F_sC_q/2(C_0 + C_s)$.

With 1,4-dioxane used as the reference solution, the frequency shifts of the ESPC and its crystal in a water–1,4-dioxane mixture are depicted in Fig. 4. The solid lines (A–C) are plotted on the basis of eqn. (6) by using the values of F_s (line E), R_q and C_0 of the crystal (shown in Fig. 5) and of C_s in this mixture. Good agreement was obtained between the results predicted theoretically and those measured experimentally.

Frequency Response of ESPC to Density and Viscosity

According to ref. 6, the frequency shift of the PQC is proportional to $(\rho\eta)^{\frac{1}{2}}$, where ρ and η are the density and viscosity, respectively, of the liquid with which the crystal is in contact. The influence of density and viscosity on the frequency of the ESPC has been investigated in sucrose solutions with known density and viscosity.[24]

With pure water used as the reference solution, the frequency shifts of the ESPC and its crystal are depicted in Fig. 6. Again the solid lines (B and C) are derived from eqn. (6) or

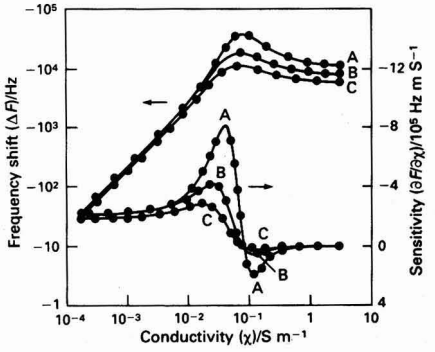

Fig. 3 Dependence of frequency shift (ΔF) and sensitivity on the specific conductivity. ESPC with cell constant (m): A, 0.0086; B, 0.0159; and C, 0.0264

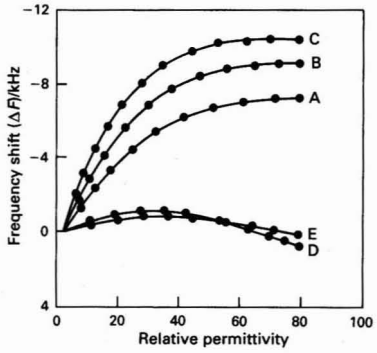

Fig. 4 Dependence of frequency shift (ΔF) on the permittivity in a water–dioxane mixture: A, ESPC with cell constant of 0.0086 m; B, ESPC with cell constant of 0.0159 m; C, ESPC with cell constant of 0.0264 m; D, oscillating frequency of the crystal; and E, resonant frequency of the crystal

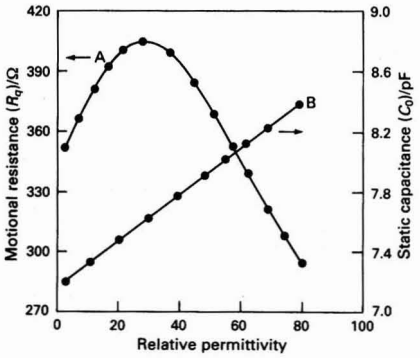

Fig. 5 Motional resistance and static capacitance of the PQC in a water–dioxane mixture: A, motional resistance; and B, static capacitance

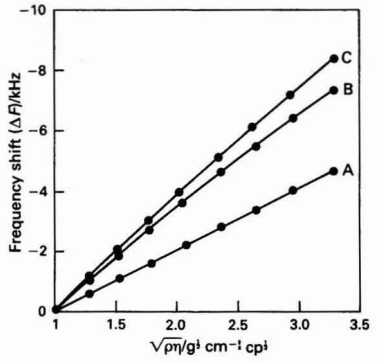

Fig. 6 Dependence of frequency shift on the density and viscosity in sucrose solutions: A, resonant frequency of the crystal; B, oscillating frequency of ESPC with cell constant of 0.0264 m; and C, oscillating frequency of the crystal

(12) by using F_s (line A), and R_q and C_s (in Fig. 7). It appears that the frequency shifts of the PQC are in linear correlation with $(\rho\eta)^{\frac{1}{2}}$, whereas the linearity of frequency shift *versus* $(\rho\eta)^{\frac{1}{2}}$ in ESPC is only approximate. Moreover, the frequency shift of the ESPC is slightly less than that of its crystal. The difference in frequency shift is due to different response characteristics

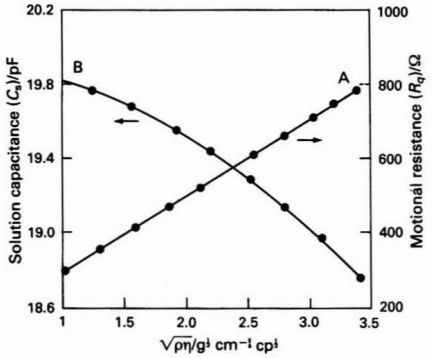

Fig. 7 Solution capacitance and motional resistance in sucrose solutions: A, motional resistance; and B, solution capacitance

between the PQC and ESPC. The difference in frequency between the ESPC and PQC, which is obtained by subtracting eqn. (12) from eqn. (6), is expressed as

$$F_{ESPC} - F_{PQC} = \frac{F_s C_q}{4C_0}$$

$$\left[\frac{C_0}{C_0 + C_s} + (1 + 4YN - 4N^2)^{\frac{1}{2}} - (1 + 4YNH - 4N^2H^2)^{\frac{1}{2}} H^{-1}\right] \quad (15)$$

Equation (15) reveals that the oscillating frequency of the ESPC is slightly greater than that of its crystal under the same solution conditions. With increasing $(\rho\eta)^{\frac{1}{2}}$, C_s decreases, and the oscillating frequency difference between the ESPC and PQC increases. Therefore, the frequency shift in the ESPC is slightly less than that of its crystal. For the same reason, the linearity of ΔF *versus* $(\rho\eta)^{\frac{1}{2}}$ for the ESPC is not good as that for the PQC.

The frequency change of the ESPC caused by density and viscosity is about 1.5 times larger than that of the normal PQC.[20] The different results could be due to the difference in the construction of the sensor and oscillator. An ESPC with two separated electrodes was used by Nomura and Yanagihara.[20]

Frequency Response of ESPC to Specific Conductivity Under Background Conductivity

With $NaNO_3$ solution of various concentrations used as the reference, the frequency shifts of the ESPC in response to the concentration of electrolyte (KCl as an example) are illustrated in Fig. 8. It is evident that the frequency shift of the ESPC can reflect a minute change in specific conductivity or in the concentration of electrolyte against a highly conducting background. In our opinion, this is the most important advantage of ESPCs over the classical conductimetric method, with respect to determinations based on conductivity. The reason why the ESPC can detect such a slight variation in specific conductivity against a highly conducting background is that it exhibits a very good signal-to-noise ratio or resolving power. The typical noise level for an ESPC is about 2 Hz and depends slightly on the conductivity, while the fundamental frequency of the crystal is 9 MHz; therefore, the small change in specific conductivity can be measured by the ESPC with ease even against a background of high conductivity. As predicted from eqn. (14), the slopes of these response curves are relevant to the value of the background conductivity. Because the solution conductivity depends directly on the cell constant, the sensitivity of the ESPC can be changed by adjusting the distance between the separated electrode and the crystal.

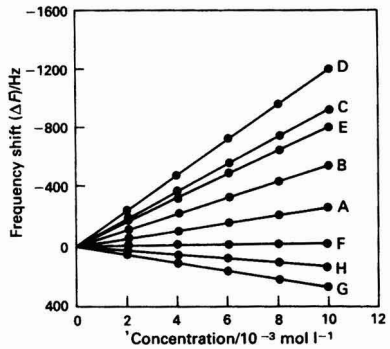

Fig. 8 Response curves of ESPC in the presence of a foreign electrolyte. Concentration of $NaNO_3$ (10^{-3} mol l^{-1}): A, 0; B, 1; C, 2; D, 3; E, 4.5; F, 6; G, 10; and H, 15

Conclusions

The characterization of an ESPC with one separated electrode is discussed theoretically. The frequency of the ESPC is sensitive to the change in permittivity and conductivity of a liquid. The frequency shift arising from the change in density and viscosity is slightly less than that of a normal PQC that operates under the same conditions. It is more important that the ESPC can detect a minute conductivity change even against a highly conducting background.

This work has been supported by the National Science Foundation and the Education Commission Foundation of China.

References

1 Deakin, M. R., and Buttry, D. A., *Anal. Chem.*, 1989, **61**, 1147A.
2 McCallum, J. J., *Analyst*, 1989, **114**, 1173.
3 Buttry, D. A., in *Electroanalytical Chemistry*. ed. Bard, A. J., Marcel Dekker, New York, 1991, vol. 17, pp. 1–85.
4 Thompson, M., Kipling, A. L., Duncan-Hewitt, W. C., Rajaković, L. V., and Čavić-Vlasak, B. A., *Analyst*, 1991, **116**, 881.
5 Sauerbrey, G., *Z. Phys.*, 1959, **155**, 206.
6 Kanazawa, K. K., and Gordon, J. G., II, *Anal. Chim. Acta*, 1985, **177**, 99.
7 Nomura, T., and Okuhara, M., *Anal. Chim. Acta*, 1982, **142**, 281.
8 Yao, S. Z., and Zhou, T. A., *Anal. Chim. Acta*, 1988, **212**, 61.
9 Endo, H., Sode, K., Karube, I., and Muramatsu, H., *Biotechnol. Bioeng.*, 1990, **36**, 636.
10 Muramatsu, H., Tamiya, E., Suzuki, M., and Karube, I., *Anal. Chim. Acta*, 1988, **215**, 91.
11 Muramatsu, H., Tamiya, E., Suzuki, M., and Karube, I., *Anal. Chim. Acta*, 1989, **217**, 321.
12 Yao, S. Z., and Mo, Z. H., *Anal. Chim. Acta*, 1987, **193**, 97.
13 Yao, S. Z., Mo, Z. H., and Nie, L. H., *Anal. Chim. Acta*, 1990, **229**, 205.
14 Mo, Z. H., Nie, L. H., and Yao, S. Z., *Sci. China (Ser. B)*, 1991, **1**, 1.
15 Mo, Z. H., Nie, L. H., and Yao, S. Z., *Anal. Chim. Acta*, 1991, **246**, 421.
16 Wei, W. Z., Nie, L. H., and Yao, S. Z., *Anal. Chim. Acta*, 1992, **263**, 77.
17 Wei, W. Z., Nie, L. H., and Yao, S. Z., *Anal. Chim. Acta*, 1992, **269**, 149.
18 Nomura, T., and Tanaka, F., *Bunseki Kagaku*, 1990, **39**, 773.
19 Nomura, T., and Takada, K., *Bunseki Kagaku*, 1991, **40**, 567.
20 Nomura, T., and Yanagihara, T., *Anal. Chim. Acta*, 1991, **248**, 329.
21 Nomura, T., Tanaka, F., and Yamada, T., *Anal. Chim. Acta*, 1991, **243**, 273.
22 Mo, Z. H., Nie, L. H., and Yao, S. Z., *J. Electroanal. Chem. Interfacial Electrochem.*, 1991, **316**, 79.
23 Zhou, T. A., Nie, L. H., and Yao, S. Z., *J. Electroanal. Chem. Interfacial Electrochem.*, 1991, **293**, 1.
24 *Handbook of Chemistry and Physics*, ed. Weast, R. C., CRC Press, Boca Raton, FL, 64th edn., 1984–1985, D-270.

Paper 3/00353A
Received January 20, 1993
Accepted March 17, 1993

Enzymic Assays of Organic Peroxides in Microemulsion Systems

Joseph Wang and A. Julio Reviejo*
Department of Chemistry and Biochemistry, New Mexico State University, Las Cruces, NM 88003, USA

Microemulsions are shown to extend the scope of enzymic amperometric assays towards both hydrophobic and hydrophilic compounds. This possibility is illustrated for amperometric monitoring of organic peroxides in oil-in-water emulsions containing horseradish peroxidase. Enhanced sensitivity (compared with work in pure aqueous solution) is observed also for water-soluble analytes, and is attributed to changes in the local substrate concentration. The effect of the emulsion structure on the biocatalytic activity and analytical performance is explored. Both hydrophobic and hydrophilic mediators can be used. Amperometry can also be used for elucidating biocatalytic conversions in microemulsions. Future prospects are discussed.

Keywords: *Enzymic assay; organic peroxide; microemulsion; peroxidase*

The interest in organic-phase enzymic assays is growing rapidly.[1,2] Several useful enzyme electrodes and unique applications utilizing non-aqueous environments have already been reported.[3–8] Similar analytical opportunities can accrue from the use of microemulsion systems (*i.e.*, mixtures of water and oil separated by a surfactant-rich film). Many studies have been devoted to biocatalytic conversions in microemulsions (particularly reverse micellar systems).[9–12] Analytical advantages accrued from the coupling of enzymic–chemiluminescence detection schemes have been documented,[13,14] but enzymic electrochemical assays utilizing these media have not been reported.

The aim of this investigation was to demonstrate the analytical possibility of using amperometry for monitoring enzymic processes in microemulsions. The main analytical advantage resulting from using such environments is solubility, namely, microemulsions are good solvents for both hydrophobic and hydrophilic compounds, and for compounds of intermediate character. The large (water/oil) interfacial area offers a rapid exchange of such analytes between the organic and water domains, hence facilitating their conversion by the enzyme (present in the aqueous phase). In addition, microemulsions have low mass transfer limitations and can be prepared rapidly. Finally, by avoiding direct contact with the unfavourable organic medium it is possible to stabilize the enzyme against the inactivating action of such solvents.

The prospects of using microemulsions for amperometric enzymic assays are illustrated here for monitoring organic peroxides in the presence of horseradish peroxidase. Organic peroxides are of great environmental, industrial and biological interest[15,16] and possess a broad solubility range. In addition to its analytical significance, the work described here illustrates the utility of amperometric electrodes for *in situ* probing of enzymic conversions in microemulsions

Experimental

Apparatus

A 10 cm^3 cell [Model VC-2, Bioanalytical Systems (BAS) W. Lafayette, IN, USA] was connected to a glassy carbon disc working electrode (Model MF-2012, BAS), an Ag–AgCl reference electrode (Model RE-1, BAS) and a platinum wire auxiliary electrode through holes in its poly(tetrafluoroethylene) cover. A magnetic stirrer and stirring bar provided the convective transport. Amperometric measurements were performed with an EG & G Princeton Applied Research (Princeton, NJ, USA) Model 174 voltammetric analyser, in conjunction with a BAS *X–Y–t* recorder. The working electrode was polished with an alumina slurry.

Reagents and Procedures

All the solutions were prepared from analytical-reagent grade chemicals and distilled water. Dimethylferrocene, butan-2-one peroxide, benzoyl peroxide, *tert*-butyl peroxide, lauroyl peroxide, dicumyl peroxide, ethyl acetate, cetyltrimethylammonium bromide (CTAB) and chloroform were obtained from Aldrich (Milwaukee, WI, USA), while cumene hydroperoxide, ferrocene and *o*-phenylenediamine were received from Sigma (St. Louis, MO, USA). Potassium hexacyanoferrate(II), Triton X-100 and sodium dodecyl sulfate (SDS) were obtained from J. T. Baker (Phillipsburg, NJ, USA). All the peroxides were dissolved in ethyl acetate. The enzyme [horseradish peroxidase (HRP) EC 1.11.1.7, Type I, 100 U mg^{-1}; (1 U = 16.67 nkat) Sigma] was dissolved in 0.05 mol dm^{-3} phosphate buffer.

Amperometric measurements were performed at room temperature, by applying the desired (−0.2 V) potential, allowing the transient currents to decay, and stirring the solution.

Preparation of Microemulsions

Different volumes of the organic solvent (containing the mediator) and of the surfactant were placed in a 10 cm^3 calibrated flask, and diluted to the mark with phosphate buffer solution (to yield final concentrations of 1–4% and 0.05–0.4%, respectively). Clear emulsions were obtained by shaking or sonicating these mixtures.

Results and Discussion

While enzymic conversions in microemulsions have traditionally relied on water-in-oil (w/o) systems, oil-in-water (o/w) emulsions are used here to demonstrate the analytical prospects of enzymic assays in emulsified media. Such o/w systems offer a broad solubility range, while maintaining high biocatalytic efficiencies. Ethyl acetate-in-water emulsions are, therefore, used here for peroxidase-based assays of organic peroxides. Such assays rely on the biocatalytic conversion of organic peroxides in the presence of a suitable mediator (M):

$$\mathrm{ROOH + M\,(red) \xrightarrow{HRP} ROH + H_2O + M\,(ox)}$$

Fig. 1 shows current–time recordings, obtained at the glassy carbon electrode immersed in emulsified (A) and aqueous (B) media, on successive additions of lauroyl peroxide (*a*) and cumene hydroperoxide (*b*). The emulsion system was stabilized by CTAB and Triton X-100 (not shown), respectively.

* Permanent address: Department of Analytical Chemistry, Complutense University, Madrid, Spain.

Determination in the pure water solution is not feasible because of the poor solubility of these highly hydrophobic peroxides. In contrast, a rapid response to these sub-millimolar additions is observed when using the emulsified media. Steady-state currents are achieved within 15 s (*a*) and 50 s (*b*). Such difference is attributed to different rates of substrate partition (from the oil pools towards the bulk aqueous phase containing the enzyme). The favourable signal-to-noise characteristics indicate detection limits in the micromolar range.

The o/w microemulsion operation can benefit also enzymic assays of water-soluble peroxides. Fig. 2 displays calibration plots for butan-2-one peroxide (over the 0.1–1.0 mmol dm^{-3} range) in aqueous and microemulsion systems, and in the presence of hexacyanoferrate(II) (*a*) and *o*-phenylenediamine (*b*) as mediators. Both the Triton X-100- and CTAB-based emulsion systems exhibit a sensitivity better than that of the corresponding water solutions. The sensitivity enhancement is particularly pronounced (11-fold) in the presence of CTAB. The reason for these improvements is discussed below.

If enzyme catalysis in microemulsions is to be of practical analytical significance, it is essential to understand the factors influencing the biocatalytic activity in such systems. Unlike w/o emulsions, o/w systems (used in the present investigation) do not exert substantial changes in the biocatalytic activity because the enzyme is confined within the bulk aqueous phase. The activity and stability of enzymes in such systems are usually of the same order of magnitude as in an aqueous environment. However, some changes in reaction rates can result from differences in the 'local' substrate concentration in the aqueous domain. For example, the higher reaction rates (than in water, *e.g.*, Fig. 2) are attributed to bringing together the substrate, mediator and enzyme in higher 'local' concentration near the interface. (The hydrophobic part of the enzyme molecule can come into contact with the phase of the organic micro-domain.) The effect of the microemulsion composition (its components and their level) on the response of the enzymic assay was therefore investigated.

The effect of various microemulsion stabilizers, including CTAB, Triton X-100 and SDS on the sensitivity was examined for successive (0.1 mmol dm^{-3}) concentration increments of butan-2-one peroxide (not shown). Such stabilizers are representative of cationic, neutral and anionic surfactants, respectively. The three emulsions displayed a very rapid and sensitive response to these additions of the peroxide substrate (yielding steady-state currents within 5–10 s). While no substantial differences were observed among the three surfactants, the CTAB-containing emulsion offered the most favourable signal-to-noise characteristics. Unlike its enzyme denaturating activity in aqueous solutions, SDS does not display such activity in the microemulsion. As shown in Fig. 3, changes in the level of different components of the emulsion system, including the percentage of the oil (A) or of the surfactant (B), and also the mediator concentration (C) and the enzyme activity (D) have little effect on the response to the peroxide substrate. No response was observed in the absence of HRP (not shown). In contrast, oil-rich w/o microemulsions, with the enzyme entrapped in the water droplets, can lead to pronounced changes in the biocatalytic activity,[12,17] and can, therefore, allow tailoring of the enzyme function (by engineering the emulsion composition) to meet the requirements of a given enzymic assay.

Enzymic assays in microemulsions can benefit from the use of mediators with a broad solubility range. For example, Fig. 4 displays calibration data for butan-2-one peroxide in emulsions formed with Triton X-100 (*a*) and CTAB (*b*), and containing the water-soluble hexacyanoferrate(II) and *o*-phenylenediamine, and also the poorly water-soluble fer-

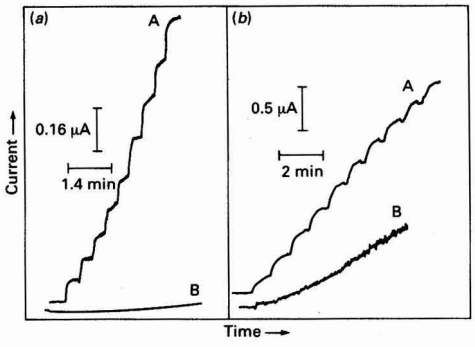

Fig. 1 Typical current–time recordings on increasing (*a*) the lauroyl peroxide and (*b*) cumene hydroperoxide concentration in steps of 0.1 and 0.5 mmol dm^{-3}, respectively. Solutions: A, emulsion (2% ethyl acetate, 97.8% phosphate buffer, 0.2% CTAB); and B, phosphate buffer (0.05 mol dm^{-3}, pH 7.4); both solutions contained 5 U HRP and 2 mmol dm^{-3} ferrocene. Operating potential, −0.2 V; stirring rate, 300 rev min^{-1}

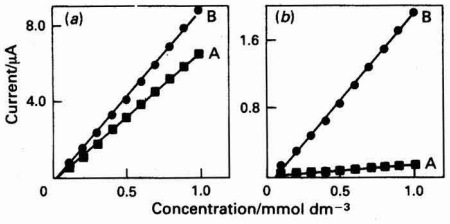

Fig. 2 Calibration plots for butan-2-one peroxide in A, aqueous and B, microemulsion media. Mediators: (*a*) hexacyanoferrate(II) and (*b*) *o*-phenylenediamine. Surfactants: (*a*) Triton X-100; and (*b*) CTAB. [Other conditons as in Fig. 1 (A)]

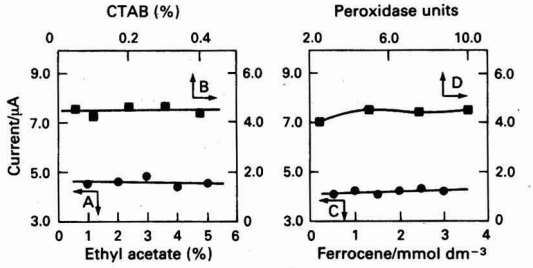

Fig. 3 Effect of: A, ethyl acetate; B, CTAB; and C, ferrocene contents; and D, enzyme activity, on the response to 0.5 mmol dm^{-3} butan-2-one peroxide. [Other conditions as in Fig. 1 (A)]

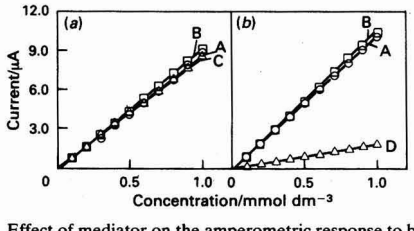

Fig. 4 Effect of mediator on the amperometric response to butan-2-one peroxide (0.1 mmol dm^{-3} additions). Mediators: A, ferrocene; B, dimethylferrocene; and C, hexacyanoferrate(II) or D, *o*-phenylenediamine. Surfactants: (*a*) Triton X-100, and (*b*) CTAB. [Other conditions as in Fig. 1 (A)]

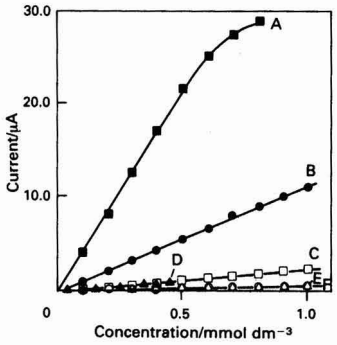

Fig. 5 Dependence of the steady-state current on the concentration of: A, benzoyl peroxide; B, butan-2-one peroxide; C, cumene hydroperoxide; D, lauroyl peroxide; E, *tert*-butyl peroxide; and F, dicumyl peroxide. [Conditions as in Fig. 1 (A)]

rocene and dimethylferrocene species. With use of the Triton X-100 based system there is no apparent difference in the sensitivity in the presence of the three different mediators. In contrast, the barley water-soluble ferrocene compounds exhibit better sensitivity in the presence of CTAB. Such behaviour indicates that the ferrocene mediators partition into the bulk water phase containing the enzyme. Note also the high linearity observed for these six experiments.

Fig. 5 illustrates the dependence of the steady-state reduction current on the concentration of six different organic peroxides (representing a broad solubility range). Convenient measurement of sub-millimolar concentrations of these peroxides is feasible. With the exception of benzoyl peroxide, all the other peroxides exhibit linearity over the entire range. The following trend in sensitivity is observed: benzoyl peroxide > butan-2-one peroxide > cumene hydroperoxide > lauroyl peroxide > *tert*-butyl peroxide = dicumyl peroxide. These concentration-dependent data and the corresponding (reciprocal) Lineweaver–Burk-type plots were used to estimate the apparent Michaelis–Menten constant ($K_{m,app}$). For example, $K_{m,app}$ values of 8.56, 7.14, 6.86 and 3.11 were obtained for butan-2-one peroxide, cumene hydroperoxide, benzoyl peroxide and dicumyl peroxide, respectively.

In conclusion, the above experiments confirm the expectation that microemulsions can serve as suitable media for performing enzymic assays. The major advantage of such an operation is the broad substrate solubility range, in connection with 'class-selective' enzymes. While the concept is presented within the framework of organic peroxides, these observations are likely to stimulate investigations into other classes of analytes possessing a broad solubility range. The microemulsion peroxide assays can be readily adapted to an on-line (*e.g.*, flow injection) operation to offer fast monitoring of organic peroxides in relevant environmental or industrial samples. Although o/w emulsions were used in the present work, w/o emulsions should also offer analytical advantages, particularly for manipulating the biocatalytic activity to address specific analytical needs. Such an operation should also allow a convenient recovery and re-utilization of the enzyme.[18]

This work was supported in part by the US Environmental Protection Agency (Grant No. CR-81 7936-010). Mention of trade names or commercial products does not constitute endorsement or recommendation by the Agency. A. J. R. acknowledges a fellowship from the Spanish Ministry for Science and Education.

References

1 Klibanov, A. M., *Chemtech.*, 1986, **16**, 354.
2 Saini, S., Hall, G. F., Downs, M. E., and Turner, A. P., *Anal. Chim. Acta*, 1991, **249**, 1.
3 Hall, G., Best, D., and Turner, A. P., *Anal. Chim. Acta*, 1988, **213**, 113.
4 Wang, J., Naser, N., Kwon, H., and Cho, M., *Anal. Chim. Acta*, 1992, **264**, 7.
5 Hall, G., and Turner, A. P., *Anal. Lett.*, 1991, **24**, 1375.
6 Wang, J., Reviejo, A., and Mannino, S., *Anal. Lett.*, 1992, **25**, 1399.
7 Schubert, F., Saini, S., and Turner, A. P., *Anal. Chim. Acta*, 1992, **245**, 133.
8 Wang, J., Lin, Y., and Chen, Q., *Electroanalysis*, 1993, **5**, 23.
9 Martinez, K., Klyachko, N., Kabanov, A., Khmelnitsky, Y., and Levashov, A., *Biochim. Biophys. Acta*, 1989, **981**, 161.
10 Luisi, P. L., and Larane, C., *Trends Biotechnol.*, 1986, **4**, 153.
11 Larsson, K., Ph.D. Thesis, Lund University, 1990.
12 Hedstrom, G., Slotte, J. P., Molander, O., and Rosenholm, J., *Biotechnol. Bioeng.*, 1992, **39**, 218.
13 Igarashi, S., and Hinze, W., *Anal. Chem.*, 1988, **60**, 446.
14 Abdel-Latif, M., and Guilbault, G., *Anal. Chem.*, 1988, **60**, 2671.
15 Glaze, W., *Environ. Sci. Technol.*, 1987, **21**, 224.
16 Silbert, L., in *Organic Peroxides*, ed. Swern, D. Wiley-Interscience, New York, 1971, vol. II, p. 755.
17 Sarcar, S., Jain, T., and Maitra, A., *Biotechnol. Bioenerg.*, 1992, **39**, 1992.
18 Larsson, K., Aldercreutz, P., and Mattiasson, B., *Biotechnol. Bioeng.*, 1990, **36**, 135.

Paper 3/00779K
Received February 9, 1993
Accepted April 6, 1993

Determination of Microgram Amounts of Uranium in Thorium by Differential-pulse Polarography

Sulobh K. Das
Fuel Reprocessing Division, Bhabha Atomic Research Centre, Bombay-400 085, India
Achyut V. Kulkarni and Ramesh G. Dhaneshwar
Analytical Chemistry Division, Bhabha Atomic Research Centre, Bombay-400 085, India

A differential-pulse polarographic (DPP) method for the determination of uranium(VI) in the presence of a large excess of thorium without any prior separation of the latter is described. Disodium ethylenediaminetetraacetate and sodium carbonate–hydrogencarbonate buffer (pH 10) was used as the supporting electrolyte. The interference of several impurities expected in the Thorex process while processing irradiated thorium was overcome by using the above supporting electrolyte. A relative standard deviation of 2.4% for the determination of uranium at the 5 ppm level was obtained. The uranium(VI) values obtained by the proposed DPP method were compared with those obtained by inductively coupled plasma atomic emission spectrometry.

Keywords: *Uranium determination; thorium metal analysis; differential-pulse polarography*

The irradiation of thorium by neutrons results in the production of fissile ^{233}U, which can be used as a fuel in future nuclear programmes. This necessitates the development of a method for the determination of small amounts of uranium in the presence of a large excess of thorium. Radiometric[1] and spectrophotometric[2] methods of determining uranium in thorium exist but they involve a prior separation of uranium from the thorium matrix. In the separation procedure using trioctylphosphine oxide, thorium is also extracted along with uranium and interferes in its subsequent spectrophotometric determination.[3] In the inductively coupled plasma atomic emission spectrometric (ICP-AES) method,[4] the total dissolved solids in the sample must be restricted, otherwise easy transportation of the sample to the ICP is not possible. It was therefore necessary to develop an alternative method that is capable of determining uranium in the presence of an excess of thorium without its interference.

Uranyl ion (UO_2^{2+}) is one of the few electroactive species that is only weakly complexed by disodium ethylenediaminetetraacetate (Na_2-EDTA) and related chelating agents. The standard potentials of U^{VI}–U^{IV} and Th^{IV}–Th^{O} are well separated from one another.[5] This factor, coupled with the strong complexation between EDTA and other metal ions present, prompted Pribil and Blazek[6] and Auerbach and Kissel[7] to investigate systematically the polarography of uranium in an EDTA-containing medium and to develop a method for the determination of uranium in the presence of several elements whose half-wave potentials are significantly displaced towards more negative values by chelation with EDTA.

Uranium(VI) forms a strong complex with carbonate ion.[8] The polarographic behaviour of U^{VI} has been extensively studied in a carbonate medium,[9–12] although only Perec[11] found a linear relationship between concentration and limiting current of U^{VI} in the narrow concentration range from 0.5×10^{-3} to 4×10^{-3} mol l^{-1} in a supporting electrolyte of carbonate–hydrogencarbonate buffer.

A differential-pulse polarographic (DPP) method for the determination of uranium in a thorium matrix is reported in this paper. Advantage was taken of the weak complexation between U^{VI} and EDTA and of the strong complexation between thorium and EDTA in an alkaline carbonate–hydrogencarbonate buffer medium to develop a DPP procedure for U^{VI} determination. This approach helped in suppressing the hydrolysis of Th^{IV}, at the same time retaining the strong complexation between U^{VI} and carbonate ions. Several impurities (Al^{III}, Ca^{II}, Cr^{VI}, Cu^{II}, Mg^{II}, Mn^{II}, Zn^{II}, Fe^{III}, *etc.*) might be present when irradiated thorium fuel rods are dissolved in nitric acid in the Thorex process for fuel reprocessing. These impurities, if not complexed with EDTA, interfere in the DPP determination of U^{VI} and the supporting electrolyte chosen removes their interference together with that of Th^{IV}.

Experimental

Differential-pulse polarographic experiments were performed on a Model 174A polarographic analyser in conjunction with a Model 303A static mercury drop electrode (SMDE) and a Model RE 0089 *x*–*y* recorder, all from EG & G Princeton Applied Research (Princeton, NJ, USA). pH measurements were made on a Model 330A digital pH meter manufactured by EMCO (Bombay, India).

A linear-sweep ramp (scan rate 5 mV s^{-1}) superimposed with pulses of 50 mV amplitude was applied to the SMDE (small drop size) in the mode of a hanging mercury drop electrode (HMDE). A saturated Ag–AgCl electrode was used as the reference electrode and platinum wire as the auxiliary electrode.

Reagents

Stock solutions of uranium and thorium were prepared by dissolving their respective nitrates of Specpure grade (Johnson Matthey, London, UK) in 0.1 mol l^{-1} nitric acid. All acids were of Aristar grade (BDH, Poole, Dorset, UK). All other salts were of general-reagent grade (Merck, Darmstadt, Germany). High-purity nitrogen gas of IOLAR grade (Indian Oxygen, Bombay, India) was used for removing dissolved oxygen from the polarographic solution. Uranium solutions were standardized following a modification of the method of Davies and Gray.[13]

Procedure

A suitable aliquot of synthetic sample solution containing thorium (10–50 mg) and uranium (10–50 μg) together with other impurities, mainly Fe^{III} in the range 20–100 μg and Al^{III}, Ca^{II}, Cr^{VI}, Cu^{II}, Mg^{II}, Mn^{II}, Mo^{VI}, Ni^{II}, Pb^{II} and Zn^{II}, *etc.*, each in the range 1–5 μg, was placed in a 10 ml calibrated flask. About 0.5 g of Na_2-EDTA (solid) was added to the solution and warmed to dissolve it. The amount of EDTA was

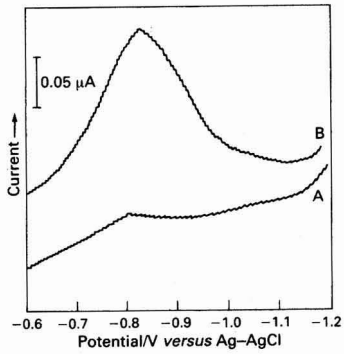

Fig. 1 Differential-pulse polarograms of U^{VI} in 0.1 mol l^{-1} sodium carbonate–hydrogencarbonate buffer (pH 10) containing Na_2-EDTA. A, Blank; and B, 10 ppm of U^{VI}

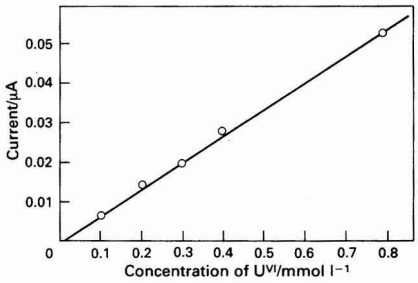

Fig. 2 Differential-pulse polarogram of peak current *versus* concentration of U^{VI} in the presence of 0.1 mol l^{-1} thorium

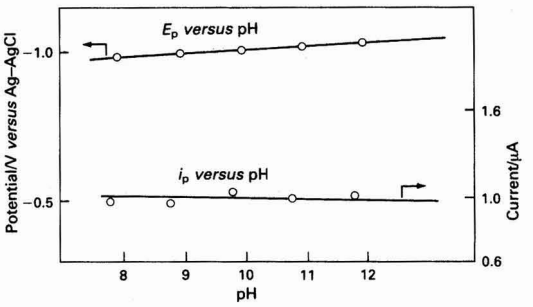

Fig. 3 Effect of pH on peak potential and peak current of 0.1 mmol l^{-1} of U^{VI}. Suporting electrolyte: 0.1 mol l^{-1} of sodium carbonate–hydrogencarbonate buffer (pH 10) containing Na_2-EDTA (10 mmol l^{-1}) (pH adjusted with dilute NaOH solution)

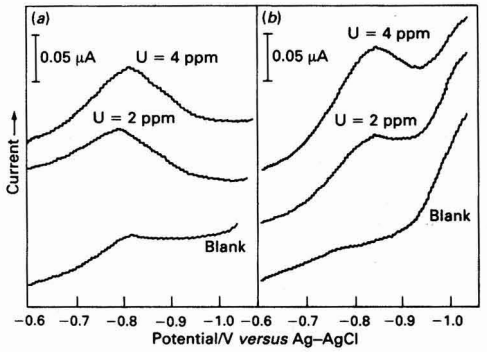

Fig. 4 Differential-pulse polarograms of U^{VI} in the absence and presence of thorium in 0.1 mol l^{-1} sodium carbonate–hydrogencarbonate buffer (pH 10) containing 0.5 g of Na_2-EDTA (solid) in 10 ml. (*a*) Thorium absent. (*b*) Thorium present (5 g l^{-1})

sufficiently in excess over the stoichiometric amount required by all the metal ions (thorium and other impurities) present. The pH of the solution was raised to the alkaline region by adding NaOH solution. A 1.0 ml volume of 1.0 mol l^{-1} carbonate–1.0 mol l^{-1} hydrogencarbonate mixture was added to the above solution and the pH was adjusted to 10. The volume was made up to 10 ml with distilled water and the solution was subjected to polarography.

Results and Discussion

Fig. 1 shows a typical differential-pulse polarogram of U^{VI} in 0.1 mol l^{-1} sodium carbonate–hydrogencarbonate buffer solution (pH 10) containing Na_2-EDTA. The effects of changes in pH, EDTA concentration and carbonate buffer concentration were studied to establish the optimum experimental conditions for U^{VI} reduction. The linear relationship between U^{VI} concentration and DPP peak current is shown in Fig. 2.

It is known that the U^{VI}–carbonate complex is very strong, the equilibrium constant being 2×10^{18} for the complex $[UO_2(CO_3)_3]^{4-}$.[8] The choice of a suitable pH for U^{VI} reduction was dictated by the presence of other metal ions (including Th) that are hydrolysed in the alkaline medium. The EDTA complexes of Th^{IV} and other cationic impurities present in the solution after dissolution of the thorium fuel rods in nitric acid are stable in alkaline solutions. Hence the addition of Na_2-EDTA and the use of an alkaline pH not only prevents the hydrolysis of the bulk Th^{IV} matrix and most of the divalent and trivalent impurities, but also shifts their reduction potentials well beyond the hydrogen discharge potential (−1.4 V *versus* Ag–AgCl). This effectively eliminates the interferences in the determination of U^{VI}.

Plots of peak potential (E_p) and peak current (i_p) for U^{VI} reduction *versus* pH reveal that both the potential and current are nearly constant over the pH range 8–12 (Fig. 3). This is in agreement with the observations of Jung *et al.*[14] As E_p and i_p were both constant in the pH range 8–12, a pH of 10 was chosen for further studies.

Fig. 4 shows differential-pulse polarograms of U^{VI} in the absence and presence of thorium. It is clear that the polarograms are not affected to any significant extent by the presence of large amounts of thorium, except for an alteration in the shapes of the differential-pulse peaks and the nature of the blank polarograms.

Analysis of Thorium Samples for Uranium Content

Uranium(VI) in thorium was determined by the proposed method and the values obtained were compared with those obtained by the ICP-AES method as developed in our laboratory.[15] The sample solutions provided for the ICP-AES analysis were diluted so as to give about 1 g l^{-1} of thorium, whereas the polarographic solution contained as much as 5 g l^{-1} of thorium. The DPP procedure yielded uranium values with a relative standard deviation of 2.4% at the 5 ppm level.

Synthetic samples containing thorium and uranium in ratios from 50 to 1000 along with other impurities were analysed by the DPP and ICP-AES methods. The results are given in Table 1.

Table 1 Analysis of uranium samples by ICP-AES and DPP. Samples containing thorium and other impurities. Supporting electrolyte: Na_2CO_3 + $NaHCO_3$ buffer containing 0.5 g of Na_2-EDTA (solid) at pH 10. Thorium content: 1 g l^{-1}

	U concentration/μg ml^{-1}	
Sample	ICP-AES	DPP
A	1.3	1.5
B	5.8	5.6
C	10.3	10.5
D	19.0	18.0

It should be noted that the spectrophotometric procedure involves a prior extraction step[1-3] whereas the present DPP method is capable of determining uranium in solutions after dilution but without involving any prior extraction step. The thorium content in the present method does not significantly influence the differential-pulse polarograms of U^{VI}, as can be seen from Fig. 4, because the Th^{IV}–EDTA complex itself serves as the inert supporting electrolyte.

It is concluded that DPP can be applied to the rapid and precise determination of low levels of uranium in thorium without the need for a prior extraction or separation step.

The authors thank Sri A. N. Prasad, Director, Fuel Reprocessing and Nuclear Waste Management Group, BARC, Sri M. K. Rao, Associate Director, FR and NWM Group, and Dr. R. K. Dhumwad, Head, Laboratory Section, Fuel Reprocessing Division, BARC, for their encouragement in this work. They also thank Dr. S. Gangadharan, Head, Analytical Chemistry Division, BARC, for his interest in this work.

References

1 Clayton, R. F., Hardwick, W. H., Moreton-Smith, M. and Todd, R., *Analyst*, 1958, **83**, 13.
2 Harton, C. A., and White, H. C., *Anal. Chem.*, 1958, **30**, 1779.
3 Mukherjee, A., and Rege, S. G., in *Proceedings of Radiochemistry and Radiation Chemistry Symposium, University of Poona*, Board of Research in Nuclear Sciences, Department of Atomic Energy, Bombay, 1982, paper RA-7.
4 Thompson, M., and Walsh, J. N., *A Handbook of Inductively Coupled Plasma Spectrometry*, Blackie, Glasgow, 1983, p. 20.
5 Latimer, W. M., *The Oxidation States of the Elements and Their Potentials in Aqueous Solutions*, Prentice Hall, Englewood Cliffs, NJ, 2nd edn., 1956, p. 299–301.
6 Pribil, R., and Blazek, A., *Collect. Czech. Chem. Commun.*, 1953, **16**, 567.
7 Auerbach, C., and Kissel, G., *Talanta*, 1964, **11**, 85.
8 Katz, J. J., and Seaborg, G. T., *The Chemistry of Actinide Elements*, Methuen, London, 1957, p. 190.
9 Harris, W. E., and Kolthoff, I. M., *J. Am. Chem. Soc.*, 1947, **69**, 446.
10 Stabrovskii, A. I., *Zh. Neorg. Khim.*, 1960, **5**, 811.
11 Perec, M., *Nukleonika*, 1961, **6**, 357.
12 Branica, M., and Pravdic, V., in *Polarography (1964)* (Proceedings of the 3rd International Congress of Polarography, Southampton, 1964), ed. Hills, G. J., Macmillan, London, 1966, vol. I, p. 435.
13 Chitnis, R. T., Kulkarni, R. T., Rege, S. G., and Mukherjee, A., *J. Radioanal. Chem.*, 1978, **45**, 331.
14 Jung, K.-S., Sohn, S. C., Ha, Y. K., Eom, T. Y. and Yun, S. S., *J. Electroanal. Chem.*, 1991, **315**, 113.
15 Dhumwad, R. K., Patwardhan, A. B., Joshi, M. V., Kulkarni, V. T., and Radhakrishnan, K., in *Proceedings of the Radiochemistry and Radiation Chemistry Symposium, Kalpakkam, India*, 1989, paper RA-17.

Paper 3/01051A
Received February 22, 1993
Accepted April 21, 1993

Electrochemical Reduction at Mercury Electrodes and Differential-pulse Polarographic Determination of Pentamidine Isethionate

M. Valnice B. Zanoni and Arnold G. Fogg*
Chemistry Department, Loughborough University of Technology, Loughborough, Leicestershire, UK LE11 3TU

Reduction processes are observed for pentamidine isethionate at a dropping mercury electrode above pH 7: the reduction potential is independent of pH below about pH 10. Below pH 10, adsorption of the reduced species is observed, whereas above pH 10 there is a large contribution owing to adsorption of pentamidine isethionate. For the polarographic determination of pentamidine isethionate, a pH of 8–9 is recommended with the addition of Triton X-100 as a maximum suppressor. Pentamidine isethionate can be determined by differential-pulse polarography down to about 5×10^{-6} mol l^{-1}.

Keywords: *Pentamidine isethionate determination; differential-pulse polarography*

Amidines are important medical and biochemical agents and can be identified in numerous cyclic derivatives of biological interest. Many of the compounds of this type have been examined as potential antibacterial and antiprotozoal drugs in humans and domestic animals.[1] Most of the active compounds possess two benzamidine residues, which are separated by a structural unit containing one or more atoms. A striking feature is that all of these compounds contain an unsubstituted amidine group.

Pentamidine isethionate [4,4′-(pentamethylenedioxy)dibenzamidine bis(2-hydroxyethanesulfonate)] belongs to this class of compound, and is used in the treatment of patients with pneumocystis carinii pneumonia.[2] This is a parasitic infection that attacks patients with severe immunosuppression. Since 1981, the occurrence of acquired immunodeficiency syndrome (AIDS) has been accompanied by a dramatic increase in the incidence of pneumocystis carinii pneumonia. A corresponding increase in the use of pentamidine isethionate has highlighted the need to develop rapid and reliable analytical methods for evaluating the quality of the drug and with sufficient sensitivity to quantify it at low levels in human patients.

Several analytical methods have been employed for these purposes, *viz.*, thin-layer chromatography, liquid chromatography, ultraviolet (UV) spectrophotometry, mass spectrometry and infrared spectroscopy.[3,4] A spectrofluorimetric method for determining pentamidine isethionate in plasma, urine and tissue,[5] and a high-performance liquid chromatographic method for its determination in blood serum[6] and whole-blood plasma and urine[7–9] have also been published.

Although some amidines and related compounds can be reduced or oxidized at electrodes,[1,10] only in recent years has increasing attention been paid to electrochemical studies of cyclic amidines, particularly the biologically active amidines. However, few electrochemical studies involving benzamidines in aqueous solution are found in the literature.[11,12] The reduction of substituted benzamidines is postulated to occur in two diffusion-controlled two-electron waves,[12] in contrast to earlier results for unsubstituted benzamidine,[11] which is reduced in a single four-electron step. The over-all process is usually pH-dependent and involves the saturation of double bonds and a cleavage of C–N bonds.

The aim of the present work was to investigate the possibility of using polarography for the determination of pentamidine isethionate in aqueous solution.

* To whom correspondence should be addressed.

Experimental

Apparatus

For differential-pulse polarographic and cyclic voltammetric measurements a Metrohm E612 VA scanner, an E611 VA-detector and a 663 VA stand were used in conjunction with a Houston Instruments Model 2000 *x–y* recorder. The multimode electrode in the VA stand was used in both the dropping mercury electrode and the hanging mercury drop electrode modes. The three-electrode system was completed by means of a glassy carbon auxiliary electrode and an Ag–AgCl reference electrode. All potentials are given relative to this Ag–AgCl (3 mol l^{-1} KCl) electrode. The d.c. and a.c. polarographic studies were carried out using a Metrohm E506 Polarecord with the 663 VA stand.

All pH measurements were made with a Corning combined pH reference electrode using a Radiometer PHM 64 pH meter, previously calibrated.

Reagents

All chemicals were of analytical-reagent grade. Water was obtained from a LiquiPure system.

Pentamidine isethionate was supplied by Fisons Pharmaceuticals. Stock standard solutions of the drug (1.0×10^{-3} mol l^{-1}) were prepared from the dried pure substance. All stock solutions were freshly prepared weekly and more dilute solutions were prepared as required from the stock solutions.

The supporting electrolyte was Britton–Robinson (B–R) buffer prepared in the usual way, *i.e.*, by adding to a solution 0.04 mol l^{-1} orthophosphoric acid, 0.04 mol l^{-1} in acetic acid and 0.04 mol l^{-1} in boric acid with the appropriate amount of 0.2 mol l^{-1} sodium hydroxide solution.

Procedures

The general procedure adopted for obtaining polarograms was as follows. An aliquot (10 ml) of B–R buffer or sodium hydroxide solution was placed in a clean, dry voltammetric cell and the required volume of standard pentamidine isethionate was added by means of a micropipette. The solution was purged for 15 min and the polarogram was recorded.

The differential-pulse mode was used with a pulse amplitude of 50 mV, a drop time (t_d) of 1 s and a scan rate of 3 mV s^{-1}, unless stated otherwise. The phase-selective a.c. polarographic behaviour was studied using a superimposed alternating voltage (U) of 8 mV and a phase angle of 0 or 90°.

Results and Discussion

D.c. and Differential-pulse Polarography

Pentamidine isethionate contains reducible amidine groups that provide the basis for its polarographic determination. In B–R buffer solutions, pentamidine isethionate is readily reduced in the pH range 7.0–12.0: the half-wave potentials ($E_{\frac{1}{2}}$), wave heights, shapes and the number of waves, depend on the pH, the drop time and the pentamidine isethionate concentration. In acidic solution (*i.e.*, pH <6.0), the reduction wave is masked by the electrolyte discharge.

Effect of pH

Differential-pulse polarograms of 0.5×10^{-5} mol l^{-1} pentamidine isethionate solutions, recorded at a drop time of 2 s and a pulse amplitude of 50 mV, exhibit one cathodic peak in the pH range 7.0–9.0. This peak becomes broader as the pH increases and becomes a double peak in solutions of pH 12.0, as is shown in Fig. 1. Plots of peak potential *versus* pH show two distinct regions (see Fig. 2): over the pH range 7.0–10.0 the peak potential is independent of pH, but above pH 10 it shifts linearly towards more negative values (slope of 38 mV per pH unit). The effect of the drop time on this peak, also shown in Fig. 2, is discussed below. The height of the peak decreases continuously above pH 9, being only about one-third of its original height at pH 12 (see Fig. 3). The heights of the d.c. wave and differential-pulse peaks within the pH range studied remained constant at room temperature for a period of at least 12 h after preparation of the solution for polarography.

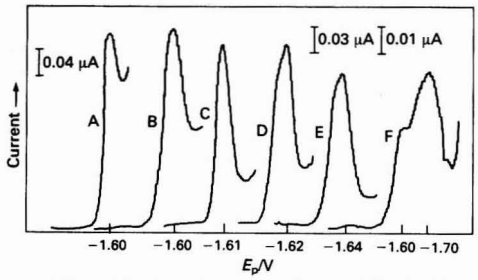

Fig. 1 Differential-pulse polarograms of pentamidine isethionate in B–R buffers. Pentamidine isethionate concentration = 0.5×10^{-5} mol l^{-1}. pH: A, 7.0; B, 8.0; C, 9.0; D, 10.0; E, 11.0; and F, 12.0. Drop time = 2 s, pulse amplitude = 50 mV, scan rate = 3 mV s^{-1}

Analysis of the shapes of the differential-pulse peaks indicates a degree of irreversibility, with peak half-width values of about 78 mV at pH 7–9, and even higher half-width values at higher pH values (82.7 and 102.4 mV at pH 10.0 and 11.0, respectively). The irreversibility of the system was confirmed by applying the criterion of Birke *et al.*,[13] when comparing forward and reverse differential-pulse scans. Differential-pulse polarograms obtained for pentamidine isethionate at a pulse amplitude of 50 mV (cathodic peak, forward scan) and 50 mV (anodic peak, reverse scan) yielded a ratio of the heights of the cathodic (i_{pc}) and anodic (i_{pa}) peaks of about 0.35 (pH 7.0–9.0) and a value of $E_{pc} - E_{pa}$ (E_{pc} = cathodic peak potential; E_{pa} = anodic peak potential) (about 39 mV) of less than the pulse amplitude. In strongly alkaline solutions, values of i_{pa}/i_{pc} and $E_{pc} - E_{pa}$ became slightly larger. However, although two peaks are observed using a pulse amplitude of 50 mV at pH 12.0, only one peak is observed in the reverse scan (pulse amplitude, 50 mV).

An interesting effect was observed when differential-pulse polarograms were recorded using a drop time of 1 s, in that it was possible to distinguish two peaks between pH 7.0 and 12.0. Whereas the second (main) peak shows the same behaviour as that observed with a drop time of 2 s (see Fig. 2), the peak potential of the pre-peak (at the less negative potential) is independent of pH over the pH range 7–12, and its peak height (see Fig. 3) is slightly smaller than that observed for the second peak. However, the heights of both peaks are affected equally by variation of pH. These results could indicate either that the electrode process occurs in two cathodic steps having very close reduction potentials, or that the reduction is associated with a strong adsorption process.

In order to distinguish between these two alternatives the reduction of pentamidine isethionate was studied further by d.c. and a.c. polarography and by cyclic voltammetry. Typical polarograms and voltammograms in B–R buffer of pH 9.0, which are representative of the pH range 7.0–9.0, are shown in Fig. 4. The d.c. polarographic parameters ($E_{\frac{1}{2}}$; i_l; $E_{\frac{1}{2}} - E_{\frac{1}{4}}$ and αn_a) (αn_a = electron transfer coefficient) were obtained from polarograms recorded with 0.5×10^{-4} mol l^{-1} pentamidine isethionate with a drop time of 0.4 s (see Table 1): these experimental conditions favoured the occurrence of a single well-defined wave over the pH range studied.

As indicated above, in the pH range 7.0–9.0, the half-wave potential was almost independent of pH and the limiting current was virtually constant. Logarithmic analysis of the waves resulted in straight lines, and, by applying the treatment of Meites and Israel,[14] the αn_a values point to an irreversible reduction process with $\alpha n_a = 1.38$. At higher pH values the

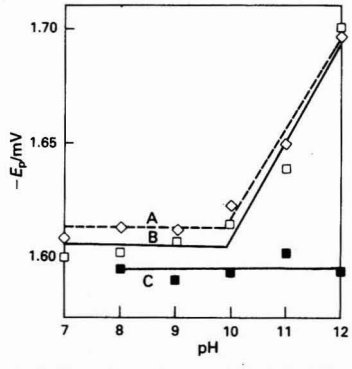

Fig. 2 Effect of pH on the peak potentials of the differential-pulse polarographic peaks obtained for a 0.5×10^{-5} mol l^{-1} solution of pentamidine isethionate in B–R buffer. A, Potential of single peak obtained with a drop time of 2 s; B, potential of second (main) peak (drop time = 1 s); and C, potential of first (pre-) peak (drop time = 1 s)

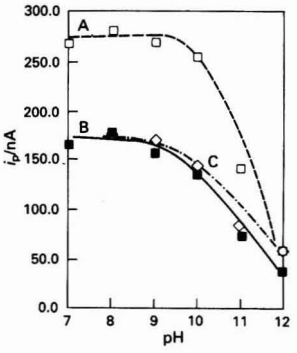

Fig. 3 Effect of pH on the peak currents of the differential-pulse polarographic peaks obtained for a 0.5×10^{-5} mol l^{-1} solution of pentamidine isethionate in B–R buffer. A, Peak obtained at a drop time of 2 s; B, second (main) peak obtained at a drop time of 1 s; and C, first (pre-) peak obtained at a drop time of 1 s

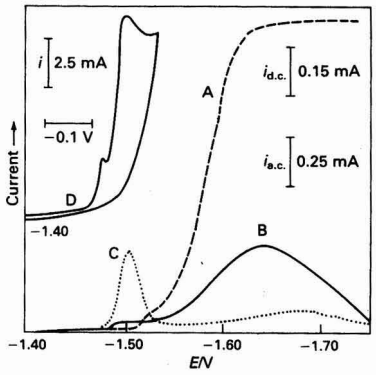

Fig. 4 Response of pentamidine isethionate (0.5×10^{-4} mol l^{-1}) in B–R buffer (pH 9.0); drop time = 1 s: A, d.c. polarography; B, a.c. polarography, phase angle 0° and U = 8 mV; C, a.c. polarography, phase angle 90° and U = 8 mV; and D, cyclic voltammogram of pentamidine isethionate at a concentration of 5.0×10^{-4} mol l^{-1} at a scan rate of 20 mV s^{-1}

Table 1 Effect of pH on d.c. polarograms of 0.5×10^{-4} mol l^{-1} pentamidine isethionate in B–R buffer (t_d = 1 s), and a.c. polarographic waves of 1×10^{-4} mol l^{-1} pentamidine isethionate obtained with phase angles of 90 and 0° and a superimposed potential of 8 mV

				0°		90°	
pH	$-E_i$/V	i_i/mA	αn_a	i_p/mA	$-E_p$/V	i_p/mA	$-E_p$/V
7.0	1.610	0.86	1.38	0.27	1.64	0.32	1.52
8.0	1.608	0.73	1.38	0.20	1.63	0.37	1.51
9.0	1.615	0.73	1.38	0.28	1.64	0.33	1.51
10.0	1.620	0.77	1.17	0.16	1.64	0.75	1.51
11.0	1.644	0.39	0.81	0.07	1.68	0.81	1.52
12.0	1.690	0.37	0.65	—	—	1.08	1.53

half-wave potentials are shifted linearly to more negative values (see Table 1), and the slope of the relationship E_i *versus* pH can be expressed as $E_i = -1.266 - 0.039$ pH. As indicated in Table 1, the change in the character of the reduction process observed above pH 10.0 is accompanied by an increase in the degree of irreversibility, and the waves diminish in height. Hence, it can be suggested that at pH values >10.0, the reduction of pentamidine isethionate probably involves preceding chemical reactions with participation of protons and/or strong adsorption effects.

Effect of Pentamidine Isethionate Concentration, Pulse Amplitude and Drop Time

In order to obtain further information on the nature of the electrode reaction, the influence of concentration and drop time was investigated at two pH values, *viz.*, 9.0 and 12.0, which are representative of the polarographic behaviour in the pH ranges 7.0–9.0 and 10.0–12.0, respectively. It was observed that the drop time directly affected the polarographic response at drop times from 0.4 to 3.0 s. Differential-pulse polarograms obtained at pH 9.0 show two cathodic peaks when shorter drop times are used [Fig. 5(*a*)].

In the same way, when the concentration is decreased and adsorption effects are minimized, the polarograms change from one with two peaks to one with a single peak [Fig. 6(*a*)]. Also, the differential-pulse polarographic response is influenced by pulse amplitude. For the same drop time (t_d = 1 s) there is a coalition of the two peaks when the pulse amplitude is decreased and only one peak can be observed at more negative potentials for pulse amplitudes less than −40 mV.

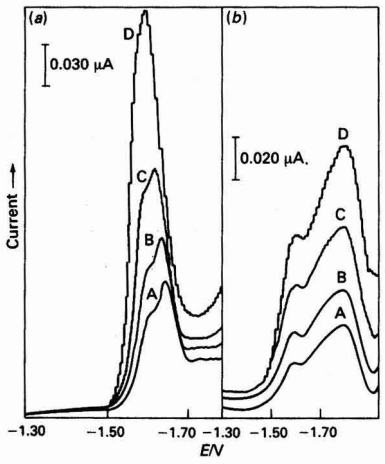

Fig. 5 Influence of the drop time of the DME on the differential-pulse polarographic reduction of 1×10^{-5} mol l^{-1} pentamidine isethionate in (*a*) B–R buffer (pH 9.0) and (*b*) B–R buffer (pH 12.0) at drop times of: A, 0.4; B, 0.6; C, 1.0; and D, 2.0 s

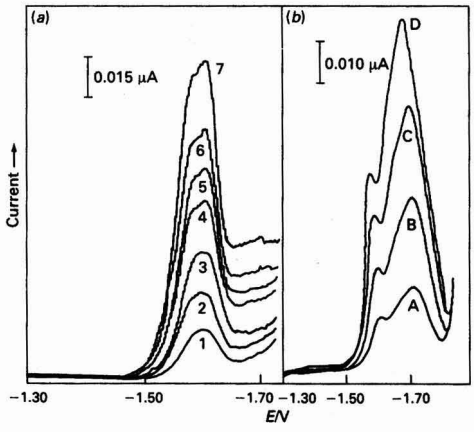

Fig. 6 (*a*) Differential-pulse polarograms of pentamidine isethionate in B–R buffer (pH = 9.0) at different concentrations: 1, 0.6×10^{-6}; 2, 1.2×10^{-6}; 3, 2.0×10^{-6}; 4, 2.6×10^{-6}; 5, 3×10^{-6}; 6, 4×10^{-6}; and 7, 5×10^{-6} mol l^{-1}. (*b*) Differential-pulse polarograms obtained in B–R buffer (pH 12.0): A, 0.5×10^{-5}; B, 1.0×10^{-5}; C, 2.0×10^{-5}; and D, 3.0×10^{-5} mol l^{-1} pentamidine isethionate

A comparison was made between a differential-pulse polarogram with a negative-going potential scan and a differential-pulse polarogram recorded with a positive-going potential scan. Although two cathodic peaks are observed on the forward scan for shorter drop times (t_d = 0.4 s), only one anodic peak is obtained on the reverse scan. In contrast, although one cathodic peak is observed on the forward scan (t_d = 2 s), this is split into two peaks at higher pulse amplitudes. Hence the behaviour is not that reported in the literature for an electrode process controlled either kinetically or by diffusion.[15–17] These results can be explained by the occurrence of a strong adsorption phenomenon coupled with electron transfer.[18,19] Double peaks can occur in differential-pulse polarograms when saturation of the electrode occurs before the application of the pulse. Hence at longer pulse amplitudes and higher concentrations, the main diffusion-controlled peak appears next to the adsorption peak. In

contrast, if the pulse application and sampling times are kept constant, two peaks are observed at shorter drop times, when the surface area is such that it promotes the situation where the sampling time is shorter than the time required to achieve maximum coverage.

Direct current polarograms confirm this diagnosis. Studies in the concentration range from 0.2×10^{-4} to 2.0×10^{-4} mol l^{-1} pentamidine isethionate, at pH 9.0, lead to the appearance of a new wave at a less negative potential when the concentration is increased to 0.7×10^{-4} mol l^{-1} (see Fig. 7, curve B). When the concentration was increased further, the height of the main wave (i) increased steadily and the height of the wave at the less negative potential (i') remained virtually constant. This indicates that the electrode reaction is controlled by adsorption of the reduced form of the compound.[20] Polarograms obtained in the same concentration range but using a drop time of 0.4 s show a single wave (Fig. 7, curve A), for which the peak height increases linearly with an increase in the pentamidine isethionate concentration in the same concentration range discussed above.

At pH 9.0, d.c. polarograms obtained at lower concentrations (0.2×10^{-4} mol l^{-1}) of pentamidine isethionate exhibited a diffusion-limited current, as the limiting current varied in a direct proportion to $t^{\frac{1}{6}}$. However, at 1.0×10^{-4} mol l^{-1}, the wave obtained at a drop time >1.0 s splits into two waves (see Fig. 7, curve II), for which the total limiting current decreases linearly with $t^{-\frac{1}{6}}$, indicating that the current is adsorption-controlled.[20] However, at pH 12.0, two peaks are observed in the pulse polarograms at any drop time or concentration, as is shown in Figs. 5(b) and 6(b). The linearity between the peak current (i_p) and $t^{\frac{1}{6}}$, where t, the drop time, varies between 0.4 and 3.0 s, suggests that the first electrode process is diffusion-controlled. The same conclusion was reached from the fact that the peak height increased linearly with concentration in the range from 1.0×10^{-5} to 7.0×10^{-5} mol l^{-1}. The second peak is broader than the first peak and the peak current showed deviations from linearity at high concentrations, which clearly indicates the presence of a strong adsorption phenomenon.

Direct current polarograms at pH 12.0 exhibit polarographic maxima (Fig. 8, curve A), which become more distorted at high concentrations. This behaviour is typical in the presence of an adsorption process, and the polarographic maximum hindered accurate current evaluation.

In an attempt to finalize the conclusions, the effect of the addition of Triton X-100 on the differential-pulse polarograms was studied for conditions where two peaks are observed. Polarograms recorded at pH 8.50 and at a drop time of 1.0 s in the presence of Triton X-100 show only one well-defined peak at all concentrations [Fig. 9(a)]. It is probable that the effect of the surface-active agent is to contribute to complete coverage of the electrode surface and to promote the suppression of the adsorption process coupled with the reduction of the pentamidine isethionate.

In contrast, differential-pulse polarograms obtained at pH 12.00 in the presence of Triton X-100 exhibit two peaks. The first peak is slightly larger and the second peak is smaller and

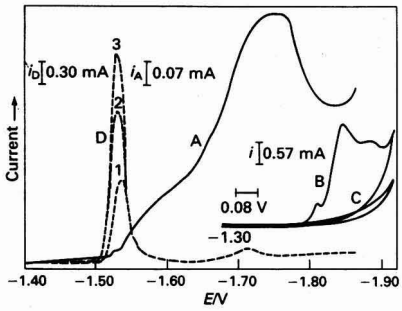

Fig. 8 Response of pentamidine isethionate (1.0×10^{-4} mol l^{-1}) in B–R buffer (pH 12.0) (drop time 1 s): A, d.c. polarography; B and C, first and second cyclic voltammograms at 5×10^{-4} mol l^{-1} pentamidine isethionate at a scan rate of 20 mV s^{-1}; and D, a.c. polarography, phase angle 90° and U = 8 mV at a pentamidine isethionate concentration of 1, 0.5×10^{-4}; 2, 1.0×10^{-4}; and 3, 1.5×10^{-4} mol l^{-1}

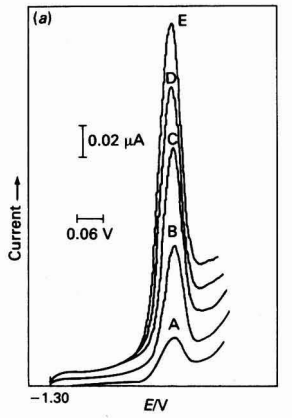

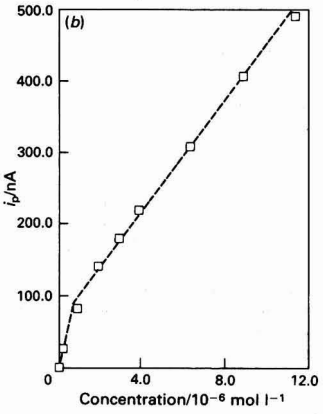

Fig. 9 (a) Differential-pulse polarograms of pentamidine isethionate in B–R buffer (pH 8.50) (drop time 1 s) at different concentrations: A, 0.2×10^{-6}; B, 0.9×10^{-6}; C, 1.9×10^{-6}; D, 2.9×10^{-6}; and E, 3.9×10^{-6} mol l^{-1}. (b) Calibration graph obtained at pH 8.50 in the presence of 0.001% Triton X-100

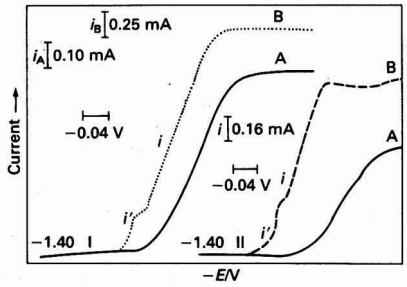

Fig. 7 (II) D.c. polarograms of 1×10^{-4} mol l^{-1} pentamidine isethionate measured in B–R buffer (pH 9.0) at a drop time of: A, 0.4 and B, 2.0 s. (I) D.c. polarograms obtained at pH 9.0 (drop time 0.4 s) in A, 0.5×10^{-4}; and B, 2.0×10^{-4} mol l^{-1} pentamidine isethionate

narrower than in the absence of Triton X-100. It is evident that the electrode process in very alkaline solution is coupled with stronger adsorption than that at pH values <9.0.

A.c Polarography and Cyclic Voltammetry

The phase-selective a.c. polarographic behaviour of pentamidine isethionate was studied in the pH range 7.0–9.0 for phase angles of 90 and 0°. Although at lower concentrations only one peak can be observed, a smaller peak is coupled with the main a.c. peak when the polarograms are recorded at 0° at the higher concentration of 1.0×10^{-4} mol l^{-1} (Fig. 4, curve B). The d.c. polarogram is sho ı for comparison. The main peak is much smaller than the corresponding d.c. limiting current at all pH values, as is shown in Table 1. The peak potential (E_p) is distinctly more negative than $E_{\frac{1}{2}}$ and the waves are very broad, emphasizing the presence of irreversibility and/or an adsorption phenomenon.[20] However, this small peak becomes very well-defined at about −1.52 V, when the polarograms are recorded at 90°, which confirms that an adsorption phenomenon is coupled with the electron-transfer reaction. The adsorption of the product of electron transfer was characterized by the appearance of a pre-peak in the cyclic voltammogram recorded at a low scan rate, as is shown in Fig. 4 (curve D).

A comparison of the peak heights obtained at 0 and 90° at different pH values is shown in Table 1. Analysis shows that the capacitive current increases markedly above pH 10.0. Concomitantly, the faradaic peak decreases in size, and it is evident that the electrode process is more significantly influenced by adsorption in very alkaline solutions.

At pH 12.0, the a.c. polarograms recorded at 0° do not show appreciable faradaic current, but at 90° one well-defined capacitive peak at −1.54 V can be observed, and this increases with concentration, as is shown in Fig. 8. This behaviour suggests that adsorption of the reactant might also be contributing to the process. This is confirmed by cyclic voltammograms obtained at pH 12.0, which show pre- and post-peaks in relation to the main peak at −1.60 V (see Fig. 8, curve C). In addition, multi-scan cyclic voltammograms show the absence of current on the second scan (Fig. 8), indicating that the reduction mechanism could involve spontaneous adsorption of the drug in this pH range.

Over-all Characteristics of the Reduction of Pentamidine Isethionate

The foregoing experiments show that adsorption phenomena strongly affect the reduction mechanism of pentamidine isethionate. The presence of a pre-wave under the determined conditions demonstrates that the reduction of the species is more strongly affected by adsorption of the electrode product at pH values <9.0. In contrast, although product adsorption cannot be neglected, in strongly alkaline solutions the preponderant form of pentamidine isethionate probably adsorbs spontaneously on mercury and provokes maxima and other distortions in the wave.

Under exceptional experimental conditions, when adsorption complications were minimized, it was possible to observe a break in the $E_{\frac{1}{2}}$ *versus* pH and E_p *versus* pH relationships at about pH 10.0 and a clear diminution of the peak height. This could indicate the presence of an acid–base equilibrium with at pK_a of about 10.0 or possibly the hydrolysis of the amidine group.

Because hydrolysis reactions of amidine compounds generally involve bond-cleavage,[21] some quantitative polarographic determinations were carried out to check the stability to hydrolysis of the species which predominate in pentamidine isethionate solutions at pH 8.0 and 12.0. Pentamidine isethionate was found to degrade considerably in 1 mol l^{-1} sodium hydroxide solution. However, by polarographing the same solution at pH 8.0, then at pH 12.0, and then again at pH 8.0, an 85% recovery of the pentamidine isethionate was evident in the final polarograms at pH 8.0. This relative stability to hydrolysis at pH 12 was confirmed by UV spectrophotometry, as illustrated by the spectra in Fig. 10. The absorption spectrum of pentamidine isethionate (λ_{max} = 260 nm) can be restored fully after addition of acid to a pentamidine isethionate solution in 0.2 mol l^{-1} sodium hydroxide (in which λ_{max} = 245 nm). Hence the preponderant form of pentamidine isethionate in strongly alkaline solution appears to be the species containing the unprotonated amidine group. This would be in agreement with the chemistry of unsubstituted benzamidines, for which the dissociation equilibria are characterized by protonation of the imino nitrogen, and for which the pK_a values[22] are about 11.2.

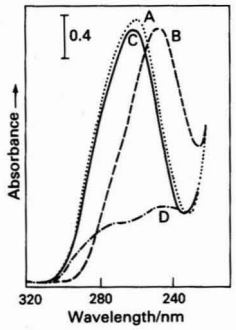

Fig. 10 UV spectra of 1×10^{-4} mol l^{-1} pentamidine isethionate at A, pH 8.0; B, in 0.20 mol l^{-1} sodium hydroxide; C, at pH 8.0 restored; and D, in 1 mol l^{-1} sodium hydroxide

Hence, with the knowledge that amidine groups can be reduced in aqueous solutions in a two-electron process,[10] it seems probable that four electrons would be involved in the reduction of pentamidine isethionate, which has two amidine groups. This is consistent with the value of αn_a = 1.38 found by d.c. polarography (α = 0.35 for n = 4) at pH <10. Therefore, as with other aromatic amidine compounds,[11,12] the over-all course of the reduction of pentamidine isethionate probably involves reductive cleavage of the amidine group, which can be represented as follows:

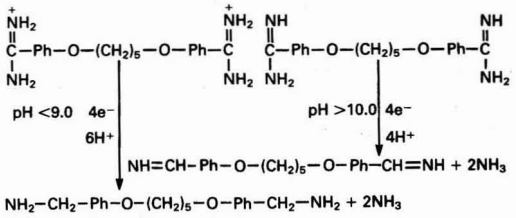

Determination of Pentamidine Isethionate

A pH of about 8.0–9.0 was chosen as optimum for analytical purposes, because it yielded the highest peak currents and gave the best separation from the background electrolyte reduction. The limiting diffusion currents obtained from d.c. polarograms were found to be a linear function of the pentamidine isethionate concentration only when shorter drop times, *e.g.*, 0.4 s, were utilized. Satisfactory calibration graphs were obtained over the concentration range from 0.5×10^{-4} to 2.0×10^{-4} mol l^{-1}.

Differential-pulse polarography permitted quantitative measurements to be made at lower concentration ranges, the limit of determination for pentamidine isethionate being

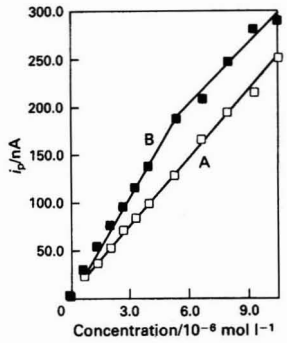

Fig. 11 Effect of the pentamidine isethionate concentration on calibration graphs obtained at pH 8.50 using different drop times: A, 1 s (second peak); B, 2 s

about 5×10^{-7} mol l^{-1}. Differential-pulse polarographic calibration graphs could be obtained over the concentration range from 0.5×10^{-6} to 10×10^{-6} mol l^{-1} at pH 8.5 for the second peak when a drop time of 1 s was utilized (see Fig. 11, curve A). The slope obtained, 2.25×10^{7} nA mol^{-1}, and the correlation coefficient, 0.9977, indicate excellent linearity. The height of the first peak shows a slight deviation from linearity for concentrations up to 7×10^{-6} mol l^{-1}. At a drop time of 2 s, where only one peak is observed, a linear relationship between peak height and the concentration of pentamidine isethionate can be obtained only over the range from 0.6×10^{-6} to 5.0×10^{-6} mol l^{-1} (see Fig. 11, curve B). At higher concentrations, adsorption effects promote deviation of the calibration graphs.

Although two peaks are observed at pH 8.50 and at a drop time of 1 s, as discussed earlier, differential-pulse polarograms at different concentrations of pentamidine isethionate in the presence of 0.001% Triton X-100 exhibit only one well-defined and reproducible peak, which is excellent for analytical purposes. There is a linear dependence with increase in concentration above about 1×10^{-6} mol l^{-1} pentamidine isethionate, as is shown in Fig. 9(*b*). The uniform enhancement of peak height above this concentration in the presence of Triton X-100 is apparent, and hence if a linear calibration graph is constructed it passes through the current axis above the origin.

The results obtained indicate that polarographic techniques are suitable for the determination of pentamidine isethionate. Preliminary results have shown that improvements in sensitivity can be achieved by using adsorptive stripping voltammetry in strongly alkaline solution, and that this technique can be used to some extent directly on urine samples. This work will be reported later.

The authors thank Fisons Pharmaceuticals plc for providing samples, and for their interest in this project. M. V. B. Z. thanks the FAPESP (Brazil) for financial support, and the University of Araraquara, Brazil, for leave of absence.

References

1 Grout, R. J., in *The Chemistry of Amidines and Imidates*, ed. Patai, S., Wiley, Bristol, 1975, vol. 1, pp. 255–277.
2 Goal, K. L., and Campoli-Richards, D. M., *Drugs*, 1987, **33**, 242.
3 *Martindale: The Extra Pharmacopoeia*, ed. Reynolds, J. E. F., The Pharmaceutical Press, London, 29th edn., 1989, pp. 675–677.
4 Mount, D. L., Miles, J. W., and Churchill, F. C., *J. Assoc. Off. Anal. Chem.*, 1986, **69**, 624.
5 Waalkes, T. P., and De Vita, V. T., *J. Lab. Clin. Med.*, 1970, **75**, 873.
6 Dickinson, C. M., Naviland, T. R., and Churchill, C., *J. Chromatogr.*, 1985, **345**, 91.
7 Lin, J. M. H., Shi, R. J., and Li, E. T., *J. Liq. Chromatogr.*, 1986, **9**, 2035.
8 Dusci, L. J., Hackett, L. P., Forbes, A. M., and Ilett, K. F., *Ther. Drug. Monit.*, 1987, **9**, 422.
9 Ericsson, O., and Rais, M., *Ther. Drug Monit.*, 1990, **12**, 362.
10 Jaworski, J. S., and Kaalinowski, M. K., in *The Chemistry of Amidines and Imidates*, eds. Patai, S., and Rappoport, Z., Wiley, Bristol, 1991, pp. 789–846.
11 Sevcik, J., *Acta Univ. Palacki. Olomuc., Fac. Rerum Nat.*, 1977, **53**, 37.
12 Kane, P. O., *Fresenius' Z. Anal. Chem.*, 1960, **173**, 50.
13 Birke, R. L., Kim, M., and Strassfeld, M., *Anal. Chem.*, 1981, **53**, 852.
14 Meites, L., and Israel, Y., *J. Am. Chem. Soc.*, 1961, **83**, 4903.
15 Rodriguez-Monge, L. M., Munoz, E., Avila, J. L., and Camacho, L., *Anal. Chem.*, 1988, **60**, 2269.
16 Munoz, E., Avila, J. L., and Camacho, L., *Anal. Chem.*, 1991, **63**, 1574.
17 Maestre, M. S., Munoz, E., Avila, J. L., and Camacho, L., *Electrochim. Acta*, 1992, **37**, 1129.
18 Flanagan, J. B., Takahashi, K., and Anson, F. C., *J. Electroanal. Chem.*, 1977, **81**, 261.
19 Pizeta, I., Lovric, M., Zelic, M., and Branica, M., *J. Electroanal. Chem.*, 1991, **318**, 25.
20 Bond, A. M., *Modern Polarographic Methods in Analytical Chemistry*, Marcel Dekker, New York, 1980, pp. 84–166 and 288–316.
21 Wolfe, R. H., in *The Chemistry of Amidines and Imidates*, ed. Patai, S., Wiley, Bristol, 1975, vol. 1, ch. 8, pp. 349–365.
22 Smith, J. A., and Taylor, H., *J. Chem. Soc. B*, 1969, 66.

Paper 3/00855J
Received February 12, 1993
Accepted May 6, 1993

Cathodic Stripping Voltammetric Determination of Pentamidine Isethionate at a Hanging Mercury Drop Electrode

M. Valnice B. Zanoni and Arnold G. Fogg*
Chemistry Department, Loughborough University of Technology, Loughborough, Leicestershire, UK LE11 3TU

Differential-pulse cathodic stripping voltammetry was used for the determination of trace amounts of pentamidine isethionate at a hanging mercury drop electrode using its reduction peak at −1.57 V in 0.2 mol l^{-1} sodium hydroxide. The optimum accumulation potential and accumulation time were −1.1 V and up to 180 s, respectively. Linear calibration graphs were obtained up to 1×10^{-6} mol l^{-1}: the limit of detection was calculated to be 3.0×10^{-10} mol l^{-1}. The effect of various components of urine on the voltammetric response was studied, and albumin, creatinine and uric acid caused interference in the method. The direct determination of the drug (>1×10^{-7} mol l^{-1}) in urine can be effected using a high dilution of the sample.

Keywords: *Pentamidine isethionate determination; cathodic stripping voltammetry*

Pentamidine isethionate [4,4′-(pentamethylenedioxy)dibenzamidine bis(2-hydroxyethanesulfonate)], an aromatic diamidine derivative, is an antiprotozoal agent used in the treatment of pneumocystis carinii pneumonia.[1–3] Modern applications of this drug, and the various methods of determining it, have been discussed previously.[4] In the earlier paper[4] the electrochemical reduction at mercury electrodes and the differential-pulse polarographic determination of the drug were reported. A cathodic wave is observed at pH >7.0, and the reduction potential (−1.60 V *versus* Ag–AgCl) is independent of pH to just below pH 10 (pK_a of pentamidine isethionate ≈10). Below pH 10, product adsorption is apparent, whereas above pH 10 the determinand adsorbs strongly. For the determination of pentamidine isethionate down to about 1×10^{-6} mol l^{-1}, a pH of 8–9 is recommended using Triton X-100 as a maximum suppressor.

The aim of the present work was to investigate the possibility of increasing the sensitivity and rapidity of the voltammetric determination of pentamidine isethionate by using cathodic stripping voltammetry, based on the adsorptive accumulation of the drug on the surface of a hanging mercury drop electrode (HMDE) above pH 10.

Experimental

Apparatus

For voltammetric measurements a Metrohm E612 voltammetric scanner and E611 voltammetric detector were used with a Houston Instruments Model 2000 *x–y* recorder. A Metrohm 663 VA stand was used in the HMDE mode. The three-electrode system was completed by means of a glassy carbon auxiliary electrode and an Ag–AgCl reference electrode. All potentials given are relative to this Ag–AgCl (3 mol l^{-1} KCl) electrode.

Reagents

All chemicals were of analytical-reagent grade. De-mineralized water was obtained from a LiquiPure system.

Pentamidine isethionate stock standard solutions (1×10^{-4}–4×10^{-4} mol l^{-1}) were prepared from the dried pure substance (kindly supplied by Fisons Pharmaceuticals) in de-mineralized water. All solutions were freshly prepared daily and more dilute solutions were prepared from the stock solutions as required.

Procedures

The general procedure adopted for obtaining cathodic stripping voltammograms was as follows. An aliquot (20 ml) of sodium hydroxide solution of the required concentration was placed in a clean, dry voltammetric cell and the required volume of standard pentamidine isethionate was added by means of a micropipette. The stirrer was switched on, and the solution was purged for 15 min. An accumulation potential was applied to the working electrode while the solution was stirred continuously. After accumulation for 15 s, a negative-going differential-pulse scan was initiated, the resulting voltammograms being recorded. The operational parameters used were: pulse amplitude, 50 mV; scan rate, 10 mV s^{-1}; and pulse interval, 1 s.

Results and Discussion

Preliminary studies in Britton–Robinson (B–R) buffers showed a single stripping peak for 1×10^{-5} mol l^{-1} pentamidine isethionate at pH values >10.0 with an accumulation time of 180 s. The peak height is much greater than that obtained with differential-pulse polarography. It was observed that the peak height decreased gradually with decreasing pH and the peak disappeared completely at about pH 9.5. Although it was initially considered that this adsorption at high pH might have been due to hydrolysis of the pentamidine isethionate and the peak obtained be due to reduction of the adsorbed hydrolysis product, this was shown not to be the case. The adsorption and reduction are of the neutral pentamidine isethionate molecule.

It was considered that this adsorption could be used as an effective preconcentration step prior to the voltammetric determination of pentamidine isethionate in very alkaline solutions in which the differential-pulse polarographic peaks had previously been shown to be very small.[4]

Cyclic voltammetric studies showed that pentamidine isethionate is rapidly accumulated on an HMDE from a stirred solution. Typical cyclic voltammograms of a 1×10^{-6} mol l^{-1} solution of pentamidine isethionate in 0.2 mol l^{-1} sodium hydroxide solution are shown in Fig. 1. A narrow cathodic peak, corresponding to an irreversible process, can be seen at −1.58 V. The peak is absent in the subsequent scan, indicating rapid desorption from the electrode (curve B). The height of the peak was shown to be directly proportional to the scan rate within the range 10–100 mV s^{-1} and the peak potential shifts linearly to more negative potentials when the scan rate is increased, indicating that the reduction is that of an adsorbed species.[5]

* To whom correspondence should be addressed.

Comparison of the voltammetric responses obtained with the linear scan and differential-pulse waveforms showed that the use of the pulse technique improves the sensitivity. Differential-pulse adsorptive stripping voltammograms of 5.8 $\times$ 10^{-7} mol l^{-1} pentamidine isethionate solutions in 0.2 mol l^{-1} sodium hydroxide using accumulation times of 0 and 180 s are shown in Fig. 2. Well-defined stripping peaks were observed with peak potentials at -1.60 V and peak half-widths of 31 mV. Voltammograms obtained without previous accumulation exhibit a much smaller peak.

Several parameters directly affect the voltammetric response. The peak current is linearly related to the pulse amplitude between 20 and 80 mV: a value of 50 mV was chosen as optimum as there is a loss of resolution at higher values. The peak current increased with the drop size on the voltammetric stand, and the larger drop size (nominally 0.4 mm^2) was chosen as the optimum. Forced convection (*i.e.*, stirring) during the accumulation step also affected the resulting stripping peak current. Tests were carried out between stirring positions 0 and 6 on the voltammetric stand. The peak current increases with increasing stirring speeds but becomes approximately constant at and above stirring speed 3 (approximately 1500 rev min^{-1}), and this speed was chosen as giving the best results.

The effect of accumulation potential (E_{acc}) on the stripping current at potentials between -0.1 and -1.5 V for solutions of 3.7 $\times$ 10^{-7} mol l^{-1} pentamidine isethionate in 0.2 mol l^{-1} NaOH using an accumulation time (t_{acc}) of 180 s is shown in Fig. 3. The peak height decreases when accumulation potentials more negative than -1.4 V are used and the reduction potential of pentamidine isethionate is approached. The current is maximum for accumulation between -1.0 and -1.2 V, but a decreased signal (decreased adsorption) is observed at potentials less negative than about -0.8 V. A potential of -1.1 V was adopted as the optimum accumulation potential.

In order to investigate the effect of basicity on the peak height and peak potential, the differential-pulse adsorptive stripping voltammetric response was studied for 5.8 $\times$ 10^{-7} mol l^{-1} pentamidine isethionate in solutions of different concentration of sodium hydroxide (see Fig. 4). The peak height increased linearly with sodium hydroxide concentration in the range from 5 $\times$ 10^{-3} to 0.4 mol l^{-1}, when the accumulation time and accumulation potential were kept constant at 180 s and -1.1 V, respectively. Also, the peak potential shifts linearly towards more negative values (with a slope of 80 mV per pH unit). The effect of accumulation time for 5.8 $\times$ 10^{-7} mol l^{-1} pentamidine isethionate at several sodium hydroxide concentrations is shown in Fig. 5. It was verified that the occurrence of a measurable peak at low concentrations of sodium hydroxide required a longer accumulation time. Similarly, for the same accumulation time, the current reaches a plateau because saturation of the electrode surface occurs more rapidly at higher sodium hydroxide concentrations.

For analytical purposes a sodium hydroxide concentration of 0.2 mol l^{-1} was therefore chosen. At this concentration a large peak is obtained. No significant hydrolysis of the pentamidine isethionate appears to occur at this concentration

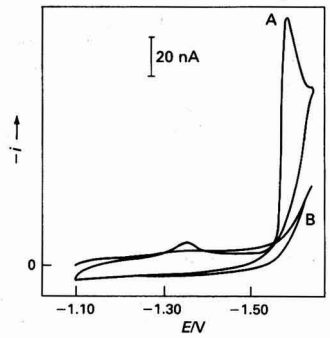

Fig. 1 Repetitive cyclic voltammograms of 1 $\times$ 10^{-6} mol l^{-1} pentamidine isethionate in 0.2 mol l^{-1} NaOH after stirring for 120 s at -1.1 V (accumulation potential). Scan rate, 70 mV s^{-1}. A, First scan and B, second scan

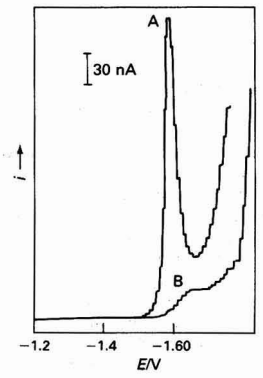

Fig. 2 Differential-pulse adsorptive stripping voltammograms of 5.8 $\times$ 10^{-7} mol l^{-1} pentamidine isethionate in 0.2 mol l^{-1} NaOH. A, Accumulation time of 180 s at -1.1 V in stirred solution and B, without accumulation

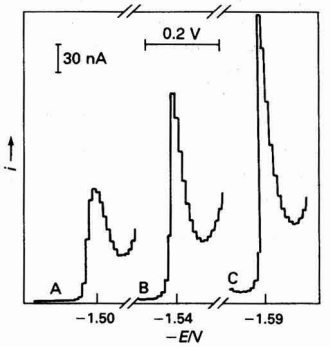

Fig. 3 Influence of accumulation potential on stripping peak current for 3.7 $\times$ 10^{-7} mol l^{-1} pentamidine isethionate in 0.2 mol l^{-1} NaOH with t_{acc} = 180 s

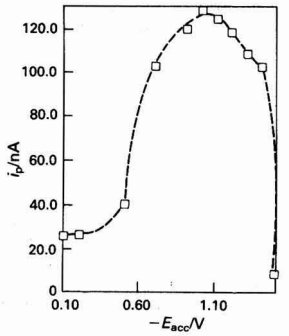

Fig. 4 Differential-pulse adsorptive stripping voltammograms of 5.8 $\times$ 10^{-7} mol l^{-1} pentamidine isethionate in A, 0.005; B, 0.02; and C, 0.1 mol l^{-1} NaOH. t_{acc} = 180 s; E_{acc} = -1.1 V

of sodium hydroxide, and the peak height is stable with time. The effect of accumulation time on the peak heights observed for 3.7×10^{-7} and 1.0×10^{-6} mol l^{-1} pentamidine isethionate solutions showed that there was a rectilinear relationship up to accumulation times of about 210 and 60 s, respectively. Above this time saturation of the mercury drop was observed. Hence the choice of accumulation time depends on the range of analyte concentration being determined.

The peak height is linearly dependent on the pentamidine isethionate concentration. As shown in Fig. 6, linear calibration graphs can be obtained from voltammograms recorded at accumulation times between 30 and 180 s from 1×10^{-7} to 1×10^{-6} mol l^{-1} pentamidine isethionate in 0.2 mol l^{-1} sodium hydroxide solution. An accumulation time of 180 s and a sodium hydroxide concentration of 0.2 mol l^{-1} are recommended as optimum conditions for the determination of the drug up to 1×10^{-7} mol l^{-1}.

The reproducibility of the method was determined by successive measurements of ten solutions of 5.0×10^{-7} mol l^{-1} pentamidine isethionate in 0.2 mol l^{-1} sodium hydroxide. Relative standard deviations of 4.4% were obtained with preconcentration times of 180 s. The limit of detection was calculated to be 3.0×10^{-10} mol l^{-1} with an accumulation time between 5 and 10 min. At lower concentrations ($<5.0 \times 10^{-9}$ mol l^{-1}) the peak is present but it was sometimes difficult to measure owing to the supporting electrolyte discharge. However, it is possible to obtain a linear concentration dependence for this peak within the concentration range from 5.0×10^{-9} to 1×10^{-8} mol l^{-1} with an accumulation time of 5 min in stirred solutions.

In order to investigate the possibility of applying cathodic stripping voltammetry to the determination of pentamidine isethionate in urine samples, a study was carried out of the influence of various urine components on the stripping peak currents of the drug. The following urine constituents were selected: albumin, uric acid, urea, glucose, creatinine, potassium, chloride and phosphate. It was demonstrated that there is no significant interference from phosphate, chloride and potassium in amounts at least four times higher than those usually found in urine. Fig. 7 shows the effect of the addition of increasing amounts of each urine constituent on the peak current. Albumin and uric acid, even at the low levels at which they are usually present in urine, lower the signal by 60 and 80%, respectively, and the peak disappears completely in the presence of 50 mg ml^{-1} of these components. Glucose has virtually no effect on the adsorption and reduction of pentamidine isethionate. Urea and creatinine at concentrations above 60 mg ml^{-1} lowered the voltammetric response by 60%.

The possibility of determining pentamidine isethionate in human urine was investigated. It was found that the direct determination of pentamidine isethionate in urine is possible by employing a high dilution of the sample with the supporting electrolyte. Urine was spiked to a concentration of 2.2×10^{-5} mol l^{-1} in pentamidine isethionate and 0.50 ml aliquots of this sample were added to 20 ml of 0.2 mol l^{-1} sodium hydroxide in the cell. The voltammogram was recorded after accumulating for 180 s at −1.1 V. The peak potential was slightly shifted to a less negative potential but the peak height was not affected by the presence of urine. Quantification of the urine content of the drug was accomplished by two standard additions. The recovery obtained was 70% and typical voltammograms are shown in Fig. 8(*b*). However, the peaks obtained for urine samples containing lower concentrations of pentamidine isethionate were partially suppressed. In addition, it was shown that direct dilution of 1 ml of urine, spiked to a concentration of 7×10^{-7} mol l^{-1} with pentamidine isethionate by adding it to 19 ml of 0.2 mol l^{-1} sodium hydroxide solution in the voltammetric cell, lowered the voltammetric response by 5% in relation to that obtained in the absence of urine [see Fig. 8(*a*)]. Further dilutions involving more than 4 ml of urine to 16 ml of sodium hydroxide lead to a depression of the pentamidine isethionate peak of 70%.

Taking into account the above results, the direct determination of pentamidine isethionate in human urine is possible, but only under exceptional conditions. It is not possible to determine pentamidine isethionate in urine samples containing very low concentrations of this drug or by using a higher ratio of urine in relation to the supporting electrolyte, probably owing to the effective inhibition of the preconcentration process on the electrode. Further, some natural constituents of the urine give rise to peaks close to that of pentamidine

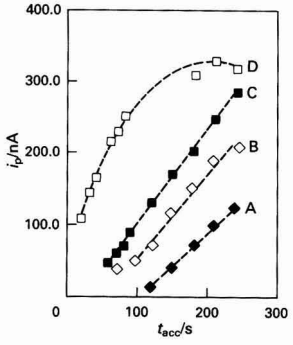

Fig. 5 Effect of accumulation time on peak current for pentamidine isethionate (5.8×10^{-7} mol l^{-1}) obtained for various concentrations of NaOH: A, 0.005; B, 0.1; C, 0.2; and D, 0.4 mol l^{-1}. $E_{acc} = -1.1$ V

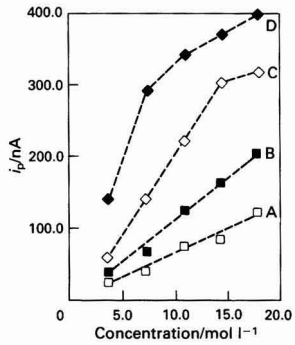

Fig. 6 Calibration graphs for pentamidine isethionate obtained for various accumulation times in 0.2 mol l^{-1} NaOH: A, 30; B, 60; C, 120; and D, 180 s

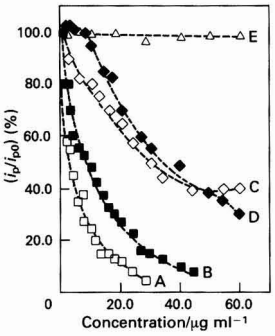

Fig. 7 Effects of various urine components on stripping peak current for 5.8×10^{-7} mol l^{-1} pentamidine isethionate in 0.2 mol l^{-1} NaOH, with an accumulation time of 180 s at −1.1 V. A, Albumin; B, uric acid; C, urea; D, creatinine; and E, glucose

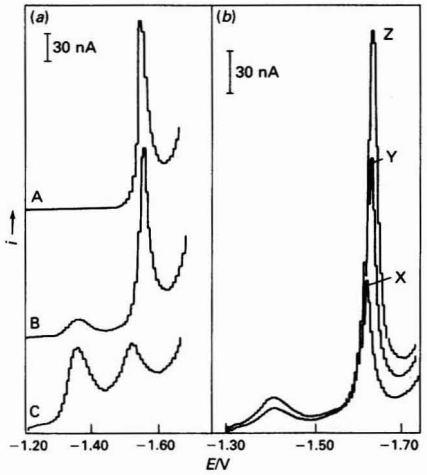

Fig. 8 (*a*) Differential-pulse adsorptive stripping voltammograms of 7×10^{-7} mol l^{-1} pentamidine isethionate in 0.2 mol l^{-1} NaOH in the presence of urine diluted: A, without urine; B, 1 + 19 ml in urine–electrolyte; and C, 5 + 15 ml in urine–electrolyte. t_{acc} = 120 s; E_{acc} = − 1.1 V; scan rate = 10 mV s^{-1}. (*b*) Stripping curves obtained using the standard additions method. X, 0.5 ml of urine spiked with pentamidine isethionate in 20 ml of 0.2 mol l^{-1} NaOH; Y, addition of 0.2 ml of a 2×10^{-5} mol l^{-1} standard pentamidine isethionate solution; and Z, further addition of 0.2 ml of standard solution

isethionate [see Fig. 8(*a*)]. Hence a urine sample clean-up procedure would be necessary prior to the determination of pentamidine isethionate. Previous workers[6,7] have used solid-phase extraction with adsorptive stripping voltammetry, and this might prove a fruitful route.

The authors thank Fisons Pharmaceuticals plc for providing samples of pentamidine isethionate, and for their interest in this work. M. V. B. Z. thanks FAPESP (Brazil) for financial support and the Instituto de Quimica (UNESP), Araraquara, Brazil, for leave of absence.

References

1 *Martindale: The Extra Pharmacopoeia*, ed. Reynolds, J. E. F., The Pharmaceutical Press, London, 29th edn., 1989, pp. 675–677.
2 Pearson, R. D., and Hewlett, E. L., *Ann. Intern. Med.*, 1985, **103**, 782.
3 Sands, M., *Rev. Infect. Dis.*, 1985, **7**, 625.
4 Zanoni, M. V. B., and Fogg, A. G., *Analyst*, 1993, **118**, 1157.
5 Laviron, E., *J. Electroanal. Chem.*, 1974, **52**, 35.
6 Hernandez, L., Zapardiel, A., Lopes, J. A. P., and Bermejo, E., *Talanta*, 1988, **35**, 287.
7 Telting-Diaz, Miranda Ordieres, A. J., Costa Garcia, A., Tuñón Blanco, P., Diamond, D., and Smyth, M. R., *Analyst*, 1990, **115**, 1215.

Paper 3/00992K
Received February 19, 1993
Accepted May 6, 1993

Direct Determination of Ethanol in all Types of Alcoholic Beverages by Near-infrared Derivative Spectrometry

Máximo Gallignani, Salvador Garrigues and Miguel de la Guardia*
Department of Analytical Chemistry, University of Valencia, 50 Dr. Moliner St. 46100, Burjassot (Valencia), Spain

A rapid and accurate method has been developed for the direct determination of ethanol in all types of alcoholic beverages. The method, which does not require any sample treatment (except for simple de-gassing for beer samples or dilution with distilled water for spirits), is based on the use of the first derivative of the near-infrared absorbance spectrum. Measurements, carried out between the 1680 nm peak and the 1703 nm valley, provide a typical calibration graph [$dA/d\lambda = 0.0000_2 + 0.0127c$ (where c is the concentration of ethanol in % v/v)] for a concentration range up to 25% v/v with a regression coefficient of 0.999992 and a limit of detection (for $k = 3$) of 0.1% v/v. The interference of sugars in the determination of ethanol can be seen by the presence of bands in the derivative spectrum in the range between 1300 and 1800 nm and can be corrected. Results comparable to those found by a reference pycnometric procedure or by gas chromatography were obtained when the proposed method was applied to the determination of ethanol in beer, white and red wines, whisky, gin and rum samples and also in sweet wines and fruit liqueurs.

Keywords: *Near-infrared derivative spectrometry; ethanol determination; alcoholic beverage*

The determination of ethanol in alcoholic beverages is a very important problem for social and economic reasons, particularly in relation to the taxes imposed on alcohol in different countries. This type of analysis is carried out in many laboratories, not only by producers but also in state and customs laboratories. Hence attempts have been made to simplify the methods available for the determination of ethanol and to develop new strategies that can be used with low-cost instrumentation and without complex sample treatment procedures.

The current official methods for the determination of ethanol are based on physical measurements, carried out after a previous distillation of the sample in order to separate the ethanol.[1–4] However, chemical methods can be used, based on the oxidation of ethanol to acetic acid with potassium dichromate and the determination of the excess oxidizing agent by using Fe^{II} or by iodimetry.[5]

Instrumental methods can also be employed for the determination of ethanol, and gas chromatography,[6,7] liquid chromatography,[8,9] potentiometry[10] and nuclear magnetic resonance spectroscopy[11,12] have been proposed.

In recent years the enzymic determination of ethanol has undergone considerable development and a series of enzymic methods, based on different techniques, which can be carried out in batch or flow injection mode, have been proposed.[13–16]

Infrared (IR) spectrometry, both in the mid and the near range, provides interesting possibilities for the determination of ethanol.

In the mid-IR range, ethanol has been determined using cells of an appropriate material, to avoid damage from water, and with a small thickness, in order to reduce the high absorbance of IR radiation by ethanol and water solutions.[17] In order to carry out these determinations a series of mathematical treatments, such as the use of orthogonal functions[17–19] or derivative spectrometry,[17,20,21] have been proposed.

The near-infrared (NIR) offers the possibility of determining ethanol in the presence of water by using ordinary glass cells, without the need for short pathlengths. A series of methods based on the use of NIR reflectance analysis have been applied to the determination of ethanol in beer[22–24] and wines.[25] Transmission NIR spectrometry has been employed for the determination of ethanol in beers[26] and molasses.[27] Also, methods employing optical fibres can be used for the monitoring of fermentation processes[28] and for the analysis of wines.[29] However, in general, methods based on NIR have been applied to the determination of ethanol in only one type of alcoholic beverage, *viz.*, beers or wines, and there appears to be no general procedure which permits the direct determination of ethanol in all types of alcoholic beverages, even in samples with a high sugar content. Hence, the aim of the present work was to develop a suitable methodology for this purpose.

Experimental

Apparatus

A Perkin-Elmer Lambda 9 double-beam ultraviolet/visible/near-infrared (UV/VIS/NIR) spectrometer, equipped with a tungsten–halogen lamp source and a PbS detector was used to carry out absorbance measurements. The spectrometer covers a wavelength range from 185 to 3200 nm and is equipped with a monochromator with a 260 lines per mm grating to enable it to operate in the NIR region. An Epson EL 2 computer, with a PECSS software package for UV/VIS/NIR (from Perkin-Elmer, release 4.01), controls the spectrometer functions and permits absorbance measurements to be carried out and the corresponding derivative to be calculated. Glass cells, with 1 cm and 1 mm pathlengths, were employed to carry out the direct determination of ethanol in alcoholic beverages.

For the chromatographic determination of ethanol, a Perkin-Elmer Model Sigma 3 gas chromatograph with a flame-ionization detector was employed; it was equipped with a 2 m × 2 mm i.d. glass column with 15% m/m Carbowax on Chromosorb (80–100 mesh).

For the determination of ethanol by the pycnometric procedure a Gibertini Hydromatic hydrostatic balance was employed.

General Procedure

NIR derivative spectrometry

For the NIR derivative spectrometric determination of ethanol in alcoholic beverages two alternative procedures were carried out, depending on the sugar content of the samples to be analysed. However, in both instances the only

* To whom correspondence should be addressed.

sample preparation required was the de-gassing of the beer samples and a 10 + 25 dilution of the spirit samples. For samples with a low sugar content, the direct measurement of $dA/d\lambda$ between the peak at 1680 nm and the valley at 1703 nm and the interpolation of these values in the corresponding calibration graph, obtained from ethanol standards diluted with water, provides accurate results.

For samples with a high sugar content, it is necessary to carry out two measurements in the NIR derivative mode, one using the 1 cm pathlength cell between 1680 and 1703 nm and the other using the 1 mm cell at 1400 nm. From these experimental values, and from the derivative values found, under the same conditions, for standards of ethanol and sugar (taking into account the nature of the sugar present in the sample, *viz.*, natural sugars or added saccharose), the true concentration of ethanol can be obtained by solving the corresponding system of two equations with two unknowns. This system permits an estimation of the sugar content in alcoholic beverages to be obtained.

Gas chromatography

In order to check the accuracy of the proposed method, ethanol was determined in a series of samples of whisky in the laboratory of the Valencia Customs (SOIVRE) following a direct procedure which consisted of diluting the sample 1 + 9 with distilled water and injecting 1 μl of the sample into a gas chromatograph using a nitrogen carrier gas flow rate of 20–30 ml min^{-1}, an oven temperature of 105 °C and injector and detector temperatures of 250 °C. A 3.85% v/v standard, prepared from analytical-reagent grade (96% v/v) ethanol, was used as a reference.

Pycnometric procedure

Other reference values were obtained in the Laboratorio Agrario de la Conselleria de Agricultura of Burjassot using a pycnometric procedure based on the distillation of 250 ml of wine in an alkaline medium obtained from CaO and the measurement of the density of the distillate.

Results and Discussion

NIR Spectrum of Ethanol in Water Solutions

The NIR spectrum of absolute ethanol in the wavelength range from 1100 to 1800 nm [Fig. 1(a)] provides, in general, absorbance values lower than those obtained for pure water. However, in a narrow range, from 1670 to 1740 nm, the spectrum of ethanol has three well-defined bands and a shoulder, which could be clearly identified in the presence of water [see Fig. 1(b)]. On the other hand, using water as a reference, positive absorbance peaks can be obtained for ethanol in the above-mentioned range [Fig. 1(c)].

By increasing the pathlength of the cell from 1 mm to 1 cm, the sensitivity of the NIR spectrometric determination of ethanol also increases and adequate sensitivity values for the determination of ethanol in alcoholic beverages can be obtained.

Fig. 2 shows the NIR spectra of ethanol standards of different concentrations and the spectrum of a wine sample containing 12.5% v/v ethanol. From these spectra, it can be concluded that the direct determination of ethanol in alcoholic beverages by NIR spectrometry presents serious problems in the establishment of the spectral baseline, owing to the matrix. However, it can be shown that the absorbance maximum at 1693 nm is well-defined, in both standards and samples, and that it offers a series of possibilities for NIR analysis.

Derivative NIR Spectra of Ethanol

The first-derivative spectra of ethanol can be employed to correct the matrix interference in the NIR analysis of alcoholic beverages.

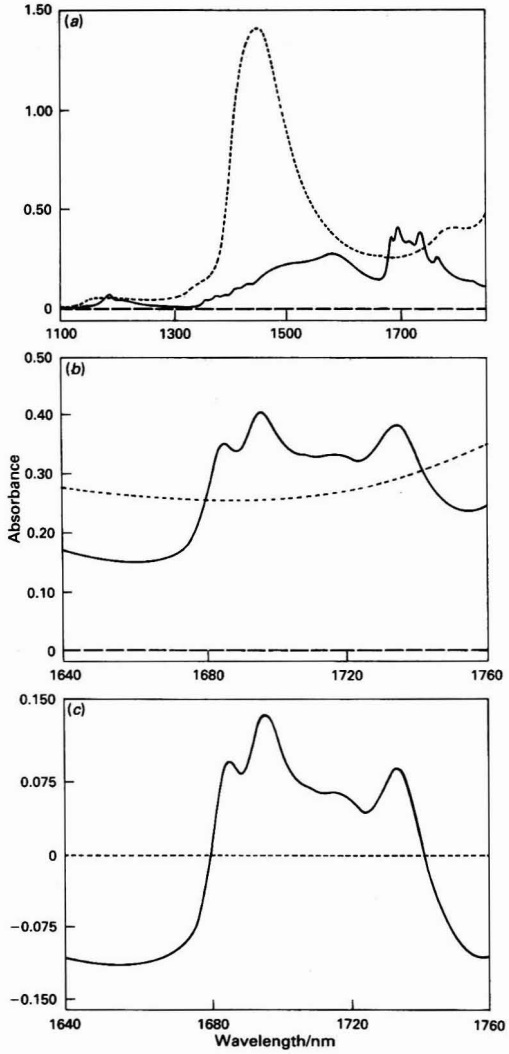

Fig. 1 NIR spectra of absolute ethanol and water: (*a*) and (*b*) using CCl_4 as a reference; (*c*) using water as a reference. Ethanol (——), water (·····) and CCl_4 (– – –). In all instances a 1 mm pathlength cell was used

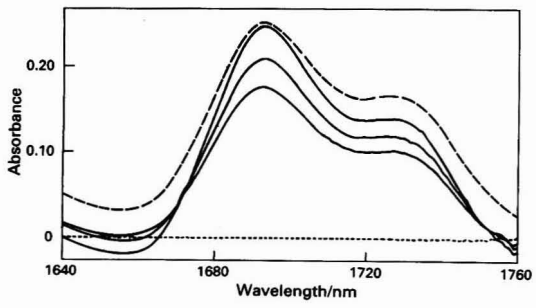

Fig. 2 NIR spectra of ethanol standards (——) containing 10, 12 and 15% v/v ethanol and the spectrum of a wine sample with 12.5% v/v ethanol (– – –). Pathlength: 1 cm. Reference: water (·····)

Fig. 3 shows the first-derivative NIR spectrum of absolute ethanol and that of pure water, using CCl_4 as reference and 1 mm pathlength cells, and, as can be seen, ethanol can be determined without interference from water in the wavelength range from 1677 to 1698 nm. On the other hand, using water as a reference [see Fig. 3(b)], well-defined peaks can be obtained.

NIR Derivative Spectrometric Determination of Ethanol

By using 1 cm pathlength cells and carrying out the peak-to-valley measurements between 1680 and 1703 nm, ethanol can be determined in alcoholic beverages by NIR derivative spectrometry with a dynamic range between 0 and 25% v/v. A typical calibration graph, under these conditions, corresponds to $dA/d\lambda = 0.0000_2 + 0.0127c$ (where c is the concentration of ethanol in % v/v) with a regression coefficient (r) = 0.999992 (see Fig 4). Under the above conditions the matrix interference found for the NIR determination of ethanol in wine, using absorbance spectra, can be avoided, as can be seen in Fig. 5.

Analytical Figures of Merit of the NIR Derivative Spectrometric Determination of Ethanol

Table 1 summarizes the main figures of merit for the determination of ethanol using both 1 mm and 1 cm pathlength cells and, in the latter instance, carrying out the measurements from peak to valley and from zero to valley.

As can be seen, the limit of detection obtained under the optimum sensitivity conditions (for $k = 3$, probability level 99.86%) corresponds to 0.1% v/v, and so the methodology developed could be applied to the analysis of all types of alcoholic beverages from beer to wines and spirits.

The repeatability of the first-derivative NIR spectrometric determination of ethanol was established from the relative standard deviation of five independent measurements of a sample containing 10% v/v ethanol (for a 1 cm pathlength cell) and 25% v/v ethanol (for a 1 mm pathlength cell). A good indication of the precision of the NIR derivative measurements can be obtained from the fact that a 10.0% v/v solution of ethanol provides a typical absorbance value of 0.1264 ± 0.0003 and that a 10.25% v/v solution of ethanol provides a value of 0.1293 ± 0.0003, carrying out the measurements between 1680 and 1703 nm and using a 1 cm pathlength cell.

Analysis of Real Samples

Ethanol was determined in real samples of alcoholic beverages and, as can be seen in Table 2, values comparable to those reported on the bottles were found for beer, red and white wine, rum, gin, brandy, whisky, vodka and fruit liqueurs. In all instances, analyses were carried out without any sample pre-treatment except for the beer sample for which a previous de-gassing was carried out by sonication in an ultrasonic water-bath, and for spirits, for which a previous dilution of 10 + 15 with distilled water is recommended in order to obtain experimental derivative values in the middle part of the linear range of the calibration graph prepared by using a 1 cm pathlength cell.

The regression between values found by the proposed method and those reported (Fig. 6) provides the equation $y = 0.10 + 0.9942x$, with $r = 0.99988$, which demonstrates that the method can be applied in all the concentration ranges studied without requiring a blank correction (the intercept is statistically equal to zero) or presenting constant relative errors (the slope is statistically equal to 1).[30]

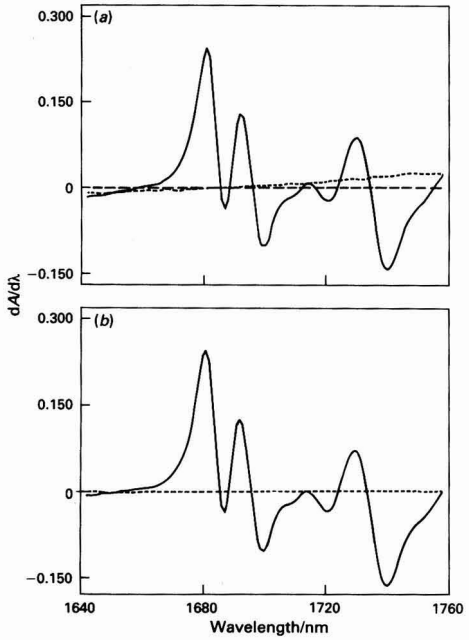

Fig. 3 First derivative spectra of absolute ethanol (——) and pure water (·····), obtained with a pathlength of 1 mm and using (*a*) CCl_4 as a reference (– – –) and (*b*) water as a reference. Pathlength: 1 mm

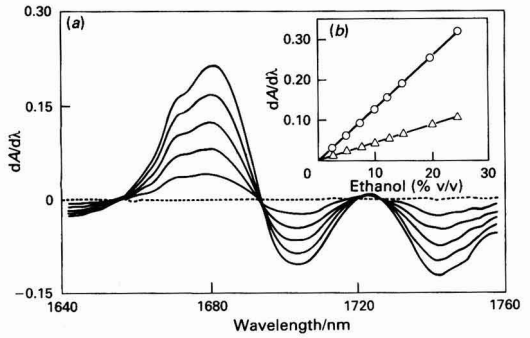

Fig. 4 Calibration graph obtained for the determination of ethanol. (*a*) Spectra of ethanol standards (from 5 to 25% v/v) (——) using water (·····) as a reference. Pathlength: 1 cm. (*b*) Calibration graph obtained by measuring $dA/d\lambda$ between 1680 and 1703 nm (○) and at 1703 nm (△)

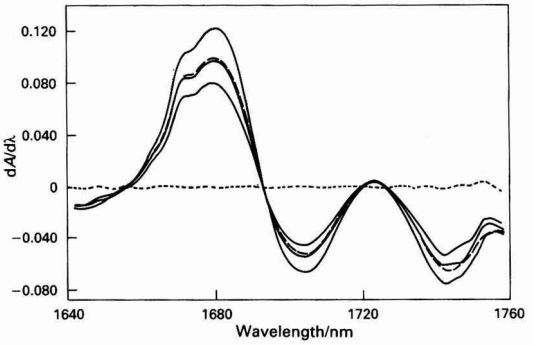

Fig. 5 NIR derivative spectra of ethanol standards containing 10, 12 and 15% v/v ethanol (——) and a wine sample (– – –) containing 12.5% v/v ethanol. Pathlength: 1 cm. Reference: water (·····)

Table 1 Figures of merit for the first-derivative NIR spectrometric determination of ethanol

	Cell pathlength		
	1 mm	1 cm	
Parameter	$(1677_p–1698_v)^*$ nm	$(1680_p–1703_v)^*$ nm	$(1703_v)^*$ nm
Calibration equation: $a_0 + bc$ (c in % v/v)	$0.0001 + 0.00262c$	$-0.0000_2 + 0.0127c$	$-0.0000_7 + 0.0043c$
Regression coefficient (r)	0.99996	0.999992	0.99986
Dynamic range (% v/v)	0.5–50	0.1–25	0.35–30
Sensitivity†	0.0262	0.0127	0.0043
Repeatability‡ (%)	0.8	0.3	4.5
Typical signal§	0.0655 ± 0.0005	0.1260 ± 0.0004	0.0430 ± 0.0020
LOD¶ (% v/v)	0.5	0.1	0.35

* The subscripts p and v indicate peak and valley, respectively.

† Sensitivity expressed in absorbance c^{-1} cm^{-1}; where c is in % v/v.

‡ Repeatability: determined by the relative standard deviation of five independent measurements of a sample containing 10% v/v ethanol for a 1 cm pathlength cell and 25% v/v ethanol for a 1 mm pathlength cell.

§ Typical derivative signal obtained for a 10% v/v ethanol content for a 1 cm pathlength cell and 25% v/v ethanol for a 1 mm pathlength cell.

¶ LOD: Limit of detection for $k = 3$; probability level 99.86%.

Table 2 NIR derivative analysis of real alcoholic beverage samples

Sample		Value reported (% v/v)	Value found by NIR* (% v/v)
Beer	1	4.50	4.47 ± 0.08
	2	5.40	5.5 ± 0.1
White wine	1	11.0	11.25 ± 0.09
	2	10.0	9.9 ± 0.1
	3	12.0	12.2 ± 0.1
Gin	1	40	39.6 ± 0.2
	2	40	40.2 ± 0.1
Dark rum	1	40	40.30 ± 0.09
	2	40	39.9 ± 0.1
	3	40	40.17 ± 0.09
	4	40	40.2 ± 0.08
	5	40	39.8 ± 0.2
White rum	1	38	37.7 ± 0.2
Vodka	1	37.5	37.3 ± 0.1
Brandy	1	39	38.9 ± 0.2
Sherry liqueur	1	25	24.96 ± 0.07
Whisky	1	40	39.6 ± 0.1
	2	40	40.16 ± 0.09
Whisky	1	43	42.4 ± 0.1
	2	43	42.6 ± 0.1
Spirit	1	40	40.2 ± 0.1

* Mean ± standard deviation ($n = 5$).

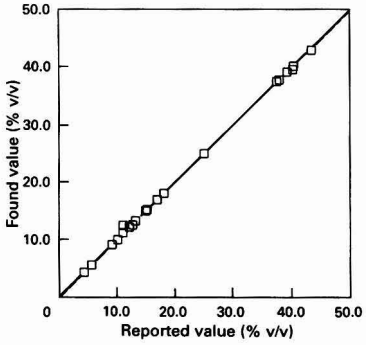

Fig. 6 Regression between values found for the determination of ethanol by NIR derivative spectrometry and those reported (– – –). Theoretical line with a slope of 1 and an intercept of 0 (————)

Table 3 Comparison between the NIR derivative spectrometric method for the determination of ethanol and gas chromatography

Sample		Stated ethanol content (% v/v)	Ethanol content found by gas chromatography (% v/v)	Ethanol content found by NIR derivative spectrometry* (% v/v)
Whisky	1	40	40.36	40.16 ± 0.09
	2	40	39.22	39.6 ± 0.1
Whisky	1	43	42.0	42.4 ± 0.1

* Mean ± standard deviation ($n = 5$).

Three whisky samples were analysed in this laboratory, using the proposed method, and by an independent laboratory, using a gas chromatographic method, and, as can be seen in Table 3, the values obtained by both procedures are comparable and of the same order as the values reported on the bottles.

Interference of Sugars in the NIR Derivative Spectrometric Determination of Ethanol

For some samples, with a high content of sugars, and also for liqueurs with added sugar, the NIR derivative spectrometric determination of ethanol, following the procedure described above leads to large errors; for example, for a sweet white wine containing 15% v/v ethanol, a value of 16.43% v/v ethanol was found, and for peppermint liqueur samples containing 25 and 30% v/v ethanol, the values found were 26.30 and 32.4% v/v, respectively.

Fig. 7(*a*) shows, as an example, the NIR derivative spectra of two standards containing 15 and 16% v/v ethanol, a sweet wine sample, with a 15% v/v ethanol content, and a peppermint sample diluted in order to obtain the same concentration of ethanol. As can be seen, the measurements between 1680 and 1703 nm are strongly affected by the matrix. For both types of alcoholic beverages, the valley at 1650 nm is deeper than previously observed. The different types of sugars present in each sample (saccharose is added to the peppermint and the equivalent of a binary mixture of fructose and glucose to the sweet wine) cause different changes in the spectra. Hence for samples with added saccharose, the peak at 1680 nm and the valley at 1703 nm provide a bathochromic shift of 7 nm, but the position of the bands is not affected by other sugars, such as glucose or fructose.

The spectra, recorded between 1300 and 1800 nm, using a 1 mm pathlength cell, [see Fig. 7(*b*) and (*c*)] show the changes caused by the presence of sugars, as compared with ethanol

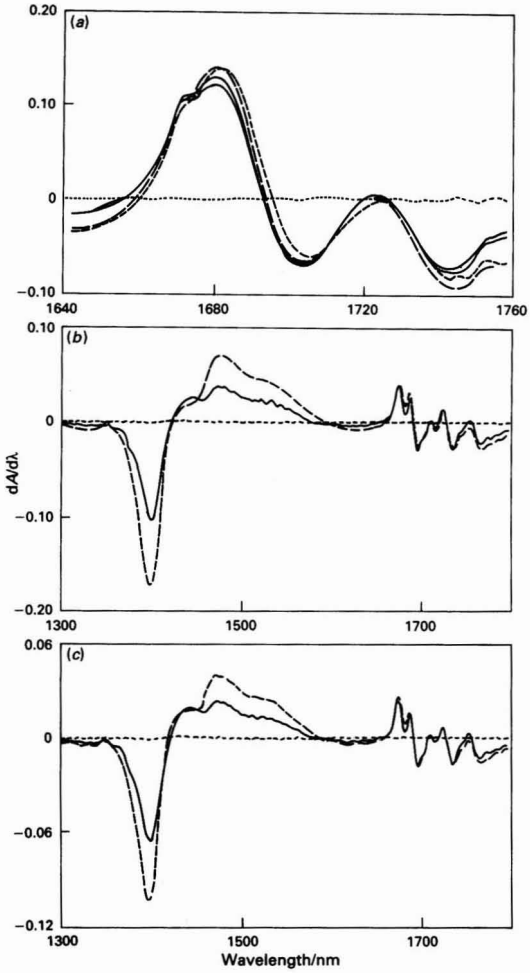

Fig. 7 (*a*) NIR derivative spectra of ethanol standards containing 15 and 16% v/v ethanol (——), a sweet wine sample (— —) and a diluted peppermint sample (– – –). Pathlength: 1 cm. Reference: water (·····). (*b*) Smoothed NIR derivative spectra of a 25% v/v ethanol standard (——) and a peppermint sample with a reported ethanol content of 25% v/v (– – –). Pathlength: 1 cm. Reference: water (·····). (*c*) Smoothed NIR derivative spectra of a 15% v/v ethanol standard (——), and a sweet wine with a 15% v/v ethanol content (– – –). Pathlength: 1 cm. Reference: water (·····)

standards. It can be seen that the smoothed first-derivative NIR spectra of samples containing both ethanol and sugars exhibit a common valley at 1400 nm, which can be used for the determination of the concentration of both compounds in the same sample. On the other hand, in the 1650–1750 nm range, the use of a 1 mm pathlength cell demonstrates that the maximum observed at 1680 nm when a 1 cm pathlength cell is used, is actually the sum of two bands at 1677 and 1689 nm and that the different types of sugars present in the sample modify either the first or the second band.

A systematic study of the interference of saccharose, fructose and glucose (from 0 to 210 g l^{-1} in each instance) in the NIR derivative spectrometric determination of ethanol was carried out. In addition the effect of 1 + 1 glucose–fructose mixture on this determination was also studied. Fig. 8(*a*) shows, as an example, the effect of the concentration of a glucose–fructose mixture on the spectrum of a 10% v/v

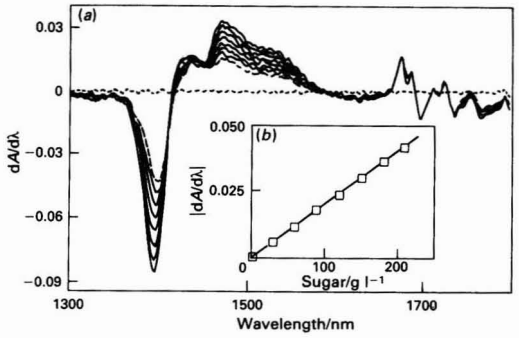

Fig. 8 (*a*) Effect of a 1 + 1 glucose–fructose mixture on the NIR derivative spectrum of a 10% v/v ethanol standard solution. Sugar content: 0(– – –), 30, 60, 90, 120, 150, 180 and 210 g l^{-1} (——). Pathlength: 1 mm. Reference: water (·····) (*b*) Variation of the absolute value of d*A*/dλ, measured at 1400 nm, as a function of the sugar concentration

Table 4 Effect of the sugar concentration on the first-derivative NIR measurement at 1400 nm by using a 1 mm pathlength cell

Sugar	$[(dA/d\lambda)] = a_0 + bc$ (c in g l^{-1})*	r
Fructose	$-0.0000_4 + 2.04 \times 10^{-4} c$	0.9989
Glucose	$0.0000_5 + 2.01 \times 10^{-4} c$	0.9991
Fructose–Glucose†	$-0.0000_6 + 2.02 \times 10^{-4} c$	0.9992
Saccharose	$0.0001 + 1.98 \times 10^{-4} c$	0.9989

* In all instances the sugar concentration range studied was between 0 and 210 g l^{-1}.

† 1 + 1 mixture of glucose and fructose.

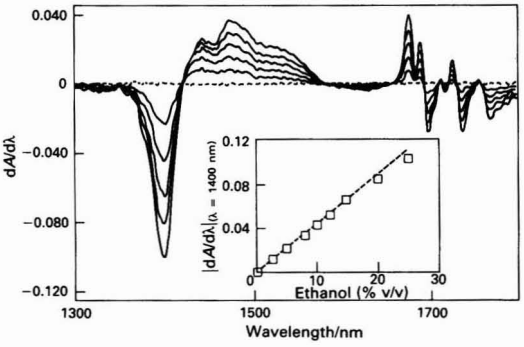

Fig 9 Calibration obtained for the NIR derivative spectrometric determination of ethanol by using a 1 mm pathlength cell. (——) Measurement at the 1400 nm band. Reference: water (·····). (Inset gives regression line)

ethanol standard, from which a linear calibration graph of d*A*/dλ for the valley at 1400 nm *versus* the sugar concentration can be prepared [Fig. 8(*b*)]. This calibration presents the typical expression $|(dA/d\lambda)_{1400\,nm}| = -0.0000_1 + 2 \times 10^{-4} c$ (c in g l^{-1}), with $r = 0.9996$, which is similar for all the different sugars tested (see Table 4).

The above-mentioned band at about 1400 nm can be related to the ethanol concentration and hence a typical regression line for ethanol, $|(dA/d\lambda)_{1400\,nm}| = 0.0000_7 + 4.45 \times 10^{-3} c$ (where c is the ethanol concentration in % v/v), with $r = 0.9991$, can be obtained (see Fig. 9).

From these two regression lines it is possible to obtain the corresponding coefficients for an equation which relates the first-derivative (d*A*/dλ) values at 1400 nm (using a 1 mm

Table 5 Effect of the sugar concentration on the first-derivative NIR measurement between 1680 and 1703 nm using a 1 cm pathlength cell

Sugar	$[(dA/d\lambda)] = a_0 + bc$ (c in g l^{-1})*	r
Glucose	$-0.0000_5 + 2.0 \times 10^{-5} c$	0.9981
Fructose	$0.0001 + 1.61 \times 10^{-4} c$	0.9997
Glucose–Fructose†	$0.0001 + 9.1 \times 10^{-5} c$	0.9992
Saccharose	$0.0000_7 + 5.8 \times 10^{-5} c$	0.9987

* In all instances the sugar concentration range studied was between 0 and 210 g l^{-1}.

† 1 + 1 mixture of glucose and fructose.

Table 6 NIR derivative spectrometric determination of ethanol in samples with a high content of sugars

Sample		Reported value (% v/v)	$NIR_{(p-v)}$* (% v/v)	$NIR_{(v)}$† (% v/v)	$NIR_{(c)}$‡ (% v/v)
White wine	1	15	16.4	15.4	14.95 ± 0.09
Peppermint	1	25	27.3	25.4	24.8 ± 0.1
Red wine	1	15.1	16.8	16.0	15.2 ± 0.1
	2	17.0	18.6	17.6	16.97 ± 0.08
	3	17.9	18.9	18.3	18.00 ± 0.09

* $NIR_{(p-v)}$: Direct determination carried out by measuring $dA/d\lambda$ between the 1680 nm peak and the 1703 nm valley.

† $NIR_{(v)}$: Direct determination carried out by measuring $dA/d\lambda$ at the 1703 nm valley.

‡ $NIR_{(c)}$: Corrected values obtained by carrying out $dA/d\lambda$ measurements with 1 mm and 1 cm pathlength cells and taking into account the parameters corresponding to the contribution of the sugar to the NIR measurements. Results given are mean ± standard deviation.

Table 7 Comparison between results found by a pycnometric procedure and by NIR derivative spectrometry for the determination of ethanol in wine samples with a high content of sugar

Sample		Pycnometric value (% v/v)	$NIR_{(p-v)}$* (% v/v)	$NIR_{(v)}$† (% v/v)	$NIR_{(c)}$‡ (% v/v)
Red wine	1	9.13	9.87	9.3	9.05 ± 0.07
	2	13.28	13.9	13.5	13.39 ± 0.09
	3	12.72	12.9	12.8	12.60 ± 0.08
White wine	1	14.82	16.2	15.3	14.90 ± 0.1
	2	11.98	13.2	12.3	12.05 ± 0.09
	3	12.21	12.6	12.3	12.10 ± 0.1

* $NIR_{(p-v)}$: Direct determination carried out by measuring $dA/d\lambda$ between the 1680 nm peak and the 1703 nm valley.

† $NIR_{(v)}$: Direct determination carried out by measuring $dA/d\lambda$ at the 1703 nm valley.

‡ $NIR_{(c)}$: Corrected values obtained by carrying out $dA/d\lambda$ measurements with 1 mm and 1 cm pathlength cells and taking into account the parameters corresponding to the contribution of the sugar to the NIR measurements. Results given are mean ± standard deviation.

pathlength cell) with the concentrations of ethanol and sugar in the sample, *i.e.*, $|(dA/d\lambda)_{1400\,nm}| = 0.00445c_{ethanol} + 2 \times 10^{-4}c_{sugar}$.

By using a 1 cm pathlength cell, a relationship can also be found between the derivative values, measured between 1680 and 1703 nm, and the concentrations of ethanol or sugars, from which a series of regression lines can be obtained. Table 5 summarizes the data obtained and, as can be seen, the parameters of these equations depend on the type of sugar; hence for the analysis of alcoholic beverages the equations to be used must be selected taking into account the nature of the sugars present in the sample. Hence, for the determination of ethanol in wines the following equation, which includes the coefficients for ethanol and for a mixture of fructose and glucose, must be employed: $(dA/d\lambda)_{1680-1703\,nm} = 0.0127c_{ethanol} + 9.1 \times 10^{-5}\,c_{sugar}$, whereas for the determination of ethanol in peppermint (which also contains added saccharose), the following equation is recommended: $(dA/d\lambda)_{1680-1703\,nm} = 0.0127\,c_{ethanol} + 5.8 \times 10^{-5}\,c_{sugar}$. Hence for the analysis of samples with a high content of sugars the determination of ethanol must be performed by carrying out NIR derivative measurements with 1 mm and 1 cm pathlength cells at 1400 nm and between 1680 and 1703 nm, respectively, and solving the corresponding system of two equations with two unknowns; the ethanol concentration is expresed in % v/v and the sugar content in g l^{-1}.

As can be seen in the equations summarized in Tables 4 and 5, the sensitivity of the NIR derivative measurements for the determination of sugars is very low and so the method, which is suitable for the determination of ethanol, only permits an estimation of the sugar concentration to be obtained. Values obtained for sugars can be used to correct the concentration of ethanol, but the values must be improved by means of other measurements in order to provide an accurate and precise determination of the sugar concentration.

Determination of Ethanol in Samples With a High Sugar Content

The above-mentioned procedure was employed for the determination of ethanol in different samples with high contents of sugars. The data in Table 6 demonstrate that the proposed method permits the correction of errors obtained by direct measurement of $dA/d\lambda$ and provides results comparable to those reported.

Comparison of the NIR Derivative Spectrometric Procedure With Other Methods

The official method for the determination of ethanol in alcoholic beverages is based on the measurement of the density of the sample, with a precision of ±0.1% v/v ethanol, after a previous distillation of the sample in an alkaline medium.

Table 7 shows the results obtained for a series of samples analysed by the pycnometric procedure and also by the proposed method. As can be seen, both procedures provide comparable results, and the precision of the NIR derivative measurements is adequate for carrying out these determinations.

One procedure, commonly employed in control laboratories for the determination of ethanol in spirits, is based on the direct analysis of samples, previously diluted with distilled water, by gas chromatography using a specific column for the determination of alcohols. This method is rapid and has been thoroughly validated. Table 3 summarizes the results found for the determination of ethanol in whisky samples by both gas chromatography and NIR derivative spectrometry. As can be seen, both procedures provide comparable results.

It can be concluded that the proposed NIR derivative method is very simple and more rapid than other methodologies described in the literature and that it provides accurate, sensitive and reproducible results. One of the major advantages of the method is that it can be applied to the direct determination of ethanol in all types of alcoholic beverages.

Compared with other published methods, based on Fourier transform IR[17–19] and NIR[22–25] analysis, the proposed method does not require any complex mathematical treatment of the data and, by using direct derivative spectra, accurate results can be obtained. The precision of the proposed NIR derivative method (±0.1% v/v) is better than that reported by Buchanan *et al.*[29] (±0.33% v/v) and Cavinato *et al.*[28] (±0.2% v/v). This could be due to the use of a 1 cm pathlength tranmission cell instead of the fibre optic systems employed in the earlier papers. The proposed method is the only procedure that can be applied to the analysis of samples of very different types without incurring problems related to the matrix. In addition, a suitable methodology for correcting errors derived from the presence of sugars has been developed.

M. G. acknowledges a grant from the Agencia Española de Cooperación Internacional to carry out Ph.D. studies and the financial support of Los Andes University and CONICIT (Venezuela). S. G. acknowledges a grant from the Conselleria de Cultura, Educació i Ciència de la Generalitat Valenciana to carry out Ph.D. studies. The authors also thank Cristina Martínez for performing the gas chromatographic analyses and Angel Orozco for carrying out the pycnometric procedure.

References

1 Commission Regulation (EEC) No. 2676/90, *Off. J. Eur. Comm.*, 1990, **33**, L272.
2 Ministerio de Sanidad y Consumo, *Análisis de Alimentos. Métodos Oficiales y Recomendados por el Centro de Investigación y Control de Calidad*, Servicio de Publicaciones del Ministerio de Sanidad y Consumo, Madrid, 1985.
3 *Official Methods of Analysis of the Association of Official Analytical Chemists*, AOAC, Washington, DC, 1990.
4 Amerine, M. A., and Ought, C. S., *Methods of Analysis of Musts and Wines*, Wiley, New York, 1980.
5 Pilone, G. J., *J. Assoc. Off. Anal. Chem.*, 1985, **68**, 188.
6 Caputi, A. J. and Mooney, D. P., *J. Assoc. Off. Anal. Chem.*, 1983, **66**, 1152.
7 Cutaia, A. J., *J. Assoc. Off. Anal. Chem.*, 1984, **67**, 192.
8 Iwachido, T., Ishimaruk, K., and Toei, K., *Anal.Sci.*, 1986, **2**, 495.
9 Morawski, J., Dincer, A. K., and Ivie, K., *Food Technol.*, 1983, **37**, 57.
10 Kakabadse, G. J., *Lab. Pract.*, 1990, **39**, 51.
11 Guillou, M., and Belanche, M., *Connaiss. Vigne Vin.*, 1989, **23**, 215.
12 Guillou, M., and Tellier, C., *Anal. Chem.*, 1988, **60**, 2182.
13 Lazaro, F., Luque de Castro, M. D., and Varcárcel, M., *Anal. Chim. Acta*, 1986, **185**, 57.
14 Lazaro, F., Luque de Castro, M. D., and Varcárcel, M., *Anal. Chem.*, 1987, **59**, 1859.
15 Junge, C., *J. Assoc. Off. Anal. Chem.*, 1987, **70**, 1089.
16 Worsfold, P. J., Růžička, J., and Hansen, E. H., *Analyst*, 1981, **106**, 1309.
17 Lopez Mahia, P., Simal Gándara, J., and Paseiro Losada, P., *Vib. Spectrosc.*, 1992, **3**, 133.
18 Glenn, A. L., *J. Pharm. Pharmacol.*, 1963, **15**, Suppl., 123T.
19 Agwu, J. V., and Glenn, A. L., *J. Pharm. Pharmacol.*, 1967, **19**, 76s.
20 Paseiro Losada, P., and Simal Lozano, J., *Anal. Bromatol.*, 1984, **36**, 97.
21 Heisz, O., *Labor Praxis*, 1989, **13**, 402.
22 Criddle, W. J., Parry, K. W., and Jones, T. P., *Analyst*, 1987, **112**, 615.
23 Halsey, S. A., *J. Inst. Brew.*, 1985, **91**, 306.
24 Halsey, S. A., *Anal. Proc.*, 1986, **23**, 126.
25 Requejo-Gómez, A., *Tec. Lab.*, 1983, **8**, 911.
26 Coventry, A. G., and Hunston, M. J. *Cereal Foods World*, 1984, **29**, 715.
27 Dumoulin, E. D., Azain, B. P., and Guerain, J. T., *J. Food Sci.*, 1987, **52**, 626.
28 Cavinato, A. G., Mayes, D. M., Zhihong, G., and Callis, J. B., *Anal. Chem.*, 1990, **62**, 1977.
29 Buchanan, B. R., Honigs, D. E., Lee, C. J., and Roth, W., *Appl. Spectrosc.*, 1988, **42**, 1106.
30 Miller, J. C. and Miller, J. N., *Statistics for Analytical Chemistry*, Wiley, New York, 1984.

Paper 3/01564E
Received March 18, 1993
Accepted May 14, 1993

Decomposition of Biological Samples for Inductively Coupled Plasma Atomic Emission Spectrometry Using an Open Focused Microwave Digestion System

Antoaneta Krushevska, Ramon M. Barnes and Chitra Amarasiriwaradena
University of Massachusetts, Department of Chemistry, Lederle Graduate Research Center, Amherst, MA 01003-0035, USA

A focused microwave digestion system operated at atmospheric pressure was applied to the preparation of milk, total parenteral nutrition, tissues (mussel, kidney, oyster and bovine liver) and urine. Reagent combinations (HNO_3, H_2SO_4 and H_2O_2) and power–time programmes were examined with respect to the residual carbon content (RCC) and element recovery. Inductively coupled plasma atomic emission spectrometry was used to determine the residual carbon and analytes (As, Ba, Ca, Cd, Cu, Fe, K, Mg, Mn, Na, P, Pb, Sr and Zn). Different reagents (HNO_3, HCl and ethylenediaminetetraacetic acid) were investigated for the final digestion step in order to improve the accuracy in the determination of elements forming low-solubility sulfates. The RCC obtained with an open-focused microwave system was similar to that obtained with high-pressure digestion, but lower than with a closed, medium-pressure microwave system.

Keywords: *Trace analysis; inductively coupled plasma atomic emission spectrometry; open-focused microwave digestion; biological sample; residual carbon*

Sample digestion is an important step in elemental analysis, because of the preparation time and possibilities for systematic errors it contributes to the analysis. Common digestion methods include conductive heating at atmospheric pressure (*i.e.*, hot-plate) with mineral acids (*e.g.*, HNO_3, $HClO_4$ and H_2SO_4) or oxidants (H_2O_2) or at elevated pressure and temperature with pressure containers or a commercial high-pressure digestion apparatus (HPA; Anton Paar, Graz, Austria)[1] with HNO_3.

Microwave heating for sample preparation has advantages compared with hot-plate digestion: the digestion time is shorter, reagent consumption and blank level are lower, and accuracy and reproducibility are better.[2] Two types of microwave system are used: closed vessels at elevated pressure and open vessels at atmospheric pressure. In the closed-vessel systems the microwave energy is dispersed throughout the cavity, whereas in the commercial open-vessel system the energy is focused on the part of the digestion vessel containing the sample. Versions of the open-focused microwave system can digest large sample masses (*e.g.*, up to 5 g in the Microdigest and 10 g in Maxidigest).[3]

Many applications for biological materials in closed systems under pressure[4–6] and in open systems at atmospheric pressure[3,7,8] have been described. The most common reagents for this type of digestion are HNO_3, H_2SO_4 and H_2O_2.[8] The effectiveness of decomposition of samples containing organic matter can be evaluated not only from the inorganic analyte recoveries, but also from the completeness of the destruction of the organic matter. Although the residual carbon content (RCC) is not crucial for some techniques such as inductively coupled plasma atomic emission spectrometry (ICP-AES) or flame atomic absorption spectrometry, RCC can introduce errors with other measuring techniques such as voltammetry or in preconcentration methods when extraction and hydride generation are applied. A comparison of different sample decomposition procedures for milk, based on the recoveries of RCC and Zn, was reported recently.[9]

Some systematic errors result from chemical reactions of the analytes during digestion. For example, elements forming sparingly soluble sulfates (*i.e.*, Ba, Pb and Sr) can precipitate whenever H_2SO_4 is used in the digestion. The loss of Pb when using HNO_3, $HClO_4$ and H_2SO_4 in the decomposition of plant materials by conductive heating is due to the presence of Ba and the precipitation of sulfates.[10] The problem of determination of Pb in poly(vinyl chloride) (PVC) with a high alkaline-earth content has been resolved through the addition of ethylenediaminetetraacetic acid, sodium salt (NaEDTA)[11,12] or HNO_3[12] in the final stage. The influence of HNO_3 on the solubility of $PbSO_4$ was described in an enrichment technique for Pb.[13] Hence, systematic errors in the determination of alkaline-earth elements resulting from the dissolution of biological materials with H_2SO_4 might be minimized with similar techniques.

An open-focused microwave system was investigated for the determination of As, Ba, Ca, Cd, Cu, Fe, K, Mg, Mn, Na, P, Pb, Sr and Zn in biological materials. The procedure was compared with other sample-digestion techniques.

Experimental

Apparatus

The apparatus used for sample digestion include an open-focused microwave system (Microdigest M 300, Prolabo, Paris, France), with 100% power at 300 W, and 50 ml glass vessels; a closed-vessel microwave system (RMS 150, Floyd, Lake Wylie, SC, USA) with double-wall, medium-pressure Teflon-PFA (perfluoroalkoxy) vessels in which pressure-control mode is used and 100% power corresponds to 600 W; and the HPA with 70 ml quartz vessels. The operating conditions for each of these systems are listed in Table 1.

The ICP–AES determinations of the analytes and carbon were performed with an automated, dual monochromator (Plasma II, Perkin-Elmer, Norwalk, CT, USA). The working conditions are presented in Table 2. Myers–Tracy signal compensation[14] was used to measure the background and the reference Sc II 424.683 nm line from 50 $\mu g\ ml^{-1}$ of Sc simultaneously. Four replicate readings were usually taken.

An element analyser (Perkin-Elmer 240) was used to determine total carbon in the original samples. A vacuum freeze-dryer (Virtis, Model 10–800, Gardiner, NY, USA) was used to remove water from the samples.

Reagents

The sample weighing and reagent additions were performed in a Class 100 clean room. Vessels were cleaned by heating at 100 °C for 24 h in HNO_3 or for the carbon determination with a

Table 1 Operating conditions for digestion systems

System	Weight/g	Reagents/ml					Programme
		HNO_3	H_2SO_4	H_2O_2	HCl	EDTA	
Prolabo M 300	1 (10 ml)	3.0	1.0				10% power/4 min 40% power/4 min or until charring occurs
				8.0			40% power/16 min
		3.75					10% power/4 min
or							
		0.75			3.0		10% power/4 min
or							
						3.0	10% power/4 min
Floyd RMS 150	0.3 (10 ml)	5.0					20 psi/2 min 40 psi/5 min 60 psi/2 min 80 psi/2 min 100 psi/2 min 120 psi/2 min 140 psi/2 min 160 psi/15 min
HPA	0.2 (5 ml)		3.0				40 °C/20 min/110 °C 110 °C/30 min/110 °C 110 °C/90 min/280 °C 280 °C/90 min/280 °C

Table 2 Instrumental parameters for ICP-AES (Plasma II)

R.f./MHz	27.12
Incident power/kW	1.0
Argon gas flow rates/l min^{-1}	
Outer	15
Intermediate	1.0
Nebulizer	1.0 for C, K and Na 0.7 for others
Observation height/mm	9 for C 15 for others
Read delay/s	60 for C 20 for others
Sampling time/ms	100
Analytical wavelengths/nm	As I 193.759 Ba II 455.403 C I 193.091 Ca II 393.366 Cd II 214.438 Cu I 324.754 Fe II 238.204 Mg II 280.270 Mn II 257.610 Pb II 220.353 Sr II 421.552 Zn I 213.856
Reference wavelength/nm	Sc II 424.683

mixture of concentrated HNO_3 and H_2SO_4 (1 + 1). They were rinsed with distilled and de-ionized water (18 MΩ cm^{-2} resistivity, Barnstead NANOpure, Sybron/Barnstead, Boston, MA, USA).

Reagents were of high purity (H_2SO_4 and H_2O_2) or pre-purified by sub-boiling (HNO_3), isothermal distillation (aqueous ammonia) or recrystallization in 2% HNO_3 (EDTA). For the carbon determination, analytical reagent-grade chemicals were used.[15] A 10% NaEDTA solution was prepared by dissolving 10 g of the reagent in 100 ml of de-ionized water. A 10% NH_4EDTA solution was prepared by dissolving 10 g of EDTA in a small volume of aqueous ammonia and diluting to 100 ml with de-ionized water. A 1000 μg ml^{-1} Sc stock solution was prepared by dissolving 0.7889 g of Sc_2O_3 (99.98%, Johnson Matthey, Ward Hill, MA, USA) in 10 ml of HNO_3 (1 + 1) and diluting, with de-ionized water, to 500 ml in a calibrated flask. Standard solutions for ICP-AES measurements were prepared in 10% v/v HNO_3. The following test standard solutions (v/v) were prepared to contain 50 μg ml^{-1} Sc: 5% HNO_3, 15% HNO_3, 12% HCl–3% HNO_3, 15% HCl and 1.2% m/v NH_4EDTA–4% H_2SO_4 neutralized with aqueous ammonia. Carbon standards were prepared from mannitol or urea.[15] A 1000 μg ml^{-1} As stock standard solution was prepared by dissolving 0.1428 g of $C_2H_6AsNaO_2 \cdot 3H_2O$ in 50 ml of de-ionized water. An artificial urine sample was prepared by dissolving 2.083 g of urea, 0.125 g of creatinine, 1.41 g of NaCl, 0.28 g of KCl, 0.0794 g of $CaCl_2.2H_2O$, 0.088 g of $MgSO_4 \cdot 7H_2O$ and 0.19 ml of aqueous ammonia in de-ionized water in a 100 ml calibrated flask.

Samples

The reference materials (RMs) investigated were National Institute of Standards and Technology (NIST) Standard Reference Material (SRH) 1577b Bovine Liver, NIST SRM 1566 Oyster Tissue, International Atomic Energy Agency (IAEA) H8 Horse Kidney, National Institute of Environmental Studies (Japan) (NIES) No. 6 Mussel, NIST SRM 1549 Non-Fat Milk Powder and NIST SRM 2670 Toxic Metals in Freeze-Dried Urine (elevated level). Samples included packaged infant formula milk, total parenteral nutrition (TPN), a 24 h urine sample and artificial urine. Liquid samples (milk and TPN) were freeze-dried and used for the determination of carbon in the original sample as well as for sample-digestion studies. Aliquots of the urine sample were either evaporated to dryness in the digestion vessel used (HPA, Floyd) before the dissolution, or during the procedure (Prolabo).

Sample Preparation

Open-focused microwave digestion (Prolabo M 300)

A 1 g (dry) or 10 g (liquid) sample was weighed into a 50 ml Prolabo flat-bottomed glass vessel, then 5 ml of HNO_3, 1 ml of H_2SO_4 and 5 ml of 250 mg l^{-1} Sc solution were added. A Vigreux reflux column was attached. Power–time programmes (Table 1) were applied until all of the HNO_3 was completely removed and the boiling-point of H_2SO_4 was reached. This corresponds usually to carbon black colour formation (*i.e.*, charring). Thereafter, the heating was stopped after 1 min, approximately 0.5 ml of 30% H_2O_2 was added dropwise, and the solution was again heated (at 40% power) for 1 min. This procedure was repeated for 16 min (*i.e.*, 8 ml of H_2O_2). The vessel was washed through the condenser with de-ionized water, and different reagents were added: 3.75 ml of HNO_3 or 3 ml of HCl plus 0.75 ml of HNO_3,

or aqueous ammonia (until precipitation occurred at pH 9) and then 3 ml of 10% NH_4EDTA. The solution was diluted with de-ionized water to approximately 15 ml and again heated (at 10% power) for 4 min. After cooling, the solution was transferred to a Nalgene tube and diluted to 25 ml with de-ionized water. When the EDTA solution was added, the pH was checked again and adjusted if necessary with drops of aqueous ammonia.

Medium-pressure microwave dissolution (Floyd RMS 150)

A dry sample (0.3 g) or liquid urine (10 g) was weighed into an 85 ml PFA double-walled vessel (the latter sample was dried in the vessel), 5 ml of HNO_3 was added, and the vessel was closed. The sample was heated in the pressure-control mode (Table 1). After cooling, the vessel was opened, and 5 ml of 250 μg ml^{-1} Sc were added. The solution was transferred to a Nalgene tube and diluted to 25 ml with de-ionized water.

High-pressure ashing

A dry sample (0.2 g) or liquid urine (5 g) was weighed into a 70 ml quartz HPA vessel (the latter sample was dried in the vessel), and 3 ml of HNO_3 was added. The vessel was covered, and the sample was heated according to the programme presented in Table 1. After cooling, 2 ml of 250 μg ml^{-1} Sc was added. The sample was transferred to a Nalgene tube and diluted to 10 ml with de-ionized water.

Procedures

ICP-AES determination

Arsenic, Ba, Ca, Cd, Cu, Fe, K, Mg, Mn, Na, P, Pb, Sr and Zn were determined by ICP-AES in the solutions obtained after sample decomposition against standard solutions in 10% HNO_3. Aliquots were taken for carbon determination and treated according to the method described previously.[15]

Sample temperature

The importance of temperature control and internal pressure has been demonstrated for closed-vessel microwave systems for various samples and reagents.[2] In the focused microwave system the microwave energy is directed only at the part of the digestion vessel containing the sample. Therefore, temperature correlations found for the closed-vessel systems are not expected to be valid for the open-vessel microwave system.

In an attempt to characterize the heating mechanism in the open-focused microwave system, solution temperatures were measured for different volumes of de-ionized water and by applying 15% power for 5 min and 30% power for 2 min.

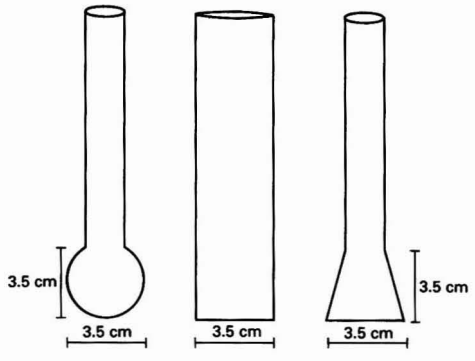

Fig. 1 Digestion containers used for temperature measurements. Prolabo vessel with round bottom; glass cylinder; Prolabo vessel with flat bottom

Three types of Prolabo glass vessel were compared (Fig. 1): 50 ml volume with a flat bottom, 50 ml with a round shape, and a cylindrical vessel with the same height (approximately 175 mm) and bottom diameter as the flat one. The Vigreux condenser was replaced by a Teflon cap to allow the rapid immersion of a thermometer. A 0–100 °C thermometer with 0.1 °C increments was immersed in the solution immediately after the microwave heating was stopped. The temperature (T_2) was measured after mixing the water well. The $\Delta T = T_2 - T_1$, where T_1 is the temperature of the water before heating, was calculated.

Insoluble sulfate formation

To characterize the formation of insoluble sulfates, test solutions were studied. Five ml of 250 μg ml^{-1} Sc, various amounts of Ba (2.5–250 μg), and 'spikes' of 25 or 125 μg of Pb, 10 or 25 μg of Sr and 25 or 2000 μg of Ca were placed in 50 ml glass beakers or Prolabo vessels. Approximately 5 ml of HNO_3 and 1 ml of H_2SO_4 were added, and the solutions were evaporated on a hot-plate or in the open-focused microwave system until SO_3 fumes evolved. After cooling, the solutions were diluted to 25 ml with: (*a*) de-ionized water; (*b*) 5, 10 or 15% v/v HNO_3; or (*c*) 11.25% HCl–3.75% v/v HNO_3, 11.6% HCl–2.8% HNO_3, 12% HCl–3% HNO_3 or 15% HCl, and heated. When EDTA salts were used, each sample (after cooling) was diluted with a small volume of de-ionized water, and aqueous ammonia was added until a precipitate appeared (pH 9), followed by 3 ml of 10% NaEDTA or 10% NH_4EDTA. The solution was heated then diluted with de-ionized water to 25 ml. The pH was checked, and, if necessary, drops of aqueous ammonia were added to bring the pH to 9. Experiments with NaEDTA at pH 2 were also performed (at this pH, NH_4EDTA precipitates). The concentrations of Ba, Ca, Pb and Sr were measured by ICP-AES.

Sample analysis

Biological samples alone or spiked with Ba, Pb or Sr were analysed. The RCC and the calculated residual carbon (RC), which represent the effectiveness of the sample decomposition,[9] and element recovery were measured for the three digestion techniques.

Results and Discussion

ICP-AES Determination

With the Myers–Tracy signal compensation technique for the ICP-AES determination,[14] 10% v/v HNO_3 standard solutions can be used for all the procedures with test solutions containing 5% v/v HNO_3, 15% HNO_3, 12% HCl–3% HNO_3, or 1.2% m/v NH_4EDTA–4% v/v H_2SO_4 neutralized by aqueous ammonia.

Sample Temperature

Temperature changes for various water volumes heated in three microwave vessels are compared in Fig. 2. The results are mean values from six replicates taken on different days. The distribution of the results was relatively low, especially for volumes above 2 ml (*i.e.*, the relative standard deviation was 10% for 2 ml and 2% for > 2 ml). With a small volume of liquid (under 8 ml), the round-bottomed vessel provided the highest temperature rise. In round-bottomed vessels the same amount of liquid occupied a height in the focused microwave cavity greater than in the two other vessels. As a result, the sample probably absorbed more energy. When the height in the vessel, instead of a fixed volume occupied, was examined (Fig. 3), the difference between the vessels could be discounted, especially for heights under 1.5 cm. For greater heights the vessel shape also influenced the temperature rise. These

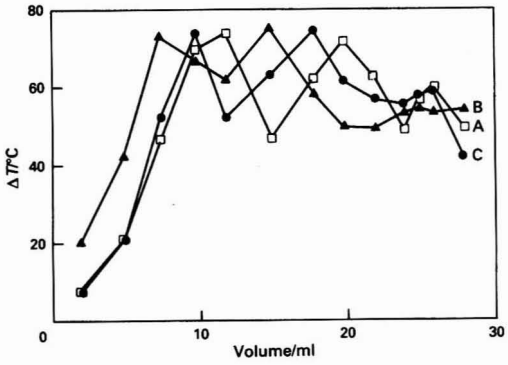

Fig. 2 Temperature change when heating different volumes of water in three type of vessels. A, Prolabo vessel with flat bottom; B, Prolabo vessel with round bottom; and C, glass cylinder

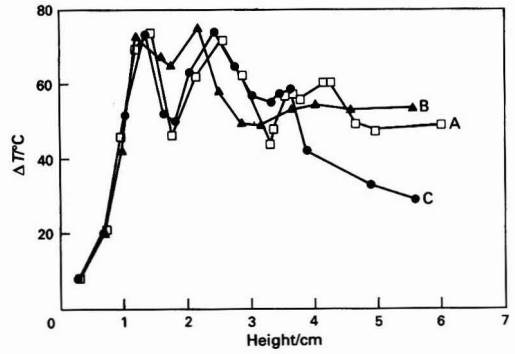

Fig. 3 Temperature change as a function of liquid height in the vessel. A, Prolabo vessel with flat bottom; B, Prolabo vessel with round bottom; and C, glass cylinder

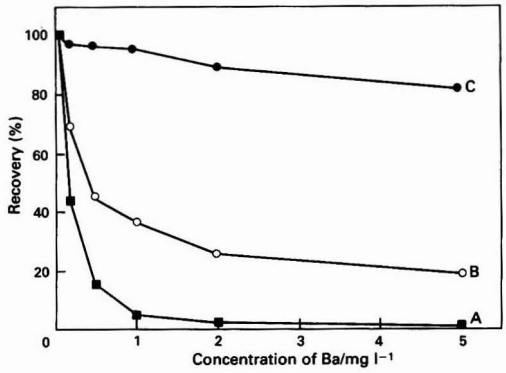

Fig. 4 Recovery of A, Ba, B, Pb, and C, Sr as a function of Ba concentration in the presence of 4% H_2SO_4

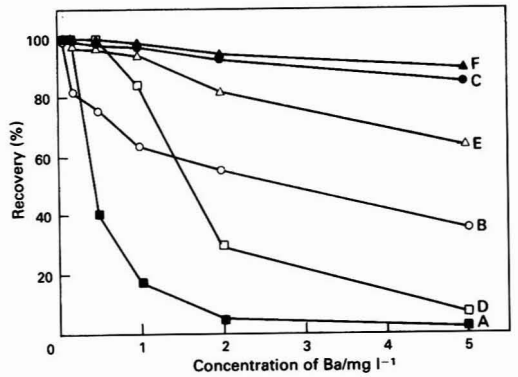

Fig. 5 Recovery of Ba, Pb, and Sr as a function of Ba concentration in the presence of 4% H_2SO_4 + 5% HNO_3: A, Ba; B, Pb; and C, Sr; and 4% H_2SO_4 + 15% HNO_3: D, Ba; E, Pb; and F, Sr

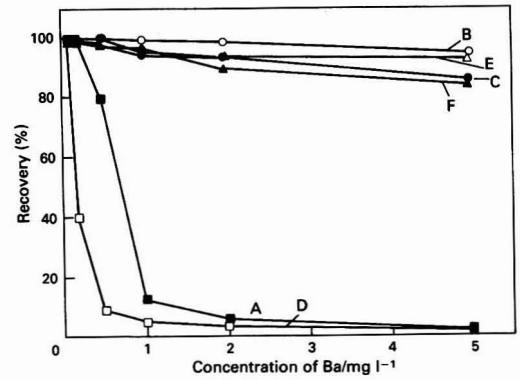

Fig. 6 Recovery of Ba, Pb, and Sr as a function of Ba concentration in the presence of 4% H_2SO_4 + 12% HCl + 3% HNO_3: A, Ba; B, Pb, and C, Sr: and 4% H_2SO_4 + 15% HCl: D, Ba; E, Pb; and F, Sr

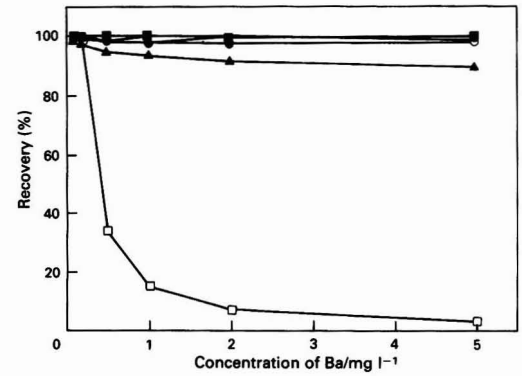

Fig. 7 Recovery of Ba, Pb, and Sr as a function of Ba concentration in the presence of 4% NH_4SO_4 + 1.2% NaEDTA or NH_4EDTA salts (pH = 9): ■, Ba; ○, Pb; and ●, Sr; and 4% H_2SO_4 + 1.2% NaEDTA (pH = 2): □, Ba; △, Pb; and ▲, Sr

results clarified our observation that, for round-bottomed vessels filled above a minimum volume, 30% power has to be used in the second heating stage instead of 40% power to avoid spilling from overheating. Also, at the same microwave power, usually a shorter time was necessary to evaporate the same amount of HNO_3 from the round-bottomed vessel.

These results can be used as guidelines for specific analytical problems. In the subsequent investigations the flat-bottomed vessels were employed, because they are somewhat easier to handle and are commonly used.

Table 3 Recovery of Ba, Pb and Sr from model solutions containing 10 μg ml^{-1} Ba and different reagents (n = 8)

Reagent	Recovery (%)		
	Ba	Pb	Sr
4% H_2SO_4	0.3 ± 0.1	12.2 ± 1.1	72.8 ± 8.5
4% H_2SO_4–5% HNO_3	0.7 ± 0.1	17.7 ± 1.0	75.0 ± 5.2
4% H_2SO_4–10% HNO_3	2.0 ± 0.8	30.0 ± 3.3	83.0 ± 4.4
4% H_2SO_4–15% HNO_3	2.4 ± 1.2	52.5 ± 4.0	86.8 ± 4.5
4% H_2SO_4–11.25% HCl–3.75 HNO_3	0.8 ± 0.4	83.2 ± 8.0	81.6 ± 6.2
4% H_2SO_4–11.6% HCl–2.8% HNO_3	0.8 ± 0.4	85.5 ± 5.4	78.5 ± 4.0
4% H_2SO_4–12% HCl–3% HNO_3	0.8 ± 0.4	85.8 ± 4.2	79.5 ± 5.3
4% H_2SO_4–15% HCl	0.5 ± 0.3	84.8 ± 3.7	76.7 ± 5.3
4% NH_4SO_4–1.2% NaEDTA	100 ± 2.8	98.5 ± 1.5	100 ± 3.0
4% NH_4SO_4–1.2% NH_4EDTA	100 ± 2.5	98.7 ± 1.6	100 ± 2.0

Table 4 Analysis of standard reference materials using open-focused microwave system and ICP-AES. Values (n = 6) are given in μg g^{-1} except where percentages are shown. Non-certified values are given in parentheses

Element	NIST SRM 1577b Bovine Liver		IAEA H8 Horse Kidney	
	Found	Reference	Found	Reference
Ca	122 ± 6	116 ± 4	944 ± 56	924 ± 77
Cd	0.51 ± 0.04	0.50 ± 0.03	208 ± 17	189 ± 4.5
Cu	162 ± 4	160 ± 8	32.8 ± 1.3	31.3 ± 1.75
Fe	188 ± 8	184 ± 15	260 ± 10	265 ± 15
Mg	610 ± 22	601 ± 28	764 ± 54	818 ± 75
Mn	10.8 ± 0.8	10.5 ± 1.7	5.99 ± 0.14	5.73 ± 0.275
P (%)	1.07 ± 0.05	1.10 ± 0.03	1.06 ± 0.05	1.12 ± 0.06
K (%)	1.04 ± 0.008	0.994 ± 0.002	1.22 ± 0.02	1.17 ± 0.075
Na (%)	0.218 ± 0.015	0.242 ± 0.006	0.91 ± 0.06	0.96 ± 0.03
Sr	0.139 ± 0.003	0.136 ± 0.001	1.1 ± 0.1	(1.1)
Zn	124 ± 7	127 ± 16	192 ± 7	193 ± 6

Element	NIES No. 6 Mussel		NIST SRM 1566 Oyster Tissue		NIST SRM 1549 Non-Fat Milk Powder	
	Found	Reference	Found	Reference	Found	Reference
Ca	0.135 ± 0.005%	0.13 ± 0.01%	0.148 ± 0.008%	0.15 ± 0.02%	1.30 ± 0.06%	1.30 ± 0.05%
Cd	<1.0	0.82 ± 0.03	3.7 ± 0.5	3.5 ± 0.4	<1.0	0.0005 ± 0.0002
Cu	5.1 ± 0.6	4.9 ± 0.3	63.7 ± 2.1	63.0 ± 3.5	0.7 ± 0.2	0.7 ± 0.1
Fe	152 ± 5	158 ± 8	194 ± 6	195 ± 34	2.7 ± 0.6	(2.1)
Mg	0.198 ± 0.006%	0.21 ± 0.01%	0.126 ± 0.002%	0.128 ± 0.009%	0.117 ± 0.03%	0.120 ± 0.03%
Mn	15.6 ± 0.9	16.3 ± 1.2	17.5 ± 0.5	17.5± 1.2	0.30 ± 0.07	0.26 ± 0.06
P (%)	0.74 ± 0.03	(0.77)	0.72 ± 0.02	(0.81)	1.00 ± 0.03	(1.05)
K (%)	0.57 ± 0.01	0.54 ± 0.02	0.967 ± 0.01	0.969 ± 0.005	1.80 ± 0.1	1.69 ± 0.03
Na (%)	0.94 ± 0.04	1.00 ± 0.03	0.52 ± 0.04	0.51 ± 0.03	0.494 ± 0.015	0.497 ± 0.010
Sr	17 ± 0.5	(17)	10.20 ± 0.43	10.36 ± 0.56	2.6 ± 0.2	Not specified
Zn	106 ± 10	106 ± 6	846 ± 31	852 ± 14	46.4 ± 0.8	46.1 ± 2.2

Table 5 Analysis of NIST SRM 2670 Toxic Metals in Freeze-Dried Urine (elevated level) with use of open-focused microwave digestion (n = 2)

Element	Found	Reference
Ca/mg ml^{-1}	0.109 ± 0.01	0.105 ± 0.005
Cd/μg ml^{-1}	0.075 ± 0.006	0.088 ± 0.003
Cu/μg ml^{-1}	0.35 ± 0.02	0.37 ± 0.03
K/mg ml^{-1}	1.4 ± 0.1	(1.5)
Mg/mg ml^{-1}	0.060 ± 0.002	0.063 ± 0.003
Mn/μg ml^{-1}	0.320 ± 0.01	(0.33)
Na/mg ml^{-1}	2.50 ± 0.20	2.62 ± 0.14

Elements Forming Insoluble Sulfates

Sulfuric acid is effective in decomposing organic matter, and the resulting solutions contain little residual carbon.[9] Low residual carbon is important for some techniques. However, H_2SO_4 can restrict the determination of elements forming low-solubility sulfates. When about 3 μmol l^{-1} of Ba was present in the digest (approximately 0.44% v/v H_2SO_4), coprecipitation of Pb occurred.[10] The ionic strength and formation of soluble complexes can strongly influence the occurrence of a precipitate and coprecipitate. In biological samples, Pb as well as Ca and Sr have to be determined. A comparison of the ionic radii and the solubility product constants shows that coprecipitation with $BaSO_4$ can be expected for Pb and Sr.[16] In the determination of Ba in waters containing sulfates, the addition of NaEDTA provided accurate results; NaEDTA was also added in the determination of Pb in PVC[11,12] by atomic absorption spectrometry, and 4% v/v HNO_3 was added to the final H_2SO_4 digest for square-wave voltammetry.[12] The increase of the lead chloride solubility in an excess of HCl and the use of an HCl and HNO_3 mixture for the analysis of a pure lead sample was reported.[17] The 11.6% HCl–2.8% HNO_3 mixture was found to be the most appropriate for element compatibility and long-term stability.[18]

These investigations have been performed with conductive heating. Microwave energy interacts on a molecular level, and some differences in precipitation and occlusion processes can be expected. Therefore, test solutions were investigated with use of both types of heating. The results obtained were statistically indistinguishable, which indicates that ionic strength and complex formation are the major influencing factors.

In all experiments with test solutions, the recovery of Ca was quantitative (95–102%). Some of the mean value results (n = 8) for both types of heating for the other elements are presented in Figs. 4–7. With only 4% H_2SO_4 in the final solutions (Fig. 4), the loss of Pb starts with the precipitation of

Table 6 Analysis of formula milk and TPN (n = 6) with use of three digestion procedures

	Formula milk			TPN		
Element	HPA	Floyd	Prolabo	HPA	Floyd	Prolabo
Ca/μg g^{-1}	3200 ± 100	3100 ± 100	3200 ± 100	67.5 ± 3	68.4 ± 4.5	67.4 ±4
Cu/μg g^{-1}	7.4 ± 0.4	7.0 ± 0.3	6.9 ± 0.3	<0.50	<0.80	<0.25
Fe/μg g^{-1}	77.9 ± 0.6	78.2 ± 0.7	76.1 ± 0.6	<0.50	<0.80	<0.25
K (%)	0.12 ± 0.2	0.13 ± 0.2	0.13 ± 0.2	0.040 ± 0.003	0.045 ± 0.004	0.043 ± 0.004
Mg/μg g^{-1}	280 ± 10	280 ± 5	300 ± 10	32.7 ± 1.8	32.6 ± 2.0	32.3 ± 2.0
Mn/μg g^{-1}	<0.50	<0.80	0.72 ± 0.02	<0.50	<0.80	<0.25
Na (%)	0.54 ± 0.07	0.58 ± 0.05	0.54 ± 0.06	0.065 ± 0.05	0.061 ± 0.04	0.060 ± 0.05
P (%)	0.29 ± 0.01	0.28 ± 0.02	0.290.01	0.023 ± 0.003	0.025 ± 0.004	0.024 ± 0.003
Zn/μg g^{-1}	46.3 ± 2.2	41.9 ± 2.2	41.3 ± 2.0	1.19 ± 0.1	1.20 ± 0.07	1.17 ± 0.05

Table 7 Recovery (%) of As, Ba, Pb and Sr from samples, spiked with 125 μg each of As, Ba and Pb (5 μg l^{-1}), for three digestion procedures with open-focused microwave digestion (n = 3)

	Recovery (%)											
	15% HNO_3				12% HCl–3% HNO_3				1.2% NH_4EDTA			
Sample	As	Ba	Pb	Sr	As	Ba	Pb	Sr	As	Ba	Pb	Sr
Bovine Liver	98.3 ± 1.5	10.4 ± 2.5	62.2 ± 2.5	90.2 ± 1.8	98.8 ± 1.5	2.4 ± 0.5	87.5 ± 3.0	84.5 ± 3.3	99.2 ± 1.0	98.8 ± 0.8	100 ± 1.0	99.5 ± 0.9
Mussel	96.2 ± 1.2	13.0 ± 3.1	55.7 ± 1.8	82.4 ± 1.6	99.5 ± 2.1	4.0 ± 1.5	81.6 ± 2.5	78.6 ± 1.9	100 ± 2.3	100 ± 1.3	96.7 ± 1.3	100 ± 0.9
Oyster Tissue	100 ± 3.0	12.0 ± 2.8	67.5 ± 2.3	89.3 ± 1.5	100 ± 2.4	3.0 ± 0.6	88.2 ± 1.0	80.7 ± 2.2	99.3 ± 2.1	100 ± 2.3	99.5 ± 2.1	99.0 ± 2.0
Horse Kidney	100 ± 2.5	14.0 ± 3.2	67.2 ± 1.8	86.5 ± 1.0	94.7 ± 0.8	6.8 ± 2.5	82.0 ± 2.6	91.0 ± 1.6	99.5 ± 1.8	100 ± 1.8	101 ± 2.6	97.8 ± 1.8
Non-Fat Milk Powder	100 ± 1.7	23.0 ± 4.0	68.5 ± 2.8	83.4 ± 1.8	96.8 ± 1.3	8.4 ± 1.1	92.1 ± 2.3	81.6 ± 2.1	98.8 ± 1.4	100 ± 1.2	96.5 ± 1.2	99.2 ± 1.9
Formula Milk	99.3 ± 1.8	9.4 ± 1.3	55.7 ± 2.3	88.8 ± 2.0	100 ± 1.5	4.4 ± 1.0	93.2 ± 1.9	92.3 ± 2.0	100 ± 1.6	100 ± 1.6	100 ± 1.9	97.5 ± 1.1
Urine Sample (24 h)	98.8 ± 2.3	9.4 ± 1.8	55.8 ± 1.6	84.2 ± 0.9	100 ± 2.0	2.8 ± 0.3	80.8 ± 1.5	93.2 ± 1.6	100 ± 2.3	96.6 ± 0.8	96.8 ± 0.8	99.5 ± 1.7
TPN	99.4 ± 2.8	19.4 ± 2.8	65.0 ± 2.4	97.2 ± 1.6	97.8 ± 1.3	14.4 ± 3.0	90.5 ± 1.8	89.0 ± 2.0	100 ± 1.8	98.4 ± 1.1	97.8 ± 1.1	100 ± 2.0

Table 8 Carbon content of original samples (c_{or})

	Carbon (%)	
Sample	Dry material	Liquid material
NIST SRM 1566 Oyster Tissue	46.64	—
NIES No. 6 Mussel	44.24	—
IAEA H8 Horse Kidney	46.64	—
NIST SRM 1577b Bovine Liver	48.14	—
NIST SRM 1549 Non-Fat Milk Powder	41.12	—
Formula milk (Similac)	50.88	4.02
TPN	38.81	4.90
Artificial urine	—	0.46
NIST SRM 2670 Toxic Metals in Freeze Dried urine	—	0.56
Urine sample	—	0.49

Ba above 0.1 μg ml^{-1} Ba. Strontium is less prone to coprecipitate above 1 μg ml^{-1} Ba. The presence of 15% HNO_3 (Fig. 5) reduced the coprecipitation, especially for Sr, but loss of Pb occurred at a Ba concentration above 1 μg ml^{-1}. The presence of HCl improved the recovery of Pb (Fig. 6), but recovery of Sr decreased slightly at high Ba concentrations. Addition of EDTA solutions at pH 9 afforded complete quantitative recovery of all the elements including Ba and Sr (Fig. 7). At lower pH, only the Pb complexes were stable. The NH_4EDTA salt was preferred to the Na salt, because the alkaline-earth elements could be determined therewith and the salt was easily purified.

The recoveries of Ba, Pb and Sr, with 10 μg ml^{-1} Ba present in the final solution, are reported in Table 3. Increasing the acid concentrations improves the recovery; HNO_3 favours more Ba and Sr, and HCl aids Pb. The EDTA dissolves all the precipitates and permits quantitative determination of all the elements investigated.

Sample Analysis

Based on investigations with these test solutions, RMs and samples were analysed to verify the efficacy of the open-focused microwave procedure. Less than 0.1 μg ml^{-1} Ba in the final solution was found in all investigated samples. For the open-focused microwave digestion, results obtained with 15% HNO_3, 12% HCl–3% HNO_3 and 1.2% NH_4EDTA were statistically indistinguishable, and means are presented for the RMs in Tables 4 and 5. The values found are in good agreement with the certified data. For the analysis of TPN and formula milk samples, the results for nine elements are compared in Table 6 for digestions with the HPA and the two microwave systems. The results agree closely.

The sample preparation and accuracy of determination were assessed for authentic samples, for Pb, Sr and Ca, which form low-solubility sulfates, and for As, which is prone to volatilization. Because of the low concentrations of Pb and As in the SRMs and the authentic samples and the poor ICP-AES sensitivity, samples were spiked with 125 μg of Pb and As, the latter element added as the Na salt of cacodilic acid. Spikes of 125 μg of Ba were also added. Element recoveries are summarized in Table 7. The recovery of As is quantitative for all samples. Similar results are obtained for the recovery of Ba, Pb and Sr from these samples and from test solutions with different reagents. These data confirm that, in the presence of a high concentration of Ba, the negative systematic error can be overcome by adding NH_4EDTA in the final preparation step.

Comparison of Sample-digestion Techniques

The RCC in the final solutions was measured for each digestion approach, by use of the operating conditions and reagents cited in Table 1, but with EDTA salts being used in the Prolabo system. To calculate the effectiveness of the procedure, the original carbon content (c_{or}) was measured by elemental analysis of the SRMs and freeze-dried TPN and formula milk. The original carbon content in SRM 2670 and a urine sample after 10-fold dilution was measured by ICP-AES.[15] The procedure was verified by comparing results for artificially prepared urine. The original sample carbon contents (Table 8) were used to calculate the total carbon left undigested (RC%) = RCC × 100/c_{or}.[9] The results obtained are presented in Table 9. With both the open digestion

Table 9 Residual carbon (RC; for definition see text) in sample digested with use of three systems (n = 2 to 6)

Sample	RC (%)		
	Prolabo	HPA	Floyd
NIST SRM 1577b Bovine Liver	0.58 ± 0.4	1.0 ± 0.2	16.4 ± 4.0
IAEA H8 Horse Kidney	0.36 ± 0.2	1.34 ± 0.5	14.2 ± 2.0
NIES No. 6 Mussel	0.54 ± 0.2	0.70 ± 0.3	16.1 ± 3.0
NIST SRM 1566 Oyster Tissue	0.38 ± 0.1	0.64 ± 0.1	14.6 ± 2.2
NIST SRM 1549 Non-Fat Milk Powder	0.15 ± 0.1	0.51 ± 0.1	6.8 ± 1.5
Formula milk	0.10 ± 0.05	0.51 ± 0.1	11.1 ± 1.0
TPN	0.15 ± 0.05	0.36 ± 0.1	2.1 ± 0.4
Artificial urine with urea	<0.2	<0.2	<0.2
Artificial urine with urea and creatinine	<0.2	<0.2	0.53 ± 0.2
NIST SRM 2670 Toxic Metals in Freeze-Dried Urine	2.70 ± 0.3	2.25 ± 0.8	9.7 ± 3.5
Urine sample	0.73 ± 0.2	0.78 ± 0.3	7.4 ± 2.0

microwave system and the HPA, the effectiveness of organic matter decomposition is similar and superior to that of the closed microwave digestion procedure.

Unexpectedly high RC results were obtained for urine. Because of the low organic carbon content in the original samples (Table 8), complete decomposition of carbon was expected. This was observed for an artificial urine sample to which only urea was added (Table 9). For some organic compounds found in urine (*i.e.*, urea, uric acid, creatinine and benzoic acid),[19] a three times higher RC was observed for creatinine, after digestion of each pure compound (0.1–0.5 g) in the open-focused system, than for the other compounds. With the addition of creatinine to the artificial urine at a concentration based on literature values,[19] a detectable difference above the detection limit for carbon[15] was observed only for the closed microwave system (Table 9). Furthermore, incomplete decomposition of carbon was observed for actual urine samples. The SRM 2670, based on the North American diet, yielded RC values higher than those for the local 24 h urine sample. Perhaps this disparity could be explained by the presence of very stable organometallic compounds, the concentrations of which can vary with the sample.[20] However, additional studies are required.

Conclusion

The investigation with the open-focused microwave system has produced an optimized method for the dissolution of biological samples. A minimal volume of H_2SO_4 (*i.e.*, 1 ml) was used to avoid nebulizer transport effects in ICP-AES, but it was sufficient to decompose the organic matter. With addition of 15% HNO_3 or 12% HCl–3% HNO_3, the accuracy in the determination of Pb and Sr can be improved. Addition of 1.2% NH_4EDTA in the final digestion step improves the recovery of Ba. In authentic biological samples, the spiked Ba recovery was quantitative. The RC obtained with the open-focused microwave system was lower than that obtained with the closed medium-pressure microwave system, and was similar to that with the HPA.

The established method can also be used with automated models of the open-focused microwave system, as well as for measuring techniques other than ICP-AES where complete decomposition of carbon is necessary. The results obtained are similar to those obtained recently for milk samples.[9]

We thank Prolabo, Floyd and Questron for their support and assistance in using their equipment. Research was sponsored by the *ICP Information Newsletter*.

References

1 Schramel, P., Hasse, S., and Knapp, G., *Fresenius Z. Anal. Chem.*, 1987, **326**, 142.
2 Kingston, H. M., and Jassie, L. B. (eds.), *Introduction to Microwave Sample Preparation*, American Chemical Society, Washington, DC, 1988, pp. 25, 26, 76, 165.
3 Grillo, A. C., *Spectroscopy*, 1989, **4**, 16.
4 Kingston, H. M., and Jassie, L. B., *Anal. Chem.*, 1986, **58**, 2534.
5 Salt, R. N., and Miller, R. O., *Anal. Chem.*, 1992, **64**, 230.
6 Stripp, R. A., and Bogen, D. C., *J. Anal. Toxicol.*, 1989, **13**, 57.
7 Hocquellet, P., and Candillier, M.-P., *Analyst*, 1991, **116**, 505.
8 Feinberg, M. H., *Analusis*, 1991, **19**, 47.
9 Krushevska, A., Barnes, R. M., Amarasiriwaradena, C. J., Foner, H., and Martines, L., *J. Anal. At. Spectrom.*, 1992, **7**, 851.
10 Temminghoff, E. J. M., and Novozamsky, I., *Analyst*, 1992, **117**, 23.
11 Belarra, M. A., Gallarta, F., Anzano, J. M., and Castillo, J. R., *J. Anal. At. Spectrom.*, 1986, **1**, 141.
12 Peddy, R. V. C., Kalpana, G., and Koshy, V. J., *Analyst*, 1992, **117**, 27.
13 Karabash, A. G., Bondarenko, L. S., Morozova, G. G., and Peizulaev, Sh. I., *Zh. Anal. Khim.*, 1960, **15**, 623.
14 Meyers, S. A., and Tracy, D. H., *Spectrochim. Acta, Part B*, 1983, **38**, 1227.
15 Krushevska, A., Barnes, R. M., Amarasiriwaradena, C. J., Foner, H., and Martines, L., *J. Anal. At. Spectrom.*, 1992, **7**, 845.
16 Weast, R. C. Astie, M. J., and Beyer, W. H. (eds.), *Handbook of Chemistry and Physics*, CRC Press, Boca Raton, FL, 65th edn., 1984, F-165 and B-222.
17 Degtyareva, O. F., and Ostrovskaya, M. F., *Zh. Anal. Khim.*, 1960, **20**, 814.
18 Que Hee, S. S., Macdonald, T. J., and Boyle, J. R., *Anal. Chem.*, 1985, **57**, 1242.
19 Lehninger, A. L., in *Principles of Biochemistry*, ed. Anderson, S., and Fox, J., Wort, New York, NY, 1982, p. 703.
20 Hanna, C. P., Tyson, J. F., and McIntosh, S., *Clin. Chem. (Winston-Salem, N.C.)*, in the press.

Paper 2/06667J
Received December 16, 1992
Accepted March 4, 1993

Determination of Trace Amounts of Thallium and Tellurium in Nickel-base Alloys by Electrothermal Atomic Absorption Spectrometry

Suh-Jen Jane Tsai and Ching-Ching Jan
Department of Applied Chemistry, Providence University, Taichung Hsien, Taiwan

A method is described for determining trace amounts of Tl in nickel-base alloys using pre-treatment with ammonia solution and electrothermal atomic absorption spectrometry. Thallium was coprecipitated when the sample solution of a nickel-base alloy was treated with ammonia solution. Background absorption was effectively eliminated in the new matrix. Nickel worked effectively as a chemical modifier for Te, and raised the charring temperature from 500 to 1000 °C. Therefore, it was possible to determine sub-nanogram levels of Te without any complicated pre-treatment. The accuracy and precision of the proposed method were elucidated through the analysis of two nickel-base alloys: spectroscopic standard certified reference material 346A IN100 Alloy and Standard Reference Material 899 Tracealloy C. There was good agreement between the expected values and the results obtained. For Tl, the results found for IN100 and Tracealloy C were 1.94 ± 0.09 μg g^{-1} (s_r = 5%) and 0.251 ± 0.005 μg g^{-1} (s_r = 2%), respectively, the reference value for IN100 being 2 and certified value for Tracealloy C being 0.252 ± 0.003 μg g^{-1}. The recoveries for these alloys were 100 ± 4 and 102 ± 3%, respectively. The detection limit was 15 pg g^{-1}. For Te, the certified values for IN100 and Tracealloy C were 9 ± 1 and 5.9 ± 0.6 μg g^{-1}, respectively. The Te contents determined by the proposed procedure were 9.03 ± 0.09 μg g^{-1} (s_r = 1%) and 5.93 ± 0.26 μg g^{-1} (s_r = 4%), with recoveries of 98 ± 4 and 97 ± 4%, respectively. The detection limit was 35 pg g^{-1}. Although the addition of Pd modifier gave a better detection limit (18 pg g^{-1}), it led to poorer results in terms of accuracy, precision and recovery.

Keywords: *Thallium and tellurium determination; nickel-base alloy; ammonia pre-treatment; nickel-base and palladium modifiers; electrothermal atomic absorption spectrometry*

The quality of nickel-base alloys is highly dependent on the amounts of trace elements present because the existence of trace elements has serious effects on the mechanical and physical properties of these high-temperature alloys.[1–5]. The determination of trace elements in nickel-base alloys had been a challenge owing to the complexity of the alloy matrices and therefore only a few studies on this subject have been reported.[6–8]

As Tl is a toxic element, the determination of trace concentrations of this element in environmental and biological samples is important. Electrothermal atomic absorption spectrometry (ETAAS) and inverse voltammetry are appropriate methods for the determination of trace amounts of Tl with detection limits at the ng ml^{-1} level, as reported in a review published in 1988.[9] Anodic stripping voltammetry had also been employed in the determination of trace amounts of Tl.[10] The determination of Tl at the μg ml^{-1} level or higher by flame AAS was usually accomplished by extracting the Tl complexes with an organic solvent such as diisopropyl ether.[11] Both complexation and extraction processes had to proceed to completion in order to obtain reliable results. Trace amounts of Tl^{III} were determined together with Ga^{III} and In^{III} by successive titrations and the detection limit thus obtained was 511 ppm.[12] Trace amounts of Tl were measured using radiochemical neutron activation analysis[13] and isotope dilution mass spectrometry[14] in addition to ETAAS.[15]

Welcher *et al.*[6] showed the potential application of non-flame AAS methods in determining ppm concentrations of Tl in high-temperature alloys. There was good agreement between the results obtained using graphite furnace atomization and by emission spectrometry. However, the precision (s_r = 11% for 3.4 ppm) could be improved. The matrix material of the nickel alloy caused about a 20% decrease in sensitivity. The very large background signals obtained need to be reduced before a satisfactory detection limit can be attained. A spiking technique was recommended by Dulski and Bixler[8] in order to compensate for the serious matrix effects of nickel-base alloys.

Difficulties were encountered in the determination of trace amounts of Tl by ETAAS. Among them, serious signal depression caused by either HCl[6] or $HClO_4$[16] both of which received much attention. The matrix interferences caused by HCl were eliminated by H_2SO_4[17] and those caused by $HClO_4$ could be reduced by using pyrolytic graphite coated graphite tubes.[18] Palladium has also been confirmed as an effective chemical modifier for Tl.[19,20] Slavin and Manning[21] confirmed that less signal depression was observed when the atomization was performed on a L'vov platform.

Coprecipitation has sometimes been employed for the separation of the analyte from interfering ions and also for preconcentration. Hafnium hydroxide is an effective collector for trace amounts of Be.[22] Niskavaara *et al.*[23] proposed a method for the separation of trace amounts of Ag, Au, Pd, Pt, Rh, Se and Te from relatively complex geological samples; reductive coprecipitation was achieved with tin(II) chloride as the reductant and mercury as the collector. The preconcentration of 16 elements, including Tl, from deep ocean sea-water and coastal water has also been achieved by tetrahydroborate reductive precipitation.[24]

Welcher *et al.*[6] also determined ppm concentrations of Te in high-temperature alloys. As certified reference materials (CRMs) of nickel-base alloys were not available at that time, the accuracy of the ETAAS procedure was evaluated based on the addition of 5 ppm of Te to various nickel-base alloys. Headridge and Nicholson[3] tried to analyse a nickel-base alloy *via* the analysis of a solid sample by ETAAS. The AAS signals of Te were monitored at 214.3 nm and the charring and the atomization temperatures were 1000 and 2900 °C, respectively. The detection limit thus obtained was 0.003 μg g^{-1}. Tellurium was reduced to the elemental state with hypophosphorous acid and collected by As before determination by ETAAS.[25] A prior extraction step with isobutyl methyl ketone (IBMK) was employed to remove trace amounts of Te from the complex matrix when geochemical samples were analysed by ETAAS.[26,27] Ion-exchange processes were required to remove interfering elements from the analyte in the determination of Te in atmospheric aerosol samples by ETAAS.[28,29] An increase in the Te signal by some mineral acids, including HCl, HNO_3 and H_2SO_4, was reported by Kunselman and Huff,[30] who consequently used an analyte addition technique.

Various metals, such as Ni, Pd, Mg and Cu[31,32] and Ir,[24] have often been employed as effective chemical modifiers. Successful measurements of trace amounts of Te in geological samples or natural water were made using a Pd-coated graphite tube.[33]

Tellurium in copper-base alloys (≥0.0002%) was determined by flame AAS with an air–acetylene flame following an extractive pre-treatment with trioctylphosphine oxide–IBMK.[34] In Hubert and Chao's work,[35] IBMK was used instead. An extractive pre-treatment was required in determining trace amounts of Te by flame AAS in order to obtain better sensitivity. A hydride generation system coupled with flame AAS was employed to determine Te in a lead alloy. However, a tedious pre-treatment was required before the metal reduction could be effected.[25] The connection of a hydride generation system with ETAAS led to the satisfactory determination of Te in a sample of silicate ore.[36] As serious interferences from nickel were reported when trace amounts of Te were determined by hydride generation AAS,[37] an effective pre-treatment would be required if complex nickel-base alloys are to be analysed by hydride generation ETAAS. Other instrumental methods such as X-ray fluorescence spectrometry[38] and differential-pulse polarography[39,40] have also been employed in the determination of trace amounts of Te.

The objective of this work was to study the determination of Tl and Te in CRMs of nickel-base alloys, namely Spectroscopic Standard (SS) CRM 346A IN 100 Alloy and National Institute of Standards and Technology (NIST) Standard Reference Material (SRM) 899 Tracealloy C, by ETAAS. For Tl determination, the effects of chemical modifiers including H_2SO_4, Pd and coprecipitation in ammonia solution on the reduction of background signals were evaluated. Pre-treatment with ammonia solution was the most effective method. This work also demonstrates the merits of a stabilized temperature platform furnace in the determination of trace amounts of Te. In spite of the complexity of alloy matrices, it was found that trace amounts of Te in nickel-base alloys can be successfully determined by measurement against nickel-containing aqueous standard solutions.

Experimental

Apparatus

A Perkin-Elmer Model 1100B atomic absorption spectrometer fitted with an HGA-700 furnace and AS-70 autosampler was used. Integrated absorbance (peak area) values were used in measurements. Experimental parameters and peak profiles were recorded with an Epson EX-800 printer. An electrodeless discharge lamp (EDL) equipped with a Perkin-Elmer EDL power supply was used for Tl determinations. The EDL was also used for Te determinations. New pyrolytic graphite coated graphite tubes (Part No. B010-9322) and pyrolytic graphite platforms (Part No. B010-9324) were used. Maximum power heating was used for the atomization step. A Barnstead Nanopure II system was employed for water purification.

Reagents and Standards

Standard solutions of Tl ($TlNO_3$ in 10% HNO_3, Tl = 1001 μg ml^{-1}), Te ($TeCl_4$ in 30% HCl, Te = 1002 μg ml^{-1}), Pb [$Pb(NO_3)_2$ in 2% HNO_3, Pb = 1001 μg ml^{-1}], Se (H_2SeO_3 in 2% HNO_3, Se = 998 μg ml^{-1}), Ga [$Ga(NO_3)_3$ in 2% HNO_3, Ga = 1000 μg ml^{-1}] and In [$In(NO_3)_3$ in 2% HNO_3, In = 1000 μg ml^{-1}] were products of Inorganic Ventures. Hafnium (atomic absorption standard solution, in 10% HCl, Hf = 985 μg ml^{-1}), Zr (atomic absorption standard solution, in 5% HCl, Zr = 1030 μg ml^{-1}) and atomic absorption standard solutions of V, Mo, Nb and Ta were products of Aldrich. Standard solutions of Ni [$Ni(NO_3)_3{\cdot}6H_2O$ in HNO_3, 0.5 mol l^{-1}], Co [$Co(NO_3)_3{\cdot}6H_2O$ in HNO_3, 0.5 mol l^{-1}], Ti ($TiCl_4$ in HCl, 0.5 mol l^{-1}), Fe [$Fe(NO_3)_3{\cdot}9H_2O$ in HNO_3, 0.5 mol l^{-1}], Cu [$Cu(NO_3)_2{\cdot}3H_2O$ in HNO_3, 0.5 mol l^{-1}], Ti ($TiCl_4$ in HCl, Pd [$Pd(NO_3)_2$ in 15% HNO_3, Pd = 10.0 ± 0.2 g l^{-1}), $K_2Cr_2O_7$, $CrCl_3{\cdot}6H_2O$, aluminium foil and concentrated ammonia solution were of analytical-reagent grade from Merck.

Concentrated HCl, HF and HNO_3 were singly distilled acids from Eastar Chemical. Working standard solutions were prepared from 1000 mg l^{-1} stock standard solutions by serial dilution. Distilled, de-ionized water (DDW) prepared with a Barnstead Nanopure II system was used for all of the determinations. The CRMs of nickel-base alloys, SSCRM 346A IN100 and SRM 899 Tracealloy C were obtained from the Bureau of Analysed Samples and NIST, respectively. Purified grade argon (99.99%) was used as the purge gas during sample analysis.

Sample Decomposition

Precise amounts of nickel-base alloys (0.04–0.12 g) were digested with 1.5 ml of HCl–HNO_3 (4 + 1 v/v). After digestion, the sample solutions were heated nearly to dryness and the residue was dissolved in a few millilitres of DDW. The heating and dissolution procedures were repeated in order to remove the excess amount of acids. For Tl determinations, the resulting solutions were treated with ammonia solution. For Te determinations, the alloy solutions were diluted to 10 ml with 0.2% HNO_3.

Thallium Determination

The above alloy solutions were further treated with ammonia solution as follows before being subjected to ETAAS. Each sample solution prepared above was treated with 5 ml of concentrated ammonia solution and the solution together with the precipitate were transferred into a 10 ml test-tube, which was then filled with concentrated ammonia solution. After the solution had been centrifuged, the precipitate was decomposed completely with 3–5 ml of HNO_3 (1 + 1 v/v). The volume of the sample solution was reduced to about 1 ml by heating gently. The above solution was diluted to 5.0 or 10.0 ml precisely with 0.2% HNO_3. These solutions were analysed by injecting 5–50 μl portions onto the platform located in a pyrolytic graphite coated graphite tube. The corresponding blank solutions were also analysed. In the measurements with a chemical modifier, 1% H_2SO_4 or Pd (1000 μg ml^{-1} Pd), sample solution was followed by 5 μl of modifier solution. Aliquots of Tl solution (0.02 μg ml^{-1}), *e.g.*, 3, 5, 10, 15, 20 and 25 μl, were injected sequentially into the graphite tube with the AS-70 autosampler to obtain the calibration graphs. Dilute HNO_3 (0.2%) was used for preparing the working solutions.

Tellurium Determination

The sample solutions prepared as described under Sample Decomposition were analysed directly by ETAAS. In the measurement with a Pd modifier, a volume of 5 μl of Pd modifier solution (1000 μg ml^{-1} Pd) was injected into the graphite tube into which sample solution had been injected. Thus, sample solutions were analysed together with the Pd modifier.

The calibration graphs were determined by injecting several aliquots of Te solution (0.05 μg ml^{-1}). Each of these aliquots contained 0.005 g of Ni, corresponding to the amount present in the nickel-base alloys. Dilute HNO_3 (0.2%) was used for preparing the working solutions.

Interferences from Foreign Ions

For interference studies, 10 μl of analyte solution (0.02 μg ml^{-1} Tl or 0.05 μg ml^{-1} Te) and 10 μl of the foreign ion

were added separately to a graphite tube. Although there was little chance of direct overlap of atom lines, the AAS signals of either Tl or Te was detected with only foreign ion in the graphite tube in order to check whether there were any spectral interferences. The optimum 'dry,' 'char' and 'atomize' HGA-700 programme developed in this laboratory was followed and the integrated areas of the absorbance peaks were recorded. The recommended analytical conditions and the temperature programmes for Tl and Te are summarized in Tables 1 and 2, respectively. Blanks were run regularly and their values were subtracted from the gross values to obtain the net values reported.

Table 1 Optimum analytical conditions for Tl determination

Supply power	6.5 W
Background corrector	Deuterium lamp
Lamp current	5 mA
Wavelength	276.8 nm
Slit	0.7 nm
Integration time	5.0 s
Characteristic mass (pg/0.0044 A s)	7.0

Furnace step No.	Furnace temperature/°C	Time/s Ramp	Time/s Hold	Gas flow/ml min^{-1}	Read on/s
1	110	10	15	300	
2	600,* 700,† 1000‡	10	30	300	
3	1350,* 1500,† 1550‡	0	5	0	0.0
4	2650	1	5	300	
5	20	5	5	300	

* Tl standard solution.
† IN100.
‡ Tracealloy C.

Table 2 Optimum analytical condition for Te determination

Light source	Te EDL
Supply power	8.5 W
Background corrector	Deuterium lamp
Technique	Atomic absorbance – background
Lamp current	5 mA
Wavelength	214.3 nm
Slit	0.2 nm
Signal processing	Integrated absorbance
Integration time	5.0 s
Internal gas	Ar, high-purity (99.99%)
Tube/site	Pyrolytic graphite/platform
Characteristic mass (pg/0.0044 A s)	25.1

Furnace step No.	Furnace temperature/°C	Time/s Ramp	Time/s Hold	Gas flow/ml min^{-1}	Read on/s
1	110	10	15	300	
2	500,* 1000,† 1250‡	10	30	300	
3	1700,† 1800*,‡	0	5	0	0.0
4	2650	1	5	300	
5	20	5	5	300	

* Te standard solution.
† IN100 and Tracealloy C.
‡ IN100 + Pd and Tracealloy C + Pd.

Results and Discussion

Ammonia Pre-treatment, Chemical Modifier and Temperature Programme

The sample solutions of the CRMs of nickel-base alloys, IN100 and Tracealloy C, were first analysed directly by ETAAS. As demonstrated in Table 3, the background signals were much higher than the AAS signals for Tl. Without the addition of any chemical modifier, the AAS signals for Tl in IN100 and Tracealloy C were −0.023 and −0.063, whereas the corresponding background absorbances were 3.019 and 9.622, respectively. Apparently, the operation of the automatic deuterium background corrector did not correct the light-scattering signals or molecular absorption of the co-volatilized salts completely. The very high background absorbances prevented direct instrumental measurement of nickel-base alloys by ETAAS. Nickel metal boils at 2840 °C, $NiCl_2$ sublimes at 973 °C[8] and Tl compounds are volatile, *e.g.*, TlCl and $TlNO_3$ boil at 720 and 430 °C, respectively.[9] It was not possible to remove the interfering molecules completely without loss of the analyte.

Chemical modification techniques have been widely applied in trace analysis by ETAAS. The addition of chemical modifiers results in an enhancement of the volatility of unwanted elements and in stabilization of the analyte during the charring stage until most of the matrix components have been vaporized.

Sulfuric acid and Pd have often been used as effective chemical modifiers for the determination of Tl in environmental samples, as mentioned earlier. The addition of H_2SO_4 allows Tl to form the more stable oxide instead of the volatile chloride[41]. The effects of these chemical modifiers on the determination of trace amounts of Tl in nickel-base alloys were, therefore, studied. The background signals were still much higher than the Tl absorption in the presence of either of the chemical modifiers, as shown in Table 3. Although background correction, chemical modification and thermal pre-treatment can often eliminate interferences in ETAAS, none of them reduced the background signals to an acceptable level when analysing nickel-base alloys.

The CRM IN100 contains over 50% Ni. The composition of IN100 as follows (all values in mg g^{-1}): C, 1.5; Cr, 100; Mo, 30; Al, 55; Co, 150; Ti, 50; V, 10; Pb, 0.022; and trace amounts of Bi, Ag, Se, Te, Tl, Sb, As, Cd, Ga, Sn, Zn, Mg, Ca and In. The reference value for Tl is 2 μg g^{-1}. The composition of Tracealloy C is as follows (all values in mg g^{-1}): C, 1.2; Cr, 120; Al, 20; Co, 85; Ti, 20; B, 0.1; W, 17.5; Nb, 9; Zr, 1; Ta, 17.5; and Hf, 12. These values are not certified but are provided for information only. The certified value for Tl is 0.252 ± 0.003 μg g^{-1}.

When ammonia solution was added to a solution of nickel-base alloys, most of the Ni^{II} would be precipitated as $Ni(OH)_2$, which would dissolve and form $[Ni(NH_3)_4]^{2+}$. The addition of ammonia solution also brought about the forma-

Table 3 Effects of ammonia solution pre-treatment and chemical modifiers on the AAS signals for Tl and the corresponding background signals for nickel-base alloys

		Chemical modifer				
Alloy	Method*	None	1% H_2SO_4	Pd	NH_3, HCl–HNO_3	NH_3, HNO_3
IN100	AA − BG	−0.023	−0.016	−0.007	0.023	0.084
	BG	3.019	0.189	1.512	0.004	0.004
Tracealloy C	AA − BG	−0.063	−0.013	0.020	0.012	0.052
	BG	9.622	3.188	3.013	0.758	0.002

AA = atomic absorbance; BG = background. The integrated absorbance was recorded.

tion of $[Co(NH_3)_6]^{2+}$ under the same conditions. Thallium was coprecipitated and separated from most of the interfering ions. The resulting mixture was centrifuged in order to avoid the adsorption of any precipitate onto the filter-paper. A volume of the decantate was injected onto the platform and analysed by ETAAS. No Tl signal was detected, as expected. When the precipitates were dissolved in a mixture of HCl and HNO_3, the background signal for Tracealloy C was still much higher than the AAS signal or of Tl. As shown in Table 3, the integrated absorbance of Tl and the background signals were 0.012 and 0.758, respectively. This indicated the interference of chloride, as reported earlier.[41–43] When the precipitates were dissolved in HNO_3 (1 + 1), a great improvement in the signal for Tl in nickel-base alloys was found. In addition, the background signals were eliminated for both IN100 and Tracealloy C, as shown in Table 3.

Pre-treatment with ammonia solution provided an effective solution to the serious background problem in the determination of trace amounts of Tl in nickel-base alloys by ETAAS.

Figs. 1(A) and 2(A) show the influence of charring and atomization temperatures on the integrated absorbances of Tl in a standard solution. For the Tl standard, the optimum temperatures for charring and atomization were 600 and 1350 °C, respectively. Figs. 1(B) and (C) and 2(B) and (C) show the effects of charring and atomization temperatures on the integrated absorbances of Tl in nickel-base alloys. The absorbances of IN100 and Tracealloy C were monitored at an atomization temperature of 1500 °C. The appropriate maximum charring temperatures for these two samples were 700 and 1000 °C, respectively. The signal intensity of the Tl standard reached a plateau when the temperature increased to 1350 °C, whereas the signal for Tl in Tracealloy C decreased rapidly above 1500 °C. The optimum atomization temperature of Tl in IN100 was 1550 °C.

As nickel has been used to stabilize volatile elements in trace analyses by ETAAS,[31,44] it was worthwhile differentiating the temperature dependence of the AAS signals for Te in a standard solution from that in nickel-base alloys. Hence, the optimum temperature for both charring and atomization steps could be found. Figs. 3 and 4 show the influence of charring and atomization temperatures on the integrated absorbances of Te in various solutions of standard Te, IN100 and Tracelloy C. Tellurium atoms in the standard solution were stable only up to 500 °C; the dramatic decrease in the AAS signals at higher temperatures was due to the expulsion of Te from the ends of the graphite tube or the injection hole. In contrast, Te atoms in the alloys were stable up to 1000 °C. This indicated that the maximum permissible charring temperature had been increased from 500 to 1000 °C as a result of thermal stabilization of Te, which formed intermetallic compounds on the platform during the charring step. In addition, the nickel modifier brought about a 100 °C decrease in the atomization temperature.

Palladium is also an effective chemical modifier in the determination of Te by ETAAS.[33,44] With the addition of Pd, Te could be converted into a more thermally stable species. The mechanisms involved in thermal stabilization by chemical modifiers can be divided into two different concepts. One is the formation of solid solutions between the analyte and the modifier and/or the atoms (ions) of the analyte replace atoms (ions) in the crystal lattice of the modifier by isomorphous substitution. The other is the less complicated formation of chemical compounds that have defined properties and structure between the analyte and the modifier.[45] Different

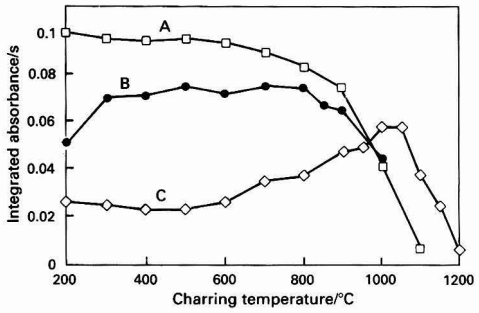

Fig. 1 Absorbance of Tl as a function of charring temperature at an atomization temperature of 1500 °C. A, 0.40 ng Tl standard; B, 0.2088 mg IN100; and C, 1.6476 mg Tracealloy C

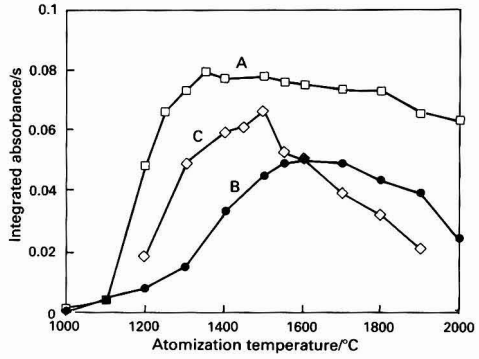

Fig. 2 Absorbance of Tl as a function of atomization temperature at different charring temperatures. A, 0.4 ng Tl standard at 600 °C; B, 0.2088 mg IN100 at 800 °C; and C, 1.6476 mg Tracealloy C at 1100 °C

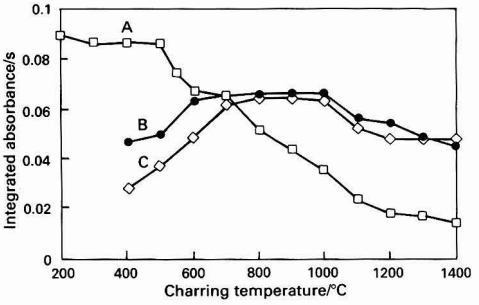

Fig. 3 Absorbance of Te as a function of charring temperature at an atomization temperature of 1650 °C. A, 1.0 ng Te standard; B, 36.0 μg IN100; and C, 45.7 μg Tracealloy C

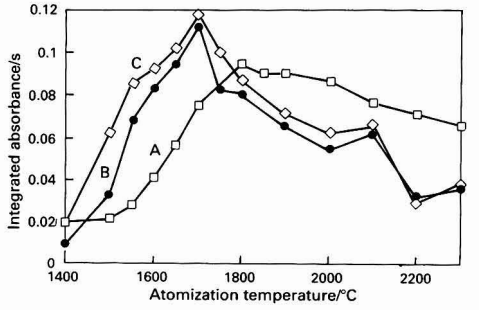

Fig. 4 Absorbance of Te as a function of atomization temperature at different charring temperatures. A, 1.0 ng Te standard at 500 °C; B, 36.0 μg IN100 at 750 °C; and C, 45.7 μg Tracealloy C at 750 °C

chemical modifiers lead to different results. An example is the work reported by Volynsky *et al.*[44] The reduction temperature of Ga_2O_3 and PbO with graphite was decreased by $PdCl_2$ whereas only the reduction temperature of Ga_2O_3 was decreased by $NiCl_2$.

Although a nickel modifier had been shown to be effective in raising the charring temperature of Te, it was of interest to establish whether there would be further a improvement with the Pd modifier. Consequently, the charring temperature was increased to 1250 °C as shown in Fig. 5. However, there was a slight increase in the peak area, by 1.7 and 3.3% for IN100 and Tracealloy C, respectively, when the atomization temperature was increased from 1700 to 1800 °C. The atomization plots are shown in Fig. 6.

Fig. 7 shows the effect of Pd on the AAS signals. The AAS signals for Te in IN100 reached a maximum when 2 μg of Pd were added. Although only 0.2 μg of Pd was required for Tracealloy C to obtain the maximum absorbance, there was a slight fluctuation in the AAS signals. In order to ensure that sufficient Pd modifier was present, an amount of 5 μg of Pd was used for each measurement.

Interference Studies

In order to understand the effects of HNO_3, HCl, HF, ammonia solution and various metal ions on the determination of Tl and Te, a number of standard solutions spiked with different foreign ions were measured by ETAAS. The relative absorbance, defined as

$$\text{Relative absorbance} = \frac{\text{absorbance of 200 pg Tl + foreign ions}}{\text{absorbance of 200 pg Tl}}$$

was monitored. For Te, an amount of 500 pg was determined instead of 200 pg.

Fig. 8 shows the variation in the relative absorbances of Tl as a function of the concentration of the acids and ammonia solution (0.020–4.60 mol l^{-1}). As $TlNO_3$, which was decomposed at 450 °C, could be converted into the more stable oxide,[41] no losses were observed with the addition of HNO_3. This was consistent with the observation reported by Fuller.[17] The very large depression of the Tl signals in the presence of HF and HCl was due to the formation of relatively volatile thallium halides.[9] Ammonia solution caused less than a 10% variation in the relative absorbances even though the concentration was increased from 0.026 to 2.60 mol l^{-1}.

Potential interfering metal ions, which included Ni, V, Mo, Nb, Ta, Fe, Cu, Co, Al, Cr, Ti, Ga, In, Zr, Hf and Pb, were studied. The relative absorbances were monitored with various concentrations of foreign ions up to 800 ppm (Table 4). Nickel and Ga caused an enhancement of the AAS signals. The relative absorbance increased from 1.20 to 2.10 as the concentration of Ni increased from 25 to 800 ppm whereas Fe gave about 20% enhancement of the Tl signal. Gallium enhanced the Tl signal to a smaller extent; the relative absorbance increased only from 1.51 to 1.72 in the same range of Ga concentration. Cobalt, Al, Zr and Hf caused severe inhibition of the Tl signals whereas Ti had no detectable effect. However, HCl in the metal ion solutions also caused some inhibition on the Tl signals. The interference thus observed could represent contributions from both acids and metal ions. By comparing the interference thus observed in Table 4 with the corresponding net effect of acids in Fig. 8, it could be concluded that Hf had a negligible effect on the Tl signals whereas Zr and Al caused serious depression of the Tl signal.

The relative absorbance increased linearly with the concentration of In at first. It then flattened to a plateau when the concentration exceeded 300 ppm. Chromium gave about a 30% enhancement of the relative absorbance in the concentration range 25–800 ppm whereas Pb caused about a 30% decrease in the same range. Tantalum caused a negligible effect up to 100 ppm. However, the Tl signal decreased rapidly at higher concentrations of Ta. Vanadium, Nb and Cu also inhibited the Tl signal to different extents. Molybdenum had a negligible effect on the signal for Tl.

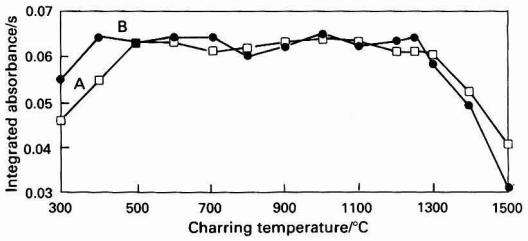

Fig. 5 Charring profiles of Te in nickel-base alloys with Pd modifier at an atomization temperature of 1700 °C. A, 36.0 μg IN100 + 5.0 μg Pd; and B, 43.2 μg Tracealloy C + 5.0 μg Pd

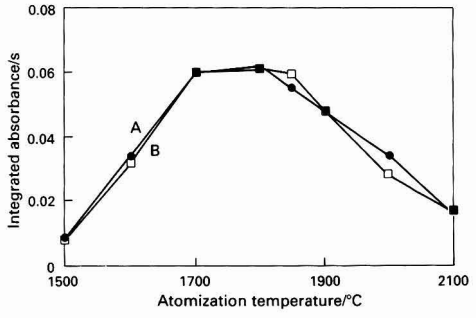

Fig. 6 Atomization profiles of Te in nickel-base alloys with Pd modifier at a charring temperature of 1250 °C. A, 36.0 μg IN100 + 5.0 μg Pd; and B, 43.2 μg Tracealloy C + 5.0 μg Pd

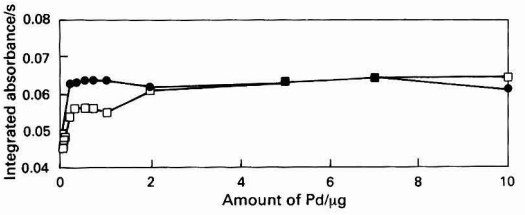

Fig. 7 Affect of Pd on the AAS signal for Te. A, 54.4 μg IN100; and B, 80.8 μg

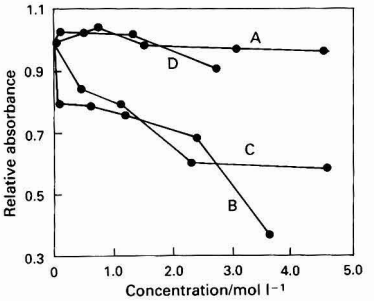

Fig. 8 Effect of ammonia solution and various acids on the signal for Tl (n = 5). A, HNO_3; B, HCl; C, HF; and D, NH_3

Table 4 Effects of various metal ions on the relative absorbances of Tl

Ion	Compound added	Concentration (ppm)	Relative absorbance*	Integrated absorbance†
Ni	$Ni(NO_3)_2$	25	1.20	
		50	1.19	
		100	1.28	
		300	1.39	
		500	2.10	
		800	2.10	0.004
Co	$Co(NO_3)_2$	25	1.02	
		50	0.94	
		100	0.66	
		300	0.32	
		500	0.19	
		800	0.08	0.005
Al	Al in 1% v/v HCl	25	1.14	
		50	1.17	
		100	1.17	
		300	1.09	
		500	0.99	
		600	0.84	
		800	0.59	0.004
Cr	$K_2Cr_2O_7$	25	1.20	
		50	1.27	
		100	1.27	
		300	1.38	
		400	1.40	
		500	1.36	
		600	1.38	
		700	1.41	
		800	1.33	0.010
Ti	$TiCl_4$	25	0.96	
		50	0.97	
		100	1.02	
		300	1.00	
		500	1.02	
		800	1.00	0.035
V	V in HNO_3	25	0.27	
		50	0.26	
		100	0.28	
		300	0.27	
		500	0.25	
		800	0.25	0.012
Mo	Mo in H_2O	25	1.03	
		50	0.92	
		100	1.05	
		300	1.00	
		500	1.06	
		800	0.97	0.003
Nb	Nb in H_2O	25	0.73	
		50	0.70	
		100	0.36	
		300	0.22	
		500	0.22	
		800	0.23	0.003
Ta	Ta in trace Hf	25	1.10	
		50	1.11	
		100	0.99	
		300	0.75	
		500	0.65	
		800	0.42	0.002
Fe	$Fe(NO_3)_3$	25	1.18	
		50	1.17	
		100	1.18	
		300	1.18	
		500	1.19	
		800	1.16	0.005
Cu	$Cu(NO_3)_2$	25	0.99	
		50	0.79	
		100	0.51	
		300	0.38	
		500	0.31	
		800	0.24	0.002
Ga	$Ga(NO_3)_3$	25	1.51	
		50	1.54	
		100	1.79	
		300	1.79	
		500	1.71	
		600	1.71	
		700	1.78	
		800	1.72	0.002
In	$In(NO_3)_3$	25	1.02	
		50	1.23	
		100	1.32	
		300	1.43	
		500	1.43	
		800	1.43	−0.004
Zr	Zr in 5% m/m HCl	25	1.06	
		50	1.03	
		100	0.95	
		300	0.78	
		500	0.64	
		800	0.53	0.017
Hf	Hf in 10% m/m HCl	25	1.09	
		50	1.02	
		100	1.05	
		300	0.86	
		500	0.88	
		800	0.71	0.006
Pb	$Pb(NO_3)_2$	25	0.69	
		50	0.67	
		100	0.63	
		300	0.65	
		500	0.62	
		800	0.64	0.002

* The relative absorbances are averages of five determinations.

$$\text{Relative absorbance} = \frac{\text{absorbance of 200 pg Tl + foreign ions}}{\text{absorbance of 200 pg Tl}}$$

† Integrated absorbances were determined with only foreign ion in the graphite tube (duplicate determinations).

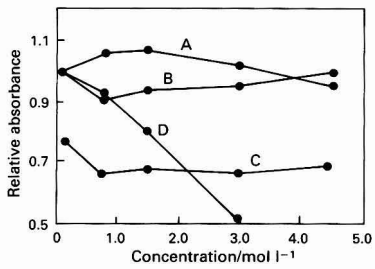

Fig. 9 Effects of ammonia solution and various acids on the absorbance signal for Te (n = 5). A, HNO_3; B, HCl; C, HF; and D, NH_3

Among these foreign ions, Cr, Ti, V and Zr showed some degree of overlapping of the absorbance spectrum with the emission spectrum of Tl. The peak areas measured with only foreign ions in the graphite tube are given in Table 4.

The results for Te are given in Fig. 9 and Table 5. Both HNO_3 and HCl had negligible effects on the relative absorbances (less than 10% deviation), even though the concentration was increased from 0.024 to 4.50 mol l^{-1}. Hydrofluoric acid caused about a 30% depression of the Te signals in the concentration range 0.046–6.90 mol l^{-1}. Ammonia solution gave a major depression of the Te signals; the relative absorbance was only 0.51 in the presence of 2.60 mol l^{-1} ammonia solution.

The effects of foreign ions on the Te signal were also investigated. The relative absorbances were monitored with

Table 5 Effects of various metal ions on the relative absorbances of Te

Ion	Compound added	Concentration (ppm)	Relative absorbance*	Integrated absorbance†
Ni	$Ni(NO_3)_2$	25	1.05	
		50	1.19	
		100	1.12	
		300	1.79	
		500	2.16	
		800	4.70	0.015
Co	$Co(NO_3)_2$	25	1.17	
		50	1.16	
		100	1.03	
		300	1.05	
		500	1.08	
		800	1.09	0.002
Al	Al in 1% v/v HCl	25	1.22	
		50	1.30	
		100	1.26	
		300	3.58	
		500	3.55	
		800	5.76	0.256
Cr	$K_2Cr_2O_7$	25	1.17	
		50	1.15	
		100	1.18	
		300	1.18	
		500	1.16	
		600	1.20	
		700	1.24	
		800	1.23	0.001
Ti	$TiCl_4$	25	1.09	
		50	1.09	
		100	0.87	
		300	0.94	
		500	0.87	
		800	0.90	0.022
V	V in HNO_3	25	0.53	
		50	0.55	
		100	0.54	
		300	0.54	
		500	0.55	
		800	0.57	0.086
Mo	Mo in H_2O	25	0.77	
		50	0.74	
		100	0.81	
		300	0.90	
		500	0.83	
		800	0.86	0.012
Nb	Nb in H_2O	25	1.04	
		50	1.03	
		100	0.90	
		300	0.89	
		500	0.87	
		800	0.89	0.270
Ta	Ta in trace Hf	25	0.71	
		50	0.69	
		100	0.69	
		300	0.70	
		500	0.73	
		800	0.73	0.179
Fe	$Fe(NO_3)_3$	25	0.70	
		50	0.71	
		100	0.75	
		300	0.97	
		500	1.12	
		800	1.29	0.137
Cu	$Cu(NO_3)_2$	25	0.55	
		50	0.57	
		100	0.55	
		300	0.56	
		500	0.57	
		800	0.56	0.208
Zr	Zr in 5% m/m HCl	25	1.02	
		50	1.05	
		100	1.05	
		300	1.07	
		500	1.19	
		600	1.21	
		700	1.26	
		800	1.22	0.168
Hf	Hf in 10% m/m HCl	25	1.21	
		50	1.25	
		100	1.30	
		300	1.40	
		500	1.40	
		800	1.41	0.025
Pb	$Pb(NO_3)_2$	25	0.80	
		50	0.80	
		100	0.81	
		300	0.73	
		500	0.76	
		600	0.71	
		700	0.71	
		800	0.75	0.015
Se	H_2SeO_3 in 2% HNO_3	25	0.93	
		50	0.96	
		100	0.98	
		300	1.02	
		500	0.99	
		800	1.02	0.007

* The relative absorbances are averages of five determinations.

$$\text{Relative absorbance} = \frac{\text{absorbance of 500 pg Te + foreign ions}}{\text{absorbance of 500 pg Te}}$$

† Integrated absorbances were determined with only foreign ion in the graphite tube (duplicate determinations).

various concentrations of foreign ions up to 800 ppm. Table 5 summarizes the effects of metal concentrations on the relative absorbances. Nickel and Al enhanced the absorbance signals of Te. The relative absorbance increased from 1.05 to 2.16 as the concentration of Ni increased from 25 to 500 ppm. Further addition of Ni would increase both the Te signals and the background signals. With 800 ppm of Ni, the relative absorbance was 4.70 whereas the corresponding background was 1.30. The relative absorbance increased from 1.22 to 5.76 in the same range of Al concentrations. However, an extremely high background absorbance with a value of 1.49 appeared when 800 ppm of Al were added. The relative absorbance increased gradually from 1.21 to 1.41 on addition of 25–800 ppm of Hf. Chromium gave about a 20% enhancement of the relative absorbance in the concentration range of 25–800 ppm and Zr gave a similar level of enhancement in the same concentration range. The effect of Se was negligible.

Although there was a small degree of fluctuation in the relative absorbance in the presence of Co and Cr, these metal ions caused only about a 10% deviation in the relative absorbance. The effect of Pb was a 20–30% suppression of the Te signal in the concentration range 25–800 ppm. The addition of V, Nb, Ta, Fe, Cu and Mo also resulted in decreases in the Te signal.

Peak areas (summarized in Table 5) measured with only foreign ions in the graphite tube showed that the Te emission spectrum overlapped with most of the absorbance spectra of foreign ions except those for Co, Cr and Se.

Quantitative Analysis

The CRMs of nickel-base alloys were analysed to validate the accuracy of the proposed procedure. The solid sample of IN100 or Tracealloy C was decomposed with a mixture of HNO_3 and HCl. A precipitate containing trace amounts of Tl was formed in ammonia solution. Thallium was then determined by ETAAS with the stabilized temperature platform furnace. Tellurium was determined directly with ETAAS.

Table 6 Analytical parameters and results of Tl determinations

Calibration graph—

Tl (ng) = K × absorbance + B

Linear range/ng	K	B	R^2
0.060–0.500	2.3853	0.0027	0.9995

Analytical results—*

	IN100	Tracealloy C
Certified value/μg g^{-1}	2†	0.252 ± 0.003
Determined value/μg g^{-1}	1.94 ± 0.09	0.251 ± 0.005
Recovery (%)‡	99.8 ± 4.0	101.8 ± 2.9
Detection limit/pg	15	15

* Results of five determinations.

† This value was not certified but given for information only.

‡ The amount of standard Tl added ranged from 0.06 to 0.60 ng.

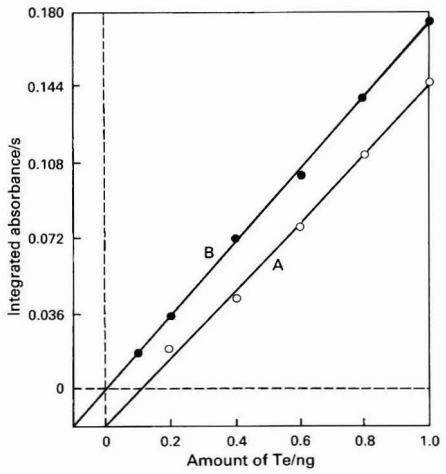

Fig. 10 Calibration graph for Te determinations. A, Established with standard Te solutions; and B, established with standard Te solutions + 0.005 mg Ni

For Tl determinations, a calibration graph with a linear range from 0.060 to 0.50 ng was established [Tl (ng) = K × absorbance + B; K = 2.3853, B = 0.0027, correlation coefficient = 0.9995]. There was good agreement between the certified values and the results obtained, as indicated in Table 6. The results found for IN100 and Tracealloy C were 1.94 ± 0.09 μg g^{-1} (s_r = 5%) and 0.251 ± 0.005 μg g^{-1} (s_r = 2%), which represent 3 and 0.4% differences from the reference value of 2 μg g^{-1} and the certified value of 0.252 ± 0.003 μg g^{-1}, respectively. By adding various amounts of standard Tl to sample solutions (0.06–0.60 ng), the results gave recoveries of 100 ± 4 and 102 ± 3% for IN100 and Tracealloy C, respectively. The detection limit, defined as 3s (s = standard deviation of 12 consecutive measurements), was 15 pg g^{-1}.

The certified values for Te in IN100 and Tracealloy C are 9 ± 1 and 5.9 ± 0.6 ppm, respectively. The need to use Ni to stabilize the volatile Te is again verified in Fig. 10, which shows the calibration graphs for standard Te solutions obtained with and without Ni modifier. The linear range is up to 4 ng of Te. The calibration graph curves towards the concentration axis at higher concentrations. A compilation of the results is given in Table 7.

The determined values obtained from the calibration graph, with a linear range from 0.100 to 1.00 ng [Te (ng) = K × absorbance + B; K = 5.7251, B = 0.0004, correlation coefficient = 0.9993], for IN100 and Tracealloy C were 9.03 ± 0.09 and 5.93 ± 0.26 μg g^{-1}, respectively. The results obtained in this work were in close agreement with the certified values. By adding various amounts of standard Te to sample solutions (0.10–0.60 ng), the results gave recoveries of 98 ± 4 and 97 ± 4% for IN100 and Tracealloy C, respectively. The detection limit was 35 pg g^{-1}.

Table 7 Analytical parameters and results of Te determinations

Calibration graph—*

Te (ng) = K × absorbance + B

Linear range/ng	K	B	R^2
0.100–1.00	5.7251	0.0004	0.9993

Analytical results—

	IN100	Tracealloy C
Certified value/μg g^{-1}	9 ± 1	5.9 ± 0.6
(1) with Ni/μg g^{-1} (n = 5)†	9.03 ± 0.09	5.93 ± 0.26
s_r (%)	1	4
Detection limit/pg g^{-1}	35	35
Recovery (%)‡	98 ± 4	97 ± 4
(2) with Ni and Pd/μg g^{-1} (n = 5)	9.04 ± 0.31	5.78 ± 0.20
Detection limit/pg	18	18
Recovery (%)	92 ± 5	91 ± 3
(3) With the standard additions method/μg g^{-1} (n = 3)	12.4 ± 1.9	11.9 ± 1.6

* Calibration graph established with standard Te solutions + 0.005 mg of Ni.

† n = Total number of determinations.

‡ The amount of standard Te added ranged from 0.10 to 0.60 ng.

Although the addition of Pd modifier resulted in a higher charring temperature, the quantitative results did not improve. As shown in Table 7, an absolute error of −0.12 μg g^{-1} for Tracealloy C was obtained. The recoveries for the nickel-base alloys were 92 ± 5 and 91 ± 3%, which were worse than those obtained without the addition of Pd modifier. Although the addition of Pd modifier gave a better detection limit (18 pg g^{-1}), it led to worse results in terms of accuracy, precision and recovery. The Te contents determined by the standard additions method were 12.4 ± 1.9 and 11.9 ± 1.6 μg g^{-1} for IN100 and Tracealloy C, respectively. Apparently, the standard additions gave poor precision and accuracy.

Conclusions

Pre-treatment with ammonia solution effectively eliminated background signals in the determination of trace amounts of Tl in nickel-base alloys by ETAAS. For Te determination, Ni worked effectively as a chemical modifier. After the solid sample of IN100 or Tracealloy C had been decomposed with a mixture of HNO_3 and HCl, the Tl present in the nickel-base alloys was coprecipitated with ammonia solution. The resulting precipitates were dissolved and analysed by ETAAS. Trace amounts of Te were determined directly without ammonia pre-treatment. The calibration graphs for the determination of Tl and Te were obtained using aliquots of HNO_3-diluted metal stock solutions; however, Ni was added to the Te standard solution. This indicated that the matrix matching of samples to calibration standards was not necessary with the ammonia solution pre-treatment. The proposed method provided precise and accurate determinations of trace amounts of Tl and Te in a nickel-base alloys with relatively low detection limits of 15 and 35 pg g^{-1}, respectively. Although the addition of Pd modifier gave a better detection limit (18 pg g^{-1}) for Te, it resulted in poor accuracy, precision and recovery.

The financial support of this work by a grant from the National Science Council of the Republic of China is gratefully acknowledged.

References

1 Andrews, D. G., and Headridge, J. B., *Analyst*, 1977, **102**, 436.
2 Bäckman, S., and Karlsson, R. W., *Analyst*, 1979, **104**, 1017.
3 Headridge, J. B., and Nicholson, R. A., *Analyst*, 1982, **107**, 1200.
4 Ford, D. A., *Met. Technol.*, 1984, **11**, 438.
5 Lowe, D. S., *Analyst*, 1985, **110**, 583.
6 Welcher, G. G., Kriege, O. H., and Marks, J. Y., *Anal. Chem.*, 1974, **46**, 1227.
7 Forrester, J. E., Lehecka, V., Johnston, J. R., and Ott, W. L., *At. Absorpt. Newsl.*, 1979, **18**, 73.
8 Dulski, T. R., and Bixler, R. R., *Anal. Chim. Acta*, 1977, **91**, 199.
9 Griepink, B., Sager, M., and Tolg, G., *Pure Appl. Chem.*, 1988, **60**, 1425.
10 Labuda, J., and Vanickova, M., *Anal. Chim. Acta*, 1988, **208**, 219.
11 Murti, S. S., Sambasiva Rao, I. V., and Rajan, S. C. S., *Talanta*, 1989, **36**, 601.
12 Hafez, M. A. E., Abdallah, A. M. A., and Wahdan, T. M. A. E., *Analyst*, 1991, **116**, 663.
13 Henke, G., *Fresenius' J. Anal. Chem.*, 1991, **339**, 245.
14 Waidmann, E., Stoeppler, M., and Heininger, P., *Analyst*, 1992, **117**, 295.
15 Flanjak, J., and Hodda, A. E., *Anal. Chim. Acta*, 1988, **207**, 283.
16 Koirytohann, S. R., Glass, E. D., and Lichte, F. E., *Appl. Spectrosc.*, 1981, **35**, 22.
17 Fuller, C. W., *Anal. Chim. Acta*, 1976, **81**, 199.
18 Slavin, W., Carnrick, G. R., and Manning, D. C., *Anal. Chim. Acta*, 1982, **138**, 103.
19 Shan, X., Ni, Z., and Zhang, L., *Talanta*, 1984, **31**, 150.
20 Manning, D. C., and Slavin, W., *Spectrochim. Acta, Part B*, 1988, **43**, 1157.
21 Slavin, W., and Manning, D. C., *Spectrochim. Acta, Part B*, 1980, **35**, 701.
22 Ueda, J., and Kitadani, T., *Analyst*, 1988, **113**, 581.
23 Niskavaara, H., and Kontas, E., *Anal. Chim. Acta*, 1990, **231**, 273.
24 Nakashima, S., Sturgeon, R. E., Willie, S. N., and Berman, S. S., *Anal. Chim. Acta*, 1988, **207**, 291.
25 Fox, G. J., *At. Spectrosc.*, 1990, **11**, 13.
26 Beaty, R. D., *At. Absorpt. Newsl.*, 1974, **13**, 38.
27 Sighinolfi, G. P., Santos, A. M., and Martinelli, G., *Talanta*, 1979, **26**, 143.
28 Chiou, K. Y., and Manuel, O. K., *Anal. Chem.*, 1984, **56**, 2721.
29 Muangnoicharoen, S., Chiou, K.-Y., and Manuel, O. K., *Talanta*, 1988, **35**, 679.
30 Kunselman, G. C., and Huff, E. A., *At. Absorpt. Newsl.*, 1976, **15**, 29.
31 Ediger, R. D., *At. Absorpt. Newsl.*, 1975, **14**, 127.
32 Donaldson, E. M., and Leaver, M. E., *Talanta*, 1990, **37**, 173.
33 Zhang, L., Ni, Z.-M., and Shan, X.-Q., *Spectrochim. Acta, Part B*, 1989, **44**, 751.
34 Bedrossian, M., *Anal. Chem.*, 1984, **56**, 311.
35 Hubert, A. E., and Chao, T. T., *Talanta*, 1985, **32**, 568.
36 Greenland, L. P., and Campbell, E. Y., *Anal. Chim. Acta*, 1976, **87**, 323.
37 Wickstrom, T., and Lund, W., and Bye, R., *Anal. Chim. Acta*, 1988, **208**, 347.
38 Corbett, J. A., and Godbeer, W. C., *Anal. Chim. Acta*, 1977, **91**, 211.
39 Ferri, T., Morabito, R., Petronio, B. M., and Pitti, E., *Talanta*, 1989, **36**, 1259.
40 Trivedi, B. V., and Thakkar, N. V., *Talanta*, 1989, **36**, 786.
41 Leloux, M. S., Lich, N. P., and Claude, J. R., *At. Spectrosc.*, 1987, **8**, 71.
42 Welz, B., Schlemmer, G., and Mudakavi, J. R., *Anal. Chem.*, 1988, **60**, 2567.
43 Hamid, H. A., Al Joboury, M. I., and Mohammed, A. K., *Anal. Chim. Acta*, 1991, **243**, 239.
44 Volynsky, A., Tikhomirov, S., and Elagin, A., *Analyst*, 1991, **116**, 145.
45 Mandjukov, P. B., Vassileva, E. T., and Simeonov, V. D., *Anal. Chem.*, 1992, **64**, 2596.

Paper 3/00783I
Received February 9, 1993
Accepted April 19, 1993

Determination of Citric Acid and Oxalacetic Acid in Foods by Enzymic Flow Injection

Milagros Plantá, Fernando Lázaro, Rosa Puchades and Angel Maquieira*
Department of Chemistry, Polytechnic University of Valencia, 46071 Valencia, Spain

A reversed-flow injection method for the determination of citric acid in foods is proposed. Two enzymes, citrate lyase and malate dehydrogenase (MDH), are used, the latter being immobilized. This method, based on the decrease in the absorbance of reduced nicotinamide adenine dinucleotide, has a linear range between 1 and 20 mg dm^{-3}, with a relative standard deviation (RSD) of 2.2%, an average recovery of 100.9% and a sampling frequency of 20 h^{-1}. Additionally, a flow injection method for the determination of oxalacetic acid in fruit juices using immobilized MDH is also proposed. The features of the method are as follows: linear range of the calibration graph 1–40 mg dm^{-3}, RSD 1.4%, average recovery 96.8% and sampling frequency 40 h^{-1}.

Keywords: *Citric acid; oxalacetic acid; enzymic flow injection; food*

Citric and oxalacetic acids are essential components in all living beings. They directly take part in the production of energy through the tricarboxylic acid cycle, as well as in several processes associated with the metabolism of fatty acids, carbohydrates and certain amino acids.[1]

Citric acid is widespread within the plant kingdom and is often predominant in the total carboxylic acid content. Therefore, it is a commonly used parameter in the analysis of plants and their derivatives. Furthermore, owing to its innocuity it is often used as an antibacterial substance and as an additive for the control of pH.[2]

Several methods have been proposed for the determination of citric acid, such as that based on oxidation with $KMnO_4$,[3] conductimetric methods[4] or spectrophotometric methods based on general reactions with carboxylic acids.[5,6] Two of these methods have involved flow injection (FI) techniques.[4,6] However, when a high specificity is required, these methods cannot be applied, as citric acid often occurs together with many organic acids. Therefore, chromatographic[7] or enzymic[8] methods are used in these instances, but these methods are time consuming .

On the other hand, oxalacetic acid is not commonly determined as it occurs at low concentrations. In the literature, only generic methods for α-ketoacids,[5] chromatographic methods[7] and bioluminescence FI methods[9,10] have been found.

The aim of this work was to establish methods for the determination of both acids in foods by using immobilized enzymes with three purposes: (*a*) to provide this enzymic determination with the advantages of FI;[11] (*b*) to minimize enzyme consumption during the analysis by means of its immobilization; and (*c*) to simplify the proposed method,[8] reducing the number of enzymes used.

The classical enzymic method[8] for the determination of citrate makes use of citrate lyase (CL), lactate dehydrogenase (LDH) and malate dehydrogenase (MDH), the consumed reduced nicotinamide adenine dinucleotide (NADH) being monitored spectrophotometrically at 340 nm. It is based on the following reactions:

$$\text{Citrate} \overset{\text{CL}}{\rightleftharpoons} \text{oxalacetate} + \text{acetate} \quad (1)$$

$$\text{Oxalacetate} \overset{\text{OD}}{\rightarrow} \text{pyruvate} + CO_2 \quad (2)$$

$$\text{Pyruvate} + \text{NADH} + H^+ \overset{\text{LDH}}{\rightarrow} \text{L-lactate} + NAD^+ \quad (3)$$

It admits the existence of oxalacetate decarboxylase (OD) together with the enzyme CL. In order to ensure that all oxalacetate reacts (despite the low amount of OD present), MDH is added:

$$\text{Oxalacetate} + \text{NADH} + H^+ \overset{\text{MDH}}{\rightarrow} \text{L-malate} + NAD^+ \quad (4)$$

The method consists of two steps:

(*i*) A mixture of LDH, MDH, NADH and buffer is added to the sample to remove all oxalacetate and pyruvate present. Reactions (3) and (4) take place. It lasts 5 min.

(*ii*) Citrate lyase, with a certain amount of OD, is added, so that the citrate formed reacts according to reactions (1)–(4), giving rise to a decrease in the absorbance of NADH (analytical signal).

Afterwards, a blank assay is carried out to measure the possible decrease in absorbance occurring due to the degradation of the NADH during the long time of analysis (10–15 min).

The proposed method for citrate determination is based on reactions (1) and (4) and avoids the use of OD and LDH for two reasons: (*a*) according to the manufacturers, the commercial product of CL contains some specified impurities, but not OD; (*b*) in the FI technique, the reactions involved are not usually required to proceed to completion.[11] As long as sufficient reaction occurs to achieve the desired sensitivity, any additional reactions resulting from impure reagents, *e.g.*, OD in the CL, will be constant and accounted for by the standard calibration.

The proposed method for oxalacetate determination is exclusively based on reaction (4), the decrease in the absorbance of NADH being controlled at 340 nm.

This reaction catalysed by MDH has already been studied, though in the opposite direction (malate → oxalacetate) to that for the determination of malic acid;[12] hence, a more exhaustive study has been carried out.

Experimental

Apparatus

A four-channel Gilson Minipuls-3 peristaltic pump (Gilson, Villiers, France), a variable-volume Rheodyne 5041 injection valve (Rheodyne, Cotati, CA, USA), a Rheodyne 5302 diversion valve, a laboratory-made poly(methyl methacrylate) mixing point, a Hellma 178.712QS flow cell (Hellma, Jamaica, NY, USA), with an inner volume of 18 mm^3 and a Philips PU-8625 spectrophotometer (Philips Analytical, Cambridge, UK), connected to a Perkin-Elmer 56 recorder (Perkin-Elmer, Analytical Instruments, Norwalk, CT, USA), were

* To whom correspondence should be addressed.

used in the determinations. Poly(vinyl chloride) pump tubing of different diameters, suited to the required flow rate, and poly(tetrafluoroethylene) coils of 0.5 mm i.d., were also used.

Reagents

Malate dehydrogenase (E.C.1.1.1.37), approximately 1200 U mg^{-1} protein (1 U = 16.67 nkat), CL (E.C.4.1.3.6), approximately 8 U mg^{-1} protein, and NADH were supplied by Boehringer Mannheim, Mannheim, Germany.

Controlled-pore glass (CPG 0240, 80/120 mesh, 240 Å mean pore diameter) (Sigma, St. Louis, MO, USA), 3-(aminopropyl)triethoxysilane (Sigma), protected from moisture and stored at 4 °C, and 25% glutaraldehyde (Sigma) were used to immobilize MDH and CL.

Standard solutions of citric and oxalacetic acids were prepared from citric acid monohydrate, analytical-reagent grade (Merck, Darmstadt, Germany), and oxalacetic acid, approximately 98% (Sigma), respectively. The oxalacetic acid solution was prepared weekly, owing to its instability.

For the determination of oxalacetic acid, a stock buffer solution of 0.5 mol dm^3 KH_2PO_4 (Merck), adjusted to pH 7.8 with KOH (Merck), was prepared, and further diluted 1 + 5 to obtain the buffer solution B (Fig. 1). The same concentration of buffer must be included in the reagent solution, R (260 mg dm^{-3} NADH) and the sample solution, S, in order to avoid problems in the analytical signal resulting from differences in the refractive index.

For the determination of citric acid, a stock buffer solution of 0.5 mol dm^{-3} glycylglycine (Boehringer Mannheim) was prepared, the pH being adjusted to 7.8 with KOH and further diluted 1 + 5 to obtain the buffer solution, B′ (Fig. 2). The sample solution, S′, and the reagent solution, R′ [0.67 U cm^{-3} CL–0.5 mmol dm^{-3} $ZnCl_2$ (Merck)–0.51 g dm^{-3} NADH] must have the same concentration of buffer as in buffer solution, B′.

Configurations and Procedures

The determination of oxalacetic acid was performed with the manifold shown in Fig. 1. It is based on the insertion of a sample volume, V, into a carrier stream, B, which then merges with the reagent solution, R. As the sample plug passes through the immobilized MDH reactor the enzyme catalyses the above described reaction (4), giving rise to an FI peak on passage of the reacting plug through the detector. This peak is negative, as it corresponds to a decrease in the absorbance of the baseline.

In food analysis it is necessary to carry out a blank assay for each sample, by changing the reagent solution R (which contains NADH) for the buffer solution B, in order to eliminate the matrix influence on the analytical signal.

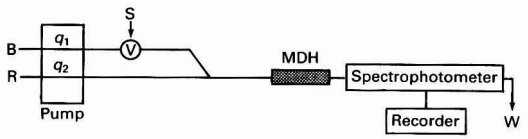

Fig. 1 Configuration for oxalacetic acid determination. B, Buffer; R, reagent; S, sample, V, injection valve; and W, waste. The values for the flow rates (q_1, q_2) and the size of the MDH reactor are shown in Table 1

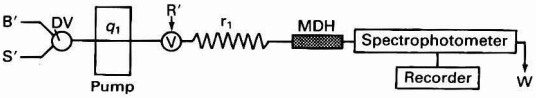

Fig. 2 Configuration for citric acid determination. B′, Buffer; R′, reagent; S′, sample; V, injection valve; DV; deviation valve; and W, waste. The values for the flow rate (q_1) and the sizes of the tubing reactor (r_1) and the MDH reactor are shown in Table 1

For the determination of citric acid, the manifold depicted in Fig. 2 was used. The reagent solution, R′, which contains CL, can be injected into a stream of sample solution, S′, or into a buffer solution, B′ (which is used as the carrier stream), by using the diversion valve (DV, reverse FI configuration). When the carrier is the buffer solution B′, the signal obtained corresponds to the absorbance (A_0) of NADH injected with the reagent solution plug, which has not reacted. On the other hand, when the carrier is the sample solution, S′, the signal obtained corresponds to the absorbance (A_1) of unconsumed NADH after the reactions (1) and (4) have been accomplished (in the r_1 and MDH reactor, respectively). The analytical signal (proportional to the concentration of citric acid) will be derived from the decrease in the absorbance ($A_0 - A_1$).

In food analysis it is not necessary to carry out a blank assay because the baseline coincides with the absorbance of the matrix.

Sample Pre-treatment

Liquid samples only require filtration and suitable dilution, but solid samples require a prior extraction step with distilled water.

Immobilization of Enzymes

The glass, after cleaning with 30% m/m HNO_3, was alkylaminated with 3-(aminopropyl)triethoxysilane and the cross-linking agent (glutaraldehyde) coupled as described by Masoom and Townshend.[13] Immobilization was performed by the following procedure: MDH, 80 mg (5600 U), or CL, 150 mg (60 U), was dissolved in 2.0 cm^3 of cold (4 °C) deoxygenated phosphate buffer (0.1 mol dm^{-3}, pH 6.0) and added to 300 mg of activated glass. This solution was kept at 4 °C overnight in a nitrogen atmosphere, then the glass was packed in a laboratory-made glass reactor [1.5 mm i.d. and the required length (200 cm)] and washed with cold phosphate buffer solution to remove unlinked enzyme.

Results and Discussion

Immobilization of Enzymes

The concentration of immobilized protein was above 99% for MDH, whereas with CL only 60% was achieved. The reactor of immobilized MDH could be used daily for at least 3 months without a noticeable loss of activity, if stored at 4 °C and in phosphate buffer solution after use. The CL reactor was found to be very unstable and, according to Fig. 3, its activity decreased exponentially with time in such a way that the initial value was reduced to 50% after 60 min and to 70% after 180 min. Hence, the CL reactor was not useful from the analytical point of view, and it was necessary to use the CL enzyme in solution.

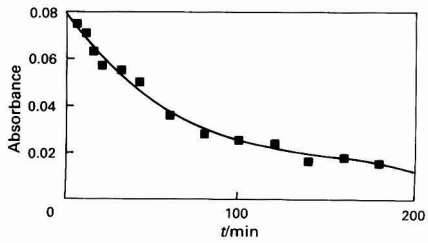

Fig. 3 Loss of activity of immobilized CL reactor *versus* time

Determination of Oxalacetic Acid

The optimization of the chemical and FI variables affecting the system was performed by a univariate method; the values taken as optimum are listed in Table 1.

A study of the pH of the phosphate buffer showed a constant analytical signal in the range 6.4–8.1, above which it significantly decreased (Fig. 4).

As regards the buffer concentration, it did not exert any influence on the analytical signal in the range studied (0.005–0.45 mol dm^{-3}). However, the concentration of NADH was very important, as the absorbance increased up to a value of 260 mg dm^{-3}, after which it remained constant.

Flow rate ($q_1 = q_2$) had no influence on the analytical signal over the range 0.25–1.00 cm^3 min^{-1}. Lower values gave rise to higher analytical signals, at the cost of an excessive time of analysis.

The analytical signal increased with increasing injected volume, although this meant a higher sample consumption and reaction time. A volume of 130 mm^3 was chosen as a compromise.

The analytical signal increased with MDH reactor lengths up to 6.0 cm, after which the signal remained constant.

Table 1 Optimum values of the variables

Variable	Oxalacetic acid*	Citric acid†
[NADH]/mg dm^{-3}	260	510
[KH_2PO_4]/mol dm^{-3}	0.1	—
[Glycylglycine]/mol dm^{-3}	—	0.1
[CL]/U cm^{-3}	—	0.67
[$ZnCl_2$]/mmol dm^{-3}	—	0.5
Buffer pH	7.8	7.8
q_1/cm^3 min^{-1}	0.50	0.28
q_2/cm^3 min^{-1}	0.50	—
r_1/cm	—	200
MDH reactor/cm	6‡	6‡
Sample volume/mm^3	130	70

* See Fig. 1.
† See Fig. 2.
‡ 1.5 mm i.d.

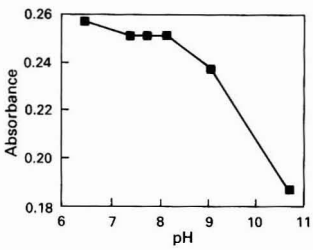

Fig. 4 Influence of pH on the analytical signal in the determination of oxalacetic acid

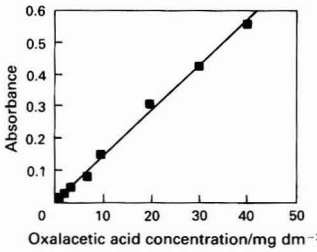

Fig. 5 Calibration graph for determination of oxalacetic acid

Under these working conditions, the calibration graph (Fig. 5) between 1.0 and 40.0 mg dm^{-3} of oxalacetic acid was a straight line given by absorbance decrease = 0.0043 + 0.01419 [oxalacetic acid]; correlation coefficient (r^2) = 0.9986. The relative standard deviation (RSD) was 1.4% for 12 determinations of 15.5 mg dm^{-3} oxalacetic acid. The sampling frequency was 40 h^{-1}.

This method was applied to the determination of oxalacetic acid in several types of fruit juice. The results obtained are presented in Table 2.

The recovery was studied by adding two different amounts (10.0 and 20.0 mg dm^{-3}) of oxalacetic acid to the same pre-treated fruit juices to obtain a mean recovery of 96.8% (range 91.8–103.9%).

Determination of Citric Acid

The initial purpose was to use immobilized CL and MDH for the determination of citric acid with these aims: (*a*) to save time and effort in the preparation of the reagents; (*b*) to re-use the same enzyme many times, thereby decreasing the cost per analysis; (*c*) to achieve a higher reproducibility in the results by always using the same concentration of enzyme; and (*d*) to simplify the FI configuration with the subsequent enhancement of sensitivity (lower dilution of the sample plug).[14]

However, owing to its low stability (Fig. 3), the CL reactor was not useful and it was necessary to use the CL in solution.

Although in FI systems it is common to inject the sample into a reagent stream, in this instance a reverse-FI configuration[15] has been used, as CL is rather expensive. In this configuration, the reagent (enzyme) is injected into the sample stream (Fig. 2).

The variables studied and the optimum values selected are summarized in Table 1. The influence of pH is small, a pH of 7.8 yielding the highest signal (Fig. 6). All buffers of this pH are not suitable, as Zn^{2+} existing in the reagent solution could precipitate with the PO_4^{3-} that occurs in many natural samples. Glycylglycine is used in order to overcome this problem.

Table 2 Study of recovery of added amounts of oxalacetic acid in spiked samples

Sample	Content of oxalacetic acid/ mg dm^{-3}	Amount added/ mg dm^{-3}	Amount recovered/ mg dm^{-3}	Recovery (%)
Apple 1	50.2	10.00	9.85	98.5
		20.00	18.54	92.7
Apple 2	2.3	10.00	10.35	103.5
		20.00	20.78	103.9
Pineapple	53.3	10.00	9.29	92.9
		20.00	18.36	91.8
Orange	100.2	10.00	9.56	95.6
		20.00	19.06	95.3

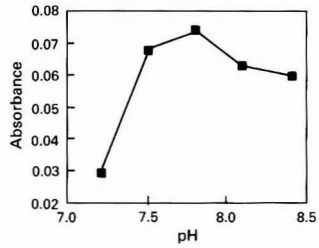

Fig. 6 Influence of pH on the analytical signal in the determination of citric acid

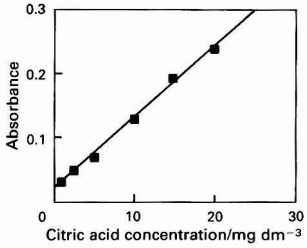

Fig. 7 Calibration graph for determination of citric acid

Table 3 Study of recovery of added amounts of citric acid in spiked samples

Sample	Content of citric acid	Amount added/ mg dm^{-3}	Amount recovered/ mg dm^{-3}	Recovery (%)
Chewing gum	1.23% m/m	5.00	5.13	102.6
		10.00	9.75	97.5
Caramel	1.77% m/m	5.00	5.12	102.4
		10.00	10.08	100.8
Asparagus*	0.82 g dm^{-3}	5.00	5.05	101.0
		10.00	9.63	96.3
Artichoke*	6.79 g dm^{-3}	5.00	4.96	99.2
		10.00	10.37	103.7
Orange (juice)	10.96 g dm^{-3}	5.00	5.33	106.6
		10.00	10.24	102.4
Lemon†	8.50 g dm^{-3}	5.00	5.10	102.0
		10.00	10.50	105.0
Sweet lime†	3.20 g dm^{-3}	5.00	4.88	97.6
		10.00	9.60	96.0

* Canned.
† Soft drink.

The concentration of NADH does not exert any influence on the analytical signal over the range 0.2–0.7 g dm^{-3}; higher values saturate the detector. On the other hand, the analytical signal increases with the concentration of CL; the maximum signal is reached with 1.4 U cm^{-3}, as the amount of NADH considered as optimum has already been consumed. As for the presence of $ZnCl_2$ (very important to avoid the loss of activity of CL[2]), the analytical signal decreases when its concentration increases. This effect can be caused by the complex formed between Zn^{2+} and oxalacetate, as Zn^{2+} hinders the reaction with MDH,[2] but it is not significant in concentrations up to 0.6 mmol dm^{-3}.

As regards FI variables, the analytical signal dramatically increases with decreasing flow rates. A value of 0.28 cm^3 min^{-1} was chosen to avoid high residence times. On the other hand, the signal increases linearly with the injected volume until the injection of the blank produces saturation of the detector.

The maximum analytical signal is obtained with a 300 cm reactor (r_1). This reflects the fact that the reaction catalysed by CL needs a certain time to proceed (10 min are required to attain the maximum signal). However, a value of 200 cm was chosen because it provides a good analytical response and a significant reduction in the analysis time. The length of the MDH reactor exerts a similar influence to that observed in the method for the determination of oxalacetic acid.

Under these working conditions, the calibration graph (Fig. 7) was linear over the range 1.0–20.0 mg dm^{-3} of citrate (absorbance = 0.0190 + 0.0111 [citric acid]; $r^2 = 0.9973$). The RSD was 2.2% (for 11 determinations of 10.0 mg dm^{-3}), and a sampling frequency of about 20 h^{-1} was achieved.

Table 4 Comparative study of the use of conventional and FI methods for the determination of citric acid

Parameter	Conventional method	Proposed FI method
RSD (%)	1.5–2.0	2.2
Linear range ratio*	20	20
Detection limit (as $A = 0.01$)/mg dm^{-3}	4.8	1.0
CL consumption per analysis/U	0.8	0.4
MDH consumption per analysis/U	12	<0.1
Mean recovery (%)	100.7	100.9
Sampling frequency/h^{-1}	≈4	≈20
Blank†	Yes	No
Number of enzymes used	3	2

* Ratio of the upper to the lower limit of the calibration graph.
† Additional measurement in order to subtract the absorbance of the matrix at the monitoring wavelength.

Table 3 shows the results obtained using the procedure previously described for the determination of citric acid in different food samples, where the citric acid is either present naturally or added.

The recoveries achieved by adding 5.0 and 10.0 mg dm^{-3} citric acid to the assayed samples was in the range 96.0–106.5%; the mean recovery was 100.9%.

Conclusions

A fast and simple method for the determination of oxalacetic acid in fruit juices has been established; it avoids the need for using sophisticated instrumentation and a greater number of enzymes, as well as the complexity of bioluminescence methods.[10] It also combines the specificity of the enzymic methods with the rapidity of the FI technique, whereas the existing chromatographic methods are much slower, with more expensive instrumentation, a longer stabilization time for the system, a more complicated sample pre-treatment and poor peak resolution. In all the methods considered, the detection limits are similar.

Finally, a comparative study between conventional[2] and proposed FI enzymic methods for citric acid determination (Table 4) leads to the following conclusions. The detection limit, defined as the concentration corresponding to a variation of the absorbance of 0.01, is lower in the FI method. The proposed method is valid for most samples as their content of oxalacetic acid is generally negligible when compared with that of citric acid; the conventional method is applicable to all types of samples. The number of enzymes involved has been reduced, as well as their consumption. Sampling frequency is five times higher in the FI method. In this method, the carrier is the sample and, therefore, no blank assay is required as the baseline coincides with the absorbance of the matrix.

The chromatographic methods proposed for the determination of citric acid show the same drawbacks as those mentioned above, together with a poorer detection limit.

The authors gratefully acknowledge financial support from the Comisión Interministerial de Ciencia y Tecnología, Project ALI 90-0633.

References

1 Lehninger, A. L., *Curso Breve de Bioquímica*, Ediciones Omega, Barcelona, 1979, pp. 214–223.

2 Moellering, H., in *Methods of Enzymatic Analysis*, ed. Bergmeyer, H. V., Verlag Chemie, Weinheim, 1983, pp. 2–12.
3 Ribéreau-Gayon, J., Peynaud, E., Sudraud, P., and Ribéreau-Gayon, P., *Traité d'Enologie. Sciences et Techniques du Vin*, Dunod, Paris, 1976, vol. I, pp. 182–284.
4 Matsumoto, K., Ishida, K., Nomura, T., and Osajima, Y., *Agric. Biol. Chem.*, 1984, **48**, 2211.
5 Pesez, M., and Bartos, J., *Colorimetric and Fluorimetric Analysis of Organic Compounds and Drugs*, Marcel Dekker, New York, 1974, pp. 62, 295, 298.
6 Dunemann, L., *Anal. Chim. Acta*, 1989, **221**, 19.
7 Saag, K., in *HPLC in Food Analysis*, ed. Macrae, R., Academic Press, London, 1982, p. 230.
8 Moellering, H., and Gruber, W., *Anal. Biochem.*, 1966, **17**, 369.
9 Kurkijärvi, K., Heinonen, T., Lövgren, T., Lavi, J., and Rannio, R., *Anal. Appl. Biolumin. Chemilumin. (Proc. Int. Symp.) 3rd 1984*, p. 125.
10 Kurkijärvi, K., Vierijoki, T., and Korpela, T., *Ann. N. Y. Acad. Sci.*, 1990, **585**, 394.
11 Valcárcel, M., and Luque de Castro, M. D., *Flow Injection Analysis. Principles and Applications*, Ellis Horwood, Chichester, 1987, p. 39.
12 Puchades, R., Herrero, M. A., Maquieira, A., and Atienza, J., *Food Chem.*, 1991, **42**, 167.
13 Masoom, M., and Townshend, A., *Anal. Chim. Acta*, 1984, **166**, 111.
14 Lázaro, F., Luque de Castro, M. D., and Valcárcel, M., *Anal. Chim. Acta*, 1988, **214**, 217.
15 Lázaro, F., Luque de Castro, M. D., and Valcárcel, M., *Fresenius' Z. Anal. Chem.*, 1985, **321**, 467.

Paper 2/05890A
Received November 4, 1992
Accepted March 1, 1993

Flow Injection Spectrophotometric Method for the Speciation of Aluminium in River and Tap Waters

Mª José Quintela, Mercedes Gallego and Miguel Valcárcel*
Department of Analytical Chemistry, Faculty of Sciences, University of Córdoba, E-14004 Córdoba, Spain

An automatic flow injection method for aluminium speciation in waters at the nanogram per millilitre level is reported, based on a Pyrocatechol Violet chelation–ion-exchange method. Data are presented on total reactive aluminium, total monomeric aluminium and non-labile monomeric aluminium. The proposed method is sensitive (detection limit, 5 μg l^{-1}), rapid and reproducible. The results obtained in the analysis of six river and tap water samples were consistent with those provided by the manual counterpart of the method.

Keywords: *Aluminium; speciation; flow injection; water; spectrophotometry*

Aluminium is the third most abundant element in the Earth's crust. Concentration of dissolved aluminium in most neutral waters are low because of the relatively low solubility of natural aluminium minerals (*e.g.*, feldspars in metamorphic and igneous rocks). Several authors[1,2] have reported average aluminium concentrations of 10 μg l^{-1} for the hydrosphere and 240 μg l^{-1} for freshwaters. There is growing concern over the environmental consequences of the geochemical mobility of aluminium in soils and aquatic systems, where its presence has increased considerably as a result of atmospheric precipitation in the form of acid rain.[3] Aluminium chemistry in acid waters is receiving increasing attention owing to the toxic effects of this element on aquatic and terrestrial organisms. Recent studies suggest a possible correlation between high concentrations of aluminium, higher than 50 μg l^{-1},[4] in drinking waters with the incidence of senile dementia.[5] The toxicity of aluminium is dependent on its speciation chemistry in water. Thus, Driscoll and co-workers[6,7] have shown positively charged aluminium hydroxy species to be much more toxic to fish than organic aluminium complexes. This has fostered the development of aluminium speciation methods.[8] Bertsch and Anderson[9] classify aluminium speciation methods into three groups: (*a*) computation that uses thermodynamic-based geochemical models; (*b*) analytical separation of aluminium species by differential reaction kinetics with chelating agents and/or the physicochemical separation of aluminium species by size or charge; and (*c*) combination of one or more analytical separation techniques and a geochemical speciation model. Driscoll[7] distinguishes three forms of aluminium based on an 8-hydroxyquinoline colorimetric method[10] combined with ion-exchange separation and liquid–liquid extraction. This allows the determination of acid-soluble aluminium, non-labile monomeric aluminium and labile monomeric aluminium. More recently, complete aluminium speciation in lake water with high suspended solids content (>20 mg l^{-1}) from Llyn Brianne reservoir (14 km north of Llandovery, Dyfed, UK), by using a colorimetric procedure based on Pyrocatechol Violet (PCV) was accomplished[11] including a study of the influence of sorption processes. Another aluminium speciation method[12] is based on a parabolic model that assumes the formation of three complexes between the metal and Morin. The speciation of aluminium in natural waters[9] and forest soil[13] using ion chromatography has been addressed by using post-column derivatization with Tiron[9] and 8-hydroxyquinoline-5-sulfonic acid[13] for identification of fluoro-, oxalato-, and citrato-aluminium complexes, and by employing a highly sensitive and selective short column for the direct determination of aluminium species of the general formula $Al(OH)_x^{(3-x)+}$, as well as fluoro species.[14]

Two automatic methods for fractionation and determination of aluminium species in natural waters use Technicon AutoAnalyzers. One method[15] is based on the ion-exchange procedure developed by Driscoll *et al.*[6] and identifies total monomeric aluminium and non-labile monomeric aluminium. The other method[16] provides fractionated inorganic monomeric and organic monomeric aluminium only. Neither method was investigated for the effect of chemical and flow variables. Finally, several flow-injection (FI) methods for the determination of total aluminium in waters,[17] dialysis concentrates[18,19] and soil extracts,[20] or monomeric aluminium species in waters[21] have been developed using different detectors.

In this work we automated a PCV method, an adaptation of the original Dougan and Wilson[22] procedure. The proposed method allows three aluminium fractions to be determined using an FI system, which includes an Amberlite IR-120 ion-exchange mini-column. The combined use of FI and ultraviolet–visible (UV–VIS) spectrophotometry for the speciation of aluminium in river and tap waters yields reproducible results with lower risks of contamination or analyte losses, and in a shorter analysis time, relative to the manual method.

Experimental

Instruments and Apparatus

A GBC UV–VIS Model 911 spectrophotometer connected to a Knauer recorder and equipped with a Hellma flow-through cell (10 mm light path, 1 mm i.d., 18 μl) was used. A Perkin-Elmer Model 1100-B atomic absorption spectrometer furnished with an HGA-700 graphite furnace and an AS-70 autosampler, and equipped with an aluminium hollow cathode lamp for the determination of total aluminium was also used. The wavelength was set to 309.3 nm and the spectral slit-width to 0.7 nm. Pyrolytic graphite coated graphite tubes were employed. The graphite furnace temperature programme is shown in Table 1. A Gilson Minipuls-2 peristaltic pump fitted with poly(vinyl chloride) (PVC) and Solvaflex (for buffer solutions) pump tubing was utilized. The injector consisted of a Rheodyne 5041 four-way valve to which a loop of the required volume was fitted; poly(tetrafluoroethylene) tubing (0.5 mm i.d.) was also used. A laboratory-constructed PVC column (10 cm × 2.5 mm i.d.) was employed for ion-exchange separations. A FIAtron 721 flow-cell accommodating a glass–calomel microelectrode connected to a Radiometer Model 62 pH meter was used for pH measurement.

Reagents

A 5×10^{-3} mol l^{-1} stock PCV solution was prepared in water. The iron-masking reagent was prepared from 2.55×10^{-2}

* To whom correspondence should be addressed.

Table 1 Graphite furnace temperature programme used for the determination of aluminium in some river and tap waters

Step	Temperature/°C	Time/s Ramp	Time/s Hold	Argon flow rate/ml min^{-1}
1	100	25	20	300
2	800	15	15	300
3	1250	15	15	300
4	2500	0	4	0 (read)
5	2650	1	1	300

Instrumental conditions:

Light source	Hollow cathode lamp
Lamp current	25 mA
Wavelength	309.3 nm
Spectral bandwidth	0.7 nm
Signal processing parameter	Peak area mode
Integrating time	5 s
Injected volume	20 µl sample

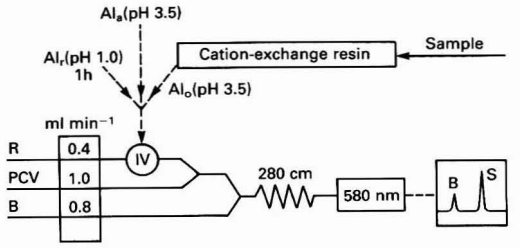

Fig. 1 Schematic representation of the FI system used for the speciation of aluminium in waters. R, iron-masking reagent (2.55 mmol l^{-1} 1,10-phenanthroline and 0.43 mol l^{-1} hydroxylammonium chloride); PCV, 5 × 10^{-4} mol l^{-1} Pyrocatechol Violet; B, 1.5 mol l^{-1} hexamethylenetetramine buffer (pH 8.2 or 8.8); Al$_a$ total monomeric aluminium; Al$_r$ total reactive aluminium; Al$_o$, non-labile monomeric aluminium; resin, Amberlite IR-120 P; B and S, blank and sample signals, respectively

mol l^{-1} (0.6% m/v) 1,10-phenanthrolinium chloride (monohydrate) and 4.3 mol l^{-1} (30% m/v) hydroxylammonium chloride in water. Two 1.5 mol l^{-1} (20% m/v) hexamethylenetetramine buffers in water (pH 8.2) or ammonia solution (pH 8.8) were used. All reagents were purchased from Merck and remained stable for at least two weeks at room temperature. A 1000 mg l^{-1} aluminium solution was prepared by dissolving 1.000 g of aluminium wire in 20 ml of concentrated H_2SO_4 and 50 ml of concentrated HNO_3, and subsequently diluting to 1 l with water. High-purity (ultrapure) water (Milli-Q) was used in all instances. For continuous introduction of the PCV and iron-masking reagents into the FI system, both the stock solutions were diluted 10-fold with water. All other reagents used were of analytical-reagent grade. The Amberlite IR-120 Plus (wet mesh 16–50) strong cation-exchange resin (Sigma) was washed twice with water and then with 1 × 10^{-3} mol dm^{-3} sodium chloride until the supernatant was clear.

Materials and Cleaning

All sample collections, storage and preparation of sample and reagent solutions were carried out in polyethylene containers (Aldrich), which are widely used to store environmental and trace component samples. All vessels were decontaminated by soaking in 10% HNO_3, for 48 h followed by rinsing five times with ultrapure water and filling with ultrapure water until used.[23]

Sample Collection and Preparation

The river and tap water samples were collected into polyethylene containers and stored at room temperature in the dark. The pH of the river and tap water at the time of collection was 6.7 and 6.5, respectively. The total aluminium content in the untreated river water (sample A) and the tap water (sample D) was about 20 and 40 µg l^{-1}, respectively, as determined by electrothermal atomization atomic absorption spectrometry (ETAAS) using the method proposed by Sanz-Medel *et al.*[24] The aluminium content in these natural waters was increased in order to make it adequate for quantitative speciation. Thus, we used six samples: unspiked river water (sample A), tap water (sample D), river water sample spiked with aluminium (as nitrate salt) to 70 (sample B) and 210 µg l^{-1} (sample C) and tap water sample spiked with aluminium to 220 (sample E) and 600 µg l^{-1} (sample F), respectively. The six water samples were analysed by ETAAS and their total aluminium concentration was found to remain virtually constant for up to 30 d, after which it decreased to a different extent depending on the type of water concerned.

Conditioning of the Ion-exchange Column

The Amberlite IR-120 P cation-exchange resin was used to determine the concentration of non-labile monomeric forms of aluminium in the water samples. The resin, in its sodium form, was packed in a 10 cm × 2.5 mm i.d. PVC column, washed with 3 ml of 1 mol l^{-1} HCl, then with 1 mol l^{-1} NaCl until the pH of effluent was 5.5, and finally conditioned by passing through a NaCl solution with the same conductivity and pH as the sample to be treated until the pH of the effluent was equal (±0.2) to that of the sample. The conductivity (µS cm^{-1}), pH of the sample and the concentration of the NaCl (×10^{-3} mol l^{-1}) used to achieve the same in the effluent, were: sample A, 203, 7.5, 1.55; sample B, 207, 7.9, 1.55; sample C, 239, 6.7, 1.80; sample D, 430, 7.2, 3.40; sample E, 430, 7.8, 3.40; and sample F, 469, 7.1, 3.7, respectively. The column was reconditioned each time it was used.

Procedures

Manual Driscoll Method

Total reactive aluminium (*Al$_r$*). A volume of 3.5 ml of water sample was acidifed to pH 1.0 by adding 50 µl of concentrated HCl. After 1 h, the sample was analysed by the PCV method (see below).

Total monomeric aluminium (*Al$_a$*). No sample pre-treatment before PCV detection of aluminium was required. However, 50 µl of concentrated HCl must be added simultaneously with the hexamethylenetetramine buffer solution prior to analysis by the PCV method (see below).

Non-labile monomeric aluminium (*Al$_o$*). The sample was aspirated through the conditioned column at a flow rate of 4.0 ml min^{-1}, the first 10 ml of sample was discarded, after which, the following 3.5 ml was collected and treated as for total monomeric aluminium.

PCV method

To a 3.5 ml volume of sample, whether standard or blank [acidified to pH 1 for 1 h (for Al$_r$ only)] 0.1 ml of the iron-masking reagent (0.1% 1,10 phenanthroline and 10% hydroxylammonium chloride) and 0.2 ml of a 0.0375% m/v PCV solution were added and mixed, then 1.0 ml of buffer solution (30% hexamethylenetetramine and 1.65% ammonia solution) and 50 µl of concentrated HCl were added (for the Al$_a$ and Al$_o$ fractions). After 10 min, the absorbance was measured at 580 nm. The linear determination range of the method was found to be between 5 and 400 µg l^{-1}.

Table 2 Fractionation of aqueous aluminium

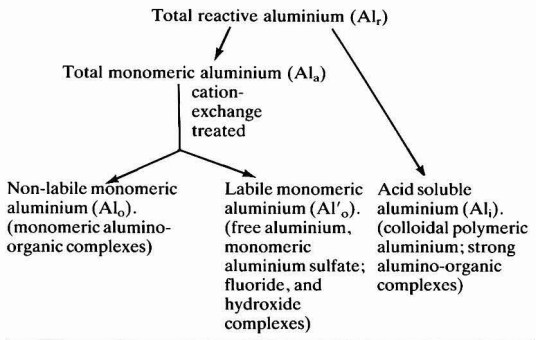

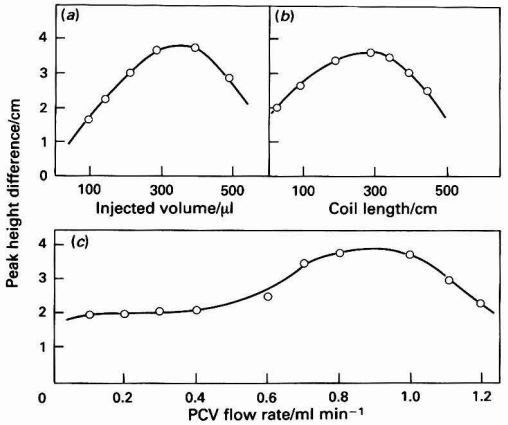

Fig. 2 Influence of the (*a*) injected volume, (*b*) coil length and (*c*) flow rate on the peak height. Sample: 0.5 μg ml^{-1} Al^{3+}; 1 cm = absorbance of 0.045

Automatic Driscoll Method

Total reactive aluminium (Al_r). A 10 ml volume of water sample was acidified to pH 1.0 by adding 150 μl of concentrated HCl. After 1 h, the sample was injected into the system shown in Fig. 1.

Total monomeric aluminium (Al_a). The water sample was rapidly injected into the FI system (Fig. 1) after adjusting the pH to 3.5.

Non-labile monomeric aluminium (Al_o). The column was positioned vertically and the water sample was aspirated at a flow rate of 4.0 ml min^{-1} through it. The first 10 ml of sample was discarded; and the following 10 ml was collected and injected into the system (Fig. 1) after adjusting the pH to 3.5.

Flow-injection Method

The proposed FI configuration for aluminium speciation is shown in Fig. 1. A 280 μl volume of sample containing between 10 and 1000 μg l^{-1} of aluminium was injected into a carrier solution including the iron-masking reagent (R) after merging with the PCV reagent, and then with the hexamethylenetetramine buffer solution of pH 8.2 (for the Al_a and Al_o, fractions) or pH 8.8 (for Al_r). Complex formation took place in the 280 cm coil (at pH 6.1–6.2). The blue colour was measured at 580 nm against an ultrapure water blank or a 0.1 mol l^{-1} HCl solution (for Al_r).

Results and Discussion

As stated above, in this work we automated the method originally developed by Driscoll[7] for the speciation of aluminium in waters, but used PCV instead of 8-hydroxyquinoline as a chelating reagent.[22] A schematic representation in the form of a flow chart is given in Table 2. The aluminium fractions determined in water samples were defined as follows: total reactive aluminium (Al_r), *i.e.*, the aluminium that was detected colorimetrically after a sample was acidified with 0.1 mol l^{-1} HCl for 1 h. Total monomeric aluminium (Al_o), *i.e.*, the aluminium detected colorimetrically in unacidified effluent from the ion-exchange column. Exchangeable or labile monomeric aluminium (Al'_o), was quantified as the difference between Al_a and Al_o. Also, the difference between total reactive aluminium and total monomeric aluminium was called acid-soluble aluminium (Al_i) and is an estimate of the aluminium that requires acid dissolution (pH 1.0) for its determination; this fraction would include colloidal aluminium and very strongly bound organic aluminium forms. If polymeric aluminium were not adsorbed onto the cation-exchange resin, then polymers might interfere with the reaction by preventing acidification of the effluent from the ion-exchange column to pH 1. Also, polymers are positively charged so they can adsorb, just as inorganic monomeric aluminium does. Consequently, the non-labile monomeric Al fraction (Al_o) is an estimate of monomeric aluminium that is organically complexed, while the labile monomeric aluminium fraction (Al'_o) includes free monomeric aluminium and aluminium sulfate, fluoride and hydroxide complexes according to Driscoll.[7]

Optimization of the Flow-injection Manifold

First, the FI manifold for the determination of aluminium by the PCV method was optimized and then was fitted to a cation-exchange column for speciation. Thus, a standard sample containing 0.5 μg ml^{-1} of aluminium was injected into the system at a pH of 2.0–6.0 (the optimal pH was 2.5–4.1). A sample pH of 3.5 was chosen for further experiments. The blank signal remained constant over the pH range 2.6–6.0; therefore, ultrapure water could be used as the blank. The concentration of PCV was varied between 1.0×10^{-4} and 14.5×10^{-4} mol l^{-1}. The sensitivity to aluminium increased with an increase in the concentration of PCV up to 5×10^{-4} mol l^{-1}, beyond which the signal remained more or less constant. Obviously, a high molar excess of PCV over aluminium was desirable in order to minimize interferences from anions which form complexes with aluminium. However, the blank signal and background absorption increased in parallel with the PCV concentration, so 5×10^{-4} mol l^{-1} (0.01875% m/v) was chosen to minimize changes in the background signal. Hexamethylenetetramine is the most commonly used buffer for the determination of aluminium by this method. The absorbance difference was constant over the range 1–2.5 mol l^{-1} hexamethylenetetramine (pH 8.2), so a 1.5 mol l^{-1} concentration was chosen.

The flow variables studied were the sample volume, coil lengths and flow rates. The effect of the injected volume on the peak height and shape at a constant flow rate was studied over the range 100–500 μl. As can be seen in Fig. 2(*a*), above 280 μl, the absorbance difference remained virtually constant up to 400 μl, beyond which the signal decreased owing to the formation of three zones in the inserted sample plug: two at the ends, which merge with the reactants, and one in the middle, where no chemical reaction takes place. This was confirmed by the appearance of two FI peaks per injected sample volume exceeding 400 μl. A sample volume of 280 μl was chosen in order to ensure that blanks yielded low signals

and hence increased reproducibility. Peak heights were scarcely affected by the length of the mixing coil used for mixing the sample and PCV, over the range 0–200 cm, because no reaction (only mixing) took place in it as the pH was still unsuitable (pH <4.0); therefore, no coil was used. As can be seen in Fig. 2(*b*), the coil length for the sample–PCV mixture and the hexamethylenetetramine buffer mixing was critical because it determined the optimal pH (6.1–6.2) required for complex formation; the length should not exceed 330 cm in order to avoid decreased signals. The influence of the flow rates of the PCV and hexamethylenetetramine solutions was investigated. Fig. 2(*c*) shows the dependence of the absorbance on the flow rate of the PCV (5×10^{-4} mol l^{-1}) solution. The signal difference between sample and blank initially remained virtually constant and then increased slightly, after which it remained constant again up to 1.0 ml min^{-1}. A PCV flow rate of 1.0 ml min^{-1} was chosen as optimum. The development of the aluminium–PCV complex depended on the flow rate of the hexamethylenetetramine buffer because the optimal pH in this coil must be maintained between 6.1 and 6.2. The optimal flow rate was between 0.4 and 0.8 ml min^{-1}. At higher flow rates, the difference between the sample and blank signal was smaller owing to increased dispersion of the complex.

Speciation of Aluminium

In the Driscoll method,[7] total reactive aluminium is determined after the water sample has been acidified with 0.1 mol l^{-1} HCl for 1 h. As shown above, the optimal pH for the sample ranged between 2.5 and 4.1 when the FI manifold was used, so the pH of the buffer solution must be higher in order to allow the most acidic sample (pH 1) to be buffered. Several hexamethylenetetramine buffers of different pH values were assayed for this purpose and a flow pH meter was included in front of the flow cell in the final flow system. Also, a standard sample containing 1.0 μg ml^{-1} of aluminium at pH 1.0 was injected into the system because the signal obtained with 0.5 μg ml^{-1} of aluminium was too low owing to dispersion of the complex in the mixing chamber of the pH meter. Finally, various 1.5 mol l^{-1} hexamethylenetetramine buffers containing different aliquots of ammonia solution (0–170 μl) were assayed. Complex formation was favoured at a pH of the sample–PCV mixture and buffer between 6.1 and 6.2 (*i.e.*, the pH obtained when standards of pH 2.5–4.1 and a hexamethylenetetramine buffer of pH 8.2 were used). Therefore, for samples of pH 1.0, the pH of the buffer solution must be increased to 8.8 in order to ensure a pH of 6.1–6.2 in the reaction coil. In summary, for the determination of Al_r, a 1.5 mol l^{-1} hexamethylenetetramine buffer of pH 8.8 in ammonia solution must be used; Al_a was determined by directly injecting the water sample after adjusting the pH to 3.5 with 1 mol l^{-1} HCl, into the FI system; Al_o was determined in the unacidified effluent from the ion-exchange column. For this purpose, after an initial sample volume (10 ml, to displace the eluent) was discarded, 10 ml was collected in a vial and adjusted to pH 3.5 prior to analysis by the proposed FI method. The cation-exchange resin had a strong affinity for aluminium. As solutions passed through the cation-exchange column, there was competition between aqueous ligands and the strong cation-exchange resin for aluminium. The affinity of the resin for aluminium was studied by using a 0.5 μg ml^{-1} of aluminium solution (from aluminium wire dissolved in an acid), and another solution containing 0.5 μg ml^{-1} of aluminium plus a strong organic ligand (100 μg ml^{-1} sodium citrate), both of which were passed through the cation-exchange column (at pH 6, similar to that of the water samples). In this experiment, detection of aluminium in the presence of citrate was complicated by the citrate competing with the PCV for aluminium and thus interfering with the determination of the metal. Citrate interferes with the proposed FI method at concentrations above 10 μg ml^{-1}; however, because a concentration of 100 μg ml^{-1} resulted in half of the original sensitivity (slope of the calibration graph for aluminium) aluminium can still be determined in spite of such a decrease. Aluminium was completely removed from the solution of inorganic aluminium (the concentration of aluminium found in the effluent was lower than the detection limit, 5 μg l^{-1}) and transferred through the cation-exchange resin in the presence of citrate. Therefore, the resin effectively retained the inorganic aluminium and eluted the organic aluminium.

Determination of Aluminium

Two calibration graphs were obtained under the optimum conditions given in Fig. 1. One graph was linear over 10–80 μg l^{-1} of aluminium and the second between 80 and 1000 μg l^{-1} of aluminium. The corresponding equations are

absorbance = $0.003 + 9.2 \times 10^{-4} x$ (x: 10–80 μg l^{-1} of aluminium)

absorbance = $0.054 + 2.3 \times 10^{-4} x$ (x: 80–1000 μg l^{-1} of aluminium)

The slope of the calibration graph for 10–80 μg l^{-1} of aluminium was higher than it was for 80–1000 μg l^{-1} of aluminium owing to the presence of excess PCV (5×10^{-4} mol l^{-1}) relative to aluminium. The detection limit (5 μg l^{-1} aluminium) was calculated as three times the absorbance for 30 injections of the ultrapure water blank by using the calibration graphs for 10–80 μg l^{-1} aluminium. The precision of the automatic method obtained for 11 samples containing 50 μg l^{-1} or 500 μg l^{-1} (intermediate concentrations of the two linear ranges) expressed as relative standard deviation, was 1.8 and 0.65%, respectively. The sample throughput, excluding the sample pre-treatment (*i.e.*, acidification, ion exchange), was 40–50 h^{-1}.

The potential interference of iron was studied by injecting samples containing 0.5 μg ml^{-1} of aluminium and different concentrations of iron(III). The metal ion was found to interfere at the same concentration level as aluminium(III) when the iron-masking reagent carrier solution (Fig. 1) was replaced with a water carrier. Iron-masking reagent solutions containing 0.03, 0.06 or 0.1% 1,10-phenanthroline plus 3% hydroxylammonium chloride suppressed the interference from iron up to 1.5, 5.5 and 9 μg ml^{-1}, respectively. An iron-masking reagent solution containing 0.06% 1,10-phenanthroline (2.55 mmol l^{-1}) and 3% hydroxylammonium chloride (0.43 mol l^{-1}) was chosen in order to avoid the interference of up to about 5.5 μg ml^{-1} of iron, which was sufficient for most waters. This iron-masking reagent also prevented interferences from Cu^{2+}, Ni^{2+}, Zn^{2+}, Pb^{2+} and Co^{2+} at concentrations of up to at least 15 μg ml^{-1}.

Analysis of Water Samples

The proposed method was applied to the speciation of aluminium in freshwaters (samples A and D) as received, and those spiked with aluminium (samples B, C, E and F). The results obtained with the proposed FI method and the manual Driscoll method[7] are given in Table 3. The total aluminium measured by ETAAS was higher than the total reactive aluminium provided by the PCV method as the determination of total aluminium by the PCV method would require pre-digestion of samples with peroxodisulfate, but pre-digestion is impossible for aluminium speciation.

Conclusions

The manual method is roughly three-times more sensitive than the proposed automatic FI method because of the increased sample dispersion in the flow system; however, the FI method

Table 3 Concentration of aluminium (μg l^{-1})* in freshwater samples by the proposed automatic (x) FI and manual (y) Driscoll methods

		Al_r		Al_a		Al_o		Al'_o	
S†	Al‡	x	y	x	y	x	y	x	y
A	20	19.6 (5.3)	15.9 (8.5)	16.5 (5.2)	13.5 (1.1)	5.4 (4.8)	4.1 (1.1)	11.1 (0.4)	9.4 (0.0)
B	70	65.2 (1.0)	59.7 (6.3)	45.6 (3.7)	42.3 (2.1)	28.3 (1.9)	14.1 (1.6)	17.3 (1.8)	28.2 (0.5)
C	210	208.7 (3.3)	139.0 (1.3)	39.9 (6.3)	33.6 (7.9)	13.9 (5.5)	10.0 (1.1)	26.0 (0.8)	23.6 (6.9)
D	40	35.2 (5.1)	29.7 (6.0)	25.6 (4.4)	22.3 (3.8)	18.3 (2.9)	14.1 (1.1)	7.3 (1.5)	8.2 (2.7)
E	220	204.3 (0.8)	196.0 (5.9)	127.1 (1.0)	99.1 (4.7)	49.9 (0.2)	45.4 (0.8)	77.2 (0.8)	53.7 (3.9)
F	600	597.7 (1.1)	507.7 (3.3)	507.3 (5.0)	467.3 (5.6)	78.5 (4.2)	45.5 (4.3)	428.8 (0.8)	421.8 (1.3)

* Relative standard deviation for five measurements of each water sample are given in brackets (%).
† A, B and C are river waters; D, E and F are tap waters; samples B, C, E and F spiked with aluminium.
‡ Total aluminium measured by ETAAS.

is more rapid and reproducible. As can be seen in Table 3, the manual method provides slightly lower concentrations because the reactants are placed directly in the sampling tubes, so losses by adsorption or precipitation on the sample tube walls are to be expected.

Because of the similarities between the proposed method and that of Henshaw *et al.*,[21] only the most salient differences between the two are commented on. Thus, Henshaw *et al.* only determine the fraction of monomeric aluminium because they only analyse the percolate from the Amberlite IR-120 cation-exchange column in an FI system similar to that used in this work. Acidification of the sample to pH 1.0 or 3.5 prior to reaction with PCV allows the determination of total reactive aluminium (Al_r) and total monomeric aluminium (Al_a). In addition, conditioning of the ion-exchange resin permits the determination of non-labile monomeric aluminium (Al_o). Also, the total aluminium content is obtained by ETAAS. In summary, as can be seen from Table 2, the proposed method, like that of Driscoll, allows up to five aluminium fractions to be determined. The results obtained in the speciation of aluminium in waters by using the manual and automatic method are compared.

Financial support from the BCR [BCR Contract No. 5311/1/9/351/90/02-BCR-E(10)] is gratefully acknowledged.

References

1 Stumm, W., and Morgan, J. J., *Aquatic Chemistry*, Wiley, New York, 1970.
2 Bowen, H. J. M., *Trace Elements in Biochemistry*, Academic Press, New York, 1966.
3 Campbell, P. G. C., Bisson, M., Boagie, R., Tessier, A., Villeneuve, J. P., *Anal. Chem.*, 1983, **55**, 2246.
4 *Standard Methods for the Examination of Water and Wastewater*, American Public Health Association, *American Water Works Association, Water Pollution Control Federation*, Washington, DC, 17th Edition, 1989.
5 Martyn, C. N., Osmond, C., Edwardson, J. A., Barker, D. J. P., Harris, E. C., and Lacey, R. F., *Lancet*, 1989, January 14, p. 59.
6 Driscoll, C. T., Baker, J. P., Bisogni, J. J., and Schofield, C. L., *Nature (London)*, 1980, **284**, 161.
7 Driscoll, C. T., *Int. J. Environ. Anal. Chem.*, 1984, **16**, 267.
8 Salbu, B., *Environ. Geochem. Health*, 1990, **12**, 3.
9 Bertsch, P. M., and Anderson, M. A., *Anal. Chem.*, 1989, **61**, 535.
10 Barnes, R. B., *Chem. Geol.*, 1976, **15**, 177.
11 Goenaga, X., Bryant, R., Willians, D. J. A., *Anal. Chem.*, 1987, **59**, 2673.
12 Browne, B. A., McColl, J. G., and Driscoll, C. T., *J. Environ. Anal.*, 1990, **19**, 65.
13 Michalas, F., Glavac, V., and Parlar, H., *Fresenius' J. Anal. Chem.*, 1992, **343**, 308.
14 Jones, P., *Int. J. Environ. Anal. Chem.*, 1991, **44**, 1.
15 Rogeberg, E. J., and Henriksen, A., *Vatten*, 1985, **41**, 48.
16 Lazerte, B. D., Chun, C., and Evans, D., *Environ. Sci. Technol.*, 1988, **22**, 1106.
17 Royset, O., *Anal. Chim. Acta*, 1986, **185**, 75.
18 Pereiro García, M. R., López García, A., Díaz García, M. E., and Sanz-Medel, A., *J. Anal. At. Spectrom.*, 1990, **5**, 15.
19 Fernández, P., Pérez Conde, C., Gutierrez, A., and Cámara, C., *Talanta*, 1991, **38**, 1387.
20 Downard, A. J., Kipton, H., Powell, J., and Xu, S., *Anal. Chim. Acta.*, 1992, **256**, 117.
21 Henshaw, J. M., Lewis, T. E., and Heithmar, E. M., *Int. J. Environ. Anal. Chem.*, 1988, **34**, 119.
22 Dougan, W. K., and Wilson, A. L., *Analyst*, 1974, **99**, 413.
23 Wilhelm, M., and Ohnesorge, F. K., *J. Anal. Toxicol.*, 1990, **14**, 206.
24 Sanz-Medel, A., Rodríguez Roza, R. M., González Alonso, R., Noval, A., and Cannata, J. B., *J. Anal. At. Spectrom.*, 1987, **2**, 177.

Paper 2/06466I
Received December 4, 1992
Accepted May 4, 1993

Selective and Sensitive Spectrophotometric Determination of Tetrafluoroborate in Waste Water After Ion-pair Extraction Using Bis[2-(5-chloro-2-pyridylazo)-5-diethylaminophenolato]cobalt(III) as a Counter Ion

Issei Kasahara, Satoshi Hosokawa, Noriko Hata, Shigeru Taguchi and Katsumi Goto
Department of Chemistry, Faculty of Science, Toyama University, Gofuku 3190, Toyama 930, Japan

A simple, selective and sensitive method has been proposed for the ion-pair extraction and spectrophotometric determination of tetrafluoroborate in waste water. Tetrafluoroborate is extracted as an ion pair with bis[2-(5-chloro-2-pyridylazo)-5-diethylaminophenolato]cobalt(III) into chlorobenzene. The absorbance of the organic phase is measured at 567 nm against a reagent blank. Beer's law is obeyed over the concentration range 0.05–1.0 mg l^{-1} of tetrafluoroborate and the detection limit (three times the standard deviation of the blank) was 0.009 mg l^{-1}. Relative standard deviations were 0.6–2.0%. Nitrate seriously interferes with the determination but can be decomposed by shaking with zinc powder after adjusting the acidity with 0.05 mol l^{-1} sulfuric acid. The proposed method can be applied satisfactorily to the determination of tetrafluoroborate in industrial and laboratory waste waters containing high concentrations of fluoride, chloride, nitrate, sulfate, borate, silicate and many other metal ions.

Keywords: *Tetrafluoroborate in waste water; ion-pair extraction; spectrophotometry; bis[2-(5-chloro-2-pyridylazo)-5-diethylaminophenolato]cobalt(III)*

Fluorine compounds, both organic and inorganic, have their specific use in modern science and technology. Water that contains fluorine is discharged from metal plating, soldering, semiconductor and fine chemicals industries and laboratories. Fluoride ion is relatively easily removed from waste water by precipitation as calcium fluoride by adding calcium salts. If, however, fluorine is present as the tetrafluoroborate ion (BF_4^-), fluorine removal is more difficult. This is mainly owing to the inertness of the tetrafluoroborate ion. In the process of water quality control or fluorine removal treatment of such kinds of waste water, it is, therefore, necessary to determine fluoride and tetrafluoroborate ions separately.

Fluoride and tetrafluoroborate ions can be determined by ion-chromatography (IC), but difficulties arise in its application to the analysis of waste water, which contains large amounts of foreign ions and suspended solids, because of overlapping peaks and deterioration of the column.

Methods of ion-pair extraction with spectrophotometric detection seem promising for the determination of tetrafluoroborate in waste water. Several cationic dyes[1–4] have already been proposed as counter ions for the determination of boron after converting the boron into the tetrafluoroborate ion. However, they are not suitable for waste water analysis because ion-pair extraction with these dyes is successful only within a narrow pH range and the reagent blank is usually high.

During the course of investigation of ion-pair extraction systems,[5] it was found that complexes of cobalt(II) with pyridylazoaminophenols are rapidly oxidized to their corresponding Co^{III} complexes, some of which are inert, and some of which are negatively or positively charged and have excellent properties for use as counter ions in ion-pair extraction with spectrophotometric determination of ionic species in water. They are intensely coloured, some have molar absorption coefficients (ε) exceeding 10^4 m^2 mol^{-1}. They have no acidic or basic groups, so that their ability for use as extraction reagents is independent of pH over a wide range. Exploiting these advantages these complex ions were applied to the ion-pair extraction and spectrophotometric determination of anionic[6] and cationic[7] surfactants in water.

In this paper, the bis[2-(5-chloro-2-pyridylazo)-5-diethylaminophenolato]cobalt(III) ion, $(Co\text{–}5\text{-}Cl\text{-}PADAP)^+$, is proposed for use as a counter ion for the ion-pair extraction and spectrophotometric determination of tetrafluoroborate. The proposed method is sensitive and reproducible and relatively free from interferences.

Experimental

Apparatus

A Hitachi U-3200 double-beam automatic recording spectrophotometer with 10 mm quartz cells was used for measurement of absorbance. A Taiyo-kagaku Type SR-II reciprocal shaker was used for equilibrating the aqueous and organic phases. A Hitachi centrifuge Model 05P-21 was used for phase separation. Measurements of pH and fluoride concentration were carried out with a Horiba Model N-8_F ion meter. A Hitachi Model 306 Super Scan ICP emission analysis system was used for the determination of metals by inductively coupled plasma atomic emission spectrometry (ICP-AES). The operating parameters of the ICP spectrometer were as follows: forward power, 1.0 kW; plasma gas flow rate 16 l min^{-1}; auxiliary gas flow rate, 0.5 l min^{-1}; nebulizer gas flow rate, 0.5 l min^{-1}; and nebulizer, concentric flow type. A Dionex Model 2000i ion chromatograph was used for the determination of anions.

Reagents

Bis [2-(5-chloro-2-pyridylazo)-5-diethylaminophenolato] cobalt(III) chloride (Co–5-Cl-PADAP)$^+$Cl$^-$ solution. The $(Co\text{–}5\text{-}Cl\text{-}PADAP)^+$ Cl^- was purchased from Dojindo Laboratory. This reagent can also be obtained from Fluka. A 0.05% m/v aqueous solution was prepared and the solution was washed three times with chlorobenzene to remove impurities.

All other reagents and solvents were of analytical-reagent grade and were used as received.

Tetrafluoroborate (BF_4^-) standard stock solution (1000 mg l^{-1}). Dissolve 0.1265 g of sodium tetrafluoroborate in 100 ml of 0.05 mol l^{-1} sulfuric acid containing 0.42 g of sodium fluoride.

Recommended Procedure

Take 20 ml of sample solution containing less than 20 μg of tetrafluoroborate into a poly(propylene) centrifuge tube with

a screw cap. Add 2 ml of 0.5 mol l^{-1} sulfuric acid and 0.1 g of zinc powder. Shake the mixture for 5 min and centrifuge for 3 min (2500 rev min^{-1}; 1100*g*). Transfer a 10 ml portion of the supernatant into another centrifuge tube. Add 1 ml each of sodium sulfate solution and (Co–5-Cl-PADAP)$^+$ solution, and 10 ml of chlorobenzene. Shake for 3 min and centrifuge for 3 min (2500 rev min^{-1}; 1100*g*). Transfer the chlorobenzene layer into a cell and measure the absorbance at 567 nm against a reagent blank. Calculate the concentration from the calibration graph.

Results and Discussion

Structure and Stability of the (Co–5-Cl-PADAP)$^+$

Fig. 1 shows the structure of (Co–5-Cl-PADAP)$^+$. Cobalt(II) forms a 1 : 2 (metal : ligand) complex with 5-Cl-PADAP, and is then oxidized to Co(III) in the complex by dissolved oxygen. The Co(III) complex is an inert, singly charged cation, stable over a wide pH range (1–13); the absorption spectrum remains the same over this pH range. Its aqueous solution gives a high absorbance at 584 nm ($\varepsilon = 9.0 \times 10^3$ m^2 mol^{-1}).

Extraction and Spectral Characteristics

Various water-immiscible solvents were examined. Benzene, toluene and xylene did not extract the ion pair of (Co–5-Cl-PADAP)$^+$ and tetrafluoroborate. *o*-Dichlorobenzene, chloroform and benzyl chloride extracted the complex cation even in the absence of tetrafluoroborate. Chlorobenzene was chosen as the solvent because the absorbance of the ion pair was highest and that of the reagent blank was lowest in this solvent. In addition, the solvent extracted the ion pair quantitatively. The absorption spectrum of (Co–5-Cl-PADAP)$^+$ extracted into chlorobenzene as an ion pair with tetrafluoroborate is shown in Fig. 2 together with that of a reagent blank. The absorption spectrum has a peak at 567 nm and this wavelength was selected for the determination.

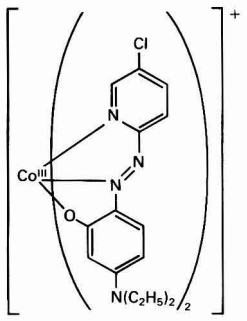

Fig. 1 Structure of (Co–5-Cl-PADAP)$^+$

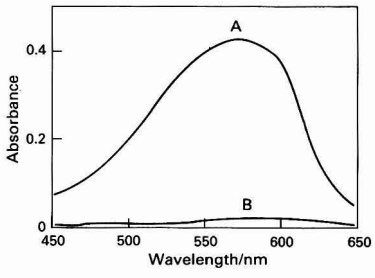

Fig. 2 Absorption spectra of the ion pairs extracted with (Co–5-Cl-PADAP)$^+$ as counter ion: A, 0.5 mg l^{-1} of BF_4^-; B, reagent blank. Conditions as for the proposed method with chlorobenzene as reference

Preservation of Stock Standard Solution

The rate of hydrolysis of tetrafluoroborate in aqueous solution is very low.[8,9] If, however, the standard solution of tetrafluoroborate is prepared with distilled water only, the tetrafluoroborate gradually hydrolyses and hence decreases in concentration, as shown in Fig. 3. To prevent the hydrolysis of tetrafluoroborate and to maintain a constant concentration, sulfuric acid and sodium fluoride were added at concentrations of 0.05 and 0.1 mol l^{-1}, respectively.

Comparison of the Results Obtained by the Proposed Method and by Ion Chromatography

A solution of sodium tetrafluoroborate in distilled water was prepared and the changes in concentration of tetrafluoroborate measured by the proposed method as well as by IC. Fig. 3 shows the relation between the results obtained by the proposed method and by IC. It can be seen in this figure that

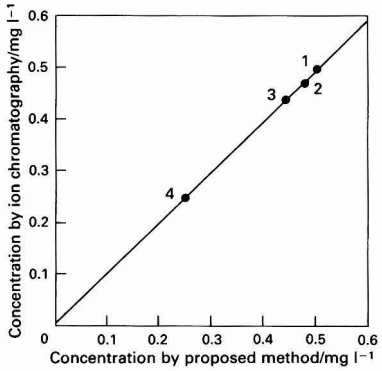

Fig. 3 Comparison of the results obtained by the proposed method and ion chromatographic method. 1, Just after preparation of standard solution; and after setting aside for: 2, 3 d; 3, 20 d; and 4, 30 d. A 1000 mg l^{-1} tetrafluoroborate solution was prepared by dissolving sodium tetrafluoroborate in distilled water. The solution was stored at room temperature and diluted 2000-fold with water for the analysis. Slope of line = 1.0

Table 1 Example of analyses of waste water samples (concentration given in mg l^{-1})

Determinand	Sample A	Sample B	Sample C	Sample D
*Element**—				
Aluminium	400	72	130	4.5
Boron	540	110	350	90
Barium	140	80	2.3	—
Calcium	41	27	1.6	7.7
Iron	6.5	1.9	1.5	0.4
Magnesium	4.0	1.1	0.8	5.1
Silicon	5800	1400	4500	24
Strontium	4.5	1.6	—	—
Zinc	—	—	190	6.0
Anion†—				
Fluoride	27000	20000	54000	160
Chloride	400	150	1000	17
Nitrate	6900	4000	19000	10
Sulfate	—	—	—	14

* Measured by ICP-AES after proper dilution.
† Measured by IC after proper dilution.

Table 2 Effect of diverse substances on the determination of BF_4^- (0.5 mg l^{-1})

Substance	Added as	Amount added/ mg l^{-1}	Absorbance at 567 nm	Error (%)
None	—	—	0.384	—
F^-	NaF	1000	0.388	+1.0
Cl^-	NaCl	1000	0.385	+0.3
SO_4^{2-}	Na_2SO_4	1000	0.384	+0.0
NO_3^-	KNO_3	1	0.492	+28*
		100	0.389	+1.3
ClO_4^-	$NaClO_4$	0.1	0.390	+1.6
$DS^{-\dagger}$	Na salt	0.1	0.385	+0.3
Na^+	NaCl	650	0.385	+0.3
K^+	KNO_3	63	0.389	+1.3
Ca^{2+}	$CaCl_2$	1000	0.384	+0.0
Mg^{2+}	$MgCl_2$	100	0.381	−0.8
Mn^{2+}	$MnSO_4 \cdot 4$–$6H_2O$	100	0.382	−0.5
Fe^{2+}	$FeSO_4 \cdot 7H_2O$	100	0.383	−0.3
Fe^{3+}	$Fe_2(SO_4)_3(NH_4)_2SO_4 \cdot 24H_2O$	100	0.381	−0.8
Ni^{2+}	$NiCl_2 \cdot 6H_2O$	100	0.384	+0.0
Cu^{2+}	$CuSO_4 \cdot 5H_2O$	100	0.386	−0.3
Al^{3+}	$Al_2(SO_4)_3$	100	0.375	−2.3
		100	0.308	−20.0‡

* Without reduction procedure.
† DS^- = dodecyl sulfate.
‡ Set aside for 1 h after addition of aluminium.

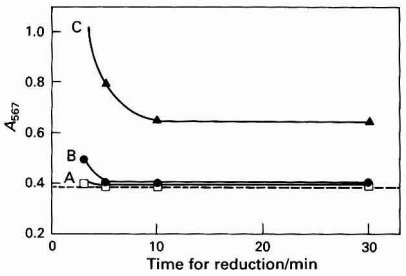

Fig. 4 Effect of time of reduction with different concentrations of nitrate. Conditions: 0.5 mg l^{-1} of BF_4^-. The broken line represents the absorbance by the proposed method in the absence of nitrate. Nitrate concentration: A, 10; B, 100; and C, 500 mg l^{-1}

correlation between the two methods is excellent (correlation coefficient, 0.999), suggesting that only tetrafluoroborate is determined by the proposed method.

Example of Determination of Fluoride in Waste Waters

The results of analyses of different kinds of waste waters that contained fluoride and borate are shown in Table 1. Samples A and B were from a university laboratory for electronic materials. Samples C and D were waste waters discharged from metal plating and soldering factories, respectively. The table shows diversity in quality of fluoride containing waste waters. It is to be noted that in addition to fluoride, boron and silicon are present at relatively high concentrations.

Effect of Diverse Ions

Table 2 shows the effects of diverse ions on the determination of tetrafluoroborate by the proposed method. Aluminium combines with the fluoride ion of the tetrafluoroborate at pH values of below 3; this is illustrated when aluminium salts are used to decompose tetrafluoroborate. Nearly all other cations have little effect. Fluoride, chloride and sulfate at high concentrations do not affect the determination. Nitrate ion has nearly the same extractability as the tetrafluoroborate ion, causing positive errors, but it can be decomposed by reduction with zinc powder; as will be described in the next section. The proposed method is very sensitive, so that original samples can be diluted for analysis by more than 100-fold in order to reduce interferences. Tetrafluoroborate seems to hydrolyse slowly to trifluorohydroxyborate,[8,9] which, however, does not interfere with the determination of tetrafluoroborate.

Table 3 Reproducibility at different BF_4^- levels. Number of measurements = 5, sample volume = 20 ml and reference = reagent blank

Concentration of BF_4^-/mg l^{-1}	Absorbance at 567 nm	s_r* (%)
0.05	0.040	2.0
0.10	0.077	1.0
0.30	0.245	1.2
0.50	0.388	1.0
0.70	0.548	0.6
1.00	0.783	0.7

* Relative standard deviation.

Table 4 Analysis of several waste water samples and results of recovery test. Each sample was analysed after dilution of the original waste water sample shown in Table 1. A′ = a 100-fold diluted solution of sample A. C′ = a 1000-fold diluted solution of sample C. D′ = a 200-fold diluted solution of sample D

Sample name	Proposed method: BF_4^- added/ mg l^{-1}	Proposed method: BF_4^- found/ mg l^{-1}	Recovery of added BF_4^-: mg l^{-1}	Recovery of added BF_4^-: %
A′	None	0.387	—	—
	0.100	0.481	0.094	94.0
	0.300	0.695	0.308	103
	0.500	0.884	0.497	99.4
C′	None	0.259	—	—
	0.100	0.357	0.098	98.0
	0.300	0.572	0.313	104
	0.500	0.755	0.496	99.2
D′	None	0.450	—	—
	0.100	0.554	0.104	104
	0.300	0.747	0.297	99.0
	0.500	0.953	0.503	101

Removal of Nitrate Interference

As shown in Table 2, nitrate seriously interferes with the determination of tetrafluoroborate by being similarly extrac-

Table 5 Application of proposed method to the analysis of waste water samples (concentrations given in mg l^{-1})

Sample*	BF_4^- found (A)	F in BF_4^- (B)	F^- (C)	Calculated total fluoride (D) = (B) + (C)	Measured total fluoride†
1	33.1	29.0	92.4	121.4	122
2	30.8	27.0	1.8	28.8	28.2
3	31.7	27.8	8.7	36.5	39.0
4	11.3	9.9	4.9	14.8	17.3
5	5.0	4.4	7.7	12.1	13.4

* Sample size = 20 ml of a 100-fold diluted sample.

† Total fluoride concentration was measured spectrophotometrically using lanthanum Alizarin Complexone after separation of fluoride by distillation.

ted. As hydrofluoric acid is used as a mixture with nitric acid in etching and other operations, nitrate interference causes a serious problem in the analysis of waste waters.

In order to attempt to decompose nitrate by reduction to other species some common reductants, such as copper powder, Devalda's alloy, hydroxylammonium chloride, hydrazinium sulfate and zinc powder, were examined. It was found that zinc powder was the most satisfactory because of low reagent blanks obtained and its ease of handling. An IC study showed that none of the nitrate remains in the samples treated with zinc powder. Fig. 4 shows the effect of time of reduction on the determination of tetrafluoroborate at different concentrations of nitrate. It can be clearly seen that up to 100 mg l^{-1} of nitrate does not interfere with the determination. Nearly identical calibration graphs were obtained both with and without the reduction process.

Precision and Detection Limit

The precision of determination is shown in Table 3 and the detection limit (defined as the concentration corresponding to a three times the standard deviation of the reagent blank) was found to be 0.009 mg l^{-1}. The absorbance of the reagent blank for this method is about 0.02.

Application to Waste Water Samples and Recovery Test

The proposed method was applied to the analysis of various waste water samples. Table 4 shows the results of the analyses of the original samples and samples to which known amounts of tetrafluoroborate had been added. The recovery of the spiked tetrafluoroborate was almost quantitative.

Tetrafluoroborate in waste water samples treated by different methods of fluoride removal was also determined by the proposed method. Determination of total fluoride and free fluoride ion was also carried out. Total fluoride was determined spectrophotometrically using lanthanum Alizarin Complexone after separation of the fluoride by distillation. Free fluoride was determined potentiometrically by using an ion-selective electrode. The results are summarized in Table 5. Sample 1 is the original waste water sample and the others are treated waters. The sum of the concentrations of free fluoride and that in the form of tetrafluoroborate agrees very well with the total fluoride concentration determined after separation of total fluoride by distillation. This result indicates that most of the fluorine in these samples is present as free fluoride and tetrafluoroborate. Other forms of fluoroborates (*i.e.*, hydroxyfluoroborates), if any, must be hydrolysed rapidly.[8,9]

Conclusion

The proposed method is applicable for the determination of tetrafluoroborate in waste water with good precision.

References

1 Ducret, L., *Anal. Chim. Acta*, 1957, **17**, 213.
2 Pasztor, L., Bode, J. D., and Fernando, Q., *Anal. Chem.*, 1960, **32**, 277.
3 Cizek, Z., and Studlarova, V., *Talanta*, 1984, **31**, 547.
4 Mikasa, H., Shirouzu, M., and Hori, Y., *Bunseki Kagaku*, 1991, **40**, 749.
5 Kasahara, I., Ohgaki, Y., Matsui, K., Kano, K., Taguchi, S., and Goto, K., *Nippon Kagaku Kaishi*, 1986, 894.
6 Taguchi, S., Kasahara, I., Fukushima, Y., and Goto, K., *Talanta*, 1981, **28**, 616.
7 Kasahara, I., Kanai, M., Taniguchi, M., Kakeba, A., Hata, N., Taguchi, S., and Goto, K., *Anal. Chim. Acta*, 1989, **219**, 239.
8 Wamser, C. A., *J. Am. Chem. Soc.*, 1951, **73**, 409.
9 Mesmer, R. E., Palen, K. M., and Baes, C. F., *Inorg. Chem.*, 1973, **12**, 89.

Paper 3/02488A
Received April 30, 1993
Accepted May 20, 1993

Spectrophotometric Determination of Lipohydroperoxides and Organic Hydroperoxides by Use of the Triiodide–Hexadecylpyridinium Chloride Micellar System

Mª Loreto Lunar, Soledad Rubio and Dolores Pérez-Bendito
Department of Analytical Chemistry, Faculty of Sciences, University of Córdoba, 14004 Córdoba, Spain

The association complex formed between triiodide ion and hexadecylpyridinium chloride (cetylpyridinium chloride; CPC) was used to develop a spectrophotometric method for the determination of hydroperoxides, based on the ability of hydroperoxides to oxidize iodide ion to iodine in an acetic acid medium. The triiodide ion thereby produced associates with CPC cationic micelles, which results in maximum absorption at 500 nm, in addition to substantially increased absorptivity and stability constant for the triiodide complex. The micellar medium allows the determination of various hydroperoxides (hydrogen peroxide, cumene hydroperoxide and *tert*-butyl hydroperoxide) at concentrations between 5×10^{-7} and 2.5×10^{-6} mol l^{-1}, with a molar absorptivity for triiodide ion of $(6.51 \pm 0.08) \times 10^3$ m^2 mol^{-1} (*i.e.*, about three times higher than those typical of methods implemented in aqueous media). The proposed method was successfully applied to the determination of lipohydroperoxides in five commercially available oil samples (olive, sunflower seed, corn, cod liver and linseed) and of various organic hydroperoxides in commercial samples (the recovery of hydroperoxides from heptane ranged between 98 and 106%). The results obtained in the determination of lipohydroperoxides are consistent with those provided by iodimetric titration.

Keywords: *Spectrophotometry; micellar media; organic hydroperoxide; lipohydroperoxide; oil*

Methods for the identification and determination of peroxides are used in a number of major industrial, environmental and clinical applications, yet few of them have proved suitable or reliable for dealing with peroxides at concentrations as low as 1 μmol l^{-1}.[1,2] The most sensitive methods for this purpose are based on fluorimetric detection. Hence, organic hydroperoxides and lipohydroperoxides at concentrations as low as 8 nmol l^{-1} have been determined by fluorimetric oxidation of dichlorofluorescein in the presence of haematin. The assay requires the dichlorofluorescein–hydroperoxide mixture to be incubated in an argon atmosphere for 50 min.[3]

Oxidation of iodide is the most widely used of all reactions in peroxide determinations. Various procedures involving iodide have been designed in order to overcome problems posed by earlier alternatives.[2] Methods based on this reaction involve oxidation of potassium iodide by hydrogen peroxide or organic peroxides, in aqueous or organic medium, in the presence or absence of ammonium molybdate as catalyst. Released iodine is determined by spectrophotometry as triiodide at 352 nm (molar absorptivity 2.3×10^3 m^2 mol^{-1}) or by titration with thiosulfate ion (this procedure is only sensitive to concentrations of approximately 5×10^{-4} mol l^{-1}, as lower concentrations give rise to errors of up to 50%[4]). The primary objective of this work was to develop a quantitative spectrophotometric method for the determination of hydroperoxides at concentrations below 1 μmol l^{-1} by using the oxidation of iodide in a micellar medium.

It is well known that micellar systems can enhance existing analytical methods by considerably improving their sensitivity and selectivity.[5] As regards the spectrophotometric determination of triiodide in micellar media, a direct method for the determination of iodine in the range 1–10 μ mol l^{-1}, based on the increase in the maximum absorbance observed at 360 nm on addition of cetyltrimethylammonium bromide to solutions containing iodine and potassium iodide, was developed.[6] The local concentration of both reagents in the micellar pseudophase also increases the apparent equilibrium formation constant of triiodide ion by a factor of about 50 relative to the aqueous medium. Similar effects have been observed in the presence of other alkylammonium cationic surfactants such as dodecyltrimethylammonium chloride.[7] In this context, it is worth noting the analytical use of the interaction between triiodide ion and hexadecylpyridinium chloride (cetylpyridinium chloride; CPC) micelles.[8] Addition of CPC to aqueous triiodide solutions has been shown to result in a bathochromic shift from 350 nm (the absorption wavelength of the triiodide complex) to 500 nm (the maximum absorption wavelength of the I_3^-–CPC association complex), in addition to a substantial increase in the absorptivity and stability constant of the triiodide complex. These effects can allow one to overcome completely or at least minimize the selectivity and sensitivity problems confronting many of the original spectrophotometric procedures that involve aqueous media for monitoring iodine. In this work, such effects were used for the determination of hydrogen peroxide and organic hydroperoxides. Under the experimental conditions used, the molar absorptivity of the triiodide ion was found to be $(6.51 \pm 0.08) \times 10^3$ m^2 mol^{-1} (*i.e.*, approximately 2.8 times that in water). The proposed method is considerably more sensitive than the recommended enzymic and non-enzymic spectrophotometric methods for the determination of hydroperoxides in the range 1–10 μmol l^{-1}.[1]

To the authors' knowledge, only the spectrophotometric methods using the *leuco* base of Methylene Blue ($\varepsilon = 7720 \pm 390$ m^2 mol^{-1}) or its *N*-benzoyl derivative ($\varepsilon = 15\,500$ m^2 mol^{-1}) are more sensitive.[9,10] These methods, however, suffer from serious drawbacks, so many analytical chemists in need of reliable trace-level analyses for peroxides have turned away from them. Hence, preparing pure enough *leuco* Methylene Blue reagent is rather difficult; also, oxygen and steam cause the dilute reagent solution to decay during storage and must, therefore, be scrupulously removed. On the other hand, both methods are highly sensitive to light, which must be excluded during the determination; in addition, the reaction with peroxides is relatively slow[2] (benzoyl peroxide takes about 30 h to react fully in the method based on the *N*-benzoyl derivative).

The proposed method was succesfully applied to the determination of lipohydroperoxides in oil samples and of organic hydroperoxides in hydrocarbon samples, with a detection limit of about 2×10^{-7} mol l^{-1} hydroperoxide.

Experimental

Apparatus

Kinetic measurements were performed on a Hitachi (Tokyo, Japan) U-2000 spectrophotometer fitted with 1 cm pathlength cells. The spectrophotometer cell compartment was thermostatically controlled by circulating water from a Neslab (Newington, NH, USA) Model RTE bath with a temperature stability of ±0.1 °C throughout.

Reagents

All the chemicals used were of analytical-reagent grade and were utilized as purchased, without further purification. Distilled water was used throughout. Solutions (1.25×10^{-2} mol l^{-1}) of hydrogen peroxide and *tert*-butyl hydroperoxide were prepared in water. A 1.25×10^{-2} mol l^{-1} solution of cumene hydroperoxide was prepared in ethanol. More dilute solutions (5×10^{-4} mol l^{-1}) were prepared from these stock solutions before each set of experiments by appropriate dilution with doubly distilled water. A 4.1 mol l^{-1} potassium iodide solution was prepared and stored in a dark glass bottle. A 1.4×10^{-3} mol l^{-1} solution of CPC was prepared by dissolving the required amount of the surfactant in distilled water. Analytical-reagent grade glacial acetic acid and chloroform were also used.

General Procedure for Calibration With Hydrogen Peroxide

A calibration graph was obtained as follows: to a 10 ml calibrated flask were added, in sequence, between 0.2 and 1 ml of 5×10^{-4} mol l^{-1} hydrogen peroxide, 1.5 ml of glacial acetic acid, 0.1 ml of 4.1 mol l^{-1} potassium iodide and distilled water up to a final volume of 2.6 ml. The mixture was swirled gently for 1 min, allowed to stand in the dark for 5 min and diluted to the mark with distilled water. A 0.5 ml aliquot of this solution was placed in a 10 ml calibrated flask. The triiodide content of each aliquot was determined as follows: 0.25 ml of 1.4×10^{-3} mol l^{-1} CPC was added, the stop-clock was started and the mixture was diluted to the mark with water. A portion of the reaction mixture was then transferred into a cell kept at 20 ± 0.1 °C, and the absorbance of the solution at 500 nm was measured as a function of time until the maximum absorbance signal was attained. Measurements were started exactly 1 min after the CPC was added and the maximum absorbance signal was generally obtained within 4 min. A blank solution containing no hydrogen peroxide was prepared and analysed similarly for each series of samples, and the resulting absorbance was subtracted from that yielded by the samples.

Procedure for the Determination of Lipohydroperoxides in Oil Samples

An accurately weighed amount of the oil (0.02–0.5 g) was placed in a 25 ml beaker and to this sample were added, in sequence, 1 ml of chloroform, 1.5 ml of glacial acetic acid and 0.1 ml of 4.1 mol l^{-1} potassium iodide. The contents of the beaker were swirled gently for 1 min and allowed to stand in the dark for 5 min, after which, 8.4 ml of distilled water were added. Immediately afterwards between 0.2 and 1 ml of the aqueous phase was pipetted into a 10 ml calibrated flask, and the triiodide content of this solution was determined as described above for the determination of hydrogen peroxide. A similarly prepared blank solution containing no oil was also analysed and the resulting absorbance was subtracted from that yielded by the samples.

The calibration graph established for hydrogen peroxide determination was used to determine lipohydroperoxides, which were expressed as 'active peroxide concentrations' (mequiv kg^{-1} of peroxide in oil). (The conversion factor of mmol to mequiv is 2.)

Procedure for the Determination of Hydroperoxides in Hydrocarbon Samples

A 10 ml hydrocarbon sample was extracted with two 2 ml portions of 1% sodium hydroxide in ethanol. If the hydrocarbon and ethanolic phases proved to be miscible, the required phase was reclaimed by extraction with 1% sodium hydroxide in ethanol–water (1 + 2 or 1 + 3). The extracts were collected together in a 10 ml calibrated flask and diluted to the mark with distilled water. A solution volume of <1 ml was pipetted into a 10 ml calibrated flask and to this were added, in sequence, 1.5 ml of glacial acetic acid, 0.1 ml of 4.1 mol l^{-1} potassium iodide and distilled water up to a final volume of 2.6 ml. The contents of the flask were swirled gently for 1 min, allowed to stand in the dark for 15 min and diluted to the mark with distilled water. The triiodide content of a 0.2–1 ml aliquot of this solution was determined as described above for hydrogen peroxide. A blank solution containing the required concentration of ethanolic sodium hydroxide was prepared and analysed similarly and the resulting absorbance was subtracted from that yielded by the samples.

The calibration graph established for hydrogen peroxide determination was used to determine hydroperoxides, which were expressed as 'active peroxide concentrations' (mmol l^{-1} of peroxide in the sample).

Results and Discussion

Study of the Hydroperoxide–Iodide System in the CPC Micellar Medium

In order to establish the optimal experimental conditions for determining hydroperoxides by reaction with iodide in the presence of CPC micelles, hydrogen peroxide, cumene hydroperoxide and *tert*-butyl hydroperoxide were used as test materials. Acetic acid was chosen as the reaction medium as it is in this solvent that iodide exhibits its reducing power in full.[2]

Iodimetric procedures exhibit an essentially constant molar response for all reactive peroxide types, thereby allowing a general calibration graph to be obtained for any conveniently available known peroxide. Inasmuch as the reactivity of hydroperoxides is a function of their structure, quantitative reduction is crucial to obtaining a constant absolute response. Under the experimental conditions used to apply the proposed procedures, the reaction between hydrogen peroxide and iodide completed quantitatively in 5 min at room temperature, while cumene and *tert*-butyl hydroperoxide took 15 min. The surfactant (CPC) had no appreciably accelerating effect on these reactions, so it was only added to the reaction medium when triiodide ion was yielded quantitatively. This allowed the hydroperoxide reduction reactions to occur under conditions of higher acidity (a previous dilution was made before measurements because pH values below 2 resulted in rapid decomposition of the triiodide–CPC association complex) and hence more rapidly.

Two steps were considered in optimizing the reaction conditions for the determination of hydroperoxides in the presence of CPC: production of triiodide and formation of the triiodide–CPC association complex. Fig. 1 shows the variation of the absorbance at 500 nm as a function of time when CPC was added to a solution containing triiodide ion. The time at which maximum absorbance was reached was between 2 and 4 min, depending on the hydroperoxide concentration.

Production of triiodide ion in the reaction between hydroperoxides and iodide was essentially affected by the iodide and acetic acid concentrations and the temperature.[2] Fig. 2 shows the final absorbance obtained for a 2×10^{-6} mol l^{-1} hydrogen peroxide concentration as a function of the iodide (*a*) and acetic acid (*b*) concentration after a reaction time of 5 min. Quantitative reaction was only obtained at iodide and acetic acid concentrations above approximately

0.14 and 9 mol l^{-1}, respectively. Iodide and acetic acid concentrations of 0.16 and 10 mol l^{-1} also assured quantitative reaction of cumene and *tert*-butyl hydroperoxide within 15 min. Higher concentrations of these reagents resulted in high blank signals and no further effect on the rate of formation of triiodide ion. The selected concentration of iodide ion (0.16 mol l^{-1}) was high enough relative to that of iodine to avoid errors arising from volatilization of iodine and from addition of iodine to unsaturated materials.[11]

Increased temperatures raised the rate of both the hydroperoxide and blank reactions. No net gain in absorbance was achieved, though, as the reaction temperature was increased. Room temperature was, therefore, believed to be the most suitable.

The experimental conditions under which the triiodide–CPC association complex shows maximum absorbance and stability are reported elsewhere.[8] The iodide concentration must be at least three times higher than the iodine concentration to cause a bathocromic shift in the triiodide spectrum. On the other hand, iodide ion forms an insoluble salt with cetylpyridinium with a solubility product of approximately 5.2×10^{-7} mol^2 l^{-2}. Under the experimental conditions described above for the determination of hydroperoxides, the iodide concentration in the solution prepared for measuring the absorbance of triiodide was 2×10^{-3} mol l^{-1}. This concentration was high enough for the triiodide–CPC association complex to be formed and for precipitation of the iodide–cetylpyridinium salt to be avoided.

The maximum absorbance signal at 500 nm for the triiodide–CPC association complex was observed at pH values between 2 and 10. Although triiodide was produced below pH 2 under the proposed experimental conditions, the solutions used to form the triiodide–CPC association complex had pH values of approximately 3 after pertinent dilution. Increased temperatures had an adverse effect on the absorbance at 500 nm of the triiodide–CPC association complex, which remained virtually constant between 10 and 20 °C.

Fig. 3 shows the absorbance maximum obtained as a function of the CPC concentration. A break point appeared at about 1.8×10^{-5} mol l^{-1} CPC, above which the absorbance remained constant throughout the range examined. A 3.5×10^{-5} mol l^{-1} CPC concentration was chosen as optimal.

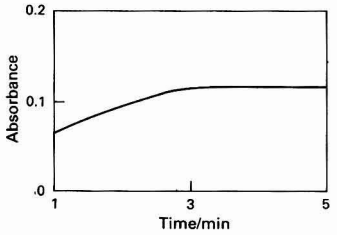

Fig. 1 Absorbance *versus* time plot for the triiodide–CPC association. $[H_2O_2] = 1 \times 10^{-6}$ mol l^{-1}. (For experimental conditions, see text.)

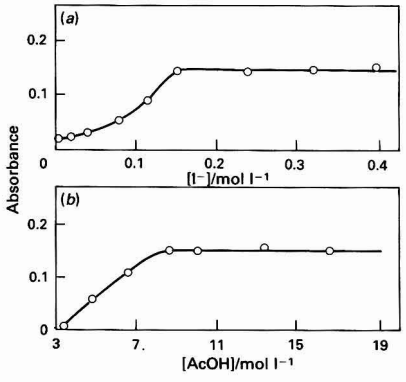

Fig. 2 Influence of the concentration of (*a*) iodide and (*b*) acetic acid on the absorbance of the reaction between iodide and hydrogen peroxide at a fixed time of 5 min. [The concentrations given in the figure are referred to the solution volume (2.6 ml) where triiodide was produced.]

Analytical Figures of Merit

Absorbance *versus* peroxide concentration calibration graphs were established for hydrogen peroxide, cumene hydroperoxide and *tert*-butyl hydroperoxide (Fig. 4). The experimental conditions used to determine the organic hydroperoxides were identical with those used for the determination of hydrogen peroxide, except that a time of 15 min was needed for the respective redox reactions to go to completion. The absorbances for the different hydroperoxides fell roughly on the same line, so the same calibration plot was used for all the samples. Alternatively, a regression equation could be used. As hydrogen peroxide was the most reactive species, it was used as a calibration standard. The determination of these hydroperoxides was feasible over the linear range (5–25) $\times 10^{-7}$ mol l^{-1}.

The standard error of the estimate was 7×10^{-3} absorbance units and the correlation coefficient was 0.992 ($n = 7$). The molar absorptivity was $(6.51 \pm 0.08) \times 10^3$ m^2 mol^{-1}. The detection limit (3σ) was 2×10^{-7} mol l^{-1} hydroperoxide. Finally, the precision of the proposed method, expressed as the relative standard deviation, was 2.3% ($n = 11$) for a 1×10^{-6} mol l^{-1} hydroperoxide concentration.

Determination of Lipohydroperoxides in Oil Samples

The iodide method most widely used for the determination of peroxides in fats and oils involves use of potassium iodide in

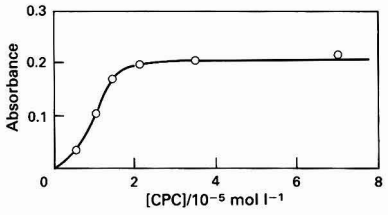

Fig. 3 Influence of the concentration of CPC on the absorbance of the triiodide ion produced from the iodide–hydrogen peroxide system at a fixed time of 5 min. (For experimental conditions, see text.)

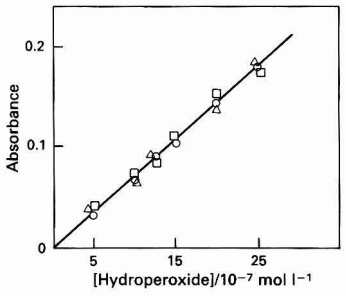

Fig. 4 Calibration graphs for (○) hydrogen peroxide; (△) cumene hydroperoxide; and (□) *tert*-butyl hydroperoxide. Times of triiodide production: (○) 5 min; and (△, □) 15 min. (For experimental conditions, see text.)

acetic acid–chloroform (3 + 2 or 2 + 1) at room temperature. The spectrophotometric determination of the triiodide produced has a serious drawback: the high absorption of fat and oil matrices at 360 nm, where the triiodide species absorbs maximally. For this reason, titration of triiodide with thiosulfate is the most commonly used procedure to determine the peroxide content in these types of sample.[12] The bathochromic shift that CPC causes in the maximum absorption of triiodide ion (λ_{max} = 500 nm) makes the iodimetric spectrophotometric method selective enough to permit reliable determinations of the peroxide content of fats and oils. In addition, the molar absorptivity for the absorption at 500 nm of the triiodide–CPC association complex (approximately 6510 m^2 mol^{-1}) makes it highly suitable for this application.

The reactivity of the lipohydroperoxides towards iodide ion was found to be similar to that of hydrogen peroxide. Accordingly, the calibration graph for hydrogen peroxide determination was also used for the lipohydroperoxides, values being expressed as 'active peroxide concentrations' (mequiv kg^{-1} of peroxide in oil). Acetic acid was used instead of acetic acid–chloroform (3 + 2) to obtain triiodide from lipohydroperoxides in oils in preparing the calibration standards both media provided equivalent results in the determination of hydrogen peroxide. The use of a relatively large excess of iodide (which assured iodine was completely converted into triiodide) and a volume of aqueous phase ten times higher than that of the organic phase ensured virtually quantitative extraction of the iodine, produced in the chloroform, into the aqueous phase. As the chloroform phase was slightly coloured after a few minutes of equilibration between the aqueous and organic phases, the aqueous aliquot used for determination of the triiodide ion was immediately separated from this extraction system, once the aqueous phase (8.4 ml) was added, in order to obtain maximum accuracy.

Table 1 lists the results obtained in the determination of lipohydroperoxides in five commercially available oil samples by the triiodide–CPC method and shows the excellent agreement with those provided by classical iodimetric titration.[12]

Determination of Hydroperoxides in Hydrocarbon Samples

The presence of hydroperoxides in many hydrocarbon distillates has been associated with sediment formation, odour and colour, and studies of hydrocarbon oxidation are in need of sensitive measurements of the hydroperoxide concentration.

Hydroperoxides can be quantitatively extracted from alkyl and aromatic hydrocarbon solutions by using ethanolic sodium hydroxide. Dialkyl and diaroyl peroxides are less acidic than hydroperoxides and do not respond to this treatment. We used this extraction procedure with slight modifications (*viz.*, the volume of hydrocarbon sample and extracts was reduced ten times, *i.e.*, 10 ml instead of 100 ml); ethanol was used instead of methanol, and two extractions were required to complete the recovery of hydrogen peroxide, cumene hydroperoxide and *tert*-butyl hydroperoxide (four extractions are needed in the original extraction procedure).

In order to assess the applicability of the triiodide–CPC method to the determination of hydroperoxides in hydrocarbon samples, commercially available analytical reagent-grade hydrocarbon samples were analysed. Hydroperoxides were undetectable in all instances. The analytical recoveries achieved at three different concentrations (7×10^{-5}, 1×10^{-4} and 2×10^{-4} mol l^{-1}) of hydrogen peroxide, cumene hydroperoxide and *tert*-butyl hydroperoxide added individually to heptane (Merck, Darmstadt, Germany) ranged between 98 and 106% (average of three determinations for each concentration of hydroperoxide). The results show the applicability of the triiodide–CPC method to the determination of hydroperoxides in hydrocarbon samples.

Table 1 Determination of the lipohydroperoxide content of oil samples

	Lipohydroperoxide content/mequiv kg^{-1}	
Oil	Triiodide–CPC method*	Iodimetric titration
Olive	9.9_9	9.7_2
Sunflower seed	8.2_9	8.2_0
Corn	4.3_8	4.4_4
Cod liver	8.7_3	8.7_3
Linseed	5.9_0	7.6_5

* Oil samples of less than 0.2 g were used in every instance.

Conclusions

The use of CPC micelles improves on the sensitivity and selectivity of the most commonly used method for the determination of hydroperoxides, which is based on the oxidation of iodide to iodine by these compounds. The proposed analytical system allows hydroperoxide concentrations below 1 μmol l^{-1} to be determined with a high precision owing to the high molar absorptivity of the triiodide–CPC association complex, which surpasses that of most spectrophotometric methods available for the determination of hydroperoxides. The bathochromic shift undergone by triiodide ion in the micellar medium overcomes one of the most serious problems confronting the spectrophotometric determination of this ion in aqueous media, namely, the strong absorption of many samples (*e.g.*, oils) at 350 nm. Although starch can also be used as a spectral shift reagent, it has so far been limited in its spectrophotometric applications because its molar absorption coefficient depends on the chain length of the starch used. The proposed method is a valid alternative to the iodimetric titration method recommended by the American Oil Chemists' Society for the determination of lipohydroperoxides in oils.[12] Hence, based on the same principle, the triiodide–CPC method is more sensitive, rapid and economic (consumption of reagents and sample is considerably reduced) and less cumbersome than the titrimetric method.

The authors gratefully acknowledge financial support from the CICyT (Project No. PB91-0840).

References

1 Frew, J. E., Jones, P., and Scholes, G., *Anal. Chim. Acta*, 1983, **155**, 139.
2 Mair, R. D., and Hall, R. T., in *Treatise on Analytical Chemistry*, eds. Kolthoff, I. M., and Elving, P. J., Wiley-Interscience, New York, 1971, vol. 14, Part II, p. 295.
3 Cathcart, R., Schwiers, E., and Ames, B. N., *Anal. Biochem.*, 1983, **134**, 111.
4 Heaton, F. W., and Uri, N., *J. Food Sci. Agric.*, 1958, **9**, 781.
5 Hinze, W. L., in *Solution Chemistry of Surfactants*, ed. Mittal, K. L., Plenum, New York, 1979, vol. 1, p. 79.
6 Cuccovia, M., and Chaimovich, H., *Anal. Chem.*, 1982, **54**, 789.
7 Hayakawa, K., Kanda, M., and Satake, I., *Bull. Chem. Soc. Jpn.*, 1979, **52**, 3171.
8 Lunar, M. L., Rubio, S., and Pérez-Bendito, D., *Anal. Chim. Acta*, 1992, **268**, 145.
9 Sorge, G., and Ueberreiter, K., *Angew. Chem.*, 1956, **68**, 486.
10 Eiss, M. I., and Giesecke, P., *Anal. Chem.*, 1959, **31**, 1558.
11 Wagner, C. D., Smith, R. H., and Peters, E. D., *Anal. Chem.*, 1947, **19**, 976.
12 *Official Methods of Analysis of the Association of Official Analytical Chemists*, ed. Horwitz, W., AOAC, Washington, DC, 1975, 12th edn., p. 489, 28.022–28.023.
13 Pobiner, H., *Anal. Chem.*, 1961, **33**, 1423.

Paper 3/00996C
Received February 19, 1993
Accepted April 6, 1993

Determination of Free State Manganese(II) in a Decoction of a Traditional Chinese Medicine Based on a Kinetic Spectrophotometric Method

Liu Jianli,* Wang Budong and Zhang Fenyan
Department of Chemical Engineering, Northwestern University, Xian, Shaanxi, 710069, People's Republic of China

The chemical state of trace elements in decoctions of traditional Chinese medicines is a new research subject in the chemical studies of traditional Chinese medicine. A simple and sensitive kinetic spectrophotometric method is proposed for the determination of free manganese(II). The method is based on the catalytic effect of manganese(II) on the oxidation of Malachite Green by potassium periodate. The reaction was followed spectrophotometrically by measuring the rate of change in the absorbance of the coloured Malachite Green at 615 nm. Trace amounts of manganese(II) (0.2–2 ng) can be determined with good accuracy and reproducibility; the detection limit is about 0.1 ng. Only iron(III) and aluminium(III) interfere in the determination but these can be masked by fluoride. This method has been used to analyse decoctions of traditional Chinese medicines for trace amounts of free manganese(II) without separation.

Keywords: *Free manganese(II) determination; kinetic spectrophotometry; traditional Chinese medicine*

The therapeutic benefit of traditional Chinese medicine (TCM), for the treatment of diseases, is based on the chemical constituents of the individual TCMs. There are thousands of organic constituents in the TCMs, some of which have biological activity, but none act independently and cannot replace the functions of TCM as a whole. Analysis of TCMs revealed that they were rich in many trace elements. It was suggested that this was the major factor in the functions of the TCMs. Trace elements were then determined in different kinds of TCM and compared with each other, in order to find the relationship between the content of trace elements and the functions of the individual TCM. However, the situation is complex, because the functions of the trace elements are critically dependent on their chemical states and environment within the TCM. Different states have different functions, toxicity and percentage absorption by the body. Therefore, research into the functions of trace elements in TCMs must consider their chemical states.[1]

The chemical states in which trace elements are found are free, complexed and organically bound. The major components of TCM are organic compounds, many of which are complex agents. Trace elements co-exist with these organic compounds in a decoction of a TCM, most will be bound to organic compounds; therefore, the concentration of the free trace elements can be very low. In order to find evidence to support the prediction that most trace elements in a TCM exist in the bound state, the free trace elements should be determined initially.

There are many sensitive methods for determining the total concentration of the trace elements present, but these do not differentiate between free and bound states. It was suggested[2] that an ion-selective electrode should be used to determine the free trace elements; however, this was not found to be sensitive enough. We have been unable to find a suitable method in the literature for determining these very low concentrations of trace elements in a decoction of a TCM.

This paper presents a kinetic spectrophotometric method to determine the free state of magnanese(II) in decoctions of TCMs, based on its catalytic effect on the oxidation of Malachite Green by potassium periodate.[3,4] Only iron(III) and aluminium(III) influence the determination and these can be masked by fluoride. Various experimental conditions are discussed in detail. The method has been successfully applied to the determination of free manganese(II) in decoctions of TCMs.

* Present address: Department of Chemistry, University of Manchester, Oxford Road, Manchester, UK M13 9PL.

Experimental

Reagents and Apparatus

All chemicals were of analytical-reagent grade. De-ionized water was used throughout.

Manganese(II) stock solution, 1000 μg ml^{-1}. Prepared by dissolving the appropriate amount of manganese sulfate ($MnSO_4 \cdot H_2O$) in hydrochloric acid. The final concentration was determined by titration with ethylenediaminetetraacetic acid.

Working manganese(II) standard solutions, 10 *and* 0.1 μg ml^{-1}. Prepared by diluting the stock solution.

Malachite Green solution. Prepared by dissolving 0.1572 g of Malachite Green in de-ionized water (1 l).

Potassium periodate. Prepared by dissolving 4.00 g of potassium periodate in de-ionized water (1 l).

Sodium fluoride solution. Prepared by dissolving 0.913 g of sodium fluoride in de-ionized water (1 l).

Buffer solution. Prepared by mixing 10 mol l^{-1} ethanoic acid with 2.6 mol l^{-1} ammonium acetate (1.6 + 1); the pH was 3.8.

A spectrophotometer (Model 721; Shanghai Third Instrument Co.) was used for the absorbance measurements and an electronic thermostated water-bath was used to control the temperature of the reagent solution.

Preparing the Sample Solution

Place 300 g of the TCM in a beaker, add 2000 ml of de-ionized water, decoct until reduced to 1200 ml then filter through four layers of absorbent gauze to remove the solid. Add 2000 ml of de-ionized water to the solid, decoct again until reduced to 1200 ml, filter through four layers of absorbent gauze then combine the filtrates and allow to stand overnight. Afterwards, filter the decoction with a microfilter to remove the granules. The filtrate was used as the sample solution.

Calibration Procedure

Transfer a series of manganese(II) standard solutions into 50 ml calibrated test-tubes fitted with ground-glass stoppers. Add

2.0 ml of buffer solution, 0.8 ml of potassium periodate, 1.0 ml of sodium fluoride, 0.8 ml of Malachite Green solution and dilute to 50 ml with de-ionized water. Place the test-tube into the thermostated water-bath at 40 °C for 30 min. Then, measure the absorbance at 615 nm and prepare a calibration graph of absorbance *versus* concentration of manganese(II).

Procedure for the Determination of Free Manganese(II)

By using 2.0 ml of the sample solution instead of the standard solution the above procedure was repeated and the absorbance measured (A). Take 2.0 ml of the sample solution, omitting the potassium periodate, and measure the absorbance (A'). The change of absorbance ($A' - A$) is due to catalysis by free manganese(II). Calculate the amount of free manganese(II) from the calibration graph prepared previously.

Procedure for the Determination of Total Manganese(II)

Weigh 2.0 ml of the sample solution into a 100 ml beaker, add 10 ml of concentrated nitric acid and heat [**Caution**: Take care to avoid a violent reaction] until a tranquil solution is produced. Cool, then slowly add 5 ml of 60–70% perchloric acid, and heat until brown fumes of nitrogen dioxide appear. If the solution has a dark colour, add 2 ml of concentrated nitric acid and continue heating until white fumes of perchloric acid appear. Continue heating until evaporated to near dryness. Then, dissolve the residue in dilute hydrochloric acid (0.1 mol l^{-1}). Use this sample instead of the standard solution in the above procedure, and measure the absorbance. Calculate the total amount of manganese(II) from the calibration graph.

Results and Discussion

Absorption Spectrum

An absorption spectrum was obtained by plotting absorbance against wavelength. The spectrum exhibited an absorption maximum at 615 nm.

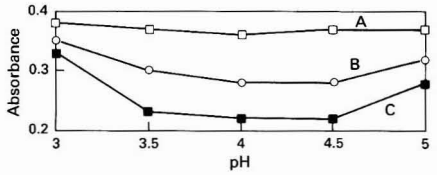

Fig. 1 Relation between pH and absorbance. A, Blank; B, 0.4 ng ml^{-1} Mn; and C, 0.8 ng ml^{-1} Mn

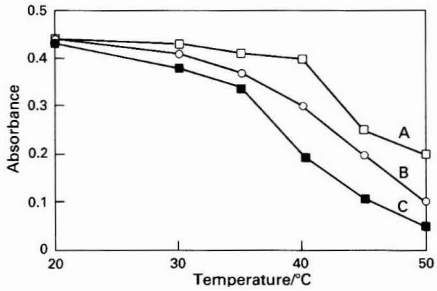

Fig. 2 Relation between temperature and absorbance. A, Blank; B, 0.4 ng ml^{-1} Mn; and C, 0.8 ng ml^{-1} Mn

Effect of pH

The influence of pH on the determination was studied by altering the pH while keeping the other conditions constant. The relation between the pH value and the rate of the catalytic reaction is shown in Fig. 1. The optimum pH range was 3.5–4.5. Outside this range, the rate of the catalytic reaction is slow and the difference between the different concentrations of manganese(II) becomes less.

Effect of Temperature

The effect of temperature was studied between 20 and 60 °C while keeping the other conditions constant. The relation between temperature and the rate of the catalytic reaction is shown in Fig. 2. The optimum temperature was 35–45 °C. If the temperature is below 35 °C, the rate of the catalytic reaction is slow and there is only a small absorbance difference between the different concentrations of manganese(II). If the temperature is higher than 45 °C, the rate of the uncatalysed reaction increases and the absorbance becomes too small to determine accurately.

Effect of Reaction Time

The influence of reaction time was studied by using a 2 ng manganese(II) standard solution and measuring the absorbance, as above, at different times. The relation between reaction time and the rate of the catalytic reaction is shown in Fig. 3. The optimum reaction time is about 30 min. If the reaction time is too short, there is insufficient change of absorbance to determine accurately. If the reaction time is too long, the absorbance is too low to determine accurately.

Effect of Reagent Volume

The effects of the volumes of reagents were studied by altering each one in turn while keeping the others constant. The volumes chosen were those which yielded the maximum slope for the calibration. The optimum conditions obtained were as follows: potassium periodate, 0.8 ml; Malachite Green, 0.8 ml; NaF, 1.0 ml; and buffer solution, 2.0 ml.

Interference Studies

The interference effects of many cations and anions on the kinetic determination of manganese(II) were examined: 10000-fold excesses of Na^+, Cl^-, Pb^{2+}, NO_3^-, K^+, Br^-, SO_4^{2-}, Cu^{2+}, Hg^{2+}, Mo^{VI}, 2000-fold excesses of Co^{2+}, Ca^{2+}, Zn^{2+}, Mg^{2+}, Cr^{3+}, I^- and 1000-fold excesses of Ag^+, V^V, Ni^{2+}, did not interfere with the determination of manganese(II). The only interference observed was by Fe^{III} and Al^{III} and these can be masked by fluoride.

There are many kinds of organic compounds in a decoction of a TCM. If these compounds react with potassium periodate or Malachite Green and form new compounds that absorb at 615 nm they will interfere. In the procedure for the determina-

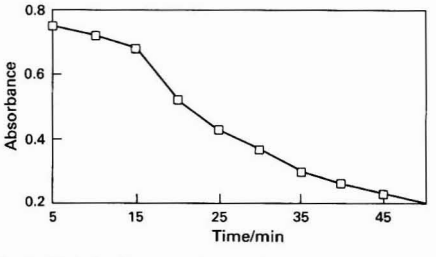

Fig. 3 Relation between the reaction time and absorbance

tion of free manganese(II), $A' - A$ subtracts the interference from the reaction between the compounds in the decoction and the Malachite Green. As there was no difference in absorbance between omitting the Malachite Green and omitting both the Malachite Green and the potassium periodate in the above procedures, this confirmed that there was no reaction, between compounds in the decoction and the potassium periodate, that produced an absorbance at 615 nm. Therefore, there was no interference in the determination of free manganese(II) by using this procedure.

Applications of the Method

A calibration graph was prepared under the optimum conditions described above. The range of linearity was 0.2–2 ng ml^{-1}, the detection limit was 0.1 ng ml^{-1}, the relative standard deviation was 3.6% for nine determinations of 1.0 ng ml^{-1} of manganese(II).

Recovery experiments were carried out by adding 2.0 μg of manganese(II) to decoctions of the TCMs. The total amount of manganese(II) was determined and the recovery calculated; this is the total recovery. The recovery of the separated free and bound states could not be obtained, because of the complex equilibrium reaction between the free and complexed states of the manganese(II). When free manganese(II) was added to the decoctions, some free manganese(II) might change to the bound state. The results are shown in Table 1.

Table 1 Recovery of manganese from TCMs

Sample	State	Mn present/ μg ml^{-1}	Mn added/ μg ml^{-1}	Mn found/ μg ml^{-1}	Recovery (%)
Cinnamoum cassia Presl	Free	0.039			
	Total	2.45	2.00	4.21	90
	Free (%)	1.6			
Zingier officinale Rosc.	Free	0.002			
	Total	5.1	2.00	6.83	95
	Free (%)	0.04			
Paeonia lactiflora Pall	Free	0.004			
	Total	2.32	2.00	4.37	102
	Free (%)	0.17			
Glycyrrhiza uralensis Fisch	Free	0.015			
	Total	1.90	2.00	3.84	97
	Free (%)	0.78			

The proposed method was used to determine the free and total amount of manganese(II) in decoctions of the TCMs. The results in Table 1 show that most of the manganese(II) in the decoctions exists in the bound state, only very low concentrations are in the free state. Therefore, a study of the functions of trace elements in a TCM must consider the chemical states. The bound state might play a more important role than the free state.

Conclusion

A spectrophotometric method was used to determine quantitatively the free manganese(II) in decoctions of TCMs without separation. The method has a low detection limit and does not suffer interference from inorganic ions and organic compounds. It might be suitable for the determination of free manganese(II) in other complex systems.

This project was supported by the National Natural Science Foundation of China. The authors thank Janet Large for the revision of English in this manuscript.

References

1 Liu, J., *Weiliang Yuansu*, 1991, Suppl. 38.
2 Zhu, T., *Zhong Chao Yao*, 1990, **21**(10), 37.
3 Liu, Z., *Huaxue Shijie*, 1983, 45.
4 Zheng, Z., Wang, Y., and Han, L., *Fenxi Huaxue*, 1989, **17**, 160.

Paper 2/04940F
Received September 15, 1992
Accepted April 30, 1993

Nitrogen Factors for Beef: A Reassessment

Analytical Methods Committee*
Royal Society of Chemistry, Burlington House, Piccadilly, London, UK W1V 0BN

Nitrogen factors (the percentage of nitrogen on a fat-free basis) for beef were estimated using a total of 43 clean beef carcases and 30 cull cow carcases from six commercial abattoirs. The sample included carcases representative of the European Community classification ranges for fatness and conformation. The nitrogen factors for the lean meat with intermuscular fat for the whole sides of clean beef and cull cow beef were 3.65 and 3.70, respectively. For beef generally, a nitrogen factor of 3.65 is recommended for use in the analysis of beef and beef products. Nitrogen factors for different commercial joints differed significantly and the appropriate joint value should be used where the nature of the joint is known. Those for cull cow beef were generally higher than those for clean beef. All factors estimated were higher than 3.55, the value recommended for beef by the Analytical Methods Committee in 1963. Fat, moisture, ash, hydroxyproline and nitrogen contents in each joint and also in the side are reported in this paper.

Keywords: *Beef; nitrogen factor; fat; moisture; hydroxyproline*

The Analytical Methods Committee has received and has approved for publication the following report from its Meat Factors Sub-Committee.

Report

The constitution of the Sub-Committee responsible for the preparation of this report was Professor R. A. Lawrie (Chairman), Miss I. Agater (from March 1991), Mr. R. A. Evans, Mr. D. J. Favell, Dr. G. Finney (until December 1991), Mr. M. W. Fogden, Professor R. S. Hannan (until July 1989), Mr. A. J. Harrison, Mr. N. Harrison, Dr. G. Hodson [Ministry of Agriculture, Fisheries and Food (MAFF) Project Officer, until April 1989], Dr. R. B. Hughes, Dr. A. J. Kempster, Mr. R. S. Kirk, Miss D. B. Lowe, Dr. R. L. S. Patterson, Mrs. K. Swan, Dr. R. Wood (MAFF Project Officer) and Dr. M. L. Woolfe (MAFF Project Officer, from April 1989), with Mr. J. J. Wilson as Secretary.

Introduction

The nitrogen factor (the percentage of nitrogen on a fat-free basis) currently used in estimating the meat content of beef and beef products was established by the Analytical Methods Committee of the Society for Analytical Chemistry in 1963.[1] The recommendation was that an average nitrogen factor of 3.55 was the best compromise for general use. This factor was based on the fat-free nitrogen of the raw comminuted lean meat with intermuscular fat, in the whole side.

As there have been major changes in beef production over the past 20 years, with greater use of continental beef breeds and more Canadian Holstein blood in dairy-bred calves, this study was carried out to provide an up-to-date factor and to examine the chemical composition of beef joints in more detail than before. It was part of a larger study carried out in order to determine the over-all chemical composition of clean beef (cattle not used for breeding) and cull cow beef (beef from cows that are no longer economically productive), which included lipid content and fatty acid profiles. These aspects will be the subject of a further paper by the Meat and Livestock Commission (MLC).

* Correspondence should be addressed to the Secretary, Analytical Methods Committee, Analytical Division, Royal Society of Chemistry, Burlington House, Piccadilly, London, UK W1V 0BN.

Experimental

The Meat Factors Sub-Committee worked closely with the MLC, the Lancashire County Council Laboratory (LCC) and five specified independent laboratories on the design and implementation of the study in all respects as it related to nitrogen factors for beef. Particular attention was paid to full compliance with written detailed protocols (approved by the Meat Factors Sub-Committee) for carcase selection, dissection, sample preparation, packaging and labelling, analytical test methods and quality control.

Forty-three clean beef carcases and 30 cull cow carcases were included in the trial. Carcases were selected at the abattoir to fall into specific conformation and fat class cells. Conformation is a subjective assessment of the surface shape of a carcase, made on the slaughterline; a carcase of conformation 'U' has more convex surfaces and thicker musculature than a carcase of conformation 'P'. An MLC 15-point numerical scale is used in the selection of carcases with an acceptability range for each European Community (EC) class. Fat classes describe the amount of fat cover on the surface of the carcase. Approximate percentage subcutaneous fat cover (SFe) allows acceptability ranges for each fat class. Details of the EC classifications are given in ref. 2. For statistical analysis the fat and conformation classes of each carcase were converted to 15-point scales (see ref. 3 and Tables 1 and 2).

Clean beef carcases of all three sexual types, *viz.*, steers, heifers and young bulls, were selected from six commercial abattoirs representing a geographical spread. The carcases covered the main EC conformation and fatness classes (Table 3).

Cull cow carcases were sampled from three commercial abattoirs. The abattoirs supplied carcases from 5–10 year old

Table 1 Relationship between the fat classes used in commercial classification and a visual assessment of carcase subcutaneous fat content to the nearest percentage unit (SFe) (from ref. 3)

	SFe	
EC fat class	Range	Mean
1	<4.5	3.00
2		
3	4.5–7.4	6.00
4L	7.5–8.9	8.25
4H	9.0–10.4	9.75
5L	10.5–13.4	12.00
5H	>13.5	15.00

Table 2 Relationship between the conformation classes used in commercial classification and conformation on a 15-point scale (C15) (from ref. 3)

EC confirmation class	C15 Range	C15 Mean
P	1	1.0
O⁻	2–3	2.5
O⁺	4–6	5.0
R	7–9	8.0
U⁻	10–12	11.0
U⁺	13–14	13.5
E	>15	15.0

Table 3 Sampling design of the clean beef trial. AC (acceptability criteria) for fat class as estimated percentage of subcutaneous fat in the carcase (SFe), and conformation on standard MLC 15-point scale. Total sample: 11 young bulls, 21 steers and 11 heifers

Conformation class	Fat class 2 (AC: 3–5)	Fat class 4L (AC: 8–9)	Fat class 5L AC: 11–13)
U⁺/U⁻ (AC: 10–13)	2 young bulls 1 steer	2 young bulls 2 steers 2 heifers	2 steers 2 heifers
R/O⁺ (AC: 4–9)	2 young bulls 4 steers	2 young bulls 4 steers 1 heifer	2 steers 4 heifers
O⁻/P (AC: 1–3)	2 young bulls 3 steers	1 young bull 3 steers 2 heifers	

Table 4 Sampling design of the cull cow trial. Each cell consists of three carcases of each of two age groups (4–7 and 8–10 years). AC (acceptability criteria) for fat class as estimated percentage of subcutaneous fat in the carcase (SFe), and conformation on standard MLC 15-point scale

Conformation class	Fat class 1/2 (AC: 1–5)	Fat class 4L (AC: 8–9)	Fat class 5L/5H (AC: 11–15)
P⁺/P⁻ (AC: 1–2)	6	6	—
O⁻/P⁺ (AC: 1–3)	—	—	6
O⁺/O⁻ (AC: 2–6)	—	6	—
R/O⁺ (AC: 4–9)	—	—	6

cows, covering the complete range of EC fat classes and the poorer conformation classes, *viz.*, R, O and P (Table 4).

Throughout this report the term 'side weight' refers to half of the mass of the dressed cold carcase. The fatness and conformation scales are referred to as SFe and C15, respectively.

Dissection and Chemical Analysis

The left side of each carcase was divided into 15 joints: brisket, jacobs ladder, fore rib, chuck, thin flank, topside, shin, leg, clod, sticking, loin, rump, thick flank, silverside and the fillet, as described by Kempster *et al.*[4] and shown in Fig. 1.

Each joint was separated into its component tissues, *viz.*, lean, intermuscular fat, subcutaneous fat and bone, and the tissues, excluding bone, were macerated. The macerated tissues of shin and leg, and of clod and sticking, were then recombined proportionally by weight on an individual tissue

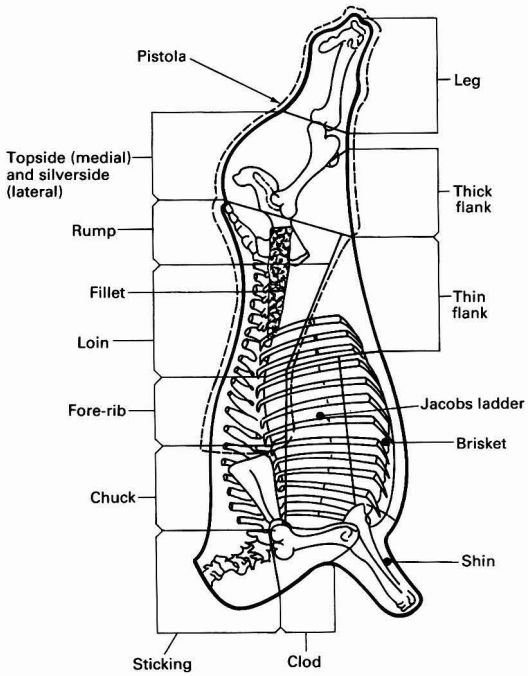

Fig. 1 Standardized joints used in MLC beef dissection technique

Table 5 Grouping of joints into pistola and residual fore quarter

Pistola	Residual fore quarter
Leg	Chuck
Topside	Sticking
Thick flank	Clod
Silverside	Shin
Rump	Jacobs ladder
Fillet	Brisket
Loin	Thin flank
Fore rib	

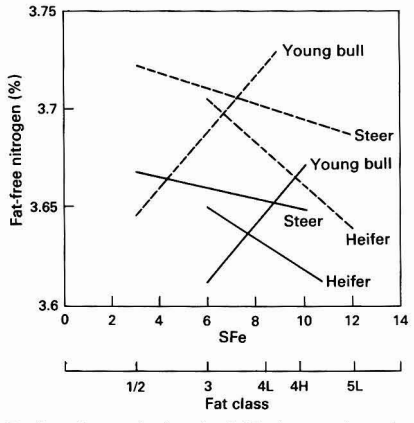

Fig. 2 Fat-free nitrogen in clean beef sides by sexual type in relation to SFe (fat class). Solid lines = lean tissue; broken lines = lean with fatty tissues

basis on all carcases. The loin, rump and fillet, and the thick flank and silverside from cull cow carcases only were recombined in the same way.

The samples, three separate tissues of each joint, were homogenized, stored at −18 °C, and then, in the context of the results reported in this paper, were analysed for lipid, moisture, ash, hydroxyproline and nitrogen contents. The LCC and MLC were the principal laboratories involved in this study. The estimated chemical compositions of the lean with intermuscular fat, and the lean with intermuscular and subcutaneous fats, were constructed mathematically from the components of the individual tissues. The tabulated results therefore show five tissue types. In addition, the estimated chemical compositions of the combined loin, rump and fillet, and the combined thick flank and silverside, were calculated for the clean beef carcases to allow comparison with those of the cull cows.

Industrial practice often separates carcases into pistola and

Table 6 Lean tissue: chemical composition and content in each clean beef joint as a percentage of total lean (standard errors in parentheses)

		Chemical composition (% of tissue)					
	% of total	Lipid	Moisture	Ash	Hydroxy-proline	Nitrogen	Fat-free nitrogen
Brisket	8.58	8.9	69.9	1.01	0.27	3.25	3.57
	(0.114)	(0.33)	(0.28)	(0.008)	(0.010)	(0.019)	(0.018)
Jacobs ladder	8.66	5.3	72.5	1.06	0.27	3.45	3.64
	(0.129)	(0.19)	(0.15)	(0.007)	(0.010)	(0.016)	(0.015)
Fore rib	3.78	7.4	70.6	1.03	0.24	3.39	3.66
	(0.055)	(0.37)	(0.29)	(0.007)	(0.006)	(0.020)	(0.018)
Chuck	15.25	5.9	72.6	1.01	0.29	3.36	3.57
	(0.145)	(0.22)	(0.21)	(0.009)	(0.011)	(0.021)	(0.022)
Thin flank	6.90	6.9	70.9	1.04	0.25	3.43	3.68
	(0.100)	(0.31)	(0.26)	(0.008)	(0.009)	(0.024)	(0.022)
Shin and leg	6.03	2.5	74.2	1.04	0.44	3.61	3.71
	(0.061)	(0.15)	(0.15)	(0.007)	(0.013)	(0.018)	(0.020)
Clod and sticking	10.12	3.8	73.8	1.06	0.35	3.45	3.59
	(0.151)	(0.16)	(0.16)	(0.007)	(0.009)	(0.021)	(0.022)
Topside	9.14	2.8	73.8	1.11	0.18	3.60	3.71
	(0.065)	(0.14)	(0.14)	(0.008)	(0.006)	(0.017)	(0.020)
Loin, rump and fillet	15.00	5.8	71.5	1.06	0.23	3.45	3.66
	(0.109)	(0.22)	(0.19)	(0.008)	(0.009)	(0.017)	(0.014)
Thick flank and silverside	16.54	3.4	73.7	1.08	0.28	3.52	3.64
	(0.112)	(0.15)	(0.14)	(0.005)	(0.026)	(0.021)	(0.021)
Side	100.00	5.1	72.5	1.05	0.28	3.45	3.64
		(0.17)	(0.15)	(0.004)	(0.006)	(0.015)	(0.015)
Pistola	48.32	4.3	72.9	1.07	0.26	3.51	3.67
	(0.177)	(0.16)	(0.17)	(0.005)	(0.007)	(0.016)	(0.016)
Fore quarter	51.67	5.9	72.2	1.03	0.30	3.39	3.61
	(0.177)	(0.19)	(0.17)	(0.005)	(0.010)	(0.015)	(0.015)

Table 7 Intermuscular fat: chemical composition and content in each clean beef joint as a percentage of total intermuscular fat (standard errors in parentheses)

		Chemical composition (% of tissue)					
	% of total	Lipid	Moisture	Ash	Hydroxy-proline	Nitrogen	Fat-free nitrogen
Brisket	19.88	74.7	18.9	0.25	0.46	1.01	4.01
	(0.281)	(0.77)	(0.57)	(0.009)	(0.033)	(0.039)	(0.112)
Jacobs ladder	12.12	73.4	20.4	0.26	0.44	0.97	3.66
	(0.228)	(0.78)	(0.59)	(0.010)	(0.027)	(0.040)	(0.130)
Fore rib	5.38	76.1	17.5	0.31	0.41	1.00	4.17
	(0.106)	(0.83)	(0.59)	(0.026)	(0.025)	(0.041)	(0.093)
Chuck	11.14	71.2	21.8	0.31	0.53	1.08	3.71
	(0.206)	(0.72)	(0.52)	(0.010)	(0.039)	(0.036)	(0.087)
Thin flank	10.56	75.1	18.0	0.23	0.047	1.10	4.41
	(0.282)	(1.06)	(0.66)	(0.008)	(0.039)	(0.064)	(0.136)
Shin and leg	3.05	50.1	36.6	0.42	1.13	2.07	4.14
	(0.129)	(1.27)	(0.86)	(0.011)	(0.063)	(0.081)	(0.098)
Clod and sticking	11.62	69.9	23.0	0.27	0.51	1.13	3.73
	(0.219)	(0.67)	(0.50)	(0.009)	(0.030)	(0.037)	(0.084)
Topside	3.19	64.9	26.2	0.34	0.56	1.35	3.84
	(0.090)	(0.97)	(0.70)	(0.013)	(0.030)	(0.049)	(0.093)
Loin, rump and fillet	12.48	76.8	16.9	0.27	0.39	0.98	4.24
	(0.257)	(0.54)	(0.39)	(0.010)	(0.017)	(0.026)	(0.052)
Thick flank and silverside	10.58	67.6	25.2	0.30	0.56	1.12	3.45
	(0.176)	(0.81)	(0.62)	(0.009)	(0.025)	(0.009)	(0.056)
Side	100.00	72.2	20.9	0.27	0.49	1.08	3.89
		(0.65)	(0.47)	(0.007)	(0.021)	(0.030)	(0.050)
Pistola	33.64	71.2	21.5	0.30	0.40	1.12	3.90
	(0.376)	(0.63)	(0.46)	(0.008)	(0.018)	(0.028)	(0.043)
Fore quarter	66.35	72.7	20.5	0.26	0.48	1.07	3.89
	(0.376)	(0.67)	(0.49)	(0.007)	(0.023)	(0.034)	(0.066)

residual fore quarter parts. The joints included in these are shown in Table 5. The chemical composition of the pistola, the residual fore quarter and the side was additionally calculated.

The analyses carried out by the LCC and MLC laboratories were separately calibrated against the five independent laboratories appointed by the Meat Factors Sub-Committee to be representative of enforcement, industrial and research laboratories (see Appendix). The methods used in the interlaboratory calibration were those of British Standard 4401[5] or approved variants that had been shown to give equivalent results. Additionally, the MLC used CEM[6] methods for fat and moisture determination and these results were reconciled with those obtained from the British Standard methods.[5]

Table 8 Subcutaneous fat tissue: chemical composition and content in each clean beef joint as a percentage of the total subcutaneous fat (standard errors in parentheses)

		Chemical composition (% of tissue)					
	% of total	Lipid	Moisture	Ash	Hydroxy-proline	Nitrogen	Fat-free nitrogen
Brisket	14.53	71.7	21.7	0.22	0.67	1.04	3.61
	(0.349)	(0.97)	(0.70)	(0.012)	(0.033)	(0.059)	(0.120)
Jacobs ladder	6.60	77.8	15.8	0.18	0.60	1.02	4.50
	(0.359)	(1.28)	(0.82)	(0.019)	(0.044)	(0.077)	(0.103)
Fore rib	3.97	85.1	10.5	0.13	0.39	0.66	4.50
	(0.141)	(1.37)	(0.93)	(0.019)	(0.033)	(0.082)	(0.213)
Chuck	7.13	77.3	15.7	0.24	0.65	1.04	4.55
	(0.192)	(1.18)	(0.87)	(0.021)	(0.044)	(0.052)	(0.138)
Thin flank	14.41	74.7	19.1	0.19	0.58	0.95	3.70
	(0.410)	(1.16)	(0.79)	(0.021)	(0.033)	(0.064)	(0.120)
Shin and leg	6.73	49.3	33.7	0.39	1.68	2.76	5.39
	(0.418)	(1.73)	(1.08)	(0.013)	(0.105)	(0.124)	(0.125)
Clod and sticking	7.96	68.5	22.0	0.26	0.86	1.44	4.47
	(0.285)	(1.39)	(0.84)	(0.017)	(0.051)	(0.099)	(0.122)
Topside	7.27	79.6	14.2	0.16	0.64	1.00	4.82
	(0.329)	(0.77)	(0.45)	(0.087)	(0.039)	(0.054)	(0.092)
Loin, rump and fillet	19.85	82.8	12.0	0.12	0.53	0.81	4.63
	(0.405)	(0.73)	(0.42)	(0.010)	(0.032)	(0.059)	(0.140)
Thick flank and silverside	11.55	68.4	21.3	0.23	0.97	1.58	4.92
	(0.396)	(1.26)	(0.84)	(0.013)	(0.052)	(0.080)	(0.119)
Side	100.00	74.3	18.3	0.20	0.72	1.16	4.41
		(0.95)	(0.60)	(0.012)	(0.036)	(0.062)	(0.085)
Pistola	47.58	75.7	16.7	0.18	0.75	1.20	4.85
	(0.606)	(0.99)	(0.61)	(0.016)	(0.060)	(0.068)	(0.101)
Fore quarter	52.42	72.9	19.8	0.22	0.69	1.12	4.07
	(0.606)	(0.98)	(0.65)	(0.012)	(0.034)	(0.060)	(0.083)

Table 9 Lean and intermuscular fat: chemical composition and content in each clean beef joint as a percentage of the total lean and intermuscular fat (standard errors in parentheses)

		Chemical composition (% of tissue)					
	% of total	Lipid	Moisture	Ash	Hydroxy-proline	Nitrogen	Fat-free nitrogen
Brisket	10.23	27.6	55.4	0.80	0.32	2.61	3.61
	(0.147)	(0.69)	(0.53)	(0.010)	(0.012)	(0.028)	(0.018)
Jacobs ladder	9.17	18.4	62.5	0.91	0.30	2.97	3.64
	(0.130)	(0.57)	(0.43)	(0.008)	(0.009)	(0.025)	(0.017)
Fore rib	4.03	20.9	60.2	0.89	0.27	2.92	3.69
	(0.057)	(0.64)	(0.49)	(0.009)	(0.006)	(0.025)	(0.019)
Chuck	14.65	13.1	67.0	0.93	0.31	3.10	3.57
	(0.137)	(0.40)	(0.34)	(0.006)	(0.013)	(0.022)	(0.021)
Thin flank	7.45	21.1	59.9	0.87	0.29	2.94	3.73
	(0.108)	(0.67)	(0.51)	(0.010)	(0.010)	(0.032)	(0.023)
Shin and leg	5.58	6.2	71.4	1.00	0.49	3.49	3.72
	(0.067)	(0.27)	(0.22)	(0.008)	(0.014)	(0.020)	(0.020)
Clod and sticking	10.34	14.7	65.5	0.93	0.37	3.07	3.59
	(0.148)	(0.48)	(0.39	(0.008)	(0.007)	(0.026)	(0.023)
Topside	8.27	6.3	71.2	1.07	0.20	3.48	3.71
	(0.064)	(0.25)	(0.20)	(0.007)	(0.006)	(0.018)	(0.017)
Loin, rump and fillet	14.63	14.8	64.7	0.96	0.25	3.14	3.68
	(0.113)	(0.45)	(0.36)	(0.008)	(0.007)	(0.020)	(0.014)
Thick flank and silverside	15.65	9.6	69.1	1.00	0.31	3.29	3.64
	(0.106)	(0.34)	(0.27)	(0.006)	(0.008)	(0.023)	(0.021)
Side	100.00	14.9	65.0	0.94	0.31	3.10	3.65
		(0.44)	(0.34)	(0.005)	(0.005)	(0.021)	(0.015)
Pistola	46.15	11.4	67.4	0.99	0.28	3.26	3.68
	(0.190)	(0.36)	(0.29)	(0.006)	(0.009)	(0.019)	(0.015)
Fore quarter	53.84	17.9	62.9	0.90	0.33	2.97	3.62
	(0.190)	(0.51)	(0.40)	(0.006)	(0.007)	(0.023)	(0.016)

Results

Clean Beef

An initial data analysis showed that the response of the chemical determinants to changes in the fat index (SFe) depended on the sexual type of the carcase, hence the model for data analysis (including effect of sexual type, regression on side weight and C15) had separate regressions on SFe for each type.

Initially, predictions were made for representative carcases of each sexual type. These were specified as follows:

Steer: side weight 158 kg, conformation R, fat class 4L
Heifer: side weight 130 kg, conformation R/O+ fat class 4L
Young bull: side weight 142 kg, conformation R, fat class 3

The national slaughter population during the sampling period consisted of approximately 57% steers, 26% heifers

Table 10 Lean and fatty tissues: chemical composition and content in each clean beef joint as a percentage of total lean and fatty tissues (standard errors in parentheses)

		Chemical composition (% of tissue)					
	% of total	Lipid	Moisture	Ash	Hydroxy-proline	Nitrogen	Fat-free nitrogen
Brisket	10.57	32.4	51.7	0.73	0.36	2.43	3.60
	(0.152)	(0.75)	(0.57)	(0.010)	(0.012)	(0.030)	(0.019)
Jacobs ladder	8.96	22.1	59.6	0.86	0.31	2.84	3.65
	(0.135)	(0.62)	(0.46)	(0.008)	(0.008)	(0.026)	(0.017)
Fore rib	4.03	25.9	56.3	0.83	0.28	2.74	3.70
	(0.058)	(0.74)	(0.57)	(0.010)	(0.005)	(0.029)	(0.020)
Chuck	14.05	15.8	64.8	0.91	0.33	3.02	3.58
	(0.130)	(0.47)	(0.39)	(0.007)	(0.012)	(0.022)	(0.021)
Thin flank	8.04	28.8	54.1	0.77	0.33	2.65	3.73
	(0.119)	(0.85)	(0.65)	(0.011)	(0.009)	(0.037)	(0.023)
Shin and leg	5.63	9.9	68.1	0.95	0.59	3.43	3.80
	(0.067)	(0.43)	(0.31)	(0.008)	(0.017)	(0.026)	(0.021)
Clod and sticking	10.15	18.2	62.7	0.89	0.40	2.96	3.61
	(0.138)	(0.59)	(0.46)	(0.009)	(0.008)	(0.030)	(0.023)
Topside	8.17	11.6	67.0	1.00	0.23	3.29	3.73
	(0.075)	(0.47)	(0.35)	(0.008)	(0.007)	(0.023)	(0.017)
Loin, rump and fillet	15.12	22.2	59.0	0.87	0.27	2.88	3.70
	(0.116)	(0.63)	(0.49)	(0.010)	(0.007)	(0.027)	(0.014)
Thick flank and silverside	15.28	13.2	66.2	0.95	0.34	3.18	3.66
	(0.110)	(0.44)	(0.34)	(0.007)	(0.009)	(0.025)	(0.021)
Side	100.00	19.7	61.2	0.88	0.34	2.94	3.66
		(0.56)	(0.43)	(0.007)	(0.005)	(0.024)	(0.015)
Pistola	46.26	16.8	63.2	0.92	0.31	3.08	3.70
	(0.175)	(0.50)	(0.39)	(0.007)	(0.009)	(0,022)	(0.015)
Fore quarter	53.74	22.3	59.5	0.85	0.35	2.82	3.63
	(0.175)	(0.61)	(0.47)	(0.007)	(0.007)	(0.026)	(0.016)

Table 11 Regression data for fat-free nitrogen (% of tissue): clean beef sides by sexual type

			Side weight/kg	C15	SFe (%)
Tissue	Sexual type	Constant	X_1	X_2	X_3
Lean	Steer	3.654	0.0001	0.001	−0.003
	Heifer	3.678	0.0001	0.001	−0.008
	Young bull	3.506	0.0001	0.001	0.014
Intermuscular fat	Steer	4.330	−0.0014	−0.006	−0.021
	Heifer	4.288	−0.0014	−0.006	−0.027
	Young bull	4.145	−0.0014	−0.006	0.019
Subcutaneous fat	Steer	6.111	−0.0047	0.005	−0.137
	Heifer	5.916	−0.0047	0.005	−0.122
	Young bull	6.116	−0.0047	0.005	−0.073
Lean with intermuscular fat	Steer	3.688	−0.0001	0.000	−0.002
	Heifer	3.723	−0.0001	0.000	−0.009
	Young bull	3.552	−0.0001	0.000	0.014
Lean with fatty tissues	Steer	3.743	−0.0001	0.001	−0.004
	Heifer	3.779	−0.0001	0.001	−0.011
	Young bull	3.610	−0.0001	0.001	0.014

Fat free nitrogen is given by the following expression:

$$\text{constant} + (X_1 \times \text{side weight}) + (X_2 \times \text{C15}) + (X_3 \times \text{SFe})$$

Example:

The fat-free nitrogen content in the lean with intermuscular fat of a young bull with side weight = 150 kg, conformation R* (equivalent to C15 = 8) and fat class 2* (equivalent to SFe = 3) is given by

$$3.552 + (-0.0001 \times 150) + (0.000 \times 8) + (0.014 \times 3) = 3.579$$

* See Tables 1 and 2 for conversion from EC grades to 15-point scales.

Table 12 Fat-free nitrogen content for the tissues of each clean beef joint and the side (% of tissue)

	Lean	Intermuscular fat	Subcutaneous fat	Lean and intermuscular fat	Lean, intermuscular and subcutaneous fat
Brisket	3.57	4.01	3.61	3.61	3.60
Jacobs ladder	3.64	3.66	4.50	3.64	3.65
Fore rib	3.66	4.17	4.50	3.69	3.70
Chuck	3.57	3.71	4.55	3.57	3.58
Thin flank	3.68	4.41	3.70	3.73	3.73
Shin and leg	3.71	4.14	5.39	3.72	3.80
Clod and sticking	3.59	3.73	4.47	3.59	3.61
Topside	3.71	3.84	4.82	3.71	3.73
Loin, rump and fillet	3.66	4.24	4.63	3.68	3.70
Thick flank and silverside	3.64	3.45	4.92	3.64	3.66
Least significnat difference*	0.07	0.34	0.47	0.07	0.07
Side	3.64	3.89	4.41	3.65	3.66
Pistola	3.67	3.90	4.85	3.68	3.70
Fore quarter	3.61	3.89	4.07	3.62	3.63

* The smallest difference between any two joints that is statistically significant.

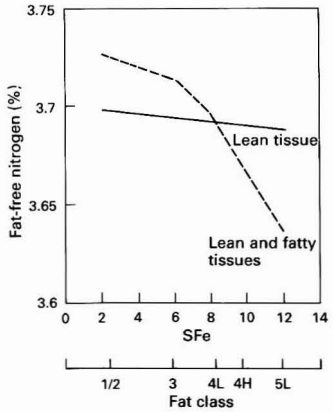

Fig. 3 Fat-free nitrogen in cull cow sides in relation to SFe (fat class)

and 17% young bulls.[7] The means of the three sexual types, weighted in this way, formed the basis for the consolidated clean beef results reported in this paper.

Side weight generally explained little of the statistical variation in the fitted models, but C15 and interactions of SFe with sexual type both contributed significantly to the models. The lipid in the fatty tissues increased at a much greater rate with SFe for the steers and heifers than for the young bulls. The fat-free nitrogen in the lean, and in the lean with fatty tissues, of the side decreased with increasing SFe for steers and heifers but increased for the young bulls, although a typical carcase of each sexual type differed little in its fat-free nitrogen content (Fig. 2). With the exception of the chuck and fore rib, each individual joint showed similar responses, *i.e.*, the fat-free nitrogen increasing with SFe for young bulls while decreasing with SFe for the other two sexual types.

Tables 6–10 show the chemical composition of the five tissue types with the contribution made by each joint to that tissue type in the side. The regressions of fat-free nitrogen in the side on weight, conformation and fatness are shown in Table 11. Table 12 gives the fat-free nitrogen for each joint and tissue with approximate least significant differences. The joints differed significantly in their fat-free nitrogen content, in particular the brisket, chuck, clod and sticking had consistently lower levels in the lean and in the lean with fatty tissues than the other joints. All determined nitrogen factors were greater than the currently recommended factor of 3.55.

Cull Cows

Initial data analysis showed a curved response to differences in SFe for some chemical determinants, especially for lipid. Models with regression on side weight, conformation and both linear and quadratic terms for SFe were therefore fitted. Predictions were made, and are presented, for a typical cull cow carcase of conformation O$^-$, fat class 4L and 135 kg side weight. The response of fat-free nitrogen in lean and in lean with fatty tissues, with fatness level is shown in Fig. 3. Tables 13–17 show the chemical composition of the five tissue types, again with the contribution made by each joint to the total of each tissue type in the side. The relationships between fat-free nitrogen in the side and the independent variables are shown in Table 18.

These regressions show how the fat-free nitrogen factors can be calculated from the important variables.

Table 19 gives the fat-free nitrogen content for each joint and each tissue with approximate least significant differences. Again the joints differed in their fat-free nitrogen contents, the pattern being similar to that for clean beef with the exception of topside, which showed a low value compared with the other joints. In general the nitrogen factors for cull cow beef were greater than those for clean beef, which probably reflects the greater age of the former animals. As with the clean beef data all exceeded the currently recommended figure of 3.55. This figure was markedly higher than the value, namely 3.4, recommended by the Analytical Methods Committee in 1952[8] and it is evident that the nitrogen factor for beef found in the present work of between 3.65 and 3.70, represents an increment of a similar order over the Analytical Methods Committee recommendation made in 1963.

Currently, the estimated national kill of beef animals consists of 20% cull cows and 80% clean beef.[9] Although such a proportion may be rather less appropriate for beef products (in which relatively more cull cow beef may be used), it is suggested that this proportion should be the present basis for establishing the general factor for beef and the factor thus derived from a mathematical recombination of the analytical results obtained is 3.65 (rounded as usual to the nearest 0.05). Beef for processing is often traded on the basis of a prescribed lean-to-fat ratio, *e.g.*, 90% visual lean. A comparison of the fat-free nitrogen figures for lean and lean with fatty tissues shows little differences (Tables 12 and 19). It can therefore be

Table 13 Lean tissue: chemical composition and content in each cull cow joint as a percentage of total lean (standard errors in parentheses)

		Chemical composition (% of tissue)					
	% of total	Lipid	Moisture	Ash	Hydroxy-proline	Nitrogen	Fat-free nitrogen
Brisket	8.85	9.0	69.9	1.00	0.26	3.38	3.71
	(0.187)	(0.51)	(0.38)	(0.024)	(0.009)	(0.038)	(0.034)
Jacobs ladder	8.96	5.5	72.4	1.07	0.26	3.56	3.76
	(0.170)	(0.23)	(0.24)	(0.019)	(0.010)	(0.025)	(0.027)
Fore rib	3.57	8.5	69.7	1.01	0.22	3.45	3.77
	(0.084)	(0.68)	(0.58)	(0.067)	(0.014)	(0.029)	(0.030)
Chuck	15.42	6.2	72.4	0.96	0.27	3.42	3.64
	(0.212)	(0.39)	(0.39)	(0.045)	(0.008)	(0.026)	(0.030)
Thin flank	7.37	3.8	71.3	0.98	0.26	3.48	3.73
	(0.143)	(0.50)	(0.39)	(0.045)	(0.012)	(0.034)	(0.032)
Shin and leg	5.76	2.6	74.7	1.03	0.39	3.71	3.81
	(0.101)	(0.52)	(0.39)	(0.031)	(0.016)	(0.033)	(0.034)
Clod and sticking	9.91	4.0	73.9	1.05	0.30	3.54	3.68
	(0.244)	(0.25)	(0.35)	(0.016)	(0.009)	(0.031)	(0.036)
Topside	8.90	2.1	73.4	1.12	0.19	3.58	3.66
	(0.106)	(0.24)	(0.21)	(0.020)	(0.009)	(0.033)	(0.030)
Loin, rump and fillet	15.53	5.1	71.3	1.04	0.22	3.47	3.66
	(0.174)	(0.46)	(0.34)	(0.014)	(0.009)	(0.028)	(0.024)
Thick flank and silverside	15.73	2.7	73.6	1.02	0.23	3.52	3.62
	(0.186)	(0.37)	(0.24)	(0.040)	(0.010)	(0.030)	(0.034)
Side	100.00	5.0	72.4	1.03	0.25	3.50	3.68
		(0.24)	(0.21)	(0.017)	(0.005)	(0.022)	(0.022)
Pistola	47.42	3.8	72.6	1.04	0.23	3.53	3.66
	(0.330)	(0.29)	(0.20)	(0.019)	(0.007)	(0.025)	(0.024)
Fore quarter	52.58	6.1	72.2	1.01	0.27	3.47	3.70
	(0.330)	(0.27)	(0.29)	(0.024)	(0.006)	(0.022)	(0.024)

Table 14 Intermuscular fat: chemical composition and content in each cull cow joint as a percentage of total intermuscular fat (standard errors in parentheses)

		Chemical composition (% of tissue)					
	% of total	Lipid	Moisture	Ash	Hydroxy-proline	Nitrogen	Fat-free nitrogen
Brisket	18.82	73.5	18.6	0.29	0.47	1.06	4.01
	(0.625)	(1.43)	(1.12)	(0.026)	(0.032)	(0.061)	(0.170)
Jacobs ladder	12.14	73.2	19.8	0.32	0.48	1.04	3.99
	(0.379)	(1.98)	(1.68)	(0.021)	(0.033)	(0.059)	(0.183)
Fore rib	5.67	77.1	15.3	0.32	0.42	0.95	4.13
	(0.295)	(1.58)	(1.31)	(0.025)	(0.029)	(0.060)	(0.157)
Chuck	11.13	70.5	21.8	0.37	0.61	1.13	3.86
	(0.442)	(1.35)	(1.14)	(0.031)	(0.060)	(0.050)	(0.118)
Thin flank	10.89	70.4	19.7	0.31	0.62	1.29	4.27
	(0.518)	(1.94)	(1.40)	(0.024)	(0.059)	(0.120)	(0.221)
Shin and leg	2.74	53.0	33.8	0.43	1.09	1.91	4.04
	(0.232)	(1.99)	(1.52)	(0.027)	(0.075)	(0.132)	(0.180)
Clod and sticking	11.58	71.2	21.2	0.32	0.60	1.14	4.02
	(0.522)	(1.79)	(1.42)	(0.025)	(0.051)	(0.070)	(0.137)
Topside	3.13	67.0	24.3	0.35	0.52	1.26	3.82
	(0.102)	(1.37)	(1.05)	(0.019)	(0.053)	(0.069)	(0.106)
Loin, rump and fillet	13.64	75.7	17.2	0.29	0.44	0.97	4.04
	(0.310)	(1.00)	(0.78)	(0.016)	(0.033)	(0.040)	(0.112)
Thick flank and silverside	10.26	68.4	23.9	0.28	0.58	1.08	3.48
	(0.419)	(1.57)	(1.35)	(0.020)	(0.036)	(0.052)	(0.185)
Side	100.00	71.8	20.2	0.31	0.54	1.11	3.97
		(1.28)	(1.08)	(0.017)	(0.024)	(0.039)	(0.100)
Pistola	34.60	71.7	20.4	0.30	0.52	1.07	3.84
	(0.673)	(1.14)	(0.97)	(0.015)	(0.026)	(0.033)	(0.101)
Fore quarter	65.40	71.9	20.1	0.26	0.63	1.13	4.04
	(0.673)	(1.45)	(1.21)	(0.036)	(0.078)	(0.050)	(0.117)

Table 15 Subcutaneous fat: chemical composition and content in each cull cow joint as a percentage of total subcutaneous fat (standard errors in parentheses)

		Chemical composition (% of tissue)					
	% of total	Lipid	Moisture	Ash	Hydroxy-proline	Nitrogen	Fat-free nitrogen
Brisket	13.83	72.2	20.0	0.23	0.63	1.18	4.21
	(1.055)	(2.57)	(1.99)	(0.024)	(0.085)	(0.099)	(0.171)
Jacobs ladder	6.74	80.2	12.9	0.26	0.49	1.00	4.92
	(0.430)	(3.55)	(2.09)	(0.041)	(0.147)	(0.236)	(0.224)
Fore rib	3.61	87.0	7.9	0.18	0.29	0.65	4.83
	(0.408)	(3.31)	(1.91)	(0.060)	(0.106)	(0.248)	(0.242)
Chuck	6.43	79.7	13.2	0.27	0.56	1.11	5.31
	(0.496)	(2.74)	(1.48)	(0.162)	(0.136)	(0.222)	(0.182)
Thin flank	13.66	73.9	19.0	0.25	0.65	1.11	4.22
	(0.845)	(2.47)	(1.87)	(0.032)	(0.089)	(0.104)	(0.204)
Shin and leg	5.80	51.5	31.1	0.42	1.51	2.64	5.43
	(0.631)	(2.09)	(1.85)	(0.032)	(0.144)	(0.211)	(0.285)
Clod and sticking	7.42	72.6	18.9	0.30	0.72	1.22	4.56
	(0.652)	(2.54)	(2.00)	(0.032)	(0.078)	(0.112)	(0.204)
Topside	6.47	78.9	14.0	0.19	0.66	1.29	6.19
	(0.815)	(2.28)	(1.53)	(0.026)	(0.068)	(0.141)	(0.272)
Loin, rump and fillet	24.71	83.8	10.0	0.17	0.47	0.96	5.86
	(1.361)	(3.42)	(1.87)	(0.034)	(0.133)	(0.274)	(0.228)
Thick flank and silverside	11.33	70.9	19.3	0.28	0.92	1.72	5.91
	(0.743)	(2.48)	(1.53)	(0.039)	(0.113)	(0.200)	(0.355)
Side	100.00	76.3	16.2	0.23	0.65	1.21	5.06
		(2.44)	(1.67)	(0.027)	(0.081)	(0.137)	(0.137)
Pistola	50.54	78.1	14.5	0.21	0.66	1.26	5.71
	(1.743)	(2.49)	(1.50)	(0.027)	(0.097)	(0.183)	(0.169)
Fore quarter	49.46	74.3	18.0	0.26	0.63	1.16	4.50
	(1.743)	(2.53)	(1.83)	(0.035)	(0.078)	(0.116)	(0.145)

Table 16 Lean and intermuscular fat: chemical composition and content in each cull cow joint as a percentage of total lean and intermuscular fat (standard errors in parentheses)

		Chemical composition (% of tissue)					
	% of total	Lipid	Moisture	Ash	Hydroxy-proline	Nitrogen	Fat-free nitrogen
Brisket	10.29	26.1	56.3	0.81	0.31	2.76	3.74
	(0.224)	(1.19)	(0.94)	(0.023)	(0.010)	(0.049)	(0.038)
Jacobs ladder	9.43	18.2	62.5	0.93	0.30	3.09	3.78
	(0.167)	(0.87)	(0.78)	(0.018)	(0.009)	(0.033)	(0.032)
Fore rib	3.88	23.0	58.2	0.87	0.26	2.92	3.80
	(0.093)	(1.18)	(0.96)	(0.051)	(0.015)	(0.042)	(0.031)
Chuck	14.80	13.2	66.9	0.90	0.30	3.17	3.65
	(0.218)	(0.63)	(0.55)	(0.040)	(0.009)	(0.030)	(0.030)
Thin flank	7.88	19.5	60.9	0.85	0.33	3.04	3.77
	(0.164)	(1.11)	(0.88)	(0.036)	(0.013)	(0.045)	(0.036)
Shin and leg	5.32	6.2	71.8	0.98	0.44	3.59	3.82
	(0.102)	(0.71)	(0.51)	(0.028)	(0.017)	(0.038)	(0.033)
Clod and sticking	10.14	15.1	65.2	0.93	0.35	3.14	3.70
	(0.261)	(0.83)	(0.75)	(0.016)	(0.010)	(0.034)	(0.038)
Topside	8.08	5.7	70.6	1.07	0.21	3.45	3.66
	(0.095)	(0.36)	(0.29)	(0.21)	(0.010)	(0.033)	(0.029)
Loin, rump and fillet	15.26	14.2	64.3	0.95	0.25	3.15	3.67
	(0.165)	(0.68)	(0.52)	(0.015)	(0.010)	(0.026)	(0.025)
Thick flank and silverside	14.92	9.1	68.7	0.94	0.26	3.28	3.61
	(0.177)	(0.40)	(0.29)	(0.036)	(0.011)	(0.027)	(0.035)
Side	100.00	14.6	64.8	0.92	0.29	3.16	3.70
		(0.58)	(0.48)	(0.016)	(0.005)	(0.023)	(0.023)
Pistola	45.56	11.2	66.9	0.96	0.26	3.26	3.67
	(0.279)	(0.44)	(0.33)	(0.017)	(0.008)	(0.021)	(0.025)
Fore quarter	54.44	17.5	63.1	0.89	0.32	3.07	3.72
	(0.279)	(0.77)	(0.66)	(0.21)	(0.006)	(0.029)	(0.026)

Table 17 Lean and fatty tissues: chemical composition and content in each cull cow joint as a percentage of total lean and fatty tissues (standard errors in parentheses)

		Chemical composition (% of tissue)					
	% of total	Lipid	Moisture	Ash	Hydroxy-proline	Nitrogen	Fat-free nitrogen
Brisket	10.60	31.2	52.3	0.75	0.34	2.58	3.76
	(0.259)	(1.35)	(1.02)	(0.022)	(0.012)	(0.056)	(0.042)
Jacobs ladder	9.21	22.3	59.3	0.89	0.30	2.94	3.80
	(0.167)	(1.16)	(0.99)	(0.019)	(0.008)	(0.043)	(0.033)
Fore rib	3.85	28.4	54.0	0.81	0.26	2.72	3.80
	(0.099)	(1.19)	(0.96)	(0.046)	(0.018)	(0.043)	(0.030)
Chuck	14.08	15.9	64.7	0.87	0.31	3.08	3.66
	(0.227)	(0.86)	(0.72)	(0.038)	(0.008)	(0.034)	(0.030)
Thin flank	8.39	27.4	54.9	0.77	0.37	2.76	3.80
	(0.206)	(1.41)	(1.12)	(0.031)	(0.017)	(0.058)	(0.041)
Shin and leg	5.34	10.4	68.1	0.93	0.54	3.49	3.90
	(0.109)	(0.97)	(0.67)	(0.025)	(0.023)	(0.056)	(0.034)
Clod and sticking	9.90	18.8	62.3	0.89	0.37	3.02	3.72
	(0.294)	(1.06)	(0.91)	(0.017)	(0.010)	(0.036)	(0.039)
Topside	7.90	10.5	66.9	1.01	0.23	3.31	3.70
	(0.137)	(0.80)	(0.58)	(0.021)	(0.010)	(0.044)	(0.031)
Loin, rump and fillet	16.15	23.9	56.9	0.84	0.27	2.83	3.73
	(0.254)	(1.33)	(0.98)	(0.021)	(0.010)	(0.046)	(0.028)
Thick flank and silverside	14.58	13.2	65.4	0.90	0.30	3.17	3.66
	(0.196)	(0.71)	(0.47)	(0.034)	(0.012)	(0.036)	(0.035)
Side	100.00	20.1	60.6	0.86	0.32	2.97	3.73
		(0.92)	(0.71)	(0.016)	(0.006)	(0.035)	(0.024)
Pistola	46.00	17.6	61.9	0.89	0.29	3.06	3.72
	(0.313)	(0.85)	(0.61)	(0.018)	(0.009)	(0.033)	(0.025)
Fore quarter	54.00	22.2	59.4	0.84	0.34	2.91	3.74
	(0.313)	(1.06)	(0.85)	(0.019)	(0.006)	(0.040)	(0.028)

Table 18 Regression data for fat-free nitrogen in cull cow sides (% of tissue)

				SFe* (%)	
		Side weight/kg	C15	Linear	Quadratic
Tissue	Constant	X_1	X_2	X_3	X_4
Lean	3.583	0.0008	0.005	−0.001	−0.000
Intermuscular fat	3.910	−0.0022	−0.031	0.104	−0.006
Subcutaneous fat	6.543	−0.0057	−0.023	−0.077	−0.000
Lean with intermuscular fat	3.596	0.0007	0.003	0.004	−0.000
Lean with fatty tissues	3.634	0.0006	0.002	0.005	−0.001

Fat-free nitrogen is given by the following expression:

$$\text{constant} + (X_1 \times \text{side weight}) + (X_2 \times \text{C15}) + (X_3 \times \text{SFe}) + (X_4 \times \text{SFe} \times \text{SFe})$$

Example:

The fat-free nitrogen content of the lean with fatty tissues of a cull cow side of weight = 140 kg, conformation P (equivalent to C15 = 1) and fat class 4L (equivalent to SFe = 8.25) is given by:

$3.634 + (0.0006 \times 140) + (0.002 \times 1.0) + (0.005 \times 8.25) + (-0.001 \times 8.25 \times 8.25) = 3.693$

* SFe has both a linear and a quadratic term.

Table 19 Fat-free nitrogen content for the tissues of each cull cow joint and the side (% of tissue)

	Lean	Intermuscular fat	Subcutaneous fat	Lean and intermuscular fat	Lean, intermuscular and subcutaneous fat
Brisket	3.71	4.01	4.21	3.74	3.76
Jacobs ladder	3.76	3.99	4.92	3.78	3.80
Fore rib	3.77	4.13	4.83	3.80	3.80
Chuck	3.64	3.86	5.31	3.65	3.66
Thin flank	3.73	4.27	4.22	3.77	3.80
Shin and leg	3.81	4.04	5.43	3.82	3.90
Clod and sticking	3.68	4.02	4.56	3.70	3.72
Topside	3.66	3.82	6.19	3.66	3.70
Loin, rump and fillet	3.66	4.04	5.86	3.67	3.73
Thick flank and silverside	3.62	3.48	5.91	3.61	3.66
Least significant difference*	0.11	0.57	0.86	0.12	0.12
Side	3.68	3.97	5.06	3.70	3.73
Pistola	3.66	3.84	5.71	3.67	3.72
Fore quarter	3.70	4.04	4.50	3.72	3.74

* The smallest difference between any two joints that is statistically significant.

assumed that a single nitrogen factor is suitable for use with different lean-to-fat ratios.

Recommendations

On the basis of these results the Meat Factors Sub-Committee makes the following recommendations, to be applied as appropriate.

1. A nitrogen factor of 3.65, on a fat-free basis for the lean meat with intermuscular fat, is appropriate when applied to beef generally and should be used in the analysis of beef products.
2. Nitrogen factors of 3.65 and 3.70, on a fat-free basis, should be used when applied to clean beef and cull cow beef, respectively.
3. The factors shown in Tables 12 and 19 are applicable to specific joints and to sides of clean beef and cull cows, respectively, when the source of the beef is thus known.
4. The data given in Tables 11 and 18 allow the calculation of the nitrogen factors for sides of clean beef and cull cows, respectively, when carcase weight and EC fatness and conformation classes are known. Changes to individual joints cannot be calculated from these data. Further advice can be obtained from the MLC.

The Analytical Methods Committee gratefully acknowledges the financial support given by the Ministry of Agriculture, Fisheries and Food, and by the Meat and Livestock Commission, to the work of this Sub-Committee.

Appendix

Statistical Analysis of the Difference Between the LCC and MLC Laboratories and the Data From the Five External Laboratories

Five external laboratories, appointed by the Meat Factors Sub-Committee and taken as a representative sample of all laboratories, were involved in the process of calibrating the results obtained from the LCC and MLC laboratories. The participating laboratories were: (*i*) Unilever Research, Sharnbrook; (*ii*) Laboratory of the Government Chemist, Teddington; (*iii*) Institute of Food Research, Bristol Laboratory; (*iv*) Avon County Council Scientific Services Laboratory, Bristol; and (*v*) Tayside Regional Council Laboratory, Dundee. Tissues from six cull cow carcases and eight clean beef carcases representing the three sexual types and a range of conformation and fatness levels were each analysed by either LCC or MLC and by one external laboratory for lipid, moisture, nitrogen, ash and hydroxyproline contents. The difference was used to adjust all LCC and MLC analytical results so that they were centred around the mean of the interlaboratory calibration laboratories for all determinations. All adjustments were small.

References

1 Analytical Methods Committee, *Analyst*, 1963, **88**, 422.
2 Meat and Livestock Commission, *Beef Yearbook*, MLC, Milton Keynes, Buckinghamshire, 1991, p. 91.
3 Kempster, A. J., Cook, G. L., and Grantley-Smith, M., *Meat Sci.*, 1986, **17**, 107.
4 Kempster, A. J., Cook, G. L., and Smith, R. J., *J. Agric. Sci.*, 1980, **95**, 431.
5 British Standards Institution, BS4401: *Analytical Methods for Meat and Meat Products, Part 1: 1980, Determination of Ash; Part 2: 1980, Determination of Nitrogen, Part 3: 1980, Determination of Moisture; Part 4: 1970, Determination of Total Fat; and Part 11: 1979, Determination of* L-(−)-*Hydroxyproline,* BSI, Milton Keynes, Buckinghamshire.
6 CEM AVC-80, *Moisture and Fat Analyser*, CEM Corp., Matthews, NC, USA.
7 Meat and Livestock Commission, *Beef Yearbook*, MLC, Milton Keynes, Buckinghamshire, 1990, p. 113.
8 Analytical Methods Committee, *Analyst*, 1952, **77**, 543.
9 Meat and Livestock Commission, *Beef Yearbook*, MLC, Milton Keynes, Buckinghamshire, 1991, p. 9.

Paper 3/02842K
Received May 18, 1993

COMMUNICATION

Material for publication as a Communication must be on an urgent matter and be of obvious scientific importance. Rapidity of publication is enhanced if diagrams are omitted, but tables and formulae can be included. Communications receive priority and are usually published within 5–8 weeks of receipt. They are intended for brief descriptions of work that has progressed to a stage at which it is likely to be valuable to workers faced with similar problems. A fuller paper may be offered subsequently, if justified by later work.

Manuscripts are usually examined by one referee and inclusion of a Communication is at the Editor's discretion.

Permeation Tubes for Calibration in Flow Injection Analysis

Stuart J. Chalk and Julian F. Tyson*
Department of Chemistry, University of Massachusetts, Amherst, MA, 01003, USA
Don C. Olson
FIA Solutions, P.O. Box 670786, Houston, TX, 77267, USA

The use of a permeation tube for the production of liquid stream calibration standards in the flow injection determination of ammonia was investigated. By varying the flow rate from 0.5 to 4.0 ml min^{-1}, calibration standards over the range 1.5–0.18 ppm could be produced. The relationship between concentration of the resulting solution and the reciprocal of the flow rate was shown to be linear. The inherent high temperature dependence of the release rate necessitated the tubes being used under thermostated conditions. The release rate was found to vary between 136 and 158 ng min^{-1} cm^{-1} over a 7 d period. Taking all sources of uncertainty into account, the 95% confidence interval for the release rate varied between 12.0 and 16.2 ng min^{-1} cm^{-1} over the same 7 d period. The device was used in a manifold for the determination of ammonia in pond water in which the method of standard additions was employed.

Keywords: *Permeation tube; flow injection; calibration; ammonia determination*

Flow injection (FI) techniques have proved to be useful for the adaptation of a variety of determinations based on aqueous solution reaction chemistry to an automated format. There is considerable interest in the use of FI procedures as the basis of process analysers for on-line monitoring of liquid process streams and waste effluents. A feature of such analysers is the requirement for the production of suitable calibration standards over the relatively long periods of unattended operation.

A number of innovative FI calibration procedures have been described in the past few years.[1–10] Most of these procedures are based on the use of a single concentrated standard from which a set of calibration standards can be produced by a number of dilution procedures that are an inherent feature of the FI dispersion process. Various gradient concentration profiles have been exploited[1–8] for continuous dilution as well as, more recently, the use of a recirculating loop to perform controlled step-wise dilution.[9,10] However, these techniques still require the production of a stock solution on a routine basis and their adaptation to the standard additions format (if needed) is not necessarily straightforward.

In this paper the use of an ammonia permeation tube for calibration of a solution spectrophotometric procedure has been investigated. For the calibration of procedures in which an analyte in a gaseous sample is determined, a range of gas permeation tubes are commercially available (Dynacal permeation tubes, VICI Metronics, Santa Clara, CA, USA). The tubes contain a concentrated solution of the volatile analyte which diffuses, at a known rate, across the tube walls into an acceptor stream containing a diluent gas. The partial pressure of the analyte is inversely proportional to the acceptor stream flow rate. Thus changing the flow rate of the acceptor stream produces different concentrations of analyte.

There are several reports of the determination of ammonia by FI procedures. Spectrophotometric,[11–13] diffusion[14,15] and various other methods[16–18] have been reported. In this paper a method based on the use of Nessler's reagent was employed.[11]

An important parameter for determining whether these devices are useful for on-line calibration is the day-to-day reproducibility of the release rate at a certain temperature. Ideally the device would be calibrated only once, at the beginning of its life. For release into a gaseous stream, VICI Metronics quotes ±1% for the first 3–4 months. After that the stability is dependent on the dryness of the gas used and can vary by up to ±5%. It is likely that over the lifetime of the tube (estimated as 7 months) stability will not be as good because of the release into aqueous solutions. Day-to-day reproducibility of the release rate was investigated along with the variation of release rate with temperature.

Experimental

Apparatus

The manifold (see Fig. 1) was constructed from 0.8 mm i.d. Teflon tubing (Omnifit, New York, NY, USA), polyethylene ethyl ketone (PEEK) nuts and ferrules (UpChurch Scientific, Oak Harbor, WA, USA), and Teflon unions (Omnifit). A six-port rotary injection valve (PhaseSep, Norwalk, CT, USA) with 0.8 mm i.d. Teflon tubing connections was used for

* To whom correspondence should be addressed.

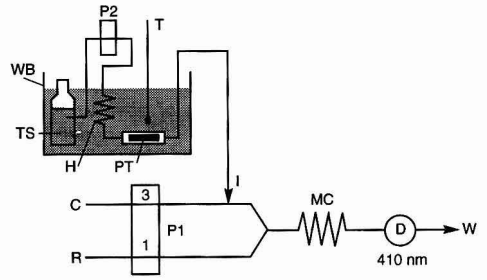

Fig. 1 Schematic diagram of the manifold used for the determination of ammonia with Nessler's reagent. Components are as follows: variable speed peristaltic pumps, P1 and P2 (numbers are approximate flow rates in ml min^{-1}); injection port, I; 25 cm mixing coil, MC; detector, D; waste, W; carrier stream, C; Nessler's reagent, R; tube stream solution, TS; permeation tube, PT; 1.5 m heat exchanger coil, H; thermometer, T; and water-bath, WB. Pulse dampers used in each flow line are not shown

sample injection. Reagent, carrier and permeation tube solutions were pumped using two Ismatec MS Reglo variable speed pumps (Cole-Parmer, Chicago, IL, USA) which were fitted with Tygon pump tubing (Cole-Parmer). The manifold was interfaced to the spectrometer using a 1 cm (18 μl) pathlength flow cell (Pye Unicam, Cambridge, UK). A Perkin-Elmer chemifold block (Perkin-Elmer, Norwalk, CT, USA) was used to merge the reagent and carrier stream. Pulse dampers were made for each line from a T-piece (Omnifit), a piece of Tygon pump tubing and a pump tube connector (Omnifit) which crimped the Tygon tube at one end.

An ammonia, controlled release, Dynacal permeation tube with an active length of 5 cm (6 mm o.d.) (VICI Metronics) was inserted into a 10 cm, 8 mm i.d. glass column (Omnifit) which was fitted with 1/4·28 end-fittings. The permeation device was allowed to rest against the wall of the tube on the rubber seals at each end. The nominal release rate into a gaseous acceptor stream at atmospheric pressure, according to the manufacturer's specifications, was 295 ng min^{-1} cm^{-1} (±10%) at 30 °C.

For temperature control a water-bath (Fisher Scientific, Pittsburgh, PA, USA) was used in conjunction with a 22–28 °C thermometer (Emil Greiner, New York, NY, USA) which was accurate to ±0.01 °C.

Real-time data acquisition of the reaction product peaks was obtained using a Lambda 6 UV/VIS spectrophotometer (Perkin-Elmer). The instrument was interfaced to an IBM PS/2 (IBM, Armonk, NY, USA) running Perkin-Elmer Computerized Spectroscopy Software (PECSS) Version 3.26. A Macintosh SE computer (Apple Computer Inc., Cupertino, CA, USA) was used for data evaluation.

Lambda 6 .SP files were converted to .DX files in the PECSS software and then transferred onto Mac using Apple file exchange (Apple). They were then processed using Excel (Microsoft Corp., Redmond, WA, USA) (removal of header and footer) and imported as text into PeaksDemo (Analog Digital Instruments, Milford, MA, USA) for height/area evaluation.

To aid peak identification a 29-point (optimized for this work) median filter recently described[19] was implemented using Excel before files were imported into PeaksDemo.

Each calibration and sample solution was injected five times. Solutions were de-gassed using nitrogen just prior to use as was the solvent used to make up the off-line standards. Any accumulated precipitate was flushed from the manifold by the passage of 2 mol l^{-1} hydrochloric acid followed by E-pure water.

Flow rates were calculated by timing the collection of the streams in 10 ml calibrated flasks.

Reagents and Samples

Nessler's reagent was made up and stored according to the procedure previously described.[20] The potassium iodide, sodium hydroxide and mercury(II) chloride were all of ACS analytical-reagent grade (Fisher Scientific).

Carrier stream and permeation tube stream solutions of 0.01 mol l^{-1} nitric acid were made by diluting 0.629 ml of concentrated nitric acid (ACS analytical-reagent grade) to 1 l. Sodium hydroxide carrier stream (3 mol l^{-1}) was made by dissolving 120 g of solid in 500 ml of E-pure water, transferred to a 1 l flask and made up to volume.

A 100 ppm stock solution of ammonia (as ammonium ion) was made by dissolving 0.3163 g of ammonium chloride (ACS analytical-reagent grade) in 250 ml of 0.01 mol l^{-1} nitric acid. Standards were made by appropriate dilution of the stock solution.

De-ionized 18 MΩ E-pure water was used throughout. A sample of water was taken from the University of Massachusetts campus pond and was acidified (pH 2) and filtered (0.45 μm) before use.

Method Development

Reaction Chemistry

Initial experiments were conducted with an acid–base indicator (Bromothymol Blue) reaction and without temperature control. The majority of the experiments were carried out using Nessler's reagent.

Most of the experimental work was conducted with an acid acceptor stream flowing around the permeation tube. The effects of the variations of flow rate of the acceptor stream and of its temperature were investigated.

Baseline Noise Reduction

A number of methods for the reduction of baseline noise were investigated, including, the addition of pulse dampers, variation of the mixing device (coil, packed-bed reactor, single bead string reactor, alternating helical reactor and stirred mixing chamber), use of a median filter for post data-acquisition smoothing, and the use of an alkaline acceptor stream.

Calibration for Ammonia

A series of calibration standards (0.2, 0.5, 1.0 and 2.0 ppm) were prepared off-line and five replicate injections of each solution were made. The solutions were prepared by dilution of the 100 ppm standard made up to volume with 0.01 mol l^{-1} nitric acid and were prepared for each calibration of the tube.

The slope of the calibration was calculated by an unweighted least squares procedure for data which did not include a blank value.

Variation of Concentration With Flow Rate

For four values of the flow rate of the acceptor stream, over the range from approximately 0.5 to 4.0 ml min^{-1}, five replicate injections of the resulting ammonia solutions were made. The slope of the plot of concentration (obtained from the absorbance *versus* concentration of the standards prepared off-line) *versus* the reciprocal of the flow rate was calculated by an unweighted least squares procedure for data which did not include blank values.

Calculation of the Release Rate

The release rate of the permeation tube may be calculated from the slope of the concentration *versus* reciprocal flow rate plot, the length of the permeation tube and a conversion factor

for the mass [eqn. (1)]. This gives a result with units that can be compared directly to the manufacturer's nominal value of the release rate into a gas stream.

$$\text{Release rate (ng min}^{-1}\text{ cm}^{-1}) = \frac{\text{calibration slope (}\mu\text{g min}^{-1}) \times 1000\text{ (ng }\mu\text{g}^{-1})}{5\text{ (cm)}} \quad (1)$$

Variation of the Release Rate With Temperature

The change in release rate as a function of temperature may be calculated from eqn. (2)

$$\log (P_2) = \log (P_1) + \alpha(T_2 - T_1) \quad (2)$$

where α is 0.034 °C^{-1}, and P_1 and P_2 are the respective release rates at T_1 and T_2. From the data supplied by the manufacturer, it may be calculated that, if the release rate into a liquid acceptor stream is the same as that into a gaseous stream, the release rate would be 157 ng min^{-1} cm^{-1} at 22 °C. It can also be seen from eqn. (2) that temperature has a significant effect on the release rate. The release rate changes by approximately 11% for every 1 °C increase. Thus a water-bath was used to keep both the permeation tube and the acceptor solution at a steady known temperature for each experiment (see Fig. 1).

A temperature variation study was performed between 22 and 28 °C.

Day-to-day Release Rate Variation

An initial study over a period of 1 week showed possible problems. Five experiments performed on different days produced values varying from 140 to 240 ng min^{-1} cm^{-1}. Modifications to the manifold were made by: (*a*) de-gassing the carrier/tube solutions and the water used for the calibration standards; (*b*) shortening, as much as possible, the tubing out of the water-bath to and from the pump; and (*c*) adding a heat exchanger coil (1.5 m) after the pump, immersed in the water-bath. This minimized any variation in the dissolved gas concentration in the carrier/tube streams and eliminated the possible heating effect of the pump on the tube solution.

Analysis of Pond Water Samples

To test that the system worked with real samples, 500 ml of campus pond water were taken for analysis. Determination of the ammonia concentration was performed using both normal calibration and standard additions (acceptor flow rates of 0.5, 1.0, 2.0 and 4.0 ml min^{-1} in both cases). Standard additions is readily performed using the permeation tube as the different additions can be generated by simply passing the sample over the tube at the different flow rates indicated. An unweighted least squares procedure was again used in the calibrations.

Results and Discussion

Reaction Chemistry

Initial experiments, performed with nitric acid and Bromothymol Blue, gave peak heights which varied with flow rate as expected. However, significant non-zero intercepts were obtained. This and the non-selectivity of the reaction prompted a change to a quantitative chemical system with selectivity for ammonia. Nessler's reaction was chosen because it has a lower detection limit and faster reaction rate in comparison with the indophenol method.[11]

Baseline Noise Reduction

Throughout the experimentation significant baseline noise was observed due to the viscosity difference between the Nessler's reagent and the acid carrier stream (which causes difficulties in obtaining rapid radial mixing downstream of the confluence point), and irregular generation and movement of bubbles through the flow cell. Indeed this is likely to be the reason for the large standard deviation (SD) of the individual results seen in Table 4 as the repeatability of injection of sample and standard solutions was typically poor (5–10%).

An investigation of different mixing devices showed that removal of some of the noise could be achieved. However, this was directly related to an increase in the mixing device volume and thus also resulted in a significant decrease in the sensitivity of the manifold. In addition, the devices did not improve the repeatability of injections and the bubble problem was not removed. The 50 cm coil used in the experiment provided the best manifold stability albeit with a large amount of baseline noise (standard deviation approximately 0.01 absorbance).

Replacing the carrier and acceptor solutions with 3 mol l^{-1} sodium hydroxide improved the repeatability of injection (3–5%). Also the sensitivity was increased by a factor of 2, due to the elimination of a decrease in the hydroxide concentration at the confluence point. No bubbles were seen which suggests that the bubbles seen in the acid manifold were due to de-gassing of the samples as they were basified at the confluence point (the pH of the resulting solution is over 13).

Table 1 Peak height *versus* concentration for ammonia solutions

Concentration (ppm)	Peak height (absorbance)
0.20	0.0235
0.50	0.0576
1.00	0.1170
2.00	0.2500

Table 2 Peak height *versus* reciprocal flow rate for an ammonia permeation tube

(1/flow rate)/ min ml^{-1}	Peak height (absorbance)
1.770	0.2700
0.898	0.1307
0.460	0.0710
0.238	0.0380

Calibration for Ammonia

A typical example calibration for ammonia (Table 1) had a slope of 0.1255 ppm^{-1} and an intercept of −0.005 with a correlation coefficient of 0.9993. No blank was included in the regression analysis.

Variation of Concentration With Flow Rate

Plotting peak height *versus* the reciprocal of the flow rate of the acceptor stream gave good linearity in all experiments (typical $r^2 = 0.999$). Table 2 shows a typical calibration with a slope of 0.1513 ml min^{-1} and an intercept of 7×10^{-5}.

Using the peak heights from this calibration, concentrations of the solutions could be calculated from the off-line calibration. From a plot of concentration *versus* the reciprocal of the flow rate (Fig. 2), it can be seen that the permeation tube shows the same behaviour with a liquid acceptor stream as it does with a gaseous one.

Calculation of the Release Rate

Taking the slope from the concentration *versus* reciprocal flow rate plot (1.20 μg min^{-1}) the release rate of the permeation tube (and the associated error) can be calculated according to eqn. (1). In this example the release rate was found to be 240 ± 23 ng min^{-1} cm^{-1}.

Variation of Release Rate With Temperature

Table 3 shows the results of the release rate variation with temperature. As can be seen the logarithm of the release rate increases linearly with temperature change (compared with the 22 °C value) and the slope is close (0.051 $°C^{-1}$, $r^2 = 0.990$) to that obtained when using the tube with a gas stream (0.034 $°C^{-1}$).

Day-to-day Release Rate Variation

Table 4 shows the results with this modified manifold configuration (Fig. 1) which was the final one used (carrier and acceptor solutions are 0.01 mol l^{-1} nitric acid). These results are much more reproducible and the average release rate (145 ± 15 ng min^{-1} cm^{-1} at 95% confidence) is now closer to the value calculated from eqn. (2). Table 5 shows the results of the same manifold using 3 mol l^{-1} sodium hydroxide instead of 0.01 mol l^{-1} nitric acid for the carrier and acceptor solutions. Surprisingly, the release rate (153 ± 22 ng min^{-1} cm^{-1} at 95% confidence) is equally as stable with a basic acceptor stream as it is with an acidic one. Indeed, as mentioned before, the repeatability of injection was improved, resulting in the lower standard deviations of the calculated release rates.

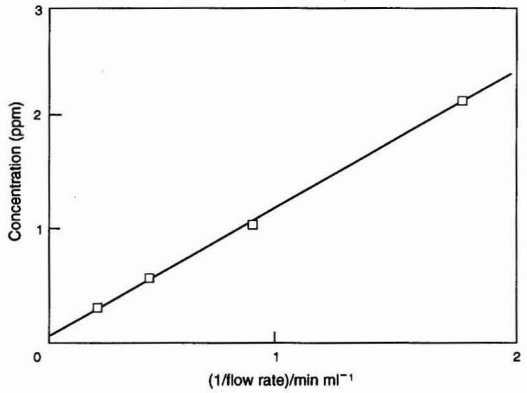

Fig. 2 Concentration *versus* reciprocal flow rate for ammonia permeation tube, $y = 0.0396 + 1.2043x$; $r^2 = 0.998$

Analysis of Pond Water Samples

Pond water ammonia concentrations using normal calibration were found to be 0.82, 0.69 and 0.71 ppm. Using standard additions the same sub-samples were found to have 0.57, 0.55 and 0.57 ppm ammonia, respectively. This clearly shows the possibility of using these tubes for on-line standard additions calibrations.

Conclusion

The use of permeation devices for FI calibration has been shown to be a viable proposition provided certain precautions are taken. The most important of these are the stability and control of the temperature of the tube, and the amount of dissolved gases present in the solutions passing across the tube. However, other important considerations should be taken into account. The stability of the pump used has a direct impact on the concentration of the solutions produced. In these experiments, an eight-roller peristaltic pump was used and a pulse damper had to be installed to minimize pulsations caused by the rollers. Transfer line tubing from the end of the permeation tube column to the injection valve was made of Teflon, the same material as the permeation tube. To reduce any possible losses in this part of the manifold it would be advisable to use a material less permeable to gases, *e.g.*,

Table 3 Variation of release rate with temperature

	Calibration		Tube solutions		Release rate/ ng min^{-1} cm^{-1}			
Temperature/°C	Slope	SD	Slope	SD	Value	SD	ΔT/°C	Log (release rate)
22.25	0.1137	0.0034	0.0803	0.0043	141.2	8.7	0	2.150
24.13	0.1137	0.0034	0.1072	0.0069	188.6	13.4	1.88	2.276
26.01	0.1104	0.0052	0.1251	0.0049	226.6	13.9	3.76	2.355
27.97	0.1104	0.0052	0.1555	0.0050	281.7	16.0	5.72	2.450

Table 4 Variation of release rate over a period of days for 0.01 mol l^{-1} nitric acid carrier and acceptor solutions (using the manifold in Fig. 1)

		Calibration		Tube solutions		Release rate/ ng min^{-1} cm^{-1}	
Day	Temperature/°C	Slope	SD	Slope	SD	Value	SD
1	22.08	0.1070	0.0059	0.0789	0.0047	147.5	12.0
2	22.10	0.1082	0.0079	0.0733	0.0044	135.5	12.8
3	22.01	0.1170	0.0068	0.0922	0.0055	157.6	13.1
4	22.01	0.1105	0.0095	0.0773	0.0060	139.9	16.2

Table 5 Variation of release rate over a period of days for 3 mol l^{-1} sodium hydroxide carrier and acceptor solutions (using the manifold in Fig. 1)

		Calibration		Tube solutions		Release rate/ ng min^{-1} cm^{-1}	
Day	Temperature/°C	Slope	SD	Slope	SD	Value	SD
1	22.06	0.2160	0.0051	0.1684	0.0103	156.0	10.2
2	22.08	0.2016	0.0065	0.1726	0.0061	171.3	8.2
3	22.01	0.2046	0.0056	0.1447	0.0046	141.4	5.9
4	22.01	0.1988	0.0070	0.1415	0.0110	142.4	12.1

PEEK tubing. The device may also be useful for standard additions calibrations, and it has a wide tolerance to the pH (2–14) of the acceptor stream.

Clearly this approach is only applicable to those analyte species for which a suitable permeation tube is available. The manufacturer's current list of approximately 110 species includes a number that are of relevance to industrial processes such as S^{2-}, SO_2, HCN methanol and ethanol. As a variety of tube lengths are available, the release rate may be selected to allow calibration over a wide range of concentrations.

Financial support by the Shell Development Company is gratefully acknowledged and Dr. Stephen Bysouth is thanked for helpful discussions.

References

1 Muller, H., and Kramer, J., *Fresenius' Z. Anal. Chem.*, 1989, **335**, 205.
2 Muller, H., and Kramer, J., *Fresenius' Z. Anal. Chem.*, 1989, **335**, 210.
3 Yang, J., Ma., C., Zhang, S., and Shen, Z., *Anal. Chim. Acta*, 1990, **235**, 323.
4 Fan, S. H., and Fang, Z. L., *Anal. Chim. Acta*, 1990, **241**, 15.
5 Sperling, M., Fang, Z., and Welz, B., *Anal. Chem.*, 1991, **63**, 151.
6 Baron, A., Guzman, M., Růžička, J., and Christian, G. D., *Analyst*, 1992, **117**, 1839.
7 MacLaurin, P., and Worsfold, P. J., *Microchem J.*, 1992, **45**, 178.
8 Starn, T. K., and Hieftje, G. M., *J. Anal. At. Spectrom.*, 1992, **7**, 335.
9 Agudo, M., Rios, A., and Valcárcel, M., *Anal. Chim. Acta*, 1992, **264**, 265.
10 Tyson, J. F., Bysouth, S. R., Grzeszczyk, E. A., and Debrah, E., *Anal. Chim. Acta*, 1992, **261**, 75.
11 Stewart, J. W. B., Růžička, J., Bergamin Filho, H., and Zagatto, E. A. G., *Anal. Chim. Acta*, 1976, **81**, 371.
12 Krug, F. J., Růžička, J., and Hansen, E. H., *Analyst*, 1979, **104**, 47.
13 Bergamin Filho, H., Reis, B. F., Jacintho, A. O., and Zagatto, E. A. G., *Anal. Chim. Acta*, 1980, **117**, 81.
14 Van Son, M., Schothorst, R. C., and Den Boef, G., *Anal. Chim. Acta*, 1983, **153**, 271.
15 Nakata, R., Kawamura, T., Sakashita, H., and Nitta, A., *Anal. Chim. Acta*, 1988, **208**, 81.
16 Mikasa, H., Motomizu, S., and Toei, K., *Bunseki Kagaku*, 1985, **34**, 518.
17 Ishibashi, N., and Imato, T., *Fresenius' Z. Anal. Chem.*, 1986, **323**, 245.
18 Hara, H., Motoike, A., and Okazaki, S., *Analyst*, 1988, **113**, 113.
19 Moore, A. W., Jr., and Jorgenson, J. W., *Anal. Chem.*, 1993, **65**, 188.
20 Bassett, J., Denney, R. C., Jeffrey, G. H., and Mendham, J., in *Vogel's Textbook of Quantitative Inorganic Analysis*, Longman, London, 4th edn., 1983, p. 731.

Paper 3/03800I
Received July 1, 1993
Accepted July 27, 1993

CUMULATIVE AUTHOR INDEX

JANUARY–SEPTEMBER 1993

Aarkrog, Asker, 1101
Aboal-Somoza, Manuel, 665
Abramović, Biljana F., 899
Adams, Michael J., 229
Akasaka, Kazuaki, 765
Alder, J. F., 395
Allag, Houssein, 401
Al-Masri, M. S., 873
Alwarthan, Abdulrahman A., 639
Amarasiriwaradena, Chitra, 1175
Analytical Methods Committee, 1089, 1217
Anderson, David R., 449
Andrew, B. E., 153
Andrews, William J., 425
Aoki, Nobumi, 909
Armstrong, Fraser A., 973
Arrigan, Damien W. M., 355
Ashok Kumar, T., 293
Avidad, Ramiro, 303
Bae, Yea-Ling, 297, 301
Baj, Stefan, 1081
Banerjee, Arun B., 937
Bangar Raju, G., 101
Bannon, Thomas, 361
Barclay, David A., 245
Barjat, Hervé, 73
Barker, Philip G., 347
Barnard Howie, Judith A., 35
Barnes, Ramon M., 1175
Bartle, Keith D., 737
Bartlett, Philip N., 371
Barwick, Ian M., 489
Baxter, Douglas C., 495, 1007
Bayo, Javier, 171
Beauchemin, Diane, 815
Bell, Jimmy D., 241
Belton, Peter S., 73
Benmakroha, Farida, 401
Beone, T., 979
Bermejo Martín-Lázaro, A., 917
Bermejo-Barrera, Pilar, 665
Bernal Suárez, M. M., 917
Bhaskar, Nilam, 1
Biondi, Cinzia, 183
Birmingham, John. J., 1
Blackburn, R., 873
Blaih, Salah M., 577
Blair, Neil, 371
Bond, Alan M., 973
Boržitsky, Juri A., 859
Bos, Albert, 323
Bos, Martinus, 323
Boudjerda, Tarik, 401
Boufenar, Rabah, 401
Bovara, Roberto, 849
Bradbury, Michael W. B., 533
Brand, Tom L., 1101
Breen, William, 415
Brereton, Richard G., 779
Brienza, Sandra Maria Boscolo, 719
Brinkman, Udo A. Th., 11
Brossier, Pierre, 1021
Brough, Paul A., 753
Brown, Marc B., 407
Bruns, Roy E., 213
Büchi, Felix N., 973
Budong, Wang, 1213
Bùi, Lân N., 463
Cai, Xiaohua, 53
Calokerinos, Antony C., 627, 633
Campanella, L., 979
Campiglio, Antonio, 545
Canela, Ramón, 171
Capitán-Vallvey, Luis Fermín, 303
Carlson, Robert G., 257
Carrea, Giacomo, 849
Casey, Vincent, 389
Cassidy, John F., 415
Catterick, Timothy, 791
Celeste, M., 895
Cepas, Juana, 923
Çerdà, V., 895
Čermák, Josef, 79
Chadima, Radko, 79
Chaisuksant, Rasamee, 179
Chalk, Stuart J., 1227
Chan, Wing-Hong, 863, 869
Chang, Qing, 839
Chartier, A., 157
Chatergoon, Lutchminarine, 947
Chen, Liang, 277
Chen, Qiang, 1131
Chen, Rong-mei, 1055
Chen, Tianyu, 541
Chokshi, Hitesh P., 257
Chowdhury, Bhabadeb, 937
Chun-Xiang, He, 1077
Cladera, A., 895
Clark, Alastair, 601
Clarke, Colin G., 229
Clifford, Anthony A., 737
Clinton, Cathriona, 415
Comber, Sean, 505
Cooke, Michael, 449
Cooper, Andrew I., 1111
Corbini, Gianfranco, 183
Cordero, Bernardo Moreno, 209
Corti, Piero, 183
Costa García, Agustin, 649
Cotsaris, Evangelo, 265
Crane, Michael, 617
Crean, G. M., 429
Crooks, Steven R. H., 447
Crosby, Neil T., 489
Crouch, Stanley R., 695
Crubellati, Ricardo O., 529
Cruz Ortiz, M., 801
Csizér, Éva, 609
Cummins, Diane, 1
Cummins, Phillip G., 1
Cunningham, K., 341
Daenens, P., 137
Dams, Richard, 1015
Danielsson, Bengt, 845
Das, Sulobh K., 1153
Davis, Willard E., 249
Day, J. Philip, 1101
Dazhong, Shen, 1143
de Andrade, João Carlos, 213
de la Guardia, Miguel, 23, 1043, 1167
de la Rosa, Francisco F., 643
de Paula Eiras, Sebastião, 213
Dean, John R., 747
Deasy, Brian, 355
Debrabandere, Lode, 137
Deftereos, Nikolaos T., 627
Delves, H. Trevor, 533
Dempsey, Eithne, 411
Dhaneshwar, Ramesh G., 1153
Diamond, Dermot, 347, 1127, 1131
Díaz, Susana, 171
Diewald, Wolfgang, 53
Djerboua, Ferhat, 401
Domanský, Karel, 335
Domínguez, Lucas, 171
Domínguez-González, Raquel, 665
dos Reis, Boaventura Freire, 719
Dowle, Chris J., 17
Dreassi, Elena, 183
Durán-Merás, Isabel, 807
Dvinin, Alexei, 859
Economou, Anastasios, 47
Edmonds, Tony E., 407, 443
Efstathiou, Constantinos E., 627
Egan, Denise A., 201, 411
Eggins, Brian R., 439
Elliott, Christopher T., 447
El-Yazbi, Fawzy A., 577
Emteborg, Håkan, 1007
Escobar, Rosario, 643
Espinosa-Mansilla, Anunciación, 89, 807
Estela, J. M., 895
Fabre, H., 1061
Faure, Uta, 475, 481
Fearn, Tom, 235
Fenyan, Zhang, 1213
Fernández Laespada, Mª. Esther, 209
Ferri, Elida, 849
Feygin, Ilya, 281
Fielden, Peter R., 47
Finglas, Paul M., 475, 481
Fitzgerald, Catherine, 361
Flaherty, T., 429
Fogg, Arnold G., 1157, 1163
Foster, Robert, 415
Fox, C. G., 157
Fraidías Becerra, Antonio J., 175
Frech, Wolfgang, 495, 1007
Friel, Sharon, 371
Frutos, G., 59
Fu, Chengguang, 269
Gaál, Ferenc F., 899
Gaind, Virindar S., 149
Gallagher, Timothy, 753
Gallego, Mercedes, 1199
Gallegos, Robyn Dahl, 1137
Gallignani, Máximo, 1043, 1167
Gangadharan, S., 1085
Gangemi, Gianni, 849
García Gómez de Barreda, Daniel, 175
García-López, Trinidad, 303
Garciá-Mesa, J. A., 891
Gardner, Julian W., 371
Garrigues, Salvador, 1043, 1167
Georges, J., 157
Gerakis, Athanasios M., 1001
Ghijsen, Rudy T., 11
Ghini, Severino, 849
Gibney, Patrick M., 425
Gilner, Danuta, 1081
Giosuè, Maria Antonietta, 849
Girotti, Stefano, 849
Givens, Richard S., 257
Glennon, Jeremy D., 355
Godovski, D. Yu., 997
Gómez-Hens, Agustina, 707
Goodfellow, Brian J., 73
Görög, Sándor, 609
Goto, Katsumi, 1205
Grau, Harald, 689
Greenfield, Stanley, 443
Greenway, Gillian, 17
Gregory, Donald P., 1
Grob, Robert, 11
Gu, Xiao-Hong, 863
Gu, Zhi-cheng, 105, 1055
Guiraúm, Alfonso, 643
Haegel, Franz-Hubert, 703
Halbig, Peter, 689
Halls, David J., 821
Halvatzis, Stergios A., 633
Hamano, Takashi, 909
Hamnett, Andrew, 973
Han, Chuan-qiang, 1055
Hanai, Toshihiko, 769, 773
Hara, Hirokazu, 549
Harris, S. J., 341
Harris, Stephen J., 1127
Hartnett, Margaret, 347
Haswell, Stephen J., 245
Hata, Noriko, 1205
Hauser, Peter C., 991
Hawkesworth, K., 395
Hawkins, Peter, 35
Hembree, Jr., Doyle M., 249
Hernández García, J., 917
Hidalgo de Cisneros, José L. Hidalgo, 175
Hill, H. Allen O., 973
Hiraide, Masataka, 537
Hirose, Tsuyoshi, 517
Hodgkinson, Mark, 1049
Hokari, Norihisa, 219
Hollman, Peter C. H., 475, 481
Hornig, James F., 933
Horváth, Kornélia S., 899
Hosokawa, Satoshi, 1205
Howard, Vyvyan C., 1
Howdle, Steven M., 1111
Huang, Ka-Lin, 205
Hughes, Catherine, 1111
Hunt, Terence P., 17
Idriss, Kamal A., 223
Iizuka, Ryuji, 165
Imai, Kazuhiro, 759
Inui, Syn-ya, 1031
Ishibashi, Mumio, 759
Ishida, Junichi, 165
Ishida, Ryoei, 1071
Ito, Yoshio, 909
Ivaska, Ari, 885
Iwachido, Tadashi, 273
Iwata, Tetsuharu, 517
Iyer, R. M., 929
Izquierdo, Pilar, 707
Izumi, Sigeru, 553
Jan, Ching-Ching, 1183
Janata, Jiří, 335
Jedrzejczak, Kazik, 149
Jefferies, Terry M., 753
Jianli, Liu, 1213
Jobling, Margaret, 1111
Johnston, Brian, 355
Johnston, Keith P., 1111
Jones, Carol L., 1
Josowicz, Mira, 335
Ju, Doweon, 253
Kalcher, Kurt, 53
Kallury, Krishna M. R., 309
Kalman, Peter G., 463
Kane, Jean S., 953
Karayannis, Miltiades I., 711, 723, 727
Kasahara, Issei, 1205
Kasumimoto, Hanae, 131
Katz, Stanley E., 281
Kawaguchi, Hiroshi, 537
Kazarian, Sergei G., 1111
Kessler, Margalith, 235
Keyes, Emmetine T., 385
Khayyami, Masoud, 845
King, Bernard, 587
Kinoshita, Toshio, 161, 769, 773
Kiranas, Efstratios R., 727
Kiss, Attila, 661
Kobayashi, Atsushi, 273
Kobayashi, Shouichi, 131
Koçak, Ali, 657
Koh, Tomozo, 669
Kojima, Nobuaki, 909
Kokot, Serge, 1049
Koltypin, E. A., 997
Konidari, Constantina N., 711
König, Monika, 703
Koshino, Yukihiro, 827, 1027
Kostov, Yordan, 987
Kotrlý, Stanislav, 79
Koupparis, Michael A., 1001
Kovanic, Pavel, 145
Krishan Puri, Bal, 85
Krushevska, Antoaneta, 1175
Kubal, Gina, 241
Kulicki, Zdzisław, 1081
Kulkarni, Achyut V., 1153
Kumar, Manjeet, 193
Kumar, Sanjiv, 1085
Kundu, Dipali, 905
Kvalheim, Olav M., 779
Lan, Chi-Ren, 189

Lang, Mark J., 425
Lannon, A. Martin, 973
Larsson, Per-Olof, 845
Laukó, Anna, 609
Lázaro, Fernando, 1193
Ledesma, Ariel G., 529
Ledingham, Kenneth W. D., 601
Lee, Albert Wai-Ming, 869
leGras, Christopher A. A., 1035
Lettington, Olwen C., 973
Lev, Ovadia, 557
Li, Ronghua, 563
Li, Xiang-Ming, 289
Liang, Wei-An, 97
Liang, Yi-Zeng, 779
Lihua, Nie, 1143
Lin, Qingxiong, 643
Lin, Yuehe, 277
Littlejohn, David, 541, 821, 1065
López Palacios, Jesús, 801
López Ruiz, B., 59
Lowdon, John, 747
Lowe, Roger D., 613
Lu, Bing-liang, 1055
Lu, Jianmin, 1131
Lunar, Mª Loreto, 1209
Lunar, María Loreto, 715
Lunte, Susan M., 257
Luque de Castro, Maria Dolores, 593, 891
Lyons, Cormac H., 361
Lyons, Michael E. G., 361
Mc Monagle, James B., 389
McArdle, Fiona A., 419
McCallum, John J., 401
McCarrick, Mary, 1127
McCaughey, William J., 447
McClean, Stephen, 511
MacCraith, Brian D., 385
McDonagh, Colette M., 385
MacDonald, Robert C., 913
McEvoy, John D. G., 447
McGilp, John F., 385
MacKay, Graham A., 741
McKeown, Neil B., 463
McKervey, M. A., 341
MacLaurin, Paul, 617
McLeod, Cameron W., 449
Magee, Robert J., 53
Maguire, Michael, 1107
Maillols, H., 1061
Malone, Michael A., 649
Mandrou, B., 1061
Maquieira, Angel, 855, 1193
Marshall, Archibald, 601
Martelli, Patricia Benedini, 719
Martin, J. P., 59
Martinez-Lozano, C., 567
Martinez-Vado, Annabelle, 1043
Masotti, Piero, 849
Mathieu, Jacques, 11
Matsubara, Chiyo, 553
Meguro, Hiroshi, 765
Mellidis, Antonios S., 179
Mertens, Bart, 235
Midgley, Derek, 41
Miller, James N., 407, 455
Miller, Richard M., 1
Mills, Andrew, 839
Mitsuhashi, Yukimasa, 909
Miura, Yasuyuki, 669
Mizuno, Takayuki, 1031
Mohan, Hari, 929
Monks, Cheryl D., 623
Moreno, Miguel A., 171
Mori, Yuichi, 553
Moriyama, Youichi, 29
Moskvina, M. A., 997
Moss, Martin C., 1
Mottola, Horacio A., 675
Moulder, Robert, 737
Munakata, Toshihide, 1071
Muñoz de la Peña, Arsenio, 807
Muñoz Leyva, Juan A., 175
Munro, C. H., 731
Nabekura, Tomiko, 273
Nacapricha, Duangjai, 623
Nagahiro, Tohru, 85
Nakagawa, Genkichi, 219
Nakai, Chie, 769, 773
Nakamura, Kayoko, 29
Nakamura, Masaru, 517
Nan, Zhou, 1077
Nanos, Christos G., 711
Narayanaswamy, Ramaier, 317
Narukawa, Akira, 827, 1027
Navalón, Alberto, 303
Neuhold, Christian, 53
Ni, Yongnian, 1049
Niazi, Shahida B., 821
Nicholson, Brenton C., 265
Nickel, Ulrich, 689
Nimura, Noriyuki, 161, 769, 773
Norman, Philip, 617
Nukatsuka, Isoshi, 1071
Nwosu, Titus, 845
O'Beirn, Brendan, 389
O'Donoghue, Eilish, 415
Ohkubo, Hiromi, 549
Ohrui, Hiroshi, 765
Ohta, Kiyohisa, 1031
Ohzeki, Kunio, 1071
Oji, Yoshikiyo, 909
Okabe, Katsuaki, 669
Okada, Tetsuo, 959
O'Kane, Edward, 511
O'Keeffe, Gerard, 385
O'Kelly, Brendan, 385
O'Kennedy, Richard, 201, 411
Olson, Don C., 1227
O'Neill, Robert D., 433
O'Sullivan, Ciara, 411
Oughton, Deborah H., 1101
Palaniappan, R., 293
Pandey, Amita, 941
Papageorgiou, Vassilios P., 179
Pasha, Akmal, 777
Paukert, Tomáš, 145
Paynter, J., 379
Pearce, Timothy C., 371
Pérez Pavón, José Luis, 209
Pérez-Bendito, Dolores, 707, 715, 923, 1209
Pérez-Ruiz, T., 567
Peris Cardells, Empar, 23
Persaud, Krishna C., 419
Petelenz, Danuta, 335
Petrukhin, Oleg M., 859
Pinatel, Henri, 831
Pitre, Krishna S., 65
Plantá, Milagros, 1193
Poliakoff, Martyn, 1111
Pramauro, Edmondo, 23
Preston, Gaynor, 245
Prevot, Alessandra Bianco, 23
Prieta, Javier, 171
Proietti, Daniela, 183
Puchades, Rosa, 855, 1193
Pyo, Dongjin, 253
Qi, Kang, 1143
Quencer, Brett M., 695
Quintela, Mª José, 1199
Radulovic, Stojan, 241
Radunović, Aleksandar, 533
Rahmani, Ali, 779
Ramachandran, Venkataraman N., 511
Ramesh, A., 945
Rauch, Pavel, 849
Raurich, Josep García, 197
Reckhow, David A., 71
Reed, Peter I., 877
Reid, Helen J., 443
Rémy, Isabelle, 1021
Répási, János, 661
Reviejo, A. Julio, 1149
Riley, David P., 407
Roda, Aldo, 849
Roe, Merrion P., 425
Romaschin, Alex D., 463
Roy, S. K., 905
Ruan, Fu-Chang, 289
Rubeška, Ivan, 145
Rubio Leal, Amparo, 89
Rubio, Soledad, 715, 1209
Růžička, Jaromir, 885
Sabot, Jean-François, 831
Sadler, Peter J., 241
Saez, José A., 801
Salbu, B., 1101
Saleh, Magda M. S., 223
Salinas, Francisco, 89, 807
Salvatore, Michael J., 281
Sammartino, M. P., 979
Sanchis, Vicente, 171
Sander, Joseph, 601
Santana Rodríguez, J. J., 917
Sanyal, Asis K., 937
Sanz, A., 567
Sanz Pedrero, P., 59
Satake, Masatada, 85
Savarino, Piero, 23
Sawai, Kaori, 549
Schneider, Jeffery A., 933
Schneider, Siegfried, 689
Schwuger, Milan Johann, 703
Scott, Steven, 1117
Seare, Nichola J., 407
Selby, Mark, 1049
Shallow, A., 429
Sharma, Devender K., 941
Shepherd, Lindsey A., 1111
Sheppard, Robert C., 1
Shibata, Masaru, 909
Shimoishi, Yasuaki, 273
Shiu, Kwok-Keung, 863, 869
Shortt, Desmond H., 447
Shouzhuo, Yao, 1143
Silva, Manuel, 681, 923
Simpson, Michael, 449
Singhal, Ravi P., 601
Singleton, Scott, 1
Slangen, Jean H., 475, 481
Slater, Jonathan M., 379
Smith, Clayton, 947
Smith, Roger M., 741
Smith, W. E., 731
Smyrl, Norman R., 249
Smyth, Malcolm R., 411, 649
Smyth, W. Franklin, 511
Snook, Richard D., 613
Somer, Güler, 657
Song, Lin, 1143
Soto-Ferreiro, Rosa M., 665
Southgate, David A. T., 475, 481
Šrámková, Jitka, 79
Srivastava, P. K., 193
Stalikas, Constantine D., 723
Stewart, Jr., Charles W., 1123
Su, Hongbo, 309
Suárez, Guillermo, 171
Subbarao, Nanda K., 913
Suliman, Fakhr Eldin O., 573
Sultan, Salah M., 573
Sun, S. W., 1061
Svehla, Gyula, 341, 355
Svendsen, C. N., 123
Swadesh, Joel K., 1123
Taguchi, Shigeru, 1205
Takamura, Kiyoko, 553
Tan, Susie S. S., 991
Tang, Gui-Na, 205
Taniguchi, Hirokazu, 29
Tanweer, Ahmad, 835
Taylor, Colin G., 623
Teasdale, P. R. , 329
Terao, Tadao, 759
Thakur, Hari K., 941
Thompson, Michael, 309, 463
Thompson, Michael (Birkbeck), 235, 1107
Timotheou-Potamia, Meropi M., 633
Tomás, C., 895
Tomás, V., 567
Tomassetti, M., 979
Torrades, Francesc, 197
Torró, Luis, 855
Toyo'oka, Toshimasa, 257, 759
Tsai, Suh-Jen Jane, 297, 301, 521, 1183
Tsionsky, Michael, 557
Tsuzuki, Wakako, 131
Tucker, Alan, 241
Tuñón Blanco, Paulino, 649
Tyson, Julian F., 1227
Tzonkov, Stoyan, 987
Tzouwara-Karayanni, Stella M., 723, 727
Uchida, Takaaki, 537
Uden, Peter C., 1123
Urusov, Yuri I., 859
Valcárcel, Miguel, 593, 891, 1199
Van Allemeersch, Françoise, 1015
Van Boven, M., 137
van der Linden, Willem E., 323
Vanhoe, Hans, 1015
Veiro, Jeffrey A., 1
Verma, Balbir C., 941
Verma, Neerja, 65
Verma, Rakesh, 1085
Versieck, Jacques, 1015
Vijaya Raju, K., 101
Vijayashankar, Yadathora N., 777
Vilchez, José Luis, 303
Viscardi, Guido, 23
Volkov, A. V., 997
Vos, Johannes G., 385
Voulgaropoulos, Anastasios, 179
Wada, Hiroko, 219
Wagstaffe, Peter J., 475, 481
Wallace, G. G., 329
Walton, Philip W., 425
Wang, Bao-Ning, 205
Wang, Joseph, 277, 411, 1131, 1149
Warwick, Peter, 489
Watt, E. J., 379
White, Peter C., 731, 791
Whiting, Robin, 947
Williams, David M., 249
Williams, Kathleen E., 245
Winefordner, James D., 1031
Wong, Kwok-Yin, 289
Wong, Wai-Cheong, 869
Worsfold, Paul J., 617
Worswick, Richard, 583
Wuchner, Klaus, 11
Xie, Bin, 845
Xie, Yuefeng, 71
Xu, Guoping, 877
Xu, Hongda, 269
Yamaguchi, Masatoshi, 165, 517
Yamanaka, Nobuhiro, 1031
Yamauchi, Shuji, 161, 769, 773
Yan, Hsiao-Tzu, 521
Yang, Mengsu, 309
Yoshida, Tomohiko, 29
Yoshioka, Hiroshi, 553
Yotova, Ljubov, 987
Yuchi, Akio, 219
Zagatto, Elias Ayres Guidetti, 719
Zanoni, M. Valnice B., 1157, 1163
Zawadiak, Jan, 1081
Zenki, Michio, 273
Zhang, D., 429
Zhang, Peixun, 1065
Zheng, Minghui, 269
Zhou, Jie, 97
Zhou, Zhauro, 563
Zhu, Zhong-liang, 105, 1055
Zoski, Cynthia G., 973
Zotou, Anastasia, 753
Zou, Shi-Fu, 97

Book Reviews

The Dynamics of Electrophoresis

By R. A. Mosher, D. A. Saville and W. Thormann. *Electrophoresis Library Series.* Edited by B. J. Radola. Pp. xv + 236. VCH. 1992. Price DM186.00; £70.00 ISBN 3-527-28379-X (VCH, Weinheim); 1-56081-192-7 (VCH, New York).

This book is dedicated to our colleague and friend Milan Bier.

In the Introduction many pages are used to define history, without giving overwhelming information on references of the past. An overview of the historical research, that grounded modern electrophoresis, gives young scientists especially a guideline to find their way in the literature. Too often it is thought that the leading figures of today are the leading figures of the past. In this book it is shown that the new generation is taking over the role of those who made and created the electrophoretic techniques.

In the classification of the electrophoretic methods it is shown that four basic principles (with and without electrophoretic flow) exist. As is well known, these four basic principles can be carried out with any electrophoretic apparatus. With such equipment one can separate small ions, anions, cations, amino acids, even peptides, proteins, DNA and RNA molecules and restriction fragments. In the two-dimensional mode it is important to know that various electrophoretic principles can be combined. It will be clear that such combinations will increase the information output of researchers. This book clearly describes what kind of principles have to be chosen or which combination. It is, therefore, of importance that techniques such as two-dimensional GC–MS, pulsed flow and micellar electrokinetic chromatography are described. In the 'simplest' forms of electrophoresis such as zone electrophoresis (ZE), isotachophoresis (ITP), micellar electrokinetic chromatography (MEC) and liquid chromatography with isoelectric focusing (LC–IEF) it is rather 'simple' to devise computer programs for both qualitative and quantitative purposes. A very good reader guide to overview this book is given on page 4.

Chapter 2 discusses the physico-chemical background of electrophoresis. It not only gives attention to electrophoresis, but also to colloid chemistry. A good compromise is found between the well-established theory and the current possibilities of using computer programs for evaluation and understanding of the data obtained. This chapter is especially recommended to those scientists who would like to become experts in the field of electrophoresis.

In Chapter 3, sophisticated computer modelling is given, both to understand the programs used and to add specific wishes for those who are trained in soft- and hardware. These programs are checked with experimental data obtained with the so-called CapScan equipment. For most scientists this chapter is difficult, because for one reason or another 'wet-chemistry' and 'colloid chemistry' no longer feature in the standard university education package. It is, therefore, a pity that so many beautiful analytical 'separation' techniques have to disappear. For this reason this book is extremely useful for physical, analytical and biochemists. Such information must at least be available in the laboratory.

In Chapter 4, moving boundary electrophoresis is described, as introduced by Arne Tiselius. Although it does not have a great analytical importance, the background of this technique has to be understood. It is the separation phase of ITP used especially for injecting samples in gel filled columns.

Chapter 5 describes zone electrophoresis. This principle is probably the most used separation technique in, for example, slab gels, paper, cellulose acetate and in capillary tubes in free solutions and in gels. In free solutions this principle can be used with and without electroosmotic flow (EOF). A clear view of various effects is given. Hybrid forms of CZE and ITP illustrate that sharpening up effects and concentrating effects due to ITP and CZE make it important to understand the background of these principles.

In Chapter 6 isotachophoresis is described. It will be clear that this technique now has a great potential, because commercial equipment has become available. Again it is important to understand the background of this technique, to use it for sharpening up the sample before zone electrophoresis is started. This is comparable to the so-called Ornstein and Davis technique, published in 1964. The computer modelling has been checked with real experiments with the apparatus.

In Chapter 7 isoelectric focusing is described. Information is given to select the pH gradient needed (wide or narrow). Sometimes just one kind of carrier ampholyte is recommended, sometimes a mixture. The reproducibility of this technique is dependent on the reproducible material (ampholytes) produced batch-to-batch, week-to-week, month-to-month and year-to-year.

In this reviwers' opinion this chapter is very important for the scientists in companies manufacturing these ampholytes. Chapter 7.6 is of particular importance for students on undergraduate courses, but also for Ph.D. students in the fields related to these techniques.

More attention could have been paid to the immobilized pH gradient (Chapter 7.2.2, pages 217–221), while the focusing of proteins in natural pH gradients is questionable (Chapter 7.8, pages 221–229).

This book should be available in any laboratory. The information given is comprehensive and will last forever. The equations can be given in classical mathematics or, for instance, in fluid dynamics. The theory behind the principles of electrophoresis is well established, and needs to be known by those scientists who wish to develop their own electrolyte systems in order to optimize their separations.

Frans M. Everaerts

Particle Size Analysis

Edited by N. G. Stanley-Wood and R. W. Lines. Pp. xx + 538. Royal Society of Chemistry. 1992. Price £57.50. ISBN 0-85186-487-2.

This book covers the proceedings of the 25th Anniversary Conference of the Particle Characterization Group of the Analytical Division, Royal Society of Chemistry, held at the University of Technology, Loughborough in September 1991. Now, if you want to know 'where particle characterization is at present' and 'where it is going', then this is the book for you. It does not, of course, forget its roots and is also a good review of the development of particle analysis over the past 25 years; indeed some of the well tried and tested methods used over this period of time are discussed in some of the contributed papers.

This book is published under the subject classifications of analytical and industrial chemistry, instrumentation and chemical engineering. The wide ranging relationship that particle characterization has with these topic areas is more than adequately served by the 58 papers that make up the publication. A subject index, which allows you to browse through this ever increasing branch of science, is provided; although X for X-ray instrumentation does not seem to make it into the index, it is certainly included in the text!

The first paper is a fine scene setter and considers the philosophy/fundamentals of particle characterization, its development over 25 years and where this development might lead us. Like the first paper, each contribution is a nugget, critically addressing, in many cases, the underlying theory of a particular instrumental or particle characterization technique, its advantages, limitations of use or performance and in a number of papers future trends.

The comprehensive nature of this book makes it difficult to say exactly who it is aimed at in terms of level. In some cases it is not for the mathematically squeamish and seems to lean towards the deeper research level, whereas other papers are suitable for undergraduates in their quest for background information. This is not a criticism, more a consequence of the way in which this science has progressed, and continues to progress.

The topics under discussion include surface area, porosity and pore structure, particle shape, field-flow fractionation, electrical sensing, sedimentation, two-dimensional sieve cascadography and a range of light- and laser-based particle sizing/shape techniques. The numerous contributions concerning the latter include applications of the more advanced techniques of diffraction, scattering, Doppler velocimetry, obscuration/extinction and photon correlation spectroscopy. Mathematical approaches to particle characterization, such as three-dimensional particle reconstruction, packing, fractal geometry, principal component analysis, particle morphology and shape change, are also discussed. Examples of applications with an industrial bias are fairly well served.

In these days of quality assured techniques, thankfully the need for standards is never in question. Hence, calibration and certified reference materials are an indispensable part of particle characterization. Several papers discuss this area in a critical and open manner. A knowledge of the limitations of a technique gives a balanced view and allows the scientist to determine the confidence of data obtained. Although this information is presented it is noted that sometimes the optimism of an interested author creeps in.

This aside, certainly industrial establishments as well as academic institutions should place this timely publication on their library shelves.

Mike Foulkes

Haaland's topic is 'Multivariate Calibration Methods Applied to the Quantitative Analysis of Infrared Spectra'. He gives a good comparison of the variety of multivariate approaches to this problem. A practical example based on the industrially important problem of quality control of borophosphosilicate glass is also presented.

Windig gives some practical industrial examples of the use of chemometric techniques in the solution of problems from Raman, FTIR microscopy and pyrolysis mass spectrometry. The technique used for the examples is the SIMPLISMA approach of self-modelling mixture analysis. One data set discussed is again a glass process, the other is a rubber triblends problem.

Naes and Isaksson present an excellent view of the use of principal components regression in near-infrared, concentrating on the assessment of the predictive capability.

Computer-Assisted Mass Spectral Interpretation: MS–MS analysis is covered by Hart and Enke. They describe work based on a combination of database techniques, pattern recognition and automated rule generation.

Meuzelaar and co-workers report work on Canonical Correlation Analysis of Multisource Fossil Fuel Data, where the spectroscopic techniques used are mass spectrometry, pyrolysis-field ionization MS and photoacoustic FTIR. Correlation of such multisource data is one of the strengths of the chemometric approach, this worked example will be useful to those new to the field.

Harrington reports on the use of fuzzy rule based expert systems in laser ionization MS of polymer thin films. The other chapters on the PAIRS knowledge based system for interpreting infrared spectra, Hadamard methods in signal recovery and the report on the work of Munk on the use of NMR spectra in structure elucidation build on several previous publications.

Signal processing in ion mobility spectrometry and multichannel atomic emission spectroscopy are covered in the final two chapters.

Overall the work is well presented but suffers from the lack of state-of-the-art reports. The print and paper of the book are of high quality, but the spine of the book is glued rather than stitched, which leads to the pages becoming detached after a short time.

R. A. Hearmon

Computer-Enhanced Analytical Spectroscopy. Volume 3
Edited by Peter C. Jurs. *Modern Analytical Chemistry Series.* Pp. xvi + 320. Plenum. 1992. Price US$175.00. ISBN 0-306-43859-3.

This is the third book of proceedings of the excellent Snowbird series of symposia on the application of computers in analytical spectroscopy. As with all conventionally produced symposia proceedings the book suffers somewhat in the gap between the meeting and the publication of the proceedings. The reported lectures were presented at the third symposium that was held in 1990, the fourth symposium in the series has since been held in 1992. Thus it is important for the proceedings to conform to the editors aim that they 'provide a cross-section of current research activities in this important and active field'. Most spectroscopic techniques are mentioned. The texts concentrate on chemometrics, knowledge-based systems and signal processing, rather than attempting to cover the full range that the title might imply.

The proceedings are presented as 11 chapters by the speakers. Some of these take the form of general overviews or comparisons of methods, others cover specific examples. The highlights of the proceedings are the chapters by Haaland and Windig.

How to Use Reverse-Phase HPLC
By Gábor Szepesi. Pp. x + 356. VCH. 1992. Price DM168.00; £63.00. ISBN 0-89573-766-3 (VCH Publishers); 3-527-27939-3 (VCH Verlagsgesellschaft).

This book contains seven chapters on various aspects of reversed-phase HPLC although in places it goes outside of this subject encompassing other HPLC modes such as ion-exchange, size-exclusion and intermediate-polarity phases, but, surprisingly, includes nothing on the use of graphitized carbon packings apart from a passing mention in the Introduction. The book is probably most suitable for analysts with some reasonable experience of HPLC and who require an introduction to the more specialized topics included in later chapters.

Chapter 1 presents some advantages and disadvantages of straight-phase *versus* reversed-phase chromatography. Chapter 2 consists of a summary of basic HPLC theory followed by a survey of different separation modes. The former section is poorly presented and this reviewer would certainly not recommend it as a training aid for inexperienced chromatographers. The latter section seems irrelevant for a book devoted to reversed-phase chromatography, although it would appear from the presentation that the author considers

ion-exchange and size-exclusion modes to be reversed-phase methods.

Chapter 3 discusses stationary phases providing quite a nice review of different packings from different sources, the importance of variations in parameters such as pore size, particle size, nature of bonded alkyl chains, extent of phase coverage, *etc.* Polymeric-based phases and chiral packings are discussed as well as further considerations of ion-exchange, and size-exclusion phases. Chapter 4 is concerned with mobile phases and discusses solvent selectivities, approaches to problems of polar adsorptions at residual silanol sites using mobile-phase additives, *e.g.*, competing amines, ion-suppression techniques and ion-pair reagents. However, the author then goes on to discuss a number of aspects of column performance, which although useful, should be included in the previous chapter on columns.

The final three chapters were considered to contain the most valuable contributions in this publication. Chapter 5 discusses some special techniques. The section on ion-pair chromatography includes useful material on how various factors influence chromatographic performance. This is followed by reasonable sections on chiral chromatography, indirect detection methods, multicolumn methods and peptide separations. Chapter 6 provides a good review of optimization techniques and includes practical examples for applying such methods and checking expert systems. The final chapter is a topical discussion on method validation and in which the most valuable section is a very interesting approach to the determination of ruggedness.

This book contains several interesting topics and most chapters provide a good selection of references, which are usually reasonably recent. However, it is spoiled by poor presentation of material in many sections sometimes due to badly expressed ideas and sometimes due to grammatical errors. Either way, readers are likely to find these sections difficult to understand. In addition, many diagrams and tables were poorly prepared in some cases rendering them incomprehensible and a number of typographical errors were found.

G. P. R. Carr

Conference Diary

Date	Conference	Location	Contact
October			
3–7	**10th Asilomar Conference on Mass Spectrometry [TOF-MS]**	Estes Park, CO, USA	**Laszlo Tokes,** Syntex Discovery Research, 3401 Hillview Avenue, Palo Alto, CA 94304, USA **Tel:** +1 415 855 5713. **Fax:** +1 415 354 7363
4–8	**ECASIA 93, 5th European Conference on Applications of Surface and Interface Analysis**	Catania, Italy	**G. Marletta,** Consorzio Catania Ricerche, V. Le Andrea Doria, 6, I-95125 Catania, Italy **Tel:** +39 95 221635. **Fax:** +39 95 339734
5–7	**34th ORNL–DOE Conference on Analytical Chemistry in Energy Technology**	Gatlinburg, TN, USA	**W. R. Laing,** Technical Program Chairman, Oak Ridge National Laboratory, P.O. Box 2008, MS 6127, Oak Ridge, TN 37831-6127, USA **Tel:** +1 615 574 4852. **Fax:** +1 615 574 4902
5–7	**Laboratory Exhibition and Conference**	London, UK	**Evan Steadman Communications Group Ltd.,** 90 Calverley Road, Tunbridge Wells, Kent, UK TN1 2UN
5–8	**5th Meeting of the Nuclear Magnetism and Biology Group**	Toulouse, France	**Professor M. Malet-Martino,** Laboratoire IMRCP, Universite Paul Sabatier, 118, route de Narbonne, F-31062 Toulouse Cedex, France
5–8	**4th ISEC. Fourth International Seminar on Electroanalytical Chemistry**	Beijing, China	**Professor Erkang Wang,** 109 Sitalin Street, Changchun Institute of Applied Chemistry, Chinese Academy of Sciences, Changchun, Jilin 130022, China
8–13	**5th BCEIA. Fifth International Beijing Conference and Exhibition on Instrumental Analysis**	Beijing, China	**General Service Office,** 5th BCEIA, Room 5412, Building No. 4, Xi Yuan Hotel, Er Li Gou, Beijing 100046, China
10–15	**Electrochemical Society Meeting**	New Orleans, LA, USA	**Electrochemical Society Inc,** 10 South Main Street, Pennington, NJ 08534-2896, USA
11–13	**VIth National Symposium on Mass Spectometry**	Dehradun, India	**Dr. Pradeep Kumar,** Indian Institute of Petroleum, Dehradun-248 005, India, and **Dr. S. K. Aggarwal,** Honorary Secretary—ISMAS, c/o Fuel Chemistry Division, Bhabha Atomic Research Centre, Bombay-400 085, Maharastra, India
11–15	**Optical Sensing for Environmental Monitoring Symposium**	Atlanta, GA, USA	**Adrianne Olsakovsky,** 3 Gateway Center, 4 West, Pittsburgh, PA 15222, USA **Tel:** +1 412 232 3444. **Fax:** +1 412 232 3450
13	**FT Microscopy–10 Years On: 4th European Seminar on FT-IR Microscopy**	Manchester, UK	**Michelle Barker,** Conference Co-Ordinator, Spectra-Tech Europe Limited, Genesis Centre, Science Park South, Birchwood, Warrington, UK WA3 7BH **Tel:** +44 (0) 925 830 250. **Fax:** +44 (0) 925 830 252
16–17	**Second National Conference on Inductively Coupled Plasma Mass Spectrometry**	Detroit, MI, USA	**Society for Applied Spectroscopy/ICP/MS Users Group,** 198 Thomas Johnson Drive, Suite-2, Frederick, MD 21702-4317, USA **Tel:** +1 301 694 8122.
17–21	**Eighth Symposium on Separation Science and Technology for Energy Application**	Oak Ridge, TN, USA	**J. T. Bell,** Oak Ridge National Laboratory, Post Office 2008, Oak Ridge, TN 37381, USA
17–22	**FACSS XX, 20th Annual Meeting of the Federation of Analytical Chemistry and Spectroscopy Societies**	Detroit, MI, USA	**FACSS,** 198 Thomas Johnson Drive, Suite S-2, Fredericks, MD 21702, USA **Tel:** +1 301 846 4789. **Fax:** +1 301 694 6860
17–23	**10th International Symposium on Biorecognition and Affinity Technology**	Gwatt/Thun, Switzerland	**Professor A. N. Eberle and Mrs. D. Affentranger,** Department of Research, University Hospital, CH-4031 Basle, Switzerland **Tel:** +41 61 2652 324. **Fax:** +41 61 2652 350
18–22	**Modern Electrochemistry in Industry and for the Protection of the Environment**	Krakow, Poland	**Dr. Andrzej Kowal,** Institute of Catalysis and Surface Chemistry, Polish Academy of Sciences, ul. Niezapiminajek 1, 30-239 Krakow, Poland
19–20	**Frederick Conference on Capillary Electrophoresis**	Frederick, MD, USA	**Margaret L. Fanning,** Conference Coordinator, PRI, NCI-FCRDC, P.O. Box B, Frederick, MD 21702-1201, USA **Tel:** +1 301 846 1089. **Fax:** +1 301 846 5866

Date	Conference	Location	Contact
19–23	**EXPOQUIMIA '93: Applied Chemistry Technical Fair**	Barcelona, Spain	**Fira de Barcelona,** Avda. Reina Mª Cristina, 08004 Barcelona, Spain
20–22	**Hygiene and Health Management in the Working Environment**	Ghent, Belgium	**3rd International Symposium,** 'Hygiene and Health Management in the Working Environment', c/o TI-K VIV, Attn. Ms. Rita Peys, Desguinlei 214, B-2018 Antwerp, Belgium
21–22	**International Conference on Analytical Chemistry, Biochemistry and Pharmaceutical Sciences**	Casablanca, Morocco	**Dr. V. M. Bhatnagar,** Alena Chemicals of Canada, P.O. Box 1779, Cornwall, Ontario, Canada K6H 5V7 **Tel:** +1 613 932 7702.
24–28	**8th Symposium on Separation Science and Technology for Energy Applications**	Gatlinburg, TN, USA	**Dr. J. T. Bell,** Oak Ridge National Laboratory, P.O. Box 2008, Oak Ridge, TN 37831-6223, USA **Tel:** +1 615 574 4934; or **Dr. J. S. Watson**, K-25 Plant, P.O. Box 2003, Oak Ridge, TN 37831-7298, USA **Tel:** +1 615 574 6795.
25–29	**Scanning Electron Microscopy Field Emission and X-ray Microanalysis**	Ellenville, NY, USA	**Dr. Angelos Patsis,** Center of Materials Science, State University of New York, New Paltz, NY 12561, USA **Tel:** +1 914 257 3800.
26–28	**The 1993 Analytical Forum—'Meeting the Challenge'**	Chepstow, UK	**Lisa Butler,** Analytical Products Group, Hewlett-Packard Ltd., Cain Road, Bracknell, Berkshire, UK RG12 1HN
November			
1–3	**Chernyaev Conference on Chemistry, Analysis, Technology and Application of Platinum Metals**	Moscow, Russia	**Dr. I. B. Baranovsky,** Kurnakov Institute of General and Inorganic Chemistry, 31 Lenin Avenue, Moscow 117907, Russia
2	**Electro-Membrane Processes**	London, UK	**Dr. T. R. Ralph,** Johnson Matthey Technology Centre, Blounts Court, Sonning Common, Reading, Berkshire, UK RG4 9NJJ **Tel:** +44 734 722811 ext. 2257. **Fax:** +44 734 723236
2–4	**KEMIA 93. Finnish Chemical Congress and Exhibition**	Helsinki, Finland	**Ms. Anita Haatainen, Tel:** +358 0 150 9207 or **Mr. Seppo Niiranen** **Tel:** +358 0 150 9215.
3	**Pharmaceutical Applications and Sample Handling Techniques**	York, UK	**Don Clark,** Physical Sciences—265, Pfizer Central Research, Ramsgate Road, Sandwich, Kent, UK CT13 9NJ **Tel:** +44 304 616036. **Fax:** +44 304 616726
3–5	**2nd International Symposium on Characterization and Control of Odours and VOC in the Process Industries**	Louvain-la-Neuve, Belgium	**Symposium Secretariat,** Société Belge de Filtration, Université Catholique de Louvain, Voie Minckelers 1, 1348 Louvain-la-Neuve, Belgium **Tel:** +32 10 47 23 26. **Fax:** +32 10 47 23 21
7–10	**Electrophoresis '93**	Charleston, SC, USA	**Mrs. Janet Cunningham,** Electrophoresis '93, c/o The Electrophoresis Society, P.O. Box 279, Walkersville, MD 21793, USA **Tel:** +1 301 898 3772. **Fax:** +1 301 898 5596
7–11	**7th International Forum–Electrolysis in Chemical Manufacture**	Lake Buena Vista, FL, USA	**Dr. N. Weinberg,** 72 Ward Road, Lancaster, NY 14086-9779, USA **Tel:** +1 716 684 0513. **Fax:** +1 716 684 0511
7–12	**Symposium on Supercritical Fluid Phenomena (1993 Annual Meeting of the AIChE)**	St. Louis, MO, USA	**Michael A. Matthews,** Chemical Engineering Department, University of Wyoming, Box 3295, University Station, Laramie, WY 82071-32, USA **Tel:** +1 307 766 5769 **Fax:** +1 307 766 4444. Or: **Ted W. Randolph**, Chemical Engineering Department, Yale University, 9 Hillhouse Avenue, New Haven, CT 06520-2159, USA **Tel:** +1 203 432 4375. **Fax**: +1 203 432 7232
8–10	**International Symposium on Plasma Polymerization/Deposition**	Las Vegas, NV, USA	**K. L. Mittal,** Skill Dynamics (an IBM Company), 500 Columbus Ave., Thornwood, NY 10594, USA **Tel:** +1 914 742 5747. **Fax:** +1 914 742 5594
11–12	**International Conferences on Analytical Chemistry, Biochemistry, Pharmaceutical Sciences, and Water Quality/Environmental Pollution**	New Delhi, India	**Dr. V. M. Bhatnagar,** Alena Chemicals of Canada, P.O. Box 1779, Cornwall, Ontario, Canada K6H 5V7 **Tel:** +1 613 932 7702.

Date	Conference	Location	Contact
11–12	**7th International Conference on Plasma Chemistry and Technology**	San Diego, CA, USA	**Research Institute of Plasma Chemistry and Technology,** P.O. Box 1653, Carlsbad, CA 92008, USA
12–13	**5th Topical Conference on Quantitative Surface Analysis (ASSD Topical Conference)**	Clearwater Beach, FL, USA	**Paul Holloway,** University of Florida, 258A Rhines Hall, Gainesville, FL 32611, USA **Tel:** +1 904 392 6664. **Fax:** +1 904 392 4911
14–19	**XV International Congress of Clinical Chemistry**	Melbourne, Australia	**1993 IFCC Congress Secretariat,** 232 Bridge Road, Richmond, Victoria, Australia **Tel:** +61 3 429 4322. **Fax:** +61 3 427 0715
14–19	**OPTCON '93**	San Jose, CA, USA	**IEEE/LEOS,** 445 Hoes Lane, P.O. Box 1331, Piscataway, NJ 08855-1331, USA **Tel:** +1 908 562 3896. **Fax:** +1 908 562 1571
15–19	**32nd Annual Eastern Analytical Symposium**	New Jersey, USA	**EAS Program Committee,** P.O. Box 633, Montchanin, DE 19710-0633, USA
22–23	**International Conferences on Analytical Chemistry, Biochemistry, Pharmaceutical Sciences, and Water Quality/Environmental Pollution**	Shanghai, China	**Dr. V. M. Bhatnagar,** Alena Chemicals of Canada, P.O. Box 1779, Cornwall, Ontario, Canada K6H 5V7 **Tel:** +1 613 932 7702.
30–3/12	**13th International Symposium on HPLC of Proteins, Peptides and Polynucleotides**	San Francisco, CA, USA	**Ms. Paddy Batchelder,** Conference Manager, 7948 Foothill Knolls Drive, Pleasanton, CA 94588, USA **Tel:** +1 510 426 9601. **Fax:** +1 510 846 2242
December			
6–8	**International Symposium on Purity Determination of Drugs**	Stockholm, Sweden	**Swedish Academy of Pharmaceutical Sciences,** P.O. Box 1136, S-111 81 Stockholm, Sweden **Tel:** +46 8 245085. **Fax:** +46 8 205511
7–9	**The First Conference in Chemistry and its Applications**	Doha, Qatar	**Professor Abdel-Fattah M. Rizk,** Department of Chemistry, Faculty of Science, University of Qatar, P.O. Box 2713, Doha, Qatar
8–10	**Laser M2P, Materials Engineering, Medicine and Biology, Physics and Chemistry**	Lyon, France	**Richard Moncorgé,** Université de Lyon 1, Bât. 205, F-69622 Villeurbanne Cedex, France
1994			
January			
5–7	**6th Winter Conference on Flow Injection Analysis**	San Diego, CA, USA	**Professor G. D. Christian,** Department of Chemistry BG-10, University of Washington, Seattle, WA 98195, USA **Tel:** +1 206 543 1635. **Fax:** +1 206 685 3478
10–15	**1994 Winter Conference on Plasma Spectrochemistry**	San Diego, CA, USA	**Dr. R. Barnes,** 1994 Winter Conference on Plasma Spectrochemistry, %ICP Information Newsletter, Department of Chemistry, Lederle GRC Towers, University of Massachusetts, Amherst, MA 01003-0035, USA **Tel:** +1 413 545 2294. **Fax:** +1 413 545 4490
11–14	**5th International Symposium on Supercritical Fluid Chromatography and Extraction**	Baltimore, MD, USA	**Larry T. Taylor,** Department of Chemistry, Virginia Polytechnic Institute, Blacksburg, VA 24061, USA
19–21	**2nd International Conference on Reactive Plasmas and 11th Symposium on Plasma Processing**	Yokohama, Japan	**T. Goto,** Department of Quantum Engineering, Nagoya University, Chikusa-ku, Nagoya 464-01, Japan
31–3/2	**HPCE '94: Sixth International Symposium on High Performance Capillary Electrophoresis**	San Diego, CA, USA	**The Symposium Manager, Shirley Schlessinger,** 400 East Randolph Street, Suite 1015, Chicago, IL 60601, USA **Tel:** +1 312 527 2011.
February			
13–17	**Second International Glycobiology Symposium: Current Analytical Methods**	San Francisco, CA, USA	**Paddy Batchelder,** P.O. Box 370, Pleasanton, CA 94566, USA **Tel:** +1 510 426 9601. **Fax:** +1 510 846 2242
21–25	**OFC '94: Optical Fibre Communications Conference**	San Jose, CA, USA	**Meetings Department,** Optical Society of America, 2010 Massachusetts Avenue, NW, Washington, DC 20036-1023, USA **Tel:** +1 202 223 9034. **Fax:** +1 202 416 6100

Date	Conference	Location	Contact
23–25	**HTC 3: Third International Symposium on Hyphenated Techniques in Chromatography**	Antwerp, Belgium	**Dr. R. Smits,** p/a BASF Antwerpen N.V., Central Laboratory, Scheldelaan, B-2040 Antwerp, Belgium **Tel:** +32 3 568 2831. **Fax:** +32 3 568 3250
28–4/3	**Pittcon '94: The 45th Pittsburgh Conference on Analytical Chemistry and Applied Spectroscopy**	Chicago, IL, USA	**Mrs. Alma Johnson,** Program Secretary, The Pittsburgh Conference, Department CFP, 300 Penn Center Boulevard, Suite 332, Pittsburgh, PA 15235, USA
March			
7–11	**4th International Symposium on Trends and New Applications in Thin Films**	Dresden, Germany	**Frank Richter,** TU Chemnitz, FB Physik, PSF 964, D-09009 Chemnitz, Germany **Fax:** +49 371 852491
13–16	**Third European Federation of Corrosion Workshop on Microbial Corrosion**	Estoril, Portugal	**César Sequeira,** Instituto Superior Técnico, Av. Rovisco Pais, 1096 Lisboa Codex, Portugal, or **A. K. Tiller**, Corrosion Centre, 23 Grosvenor Gardens, Kingston-upon-Thames, UK KT2 5BE, or **D. Thierry**, Swedish Corrosion Institute, Roslagsvägen 101, Hus 25, S-10405 Stockholm, Sweden
13–18	**207th American Chemical Society National Meeting**	San Diego, CA, USA	**Department of Meetings,** American Chemical Society, 1155-16th St., NW, Washington, DC 20036, USA **Tel:** +1 202 872 4396.
27–30	**International Federation of Automatic Control (IFAC) Symposium on Modeling and Control in Biomedical Systems**	Galveston, TX, USA	**IFAC Biomedical Symposium,** University of Texas Medical Branch, Box 55176, Galveston, TX 77555-5176, USA **Tel:** +1 409 770 6628 or 770 6605. **Fax:** +1 409 770 6825
April			
6–8	**Electroanalysis: A Tribute to Professor J. D. R. Thomas**	Cardiff, UK	**Dr. J. M. Slater,** Department of Chemistry, Birkbeck College, University of London, 29 Gordon Square, London, UK WC1H 0PP **Tel:** +44 71 380 7474. **Fax:** +44 71 380 7464
10–13	**ANATECH 94: 4th International Symposium on Analytical Techniques for Industrial Process Control**	Mandelieu La Napoule, France	**ANATECH 94 Secretariat,** Elsevier Advanced Technology, Mayfield House, 256 Banbury Road, Oxford, UK OX2 7DH **Tel:** +44 (0)865 512242. **Fax:** +44 (0)865 310981
10–15	**207th ACS National Meeting and 5th Chemical Congress of North America (with Sessions of Analytical Chemistry, Environmental Chemistry, Chemical Health and Safety, *etc.*)**	Mexico City, Mexico	**Mr. B. R. Hodson,** American Chemical Society, 1155–16th Street N.W., Washington, DC 20036, USA **Tel:** +1 202 872 4396.
10–16	**3rd International Conference on Methods and Applications of Radioanalytical Chemistry**	Kailua-Kona, Hawaii, USA	**Ned A Wogman,** Battelle, Pacific Northwest Laboratories, P.O. Box 999, P7-35, Richland, WA 99352, USA **Tel:** +1 509 376 2452. **Fax:** +1 509 376 2373
12–14	**13th Pharmaceutical Technology Conference**	Strasbourg, France	**Professor Mike Rubinstein,** 13th Pharmaceutical Technology Conference, 24 Menlove Gardens North, Liverpool, UK L18 2EJ **Tel:** +44 51 737 1993. **Fax:** +44 51 737 1070
17–19	**International Symposium on Volatile Organic Compounds (VOCs) in the Environment**	Montreal, Quebec, Canada	**Symposium Chairman, Dr. Wuncheng Wang,** US Geological Survey, WRD, P.O. Box 1230, Iowa City, IA 52244, USA. **Tel:** +1 319 337 4191, **Fax:** +1 319 354 0510; or **Co-Chairmen, Dr. Jerald Schnoor,** University of Iowa, Department of Civil and Environmental Engineering, Iowa City, IA 52242, USA. **Tel:** +1 319 335 5649, **Fax:** +1 319 335 5777; and **Dr. Jon Doi,** Roy F. Weston, Inc., 1 Weston Way, West Chester, PA 19380, USA **Tel:** +1 215 524 6167. **Fax:** +1 215 524 6175
19–22	**ANALYTICA'94: 14th International Conference on Biochemical and Instrumental Analysis**	Munich, Germany	Münchener Messe- und Ausstellungsgesellschaft mbH, Analytica '94/Werbung Postfach 12 10 09, D-8000 München 12, Germany **Tel:** +49 89 51 07 143. **Fax:** +49 89 51 07 177

Date	Conference	Location	Contact
May			
7–12	**Food Structure Annual Meeting**	Toronto, Ontario, Canada	**Dr. Om Johari,,** SMI, Chicago (AMF O'Hare), IL 60666-0507, USA **Tel:** +1 708 529 6677. **Fax:** +1 708 980 6698
8–12	**85th AOCS Annual Meeting & Expo**	Atlanta, GA, USA	**AOCS Education/Meetings Department,** P.O. Box 3489, Champaign, IL 61826-3489, USA **Tel:** +1 217 359 2344. **Fax:** +1 217 351 8091
8–13	**HPLC '94, Eighteenth International Symposium on Column Liquid Chromatography**	Minneapolis, MN, USA	**Ms. J. E. Cunningham,** Barr Enterprises, P.O. Box 279, Walkersville, MD 21793, USA **Tel:** +1 301 898 3772. **Fax:** +1 301 898 5596
8–13	**CLEO '94: Conference on Lasers and Electro-Optics**	Anaheim, CA, USA	**Meetings Department,** Optical Society of America, 2010 Massachusetts Avenue, NW, Washington, DC 20036-1023, USA **Tel:** +1 202 223 9034. **Fax:** +1 202 416 6100
9–13	**Focus 94–The Annual National Meeting and Exhibition of the Association of Clinical Biochemists**	Brighton, UK	**Focus 94,** P.O. Box 227, Buckingham, Buckinghamshire, UK MK18 5PN **Tel:** +44 2806 613. **Fax:** +44 2806 487
16–19	**24th Annual Symposium on Environmental Analytical Chemistry**	Ottawa, Canada	**Dr. M. Malaiyandi,** CAEC, Chemistry Department, Carleton University, 1255 Colonel By Drive, Ottawa, Canada K1S 5B6 **Tel:** +1 613 788 3841. **Fax:** +1 613 788 3749
16–20	**24th International IAEAC Symposium on Environmental Analytical Chemistry**	Ottawa, Ontario, Canada	**Dr. James F. Lawrence,** Food Additives and Contaminants, Health and Welfare, Tunney's Pasture, Ottawa, Ontario, Canada K1A 0L2
22–26	**5th European Conference on Electroanalysis**	Venice, Italy	**Professor Salvatore Daniele,** Department of Physical Chemistry, The University of Venice, Calle Larga, S. Marta 2137-I-30123 Venice, Italy **Tel:** +39 41 5298503. **Fax:** +39 41 5298594
24–27	**3rd Symposium on Molecular Chirality**	Kyoto, Japan	**Professor Terumichi Nakagawa,** Symp ¬ on Molecular Chirality (SMC), Faculty o Pharmaceutical Sciences, Kyoto University, Yoshida-Shimoadachi-cho, Sakyo-ku, 606 Japan **Fax:** +81 48 471 0310 (Professor Hara)
24–27	**International Symposium on Metals and Genetics: Toxic Metal Compounds in Environment and Life 5; Interrelation between Chemistry and Biology**	Toronto, Ontario, Canada	**Professor B. Sarkar,** Department of Biochemistry, The Hospital for Sick Children, 555 University Avenue, Toronto, Ontario, Canada M5G 1X8
29–1/6	**42nd ASMS Conference on Mass Spectroscopy**	Chicago, IL, USA	**ASMS,** 815 Don Gaspar, Santa Fe, NM 87501, USA **Tel:** +1 505 989 4517.
30–1/6	**Scandinavian Symposium on Infrared and Raman Spectroscopy**	Bergen, Norway	**Dr. Alfred Christy,** Department of Chemistry, University of Bergen, N-5007 Bergen, Norway
30–2/6	**14th Nordic Atomic Spectroscopy and Trace Analysis Conference**	Naantali, Finland	**Ari Ivaska,** Abo Akademi University, Laboratory of Analytical Chemistry, Biskopsgatan 8, SF-20500 Abo Turku, Finland
June			
1–3	**Biosensors 94—The Third World Congress on Biosensors**	New Orleans, USA	**Kay Russell,** Conference Department, Elsevier Advanced Technology, Mayfield House, 256 Banbury Road, Oxford, UK OX2 7DH **Tel:** +44 (0) 865 512242. **Fax:** +44 (0) 865 310981
5–11	**24th ACHEMA**	Frankfurt, Germany	**Dechema,** Theodor Heuss-Allee 25, P.O. Box 970146, D-W-6000 Frankfurt am Main 97, Germany
6–8	**Conference on Plasma Science**	Santa Fe, NM, USA	**A. Perratt,** Los Alamos National Laboratory, Group X-10, MS D-406, P.O. Box 1663, Los Alamos, NM 87545, USA
8–11	**6th International Conference on Flow Analysis**	Toledo, Spain	**Professor M. Valcárcel/Dr. M. D. Luque de Castro,** (Flow Analysis VI), Departamento de Química Analítica, Facultad de Ciencias, E-14004 Córdoba, Spain **Tel:** +34 57 218616. **Fax:** +34 57 218606
15–17	**16th Symposium on Applied Surface Analysis (ASSD)**	Burlington, MA, USA	**Joseph Geller,** Geller Microanalytical, 1 Intercontiental Way, Peabody, MA 01960, USA **Tel:** +1 508 535 5595.

Date	Conference	Location	Contact
15–18	**The Second International Symposium on Speciation of Elements in Toxicology and Environmental and Biological Sciences**	Loen, Norway	**The Second International Symposium on Speciation of Elements in Toxicology and in Environmental and Biological Sciences,** Yngvar Thomassen, National Institute of Occupational Health, P.O. Box 8149 DEP, N-0033 Oslo 1, Norway
16–17	**14th International Symposium on Environmental Pollution**	Toronto, Canada	**Dr. V. M. Bhatnagar,** Alena Chemicals of Canada, P.O. Box 1779, Cornwall, Ontario, Canada K6H 5V7 **Tel:** +1 613 932 7702.
16–17	**18th International Conference on Analytical Chemistry and Applied Chromatography/ Spectroscopy**	Toronto, Canada	**Dr. V. M. Bhatnagar,** Alena Chemicals of Canada, P.O. Box 1779, Cornwall, Ontario, Canada K6H 5V7 **Tel:** +1 613 932 7702.
19–24	**20th International Symposium on Chromatography**	Bournemouth, UK	**Mrs J. A. Challis,** Chromatographic Society, Suite 4, Clarendon Chambers, 32 Clarendon Street, Nottingham, UK NG1 5JD **Tel:** +44 602 500596. **Fax:** +44 602 500614
27–1/7	**Special FEBS Meeting on Biological Membranes**	Espoo, Suomi-Finland	**Professor Timo Korhonen,** Biochemical Society, European Federation of Biochemical Societies (FEBS), Department of General Microbiology, University of Helsinki, Mannerheimintie 172, SF-00300 Helsinki, Finland
July			
18–22	**XIII International Congress on Electron Microscopy**	Paris, France	**B. Jouffrey,** SFME 67, rue Maurice Gunsbourg, 94205, Ivry sur Seine cedex, France **Tel:** +33 1 46702844. **Fax:** +33 1 46708846
20–22	**Seventh Biennial National Atomic Spectroscopy Symposium**	Hull, UK	**Dr. Steve Hill,** Department of Environmental Sciences, University of Plymouth, Drake Circus, Plymouth, Devon, UK PL4 8AA
August			
2–6	**The Second Changchun International Symposium on Analytical Chemistry(CISAC)**	Changchun, China	**Professor Quinhan Jin,** Department of Chemistry, Jilin University, Changchun 130023, China **Tel:** +86 431 82233 (ext. 2433). **Fax:** +86 431 823907
8–12	**IGARSS '94: 1994 International Geoscience and Remote Sensing Symposium**	Pasadena, CA, USA	**Meetings Department,** Optical Society of America, 2010 Massachusetts Avenue, NW, Washington, DC 20036-1023, USA **Tel:** +1 202 223 9034. **Fax:** +1 202 416 6100
21–26	**208th ACS National Meeting (with Sessions of Analytical Chemistry, Environmental Chemistry, Chemical Health and Safety, *etc*)**	Washington, DC, USA	**Mr. B. R. Hodson,** American Chemical Society, 1155–16th Street N.W., Washington, DC 20036, USA
29–2/9	**13th International Mass Spectrometry Conference**	Budapest, Hungary	**Hungarian Chemical Society,** H-1027 Budapest, Hungary **Tel:** +36 1 201 6883. **Fax:** +36 1 15 61215
September			
5–9	**7th International Symposium on Synthetic Membranes in Science and Industry**	Tübingen, Germany	**Dechema,** P.O. Box 970146, D-W-6000 Frankfurt am Main 97, Germany
11–16	**EUCMOS XXII: XXIInd European Congress on Molecular Spectroscopy**	Essen, Germany	**GDCh-Geschäftsstelle, Abt. Tagungen,** Varrentrappestr. 40–42, Postfach 90 04 40, D-6000 Frankfurt am Main 90, Germany **Tel:** +49 69 79 17 358. **Fax:** +49 69 79 17 475
12–15	**Separations for Biotechnology**	Reading, UK	**SCI Conference Office,** 14/15 Belgrave Square, London, UK SW1X 8PS **Tel:** +44 71 235 3681. **Fax:** +44 71 823 1698

Entries in the above listing are included at the discretion of the Editor and are free of charge. If you wish to publicize a forthcoming meeting please send full details to: *The Analyst* Editorial Office, Thomas Graham House, Science Park, Milton Road, Cambridge, UK CB4 4WF. Tel: +44 (0)223 420066. Fax: +44 (0)223 420247.

Key Appointment to Boost Nottingham Trent's Scientific Research Profile

Professor Colin Creaser has been appointed Head of the Department of Chemistry and Physics at The Nottingham Trent University.

He has joined Nottingham Trent from the University of East Anglia where he was Leader of the Analytical Chemistry Group.

One of Professor Creaser's key aims for the future is to develop and expand the department's research activities. He is at the forefront of research in the field of ion trap mass spectrometry, a technique that enables the detection of trace amounts of environmental pollutants such as dioxins. It also allows the detection of substances such as veterinary drug residues in food samples.

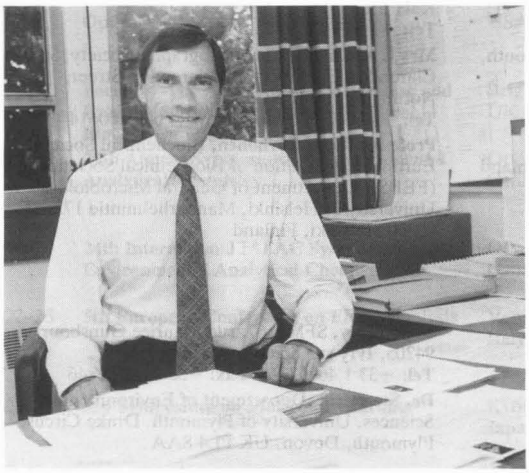

Professor Creaser's team of post-graduate and post-doctoral researchers from the University of East Anglia will also be joining the department later this summer, along with a team of four researchers from Brunel University. These moves will bring additional scientific equipment worth over £¼ million to Nottingham Trent.

Commenting on his appointment, Professor Creaser said, 'I am delighted to have joined Nottingham Trent at what is a very exciting and challenging time as it takes its place as one of the leading "new" universities'.

'The Department of Chemistry and Physics here is already known for the quality of both its teaching and its research. I hope to build on the work currently underway, develop new areas of specialist interest and help raise the department's profile in the national and international community'.

Other priorities for Professor Creaser will be to build on the department's strong record for forging international links and to develop more opportunities for students to focus on environmental themes in their courses.

Born in Surrey, Professor Creaser was brought up in Uganda but returned to the UK to attend school in Buckinghamshire and Sussex. After gaining his B.Sc. and Ph.D. at the University of Kent, he spent two years in the US conducting post-doctoral research at the University of California at Santa Barbara.

On returning to the UK in 1978, he joined the Physico-Chemical Measurements Unit at the Harwell Laboratory, where he was responsible for the mass spectrometry service. Six years later he moved to the University of East Anglia.

Professor Creaser is a member of the Royal Society of Chemistry and serves on the council of its Analytical Division.

Future Issues will Include—

Determination of Mercury Levels in Human Urine and Blood by Ultraviolet–Visible Spectrophotometry—**Hiromi Aikoh and Takashi Shibahara**

Simultaneous Determination of Ammonia Nitrogen and L-Glutamine in Bioreactor Media Using Flow Injection—**Bernhard O. Palsson, Bing Q. Shen, Mark E. Meyerhoff and Marek Trojanowicz**

Rapid Screening of Fish Tissue for Polychlorinated Dibenzo-*p*-dioxins and Dibenzofurans—**Thomas L. King, John F. Uthe and Charles J. Musial**

Determination of Phosgene (Carbonyl Chloride) in Air by High-performance Liquid Chromatography With a Dual Specific Detection System—**Weh S. Wu and Virindar S. Gaind**

Measurement of the Sorption of Actinides on Minerals Using Microanalytical Techniques—**Mark M. Cowper, John A. Berry, Hugh E. Bishop, Peter R. Fozard, John W. McMillan and Simon A. Mountfort**

Fluorescence Detection of the Glutathione S Conjugate With Aldehydes by High-performance Liquid Chromatography With Post-column Derivatization—**Mitsuaki Sano, Masahiro Fujita, Kazunori Takeda and Isao Tomita**

Use of Pattern Recognition for Signatures Generated by Laser Desorption–Ion Mobility Spectrometry of Polymeric Materials—**Michael Simpson, R. Saatchi, David R. Anderson, Cameron W. McLeod and Michael Cooke**

Reflux Pre-digestion in Microwave Sample Preparation—**Helen J. Reid, Stanley Greenfield, Tony E. Edmonds and Rafiq M. Kapdi**

Determination of Trace Elements in Laboratory-reagent Grade Sodium Salts by Atomic Absorption Spectrometry and Inductively Coupled Plasma Atomic Emission Spectrometry After Preconcentration by Column Solid-phase Extraction—**Anka Alexandrova and Sonja Arpadjan**

Inorganic Modifiers in Ion-pair Chromatographic Separation of Dicyanoaurate(I)—**John J. Byerley, Emmanuel O. Otu and Campbell W. Robinson**

Detection of Ephedrine and Phenylpropanolamine in Urine Using a Polarization Fluoroimmunoassay—**David L. Colbert, Sergei A. Eremin, A. V. Smirnov, Gerard Gallacher and David S. Smith**

Comparison of Capillary Zone Electrophoresis With Standard Gravimetric Analysis and Ion Chromatography for the Determination of Inorganic Anions in Detergent Matrices—**Emma L. Pretswell, Andrew R. Morrisson and John S. Park**

NEW PUBLICATION

HAZARDS IN THE OFFICE

The Newsletter on Health and Safety in the Office

Do you have a need for up-to-date, accurate information on the safety issues associated with the general office environment?

Are you responsible for your company's conformance to current UK and EC office legislation?

Do you work in an office and would like to be kept informed of factors affecting your health and safety?

Hazards in the Office, a new publication launched this year, can meet your requirement for information identifying hidden hazards in the office environment and necessary safety procedures. No other newsletter is devoted exclusively to office health and safety concerns.

Hazards in the Office provides:

- A convenient source of current information
- Up-to-date news on rapidly changing UK and EC office legislation
- Concise, easy-to-scan abstracts with entertaining, informative illustrations
- A feature article in each issue dealing with a topical subject
- Cited sources to assist with obtaining further information

Each bimonthly issue of **Hazards in the Office** contains around sixty short, but informative, summaries of topical articles appearing in the literature on health and safety matters. All publications with material on office safety are covered.

Hazards in the Office is a unique single source of essential information for all concerned with office safety and legislation. It can save valuable time otherwise spent searching through a diverse range of publications.

1993 Subscription Details

Published six times per year.

EC.....£48.00

USA.....$98.00

Rest of World.....£53.00

ISSN 0966-906X

Hazards in the Office *is essential reading for all responsible for, or interested in, office health and safety.*

To order please contact:
Turpin Distribution Services Ltd, Blackhorse Road, Letchworth, Herts SG6 1HN, UK.
Tel: +44 (0)462 672555. Fax: +44 (0)480947. Telex: 825372 TURPIN G.

ROYAL SOCIETY OF CHEMISTRY
Information Services

NEW EDITION

OVER 81,000 SPECTRA

EIGHT PEAK INDEX OF MASS SPECTRA

4th Edition

The essential tool for mass spectrometrists

NOW AVAILABLE – the **new 4th Edition** of the highly regarded ***Eight Peak Index of Mass Spectra.***

This quality compilation is recognised by many mass spectrometrists as the most useful index of mass spectra in print today.

THE *EIGHT PEAK INDEX* EMPOWERS YOU TO:

- ★ identify unknowns rapidly and easily
- ★ locate spectra of compounds quickly by formula or molecular weight
- ★ match spectra simply through direct peak intensity comparison
- ★ find spectra relevant to your area of interest – a wide variety of compound types are included
- ★ access the data at any time with no machine-time restrictions
- ★ use the data with confidence – extensive checks on all records have been performed

Probably the best printed index of mass spectra in the world!

For more information about the ***NEW*** edition, simply contact us at the address below for a copy of our detailed leaflet:

ROYAL SOCIETY OF CHEMISTRY

Information Services

Sales and Promotion Department
Royal Society of Chemistry
Thomas Graham House
Science Park, Milton Road
Cambridge CB4 4WF, United Kingdom
Tel: +44 (0) 223 420066.
Fax: +44 (0) 223 423623.
Telex: 818293 ROYAL

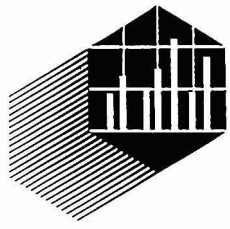

ROYAL SOCIETY OF CHEMISTRY

ACS TOXICOLOGY BOOKS

ACS Publications

Under an agreement with the American Chemical Society (ACS) the following titles are available through the Royal Society of Chemistry. All titles are hardcover unless otherwise stated.

Pesticide Residues and Food Safety

A Harvest of Viewpoints

Edited by B.G. Tweedy, *CIBA-GEIGY Corporation*
Henry J. Dishburger, *Dow Elanco*
Larry G. Ballantine, *Hazelton-Wisconsin*
John McCarthy, *National Agricultural Chemicals Association*
Jane Murphy, *Associate Editor*

In this volume a variety of experts, including chemists, toxicologists, growers, educators, regulators, food processors and distributors, representatives of consumer groups, and reporters, address the major issues surrounding food safety and pesticide residues. Its 37 chapters are divided into sections covering pesticide use, alternative agriculture production, exposure assessment, risk management, and legislative and regulatory issues. An introductory section defines the scope of the issues and a concluding section presents comments from a panel discussion on communicating risk to the public. This collection, which presents many divergent viewpoints from indivuals and organizations directly involved with pesticides, offers valuable insights into the issues covered.

ACS Symposium Series No. 446

Hardcover **360 pages**
ISBN 0 8412 1889 7 (1991) **Price £39.00**

Frontiers in Molecular Toxicology

Edited by L.J. Marnett, *Vanderbilt University*

This new volume provides concise, up-to-date articles highlighting the most recent advances in mechanisms of toxicology and the methods for studying them, examining chemical approaches to the solution of toxicologically interesting problems. Originally published in the journal Chemical Research in Toxicology, they convey the opportunity and excitement that exists at the interface of chemistry and toxicology.

Brief Contents:
Toxic Agents and their Actions; Enzymes of Activation, Inactivation, and Repair; Physical Methods; Macromolecular Modification.

Softcover **294 pages**
ISBN 0 8412 2428 5 (1992) **Price £12.50**

Immunoassays for Trace Chemical Analysis:

Monitoring Toxic Chemicals in Humans, Food, and the Environment

Edited by Martin Vanderlaan, Larry H. Shankar and Bruce E Watkins *Lawrence Livermore National Laboratory*

Dean W Roberts, *National Centre for Toxicological Research*

Increasing public concern over chemical exposures and the quality of the food supply has resulted in increased pressure on regulatory agencies to do more sampling for more chemicals. This new volume explores the use of immunoassays as alternative methods for conducting this necessary sampling. It brings together a broad range of applications of analytical immunochemistry, including immunoassays for chemical residues in food and the environment, for natural toxins, and for monitoring human exposure to toxic chemicals. Each section begins with an informative review highlighting the major issues in that section. Also included are the following three appendices that provide up-to-date compilations of references organized according to applications: environmental monitoring, mycotoxin analysis, and DNA- and protein-adduct analyses.

ACS Symposium Series No 451

Hardcover **354 pages**
ISBN 0 8412 1905 2 (1991) **Price £49.00**

Principles of Environmental Toxicology

Edited by: Sigmund F. Zakrzewski,
State University of New York at Buffalo

This volume is an ideal introductory text in environmental toxicology, offering broad coverage of the field. It opens with an examination of the basic principles of toxicology and provides a discussion of the pharmacological and metabolic processes that influence toxicity, carcinogenisis, and mutagenesis. The types, causes and effects of pollution in air, water, and on land are examined, as well as control technologies. In addition, the author offers a discussion on occupational toxicology, including kidney, liver, and respiratory toxins. **Principles of Environmental Toxicology** concludes with an examination of such environmental regulatory policies as the Clean Air Act, the Federal Water Pollution Control Act, the Safe Drinking Water Act, the Toxic Substances Control Act and others.

Hardcover **270 pages**
ISBN 0 8412 2125 1 (1991) **Price £44.00**

ROYAL SOCIETY OF CHEMISTRY

Information Services

To Order, *Please write to the:*
Royal Society of Chemistry, Turpin Distribution Services Limited, Blackhorse Road, Letchworth, Herts SG6 1HN, United Kingdom.
or telephone (0462) 672555 quoting your credit card details. We accept Access/Visa/MasterCard/Eurocard.

Turpin Distribution Services Limited is wholly owned by the Royal Society of Chemistry.

For information on other books and journals, *please write to:*
Royal Society of Chemistry, Sales and Promotion Department, Thomas Graham House, Science Park, Milton Road, Cambridge CB4 4WF, United Kingdom.

RSC Members *should obtain members prices and order from :*
The Membership Affairs Department at the Cambridge address above.

ROYAL SOCIETY OF CHEMISTRY

NEW AND RECENT ANALYTICAL BOOKS

Spectrochemical Analysis by Atomic Absorption and Emission

By Lauri H.J. Lajunen
University of Oulu, FInland

This **new** book describes both the theory of atomic spectroscopy and all the major atomic spectrometric techniques (AAS, Flame-AES, Plasma AES, AFS and ICP-MS), including basic concepts, instrumentation and applications.

Spectrochemical Analysis by Atomic Absorption and Emission is very wide in scope and will be extremely useful to both undergraduates and lecturers undertaking modern analytical chemistry courses. It contains many figures and tables which illuminate the text, covers various sample preparation methods and gives suggestions for further reading.

Contents:
Introduction; Theory of Atomic Spectroscopy; Atomic Absorption Spectrometry; Flame Atomic Emission Spectrometry; Plasma Atomic Emission Spectrometry; Inductively Coupled Plasma Mass Spectrometry; Atomic Fluorescence Spectrometry; Sample Preparation; Advantages and Mutual Comparison of Atomic Spectrometric Methods; Further Reading; Subject Index.

Softcover **xii + 242 pages**
ISBN 0 85186 873 8 **Price £18.50**
June 1992

Analytical Ultracentrifugation in Biochemistry and Polymer Science

Edited by S.E. Harding
University of Nottingham
J.C. Horton
University of Nottingham
A.J. Rowe
University of Leicester

Analytical Ultracentrifugation in Biochemistry and Polymer Science is the first book of its kind to appear for nearly two decades and gives as comprehensive a coverage as is possible of the present state-of-the-art, from the leading experts in the field. It describes the advances currently being made and assesses to what extent 'classical' methods are still applicable, providing an up-to-date guide for potential users and experienced researcher alike.

The book divides naturally into four parts. Part I describes the state-of-the-art in instrumentation including a detailed consideration of optical systems and data capture and analysis procedures. Part II focuses on sedimentation equilibrium methods for obtaining molecular weight, polydispersity and interaction information. Part III considers transport methods (both sedimentation and diffusive) and includes a detailed consideration of rigid and flexible particle conformation analysis, polydisperse and interacting systems and concentration dependence phenomena. Part IV looks at a wide range of applications to macromolecular systems in biochemistry and polymer science, including seed and membrane proteins, polysaccharides and glycoconjugates and synthetic macromolecular systems.

This important **new** book is the consequence of an exciting resurgence of interest in the technique, will assist researchers in biochemistry and polymer science to make the most of the exciting opportunity that now exists.

Hardcover **xiv + 630 pages**
ISBN 085186 345 0 **Price £85.00**
November 1992

Particle Size Analysis

Edited by N.G. Stanley-Wood
University of Bradford
R.W. Lines
Coulter Electronics Limited, Luton

Particle Size Analysis reviews the development of particle characterization over the past 25 years and also speculates on its future. Interest in the subject has increased enormously over the years and this book highlights the changes and advances made within the field.

This book is comprehensive in its coverage of particle size analysis and includes contributions on such characterization techniques as microscopy using fractal analysis, light diffraction, light scattering with the phase doppler technique, light observation, and photon correlation spectroscopy. A number of chapters address the interest in on-line in-stream particle size analysis and illustrate the progress being made in achieving this long sought after ideal of *in-situ* in-process particle characterization. Applications to other technological fields are detailed by chapters covering biological systems and the pharmaceutical industry. The subject of surface area determination is considered with particular emphasis on the measurements on porosity of powders, the characterization and comparability of reference materials, and the need for standards.

Particle Size Analysis should provide stimulating reading for technologists, scientists, and engineers involved in particle characterization and powder technology worldwide.

Special Publication No. 102

Hardcover **xx + 538 pages**
ISBN 0 85186 487 2 **Price £57.50**
June 1992

Bioanalytical Approaches for Drugs

including Anti-asthmatics and Metabolites

Edited by Eric Reid
Guildford Academic Associates
I.D. Wilson
ICI Pharmaceutical Division, Macclesfield

Methodological Surveys in Biochemistry and Analysis

Volume 22

Series Editor Eric Reid
Guildford Academic Associates

Bioanalytical Approaches for Drugs, including Anti-asthmatics and Metabolites gives a state-of-the-art account of the subject and focuses on assaying blood and other biological samples, especially drugs which are given in low dosage or which yield metabolites that need subtle investigation. It covers advances in HPLC, SFC, CZE, MS and other detectors, NMR, and automated sample handling, as well as diverse drugs. The book also looks at problems such as analyte lability, stereoselectivity and interferants.

This book is the latest volume in the 'Analysis' sub-series of **Methodological Surveys in Biochemistry and Analysis**, which is acknowledged as an integrated reference source, and contains a cumulative analyte index. It will be essential reading for researchers involved in analytical, medicinal, pharmaceutical and bio-organic chemistry.

Special Publication No. 110

Hardcover **xiv + 356 pages**
ISBN 0 85186 236 5 **Price £75.00**
September 1992

ROYAL SOCIETY OF CHEMISTRY
Information Services

To Order, *Please write to:*
Royal Society of Chemistry, Turpin Distribution Services Limited, Blackhorse Road, Letchworth, Herts SG6 1HN, United Kingdom.
or telephone (0462) 672555 quoting your credit card details. We can now accept Access/Visa/MasterCard/Eurocard.

Turpin Distribution Services Limited is wholly owned by the Royal Society of Chemistry.

For information on other books and journals, *please write to:*
Royal Society of Chemistry, Sales and Promotion Department, Thomas Graham House, Science Park, Milton Road, Cambridge CB4 4WF. UK.

RSC Members *should obtain members prices and order from :*
The Membership Affairs Department at the Cambridge address above.

The Second International Symposium on

Speciation of Elements in Toxicology and in Environmental and Biological Sciences

June 15-18, 1994, Loen, Norway.

AIMS

The Symposium will focus on recent speciation research related to the chemical, physical and morphological states of elements as they appear in various compartments in environmental and biological systems. The aims of the symposium are: to provide a forum at which recent progress in analytical methodology of element speciation can be discussed and to provide an opportunity for an interchange of ideas between analytical and other scientists investigating fundamental aspects of environmental and human toxicology, nutrition, or metal containing drugs.

THEMES

The main themes for the Symposium are:

A. Sampling, Characterization, Detection and Determination of Chemical or Particle Species

* In Air
* In Water
* In Soil
* In Biological Systems

B.Thermodynamic and Kinetic Aspects

C.Importance of Speciation in Environmental and Human Toxicology, Nutrition and Medicine.

* Speciation of the elements will be considered in the context of pathways to humans, exposure routes, uptake, distribution, metabolism, toxicological mechanisms and excretion.

SUBMISSION OF ABSTRACTS

All contributions (oral or poster) presented will be eligible for publication in a Special Symposium Issue of the journal *The Analyst*. Prospective authors should submit an abstract (A4 format) of one-page length, including tables and figures, by February 15, 1994(deadline).

ORGANIZING COMMITTEE

Yngvar Thomassen (*Symposium Chairman*) **Evert Nieboer** (*Programme Chairman*)

Rita Cornelis (*Gent, Belgium*) **Jytte Molin Christensen** (*Copenhagen, Denmark*)

Brit Salbu (*Aas, Norway*) **Wolfgang Frech** (*Umea, Sweden*)

Jan Aaseth (*Elverum, Norway*)

FOR FURTHER INFORMATION CONTACT: The Second International Symposium on Speciation of Elements in Toxicology and in Environmental and Biological Sciences, **Yngvar Thomassen**, National Institute of Occupational Health, P.O. Box 8149 DEP, N-0033 Oslo 1, Norway.

The 5th Nordic Symposium on

Trace Elements in Human Health and Disease

June 19-21, 1994, Loen, Norway

AIMS

The Symposium will focus on recent research related to trace elements and their relevance in human physiology and toxicology. The programme will emphasize cross-disciplinary issues and promote participant interaction. The conference is intended both for scientists in academia with expertise in toxicology, clinical and analytical chemistry, pathology, metabolic disorders, occupational and environmental health and nutrition, as well as environmental and health professionals.

THEMES

The main themes for the Symposium are:

* Environmental and Occupational Exposure
* Analytical and Clinical Chemistry
* Trace Element Imbalances Related to Human Diseases (*e.g.*, Cancer; Cardiovascular, Liver and Neurological Diseases)
* Dietary Levels and Critical Requirements (Essentiality *versus* Toxicity; Geomedicine)
* Reference Concentrations as Drugs, Chemotherapeutics, Diagnostic Agents, and Chelation Therapy
* Reproductive and Development Effects

SUBMISSION OF ABSTRACTS

The Organizing Committee cordially invites you to submit an abstract of original research related to the themes of the Symposium. Prospective authors should submit an abstract (A4 format) of one-page length including tables and figures by February 15, 1994(deadline). All contributions (oral or poster) presented will be eligible for publication in a Special Symposium issue of *The Analyst*

ORGANIZING COMMITTEE

Jan Aaseth, (*Symposium Chairman*) Hedmark Central Hospital, Norway

Jan Alexander, Institute of Public Health, Oslo, Norway

Evert Nieboer, McMaster University, Hamilton, Canada

Jetmund Ringstad, Ulleval Hospital, Oslo, Norway

Brit Salbu, Agricultural University, As, Norway

Yngvar Thomassen, (*Symposium Secretary*) Oslo, Norway

FOR FURTHER INFORMATION CONTACT: Trace Elements in Human Health and Disease, **Yngvar Thomassen,** National Institute of Occupational Health, P.O. Box 8149 DEP, N-0033 Oslo, Norway. TEL: 47 22466850; FAX: 47 22603276

FIRST FOLD HERE

THE ANALYST READER ENQUIRY SERVICE
For further information about any of the products featured in the advertisements in this issue, write the appropriate number on the postcard, detach and post.

FOLD HERE

THE ANALYST READER ENQUIRY SERVICE

SEP'93

For further information about any of the products featured in the advertisements in this issue, please write the appropriate number in one of the boxes below.
Postage paid if posted in the British Isles but overseas readers must affix a stamp.

PLEASE USE BLOCK CAPITALS LEAVING A SPACE BETWEEN WORDS *Valid 12 months*

1 NAME

2 COMPANY

PLEASE GIVE YOUR BUSINESS ADDRESS IF POSSIBLE. IF NOT, PLEASE TICK HERE ☐

3 STREET

4 TOWN

5 COUNTY
POST CODE

6 COUNTRY

7 DEPARTMENT/
DIVISION

8 YOUR JOB TITLE/
POSITION

9 TELEPHONE NO

OFFICE USE ONLY REC'D PROC'D

FOLD HERE

Postage will be paid by Licensee

Do not affix Postage Stamps if posted in Gt. Britain, Channel Islands, N. Ireland or the Isle of Man

BUSINESS REPLY SERVICE
Licence No. WD 106

2

Reader Enquiry Service
The Analyst
The Royal Society of Chemistry
Burlington House, Piccadilly
LONDON
W1E 6WF
England

ANALAO 118(9) 1101–1234, 107N–116N (1993) September 1993

The Analyst

The Analytical Journal of The Royal Society of Chemistry

CONTENTS

1101 **Under-determination of Strontium-90 in Soils Containing Particles of Irradiated Uranium Oxide Fuel**—Deborah H. Oughton, B. Salbu, Tom L. Brand, J. Philip Day, Asker Aarkrog

1107 **Estimating and Using Sampling Precision in Surveys of Trace Constituents of Soils**—Michael Thompson, Michael Maguire

1111 **Spectroscopic Probes for Hydrogen Bonding, Extraction Impregnation and Reaction in Supercritical Fluids**—Andrew I. Cooper, Steven M. Howdle, Catherine Hughes, Margaret Jobling, Sergei G. Kazarian, Martyn Poliakoff, Lindsey A. Shepherd, Keith P. Johnston

1117 **Determination of Derivatized Urea Herbicides in Water by Solid-phase Extraction, Methylation and Gas Chromatography With a Nitrogen–Phosphorus Detector**—Steven Scott

1123 **Comparison of Liquid Chromatographic Methods for Analysis of Homologous Alkyl Esters of Biphenyl-4,4′-dicarboxylic Acid**—Joel K. Swadesh, Charles W. Stewart, Jr., Peter C. Uden

1127 **Assessment of Three Azophenol Calix[4]arenes as Chromogenic Ligands for Optical Detection of Alkali Metal Ions**—Mary McCarrick, Stephen J. Harris, Dermot Diamond

1131 **Inverted Poly(vinyl chloride)–Liquid Membrane Ion-selective Electrodes for High-speed Batch Injection Potentiometric Analysis**—Jianmin Lu, Qiang Chen, Dermot Diamond, Joseph Wang

1137 **Titrations of Non-ionic Surfactants With Sodium Tetraphenylborate Using the Orion Surfactant Electrode**—Robyn Dahl Gallegos

1143 **Frequency Characteristics of an Electrode-separated Piezoelectric Crystal Sensor in Contact With a Liquid**—Shen Dazhong, Lin Song, Kang Qi, Nie Lihua, Yao Shouzhuo

1149 **Enzymic Assays of Organic Peroxides in Microemulsion Systems**—Joseph Wang, A. Julio Reviejo

1153 **Determination of Microgram Amounts of Uranium in Thorium by Differential-pulse Polarography**—Sulobh K. Das, Achyut V. Kulkarni, Ramesh G. Dhaneshwar

1157 **Electrochemical Reduction at Mercury Electrodes and Differential-pulse Polarographic Determination of Pentamidine Isethionate**—M. Valnice B. Zanoni, Arnold G. Fogg

1163 **Cathodic Stripping Voltammetric Determination of Pentamidine Isethionate at a Hanging Mercury Drop Electrode**—M. Valnice B. Zanoni, Arnold G. Fogg

1167 **Direct Determination of Ethanol in all Types of Alcoholic Beverages by Near-infrared Derivative Spectrometry**—Máximo Gallignani, Salvador Garrigues, Miguel de la Guardia

1175 **Decomposition of Biological Samples for Inductively Coupled Plasma Atomic Emission Spectrometry Using an Open Focused Microwave Digestion System**—Antoaneta Krushevska, Ramon M. Barnes, Chitra Amarasiriwaradena

1183 **Determination of Trace Amounts of Thallium and Tellurium in Nickel-base Alloys by Electrothermal Atomic Absorption Spectrometry**—Suh-Jen Jane Tsai, Ching-Ching Jan

1193 **Determination of Citric Acid and Oxalacetic Acid in Foods by Enzymic Flow Injection**—Milagros Plantá, Fernando Lázaro, Rosa Puchades, Angel Maquieira

1199 **Flow Injection Spectrophotometric Method for the Speciation of Aluminium in River and Tap Waters**—Mª José Quintela, Mercedes Gallego, Miguel Valcárcel

1205 **Selective and Sensitive Spectrophotometric Determination of Tetrafluoroborate in Waste Water After Ion-pair Extraction Using Bis[2-(5-chloro-2-pyridylazo)-5-diethylaminophenolato]cobalt(III) as a Counter Ion**—Issei Kasahara, Satoshi Hosokawa, Noriko Hata, Shigeru Taguchi, Katsumi Goto

1209 **Spectrophotometric Determination of Lipohydroperoxides and Organic Hydroperoxides by Use of the Triiodide–Hexadecylpyridinium Chloride Micellar System**—Mª Loreto Lunar, Soledad Rubio, Dolores Pérez-Bendito

1213 **Determination of Free State Manganese(II) in a Decoction of a Traditional Chinese Medicine Based on a Kinetic Spectrophotometric Method**—Liu Jianli, Wang Budong, Zhang Fenyan

REPORT BY THE ANALYTICAL METHODS COMMITTEE

1217 **Nitrogen Factors for Beef: A Reassessment**—Analytical Methods Committee

COMMUNICATION

1227 **Permeation Tubes for Calibration in Flow Injection Analysis**—Stuart J. Chalk, Julian F. Tyson, Don C. Olson

1233 **CUMULATIVE AUTHOR INDEX**

107N **Book Reviews**

110N **Conference Diary**

116N **New Professor of Analytical Chemistry**—Colin S. Creaser

116N **Papers in Future Issues**

Typeset and printed by Black Bear Press Limited, Cambridge, England

0003-2654(1993)9:1